

Functional analysis of the coronary artery disease associated gene *HHIPL1*

Thesis submitted for the degree of
Doctor of Philosophy
at the University of Leicester

by

Dimitra Aravani BSc, MSc

Department of Cardiovascular Sciences
University of Leicester

January 2017

Functional analysis of the coronary artery disease associated gene *HHIPL1*

Dimitra Aravani

Abstract

Genome-wide association studies have identified chromosome 14q32 as a locus for coronary artery disease in humans. The disease associated variants fall in a gene called *Hedgehog interacting protein-like 1 (HHIPL1)*, which encodes an uncharacterised sequence homologue of an antagonist of Hedgehog signalling. Here, is presented the investigation of HHIPL1 function and its role in atherosclerosis.

In vitro analysis was undertaken in order to determine the molecular and cellular function of the protein. Epitope tagged HHIPL1 protein was present in the media of transfected cells and immunoprecipitated with GFP tagged Sonic Hedgehog (SHH) protein, demonstrating that HHIPL1 is a secreted interactor of SHH. *HHIPL1* gene expression was also measured in cardiovascular cell types and found that it is expressed in aortic smooth muscle cells (HASMC), but not in other disease relevant cell types. During atherogenesis smooth muscle cells migrate and proliferate into the tunica intima. Therefore, the effect of HHIPL1 on HASMC phenotype was examined following *HHIPL1* knockdown. Down regulation of *HHIPL1* through siRNA resulted in a significant reduction in both HASMC proliferation and migration, suggesting a regulatory role for HHIPL1 in smooth muscle cell phenotype.

Next, the role of HHIPL1 in atherosclerosis *in vivo* was examined. In atherosclerotic mouse aortas (*ApoE*^{-/-}) *Hhip1* expression increased with disease progression. In order to further investigate the effect of *Hhip1* on atherosclerosis *Hhip1* knockout mice, which are phenotypically normal, were crossed onto two hyperlipidemic atherosclerosis prone backgrounds. Double knockout mice (*Hhip1*^{-/-}; *ApoE*^{-/-}, *Hhip1*^{-/-}; *Ldlr*^{-/-}) displayed a substantial reduction of over 60% in atherosclerotic lesion size compared with controls. Moreover, *Hhip1*^{-/-} lesions were characterised by reduced smooth muscle cell content, but unaltered lipid and macrophage profile.

These data represent the first experimental investigation of HHIPL1 and demonstrate that HHIPL1 is a proatherogenic protein that regulates smooth muscle cell proliferation and migration, presumably through its involvement in Hedgehog signalling.

Acknowledgements

I would like to give my gratitude to my supervisors Dr. Tom Webb and Dr. Emma Stringer for their constant mentoring, guidance and support throughout my PhD. Moreover, I would like to thank my co-supervisor Professor Nilesh Samani for giving me the opportunity to work in his group, which helped me develop as a scientist and as a person.

I would like to acknowledge all of the members of the Department of Cardiovascular Sciences who have helped me throughout my PhD, especially Dr. Veryan Codd, Dr. Pete Jones, Dr. Elisavet Kamanavi and Dr. Renata Kostogryns for their technical advice. I am also grateful to the animal unit staff at the Central Research Facility (CRF) for the great cooperation, which made all the mouse work feasible.

Thank you to my closest people in Leicester, Virag and Manolo for cheering me up and looking after me during the hardest times of my PhD.

A special thank you to my parents and sister, who have always been my reference point and source of encouragement during my studies. I am grateful for their endless love and support throughout my entire life. I'm also greatly indebted to my parents for teaching me how to set and achieve my life goals. This thesis is dedicated to my mum, dad and sister.

Table of Contents

Abstract	i
Acknowledgements	ii
Table of contents	iii
List of tables	viii
List of figures	ix
List of abbreviations	xi
1 Introduction	1
1.1 Coronary artery disease	2
1.1.1 Pathophysiology of CAD	2
1.1.2 Risk factors of CAD	10
1.2 Genetics of CAD	12
1.2.1 Heritability of CAD	12
1.2.2 Monogenic forms of CAD	14
1.2.3 Polygenic forms of CAD	15
1.2.4 Linkage studies for polygenic CAD forms	16
1.2.5 CAD Candidate gene studies	17
1.2.6 Genome wide association studies (GWAS)	19
1.2.6.1 CAD GWAS	20
1.2.6.2 Functional analysis of GWAS loci	22
1.2.6.3 14q32.2 CAD associated locus	23
1.3 Hedgehog signalling	25
1.3.1 Hh pathway and cell behaviour	28
1.3.2 Hh target genes	28
1.3.3 Non-canonical Hh signalling	29
1.3.4 Hedgehog signalling in human diseases	29
1.4 Mouse models	31
1.4.1 Mutagenesis strategies in mouse	31
1.4.1.1 Large scale gene targeting	33
1.4.2 Mouse models of atherosclerosis	34
1.4.2.1 Genetically modified atherosclerosis mouse models	35
1.4.2.2 Atherosclerosis pathophysiology in mice	37
1.5 Hypothesis	43

1.6 Aims of the thesis.....	43
2 Materials and Methods.....	44
2.1 Cell biology	45
2.1.1 Cell maintenance	45
2.1.1.1 Human embryonic kidney cells.....	45
2.1.1.2 Human aortic smooth muscle cells.....	45
2.1.1.3 Cell cryopreservation.....	45
2.1.1.4 Cell revival from liquid nitrogen	46
2.1.2 Cell transfection methods.....	46
2.1.2.1 Lipofectamine based transfection.....	46
2.1.2.2 Electroporation	46
2.1.2.3 Reverse transfection of siRNA	49
2.1.3 Behavioural assays	50
2.1.3.1 Migration assay (scratch assay)	50
2.1.3.2 Image analysis of migration assay	51
2.1.3.3 Proliferation assay.....	51
2.1.3.4 Image analysis of proliferation assay	51
2.1.4 Cell imaging	51
2.1.4.1 HEK293 fixation and staining	51
2.2 Protein methods	52
2.2.1 Western blotting	52
2.2.1.1 Cell lysate protein preparation.....	52
2.2.1.2 Concentration of conditioned media	52
2.2.1.3 SDS page.....	53
2.2.1.4 Protein transfer.....	53
2.2.1.5 Immunoblotting.....	53
2.2.2 Immunoprecipitation (IP)	54
2.2.2.1 Cell lysate protein extraction	54
2.2.2.2 Conditioned media protein preparation	54
2.2.2.3 GFP_Trap® _A beads equilibration.....	54
2.2.2.4 Protein binding	55
2.2.2.5 Western blotting of IP samples.....	55
2.3 Molecular biology	57

2.3.1	RNA isolation from mouse tissue	57
2.3.2	RNA isolation from cells	57
2.3.3	cDNA synthesis.....	58
2.3.4	Genomic DNA isolation	59
2.3.5	DNA gel extraction and sequencing.....	59
2.3.6	Primer design	59
2.3.7	Genotyping of <i>Hhip1</i> transgenic mice.....	65
2.3.8	Reverse Transcription PCR (RT-PCR).....	68
2.3.9	Quantitative-PCR (qPCR)	70
2.3.9.1	Standard curve analysis	70
2.3.9.2	qPCR conditions.....	72
2.3.9.3	Housekeeping gene validation	73
2.4	Microbiology	74
2.4.1	Plasmid cloning	74
2.4.2	Bacterial plasmid transformation	76
2.4.3	Plasmid Midiprep extraction	76
2.4.4	Plasmid sequencing	77
2.5	Animal preparations	77
2.5.1	Animal model	77
2.5.2	Mouse husbandry.....	77
2.5.3	Non invasive blood pressure measurement	78
2.5.4	Mouse termination.....	78
2.6	Tissue dissection	78
2.6.1	<i>En face</i> preparation of the aorta.....	78
2.6.2	Aortic root preparation.....	79
2.7	Histology	79
2.7.1	Tissue preparation (frozen)	79
2.7.2	Sectioning of frozen samples	79
2.7.3	Oil Red O (ORO) staining of the aorta.....	81
2.7.4	X-gal staining of frozen sections	82
2.7.5	Immunohistochemical staining of frozen sections for β -galactosidase	82
2.7.6	Immunohistochemical staining of frozen sections (MOMA-2 and α -SMA).....	83

2.7.7	ORO staining of frozen sections.....	84
2.7.8	Masson's trichrome staining for frozen sections.....	85
2.7.9	Image analysis and quantification of histological sections.....	85
2.8	Statistical analysis.....	86
2.8.1	<i>In vitro</i> data	86
2.8.2	<i>In vivo</i> data	86
2.9	<i>In silico</i> analysis	87
2.9.1	Protein domain prediction.....	87
2.9.2	Protein alignment	87
3	<i>In vitro</i> investigation of HHIPL1	88
3.1	Introduction.....	89
3.1.1	Hh signalling in vasculature maintenance	89
3.1.2	Hh signalling in vascular disease	90
3.2	Results.....	93
3.2.1	<i>In silico</i> analysis of HHIPL1	93
3.2.2	<i>In vitro</i> investigation of HHIPL1 cellular localisation	98
3.2.3	Analysis of HHIPL1-SHH interaction	102
3.2.4	Investigation of <i>HHIPL1</i> expression in vessel wall cells	104
3.2.5	Investigation of the effect of <i>HHIPL1</i> knockdown on HASMC behaviour.....	105
3.2.5.1	<i>HHIPL1</i> siRNA mediated knockdown in HASMC	105
3.2.5.2	Effect of <i>HHIPL1</i> knockdown on HASMC proliferation	108
3.2.5.3	Effect of <i>HHIPL1</i> knockdown on HASMC migration	110
3.3	Discussion	113
3.4	Conclusion	114
4	Validation and characterisation of a <i>Hhip1</i> knockout mouse model	116
4.1	Introduction.....	117
4.1.1	KOMP mutagenesis strategy.....	117
4.1.2	Hh mouse models	120
4.2	Results.....	125
4.2.1	Validation of <i>Hhip1</i> knockout first construct.....	125
4.2.2	Phenotypic characterisation of <i>Hhip1</i> ^{-/-} mouse	129
4.2.3	Analysis of <i>Hhip1</i> expression in mouse tissues.....	130

4.2.4	Histological examination of <i>Hhip1</i> expression	131
4.3	Discussion	137
4.4	Conclusion	138
5	Investigation of <i>Hhip1</i> in mouse models of atherosclerosis	139
5.1	Introduction.....	140
5.1.1	Validation of GWAS loci using mouse models of atherosclerosis .	140
5.1.2	Quantitation of atherosclerosis in mouse models.....	142
5.1.3	Atherosclerosis study design.....	143
5.2	Results.....	145
5.2.1	Investigation of <i>Hhip1</i> expression in atherosclerosis	145
5.2.2	<i>Hhip1</i> ^{-/-} mouse atherosclerosis study	149
5.2.3	Assessment of body weight and blood pressure in <i>Hhip1</i> ^{-/-} mice .	151
5.2.4	Quantitation of atherosclerosis in <i>Hhip1</i> ^{-/-} mice	154
5.2.5	Compositional analysis of atherosclerotic lesions in <i>Hhip1</i> ^{-/-} mice	157
5.3	Discussion	163
5.4	Conclusion	167
6	Discussion	168
6.1	Study limitations.....	174
6.2	Future work.....	175
6.3	Conclusion	176
7	References	177

List of tables

Table 1.1 Classification of atherosclerotic lesions-Type I to VI.....	4
Table 1.2 Heritability of atherosclerosis related phenotypes.....	13
Table 1.3 Main findings of CAD candidate genes studies.....	18
Table 1.4 Mutations in the Hh signalling pathway in human disease.....	30
Table 1.5 Atherosclerosis progression in <i>ApoE</i> ^{-/-} and <i>Ldlr</i> ^{-/-} mice.....	39
Table 2.1 Electroporation parameters for HEK293 cells.....	48
Table 2.2 siRNA target sequences.....	49
Table 2.3 Primary and secondary antibodies used for western blotting (WB)..	56
Table 2.4 Primer sequences.....	64
Table 2.5 PCR recipe for <i>Hhip1</i> genotyping.....	65
Table 2.6 PCR recipe for <i>Ldlr</i> and <i>ApoE</i> genotyping.....	66
Table 2.7 PCR conditions for genotyping.	67
Table 2.8 RT-PCR recipe using ReddyMix polymerase.....	68
Table 2.9 RT-PCR recipe using MyTaq polymerase.....	68
Table 2.10 RT-PCR conditions for each gene.	69
Table 2.11 qPCR conditions for each gene.....	72
Table 2.12 qPCR cycling conditions.	73
Table 2.13 Primary and secondary antibodies used for immunohistochemistry	84
Table 4.1 Hh mouse models and phenotypes.....	124
Table 5.1 Investigation of GWAS loci using mouse models of atherosclerosis	142

List of figures

Figure 1.1 Composition of a healthy arterial wall.....	3
Figure 1.2 Effect of LDL infiltration on the inflammatory process and the role of macrophages	7
Figure 1.3 Fibrous cap formation and rupture	10
Figure 1.4 Risk factors of CAD	11
Figure 1.5 Low and high frequency variants and disease susceptibility	15
Figure 1.6 Circular Manhattan plot summarising the CAD associated loci.	21
Figure 1.7 Regional association plot for the 14q32.2 CAD locus.....	24
Figure 1.8 Simplified vertebrate Hedgehog signalling pathway.	27
Figure 1.9 Gene targeting through homologous recombination.....	33
Figure 1.10 Plasma cholesterol levels in <i>Apoe</i> ^{-/-} mice	36
Figure 1.11 Plasma cholesterol levels in <i>Apoe</i> ^{-/-} and <i>Ldlr</i> ^{-/-} mice.	37
Figure 1.12 Distribution of atherosclerotic lesions in the major mouse arterial vasculature.....	38
Figure 1.13 Progression of mouse atherosclerotic lesions	42
Figure 2.1 Schematic representation of scratch assay.....	50
Figure 2.2 <i>Rpl4</i> standard curve and melt curve.....	71
Figure 2.3 Plasmid maps used for HHIPL1 and SHH cloning.	75
Figure 2.4 Schematic representation of the aortic root orientation and sectioning.....	80
Figure 2.5 Schematic representation of aortic root sectioning.....	81
Figure 3.1 HHIP protein family	95
Figure 3.2 <i>In silico</i> prediction of HHIPL1 localisation.....	97
Figure 3.3 Subcellular localisation of HHIPL1.	99
Figure 3.4 Detection of HHIPL1 in conditioned media.....	101
Figure 3.5 HHIPL1 interacts with SHH	103
Figure 3.6 <i>HHIPL1</i> expression in HASMC.....	104
Figure 3.7 HASMC siRNA transfection.....	106
Figure 3.8 Relative <i>HHIPL1</i> expression after siRNA treatment.....	107
Figure 3.9 HASMC proliferation following <i>HHIPL1</i> knockdown	109
Figure 3.10 Representative wound healing images in HASMCs.	111
Figure 3.11 HASMC migration following <i>HHIPL1</i> knockdown	112

Figure 4.1 <i>Hhip1</i> knock out first allele and possible allele variants.....	119
Figure 4.2 Genotyping of <i>Hhip1</i> transgenic mice.....	126
Figure 4.3 Validation of the knockout construct.....	128
Figure 4.4 <i>Hhip1</i> ^{-/-} mouse weights	129
Figure 4.5 <i>Hhip1</i> expression in mouse	130
Figure 4.6 Endogenous β -galactosidase in stomach frozen slides.....	132
Figure 4.7 <i>Hhip1</i> expression in heart vasculature.....	133
Figure 4.8 <i>Hhip1</i> expression in brain	134
Figure 4.9 Endogenous β -galactosidase expression in stomach.	136
Figure 5.1 Aortic sites included in the expression study.....	146
Figure 5.2 <i>Hhip1</i> expression pattern during atherosclerosis progression	148
Figure 5.3 Representative mouse genotypes	150
Figure 5.4 Atherosclerosis study design.....	151
Figure 5.5 Mouse weights during western-diet treatment.....	152
Figure 5.6 Blood pressure assessment.	153
Figure 5.7 Quantification of atherosclerotic lesions in <i>Hhip1</i> ; <i>Ldlr</i> ^{-/-}	155
Figure 5.8 Quantification of atherosclerotic lesions in <i>Hhip1</i> ; <i>Apoe</i> ^{-/-}	156
Figure 5.9 Compositional analysis of <i>Hhip1</i> ; <i>Ldlr</i> ^{-/-} atherosclerotic lesions	158
Figure 5.10 Compositional analysis of <i>Hhip1</i> ; <i>Apoe</i> ^{-/-} atherosclerotic lesions.	160
Figure 5.11 Cellular staining of <i>Hhip1</i> ; <i>Apoe</i> ^{-/-} atherosclerotic lesions.....	162

List of abbreviations

*Standard nomenclature is applied within the text (all capitals, italicised = human gene; all capitals, not italicised = human protein; initial capital, remaining lower case, italicised = mouse gene; initial capital, remaining lower case, not italicised = mouse protein).

ABC	ATP binding cassette
Ang*	Angiopoietin
ANOVA	Analysis of Variance
APCs	Antigen presenting cells
APOB*	Apolipoprotein B
APOE*	Apolipoprotein E
Apo B-100*	Apolipoprotein B-100
ApoB-LP*	ApoB- containing lipoproteins
α -SMA	Alpha- smooth muscle actin
B2m*	Beta-2 microglobulin
CAD	Coronary artery disease
cDNA	Complementary DNA
CETP*	Cholesteryl ester transfer protein
CNS	Central nervous system
DAPI	4',6-diamidino-2-phenylindole
DHH*	Desert hedgehog
DISP*	Dispatched
DMSO	Dimethyl sulfoxide
DTT	Dithiothreitol
ECM	Extracellular matrix
EGF	Epidermal growth factor
ENU	n-ethyl-n-nitrosourea
eQTL	Expression quantitative trait loci
ER	Endoplasmic reticulum

ES	Embryonic stem
ESS	Endothelial shear stress
EUCOMM	European Conditional Mouse Mutagenesis Program
FCS	Fetal Calf Serum
FDA	Food and Drug Administration
Fgf*	Fibroblast growth factor
Fgf10*	Fibroblast growth factor 10
FH	Familial hypercholesterolemia
FLP	Flippase recombinase
FPLC	Fast phase liquid chromatography
FRT	Flippase recognition sequences
GLI*	Glioma associated transcription factors
GWAS	Genome wide association study
HASMC	Human aortic smooth muscle cells
HDL*	High density lipoprotein
HEK293	Human embryonic kidney cells
Hh	Hedgehog
HHIPL1*	Hedgehog interacting protein like -1
HHIP*	Hedgehog interacting protein
HR	Homologous recombination
HUVEC	Human Umbilical Vein Endothelial Cells
IDL*	Intermediate density lipoproteins
IGTC	International Gene Trap Consortium
IHH*	Indian hedgehog
IKMC	International Knockout Mouse Consortium
IMPC	International mouse phenotyping consortium
IN	Input
IP	Immunoprecipitation
KO	Knockout
KOMP	Knockout Mouse Project
<i>lacZ</i>	β -galactosidase gene (<i>E. coli</i>)
LD	Linkage disequilibrium

LDL*	Low density lipoprotein
LDLR*	Low density lipoprotein receptor
<i>loxP</i>	Locus of crossover (x) in P1 bacteriophage
MAF	Minor allele frequency
MI	Myocardial infarction
Min	Minutes
MOMA-2	Intracellular antigen of macrophages and monocytes
MYH11	Smooth muscle cell myosin heavy chain
Neo	Neomycin
NorCOMM	North American Conditional Mouse Mutagenesis project
NTC	Non targeting control
ORO	Oil red O
pA	Poly adenylation site
PBS	Phosphate buffered saline
PCR	Polymerase chain reaction
PCSK9*	Proprotein convertase subtilisin/kexin type 9
PDGFB*	Platelet-derived growth factor B chain protein
Pdgf*	Platelet derived endothelial cell growth factor
PFA	Paraformaldehyde
PNAACL	Protein Nucleic Acid Chemistry Laboratory
PROTEX	Protein Expression laboratory
PSMB4	Proteasome subunit beta 4
PTCH*	Patched
qPCR	Quantitative PCR
Rpl4*	Ribosomal protein L4
RT-PCR	Reverse transcription PCR
sA	Splice acceptor site
SHH*	Sonic hedgehog
SKI*	Acyltransferase skinny hedgehog
SM22"/tagln	22-kDa SMC lineage-restricted protein
SMC	Smooth muscle cell
SMO*	Smoothened

SNP	Single nucleotide polymorphism
TCA	Trichloroacetic acid
TGF-beta*	Transforming growth factor-beta
TMH	Transmembrane helices
Vegf*	Vascular endothelial growth factor
VLDL*	Very low density lipoprotein
VPR	Volume Pressure Recording
VSMC	Vascular smooth muscle cell
36b4	Ribosomal protein, large, P0

1 Introduction

1.1 Coronary artery disease

Coronary artery disease (CAD) is the leading cause of death in the industrialised world. In the early 1990s epidemiological studies attributed 50% of deaths in USA, Europe and Japan to CAD (Ross 1993). The relative death rate has declined in recent years, however, the burden of disease is still high with 34% of deaths in before 75s in the USA caused by CAD (Go et al. 2013). CAD is a chronic inflammatory disease for which atherosclerosis is the underlying cause (Göran K Hansson 2005). A complex interaction of various cell types and pathways result in the development of plaques, which progressively narrow the lumen of the coronary artery and impair blood flow to the myocardium. Clinically this manifests as either ischemia or infarction depending on the composition of the plaque and the degree of stenosis (arterial narrowing) (Libby, Theroux 2005).

1.1.1 Pathophysiology of CAD

The healthy artery is comprised of three layers: the inner layer (tunica intima), the middle layer (tunica media) and the adventitia, which is the outer layer. The tunica intima comprises a monolayer of endothelial cells, which are in direct contact with the blood in the lumen. The tunica media predominantly consists of smooth muscle cells (SMCs), which are maintained in a complex extracellular complex. The principal components of adventitia are fibroblasts and mast cells (Majesky et al. 2011) (**Figure 1.1**).

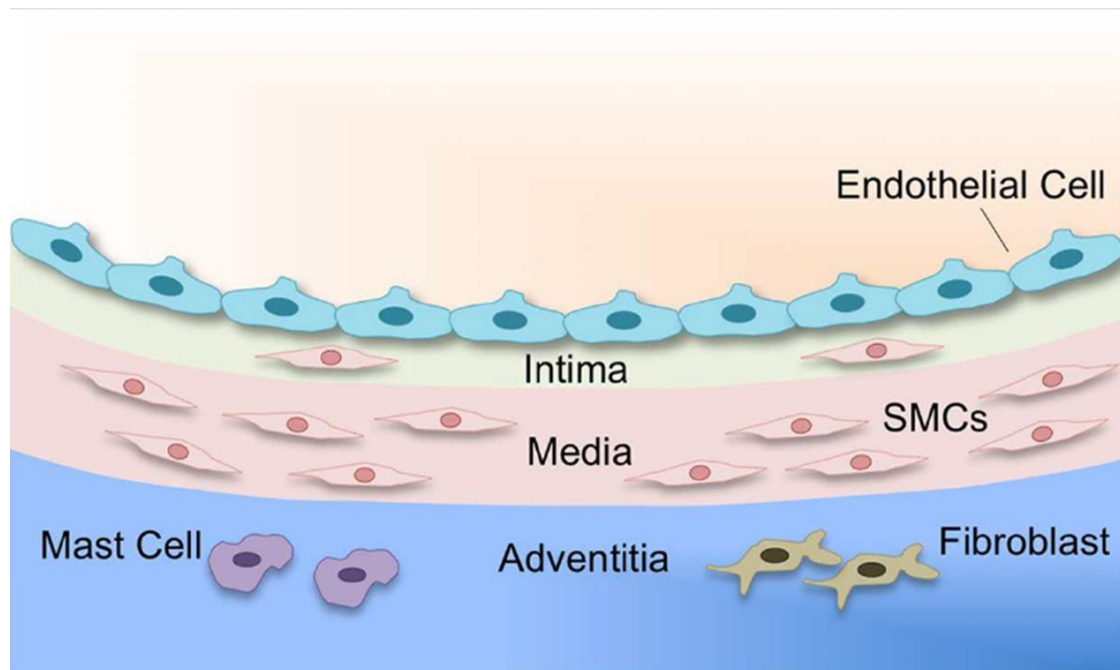


Figure 1.1 Composition of a healthy arterial wall

The endothelial monolayer of the intima is in direct contact with the artery lumen. The underlying media is mainly composed of SMCs and the outmost adventitia is a mixture of mast cells and fibroblasts (Taken from Blanco-Colio 2014) .

The formation of atherosclerotic lesions is a multistage process, involving the activation and interaction of many cells types that are either already present in the tunica intima or migrate into it during disease progression. The two major events during atherogenesis however are arterial inflammation and remodelling. The American Heart Association has classified human atherosclerotic lesions into six stages according to histological composition and structure (**Table 1.1**) (Stary et al. 1995).

Nomenclature and main histology	Sequences in progression	Main growth mechanism	Earliest onset	Clinical correlation
Type I (initial) lesion isolated macrophage foam cells	<pre> graph TD I((I)) --> II((II)) II --> III((III)) III --> IV((IV)) IV --> V((V)) V --> VI((VI)) IV --> II IV --> III V --> II V --> III V --> IV </pre>	growth mainly by lipid accumulation	from first decade	clinically silent
Type II (fatty streak) lesion mainly intracellular lipid accumulation			from third decade	
Type III (intermediate) lesion Type II changes & small extracellular lipid pools				
Type IV (atheroma) lesion Type II changes & core of extracellular lipid		accelerated smooth muscle and collagen increase	from fourth decade	clinically silent or overt
Type V (fibroatheroma) lesion lipid core & fibrotic layer, or multiple lipid cores & fibrotic layers, or mainly calcific, or mainly fibrotic				
Type VI (complicated) lesion surface defect, hematoma-hemorrhage, thrombus		thrombosis, hematoma		

Table 1.1 Classification of atherosclerotic lesions-Type I to VI

The flow diagram indicates the evolution and progression of atherosclerotic lesions, with the descriptions for each stage of the disease defined on the left. The clinical manifestations of each stage are shown on the right (Taken from Stary et al. 1995).

Stages I to III describe the clinically silent changes, which occur in the artery and gradually lead to lesion formation. The integrity of the endothelium is a critical factor in the process of atherosclerosis. Initiation of the process is characterised by endothelial injury and is caused by factors including elevated and modified low density lipoprotein (LDL), free radicals caused by cigarette smoking, hypertension, and diabetes mellitus (Ross 1999). The different causes of injury promote alterations in the normal endothelial homeostasis including increased permeability to plasma lipoproteins and other plasma constituents as well as recruitment of immune cells (Ross 1999). LDL infiltration (believed to result from excessive LDL accumulation in the plasma) and retention in the tunica intima is a major cause of endothelium and underlying smooth muscle injury. Oxidative and enzymatic modifications of LDL trigger the release of phospholipids, causing activation of endothelial cells (Leitinger 2003). It has been shown that specific segments of the artery experience distinct patterns of low blood flow (low shear stress) and contain endothelial cells that are more likely to become activated and promote the expression of adhesion molecules and inflammatory cytokines in comparison to other regions (Dai et al. 2004) (**Figure 1.2 A**). Platelets are the first blood cells to arrive at the sites of endothelial activation, coupling their glycoproteins to the surface molecules of the endothelium (Massberg et al. 2002). At this stage, monocytes also penetrate the endothelial surface and migrate into the intima forming a Type I lesion. This is due to the endothelial cells expressing leukocyte adhesion molecules, which bind the counter-receptors of the circulating monocytes and allow them to roll on the vascular surface and adhere at the activation site (Eriksson et al. 2001) (**Figure 1.2 B**). At this stage the integrity of the endothelium is compromised and the artery is subject to remodelling. Differentiation of monocytes into macrophages is promoted by an intima derived cytokine or growth factor (macrophage colony-stimulating factor) (Smith et al. 1995). Pattern recognition receptors (Toll-like and scavenger receptors) on the surface of the macrophages are up regulated possibly via the macrophage colony-stimulating factor. The scavenger receptors recognise and internalise a wide range of molecules including oxidised LDL particles (Peiser, Mukhopadhyay & Gordon 2002, Janeway, Medzhitov 2002) . The uptake of LDL into the macrophage is a critical step in the development of the plaque; if the

LDL cannot be excreted from the macrophage to a sufficient extent then it will accumulate in the cytosolic area leading to the formation of foam cells (Göran K Hansson 2005, Stary et al. 1994). These are key cells within the initiating stages of an atherosclerotic plaque and localised accumulation of these cells is termed a fatty streak (Type II lesion). The toll-like receptors initiate a signalling cascade that results in macrophage activation and propagation of the inflammatory pathway (Janeway, Medzhitov 2002) (**Figure 1.2 B**). Activated macrophages produce inflammatory cytokines, chemokines, proteases and reactive oxygen and nitrogen species, which cause further injury of the arterial tissue (Göran K Hansson 2005). Although the majority of foam cells in atherosclerotic lesions are traditionally thought to have been derived from macrophages more recent co-localisation studies *in vitro* and *in vivo* suggest that SMCs can also internalise LDL and become lipid loaded (Bennett, Sinha & Owens 2016) . Studies in humans, rabbits and rats have demonstrated that SMCs express a variety of cholesterol uptake receptors, including the LDL receptor (LDLR), very low density lipoprotein (VLDL) receptor, CD36, type I and type II scavenger receptors (Doran, Meller & Mcnamara 2008)

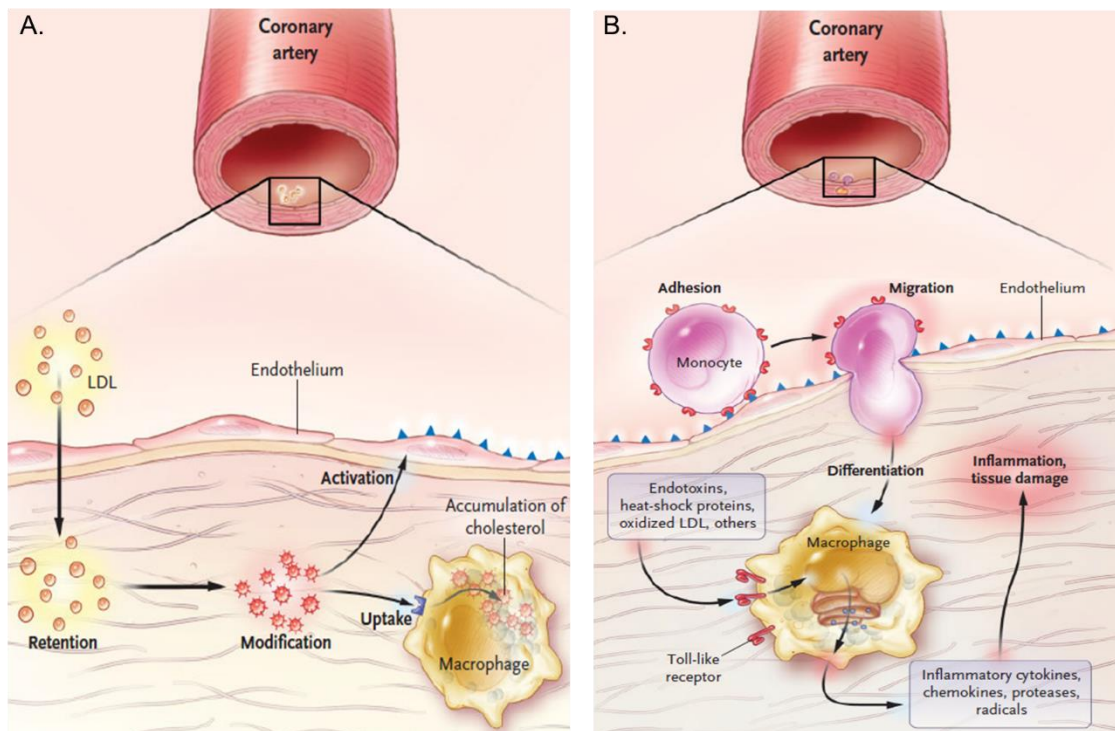


Figure 1.2 Effect of LDL infiltration on the inflammatory process and the role of macrophages

A) LDL infiltrates the artery and is retained in the intima. Oxidative and enzymatic modifications lead to the release of inflammatory lipids that activate the endothelial cells to express leukocyte adhesion molecules. B) Monocytes recruited through the activated endothelium differentiate into macrophages. The oxidised LDL particles are taken up by the scavenger receptors of macrophages, which evolve into foam cells. Several endogenous and microbial molecules also bind to pattern-recognition receptors (toll-like receptors) on the macrophages, activating them and which lead to the release of inflammatory cytokines thereby causing the recruitment of further monocytes to the area and propagation of the inflammatory pathway. This ultimately causes tissue damage
 Reproduced with permission from (Göran K Hansson 2005), Copyright Massachusetts Medical Society.

In addition to monocytes other immune cells including T cells, antigen-presenting cells (APCs), dendritic and mast cells are present in atherosclerotic plaques. T cells adhere to the endothelial surface via adhesion receptors and migrate into the intima in a similar manner to monocytes. These cells are activated by APCs and differentiate into Th1 cells that express cytokines (e.g. IFN- γ , TNF- β) and maintain the vascular inflammatory response (Göran K Hansson 2005, Libby, Ridker & Hansson 2011). Progression beyond the fatty streak stage is associated with a sequence of changes starting with the appearance of multiple scattered pools of extracellular lipids in the intimal layer due to the breakdown of the lipid-laden foam cells (Type III lesion). These lipids gradually accumulate to a large confluent mass mainly consisting of free cholesterol with its esters forming the lipid core characteristic of Type IV lesions. Further progression involves the proliferation of both migrated and resident SMCs from the tunica media into a well-defined region of the intima. Platelet-derived growth factor B chain protein (PDGFB) found within macrophages (in all stages of lesion development) and T cell secreted cytokines as well as growth factors act as chemotactic and stimulatory factors to the SMCs (Libby, Ridker & Maseri 2002). SMCs in turn synthesize extracellular matrix (ECM) containing mostly proteoglycans with scattered type I collagen fibrils and fibronectin (Doran, Meller & Mcnamara 2008, MacLeod et al. 1994). Free and esterified cholesterol becomes incorporated within this matrix. Proliferating SMCs form a layer over the luminal side of the lipid core resulting in a fibroatheroma (or fibrous cap) (Type V lesion). The plaque increases in size as additional collagen is produced and the lipid rich core becomes necrotic. The necrotic core is characterised by increased cell apoptosis, consisting of cellular debris including dead macrophages and SMCs together with an excess of free cholesterol crystals (**Figure 1.3 A**) (Libby, Theroux 2005, Zaman et al. 2000). As the lesion progresses, calcification may then occur through mechanisms similar to those in bone formation (Demer 2002).

What causes a silent atherosclerotic lesion to rupture (Type VI lesion) is predominantly due to its composition. It has been shown that the size of the atheromatous core plays a role in lesion stability and vulnerability of the plaque increases in proportion to the size of its atheromatous core (Davies et al. 1993).

Studies using post mortem aortic samples have also showed that the majority of coronary thrombi, indicative of plaque rupture, were anchored over a soft atheromatous core (Richardson, Davies & Born 1989). The softness of the core is due to a high proportion of free cholesterol and its esters, which are less viscous at body temperatures thus making the plaques softer and more prone to rupture (Small 1988). The structure and the strength of the fibrous cap can also affect plaque stability (Zaman et al. 2000). Fibrous caps can vary in thickness, cellularity, strength and stiffness and it has been shown that ruptured plaques have reduced tolerance to mechanical stress due to lower levels of collagen, glycoaminoglycans and SMCs (Falk 1992). The monocyte-macrophage dependent inflammatory process can also have an effect on plaque stability because activated macrophages, T cells, and mast cells produce several types of molecules such as inflammatory cytokines, proteases, coagulation factors, radicals, and vasoactive molecules that attack and digest the extracellular matrix of the fibrous cap and thus destabilize lesions (Göran K Hansson 2005). Finally, the location of the plaque can increase the chances of rupture; the long term repetitive cyclic mechanical forces occurring in a normal cardiac cycle can weaken and fatigue a plaque cap leading to rupture (Zaman et al. 2000). Disruption of the fibrous cap exposes the necrotic core, which is the most thrombogenic component of an atherosclerotic plaque to circulating blood. Interaction between tissue factor and the collagen fibrils contained in the necrotic core and the circulating blood leads to a platelet-rich thrombus formation (**Figure 1.3 B**) (Libby, Theroux 2005). The resultant thrombus may be sufficiently large to totally occlude the vessel lumen causing an infarct in the case of the coronary artery or the plaque fissure will reseal, lyse the thrombus and incorporate it into the plaque resulting in a complex lesion (Zaman et al. 2000). Individual plaques, however, vary greatly in composition and consistency and the risk of any individual with coronary atherosclerosis developing an acute ischemic event depends on the number of vulnerable plaques present (Zaman et al. 2000).

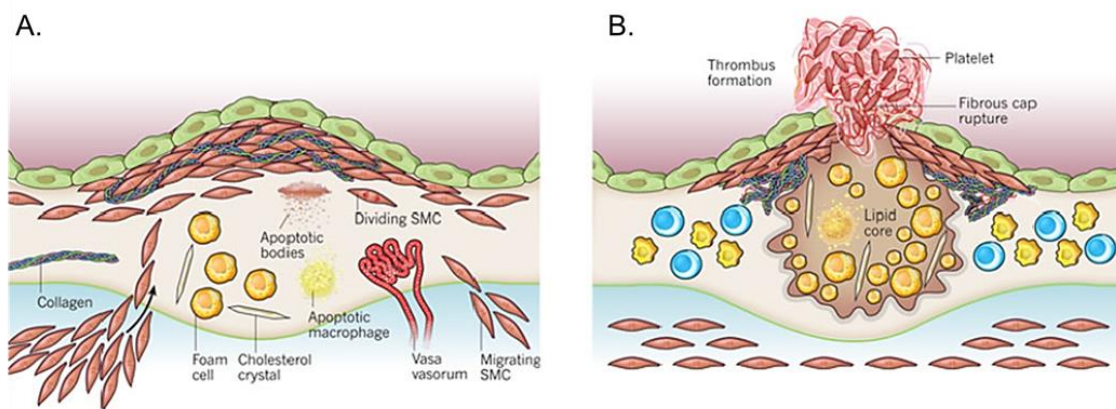


Figure 1.3 Fibrous cap formation and rupture

A) SMCs proliferate and migrate from the media to the intima and secrete ECM components creating a fibrous cap over the luminal side of the lipid core. The lipid core becomes avascular and almost acellular consisting of apoptotic macrophages and SMCs together with free and esterified cholesterol. B) Fibrous cap rupture exposes the thrombogenic material of the atheromatous plaque to the circulating blood, leading to platelet-rich thrombus formation (Taken from Libby, Ridker & Hansson 2011) .

1.1.2 Risk factors of CAD

Research into the risk factors contributing to development of CAD commenced in 1948, when the Framingham Heart Study was launched in Framingham, Massachusetts (Dawber, Meadors & Moore 1951) . This was a longitudinal study following subjects over 50 years. In 1971 the study enrolled a second generation, called the Framingham Offspring Study (Dawber, Moore & Mann 1957) with further generations enrolled over the years. The first CAD associated risk factors reported in this study included high blood pressure, high blood cholesterol, smoking, obesity, diabetes, family history and physical inactivity as well as a great deal of valuable information on the effects of related factors such as age, gender, and psychosocial issues (Marmot et al. 1991). The identification of these risk factors led to the introduction of the 10-year CAD Framingham Risk Score calculator (Wilson et al. 1998). Since then other association studies have been conducted such as the Northwick Park Heart Study confirming the same traditional CAD risk factors (Hawe et al. 2003). Whilst risk factors that are due to environmental effects (i.e. high blood

pressure, high blood cholesterol and smoking) can clearly be modified, risk factors that are genetically determined (or a combination of the two) cannot be altered. Ultimately progression of CAD is affected by an interplay between both environmental and genetic factors, with the latter exerting their effects either directly or by having a secondary affect upon another known CAD risk factors (**Figure 1.4**).

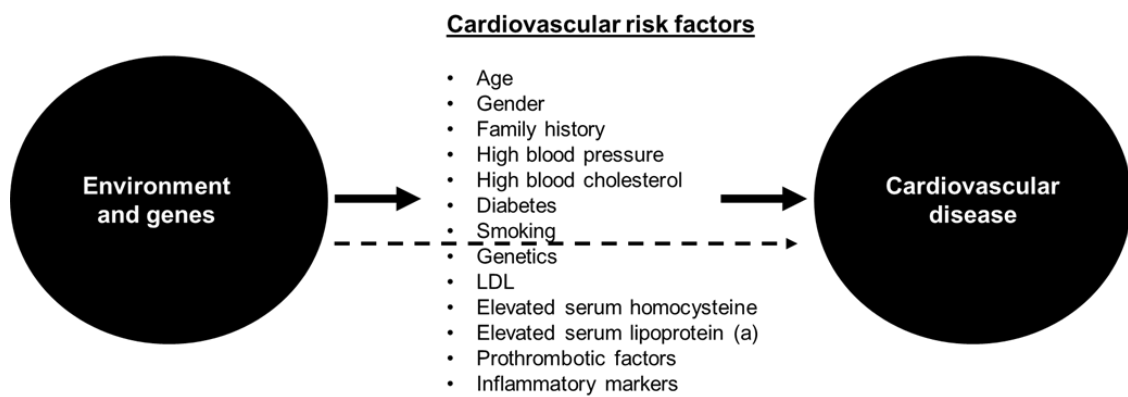


Figure 1.4 Risk factors of CAD

Environmental factors and genetics can trigger CAD either directly or through known intermediate risk factors (Adapted from Sayols-Baixeras et al. 2014) .

1.2 Genetics of CAD

1.2.1 Heritability of CAD

The dissection of the genetic contribution to CAD has proven to be quite challenging. Although traditional risk factors seem to be better predictors of CAD than genetic markers, twin studies and familial clustering have shown that CAD has a strong genetic component, with heritability estimates ranging from 30 to 60% (Marenberg et al. 1994, Lusia, Mar & Pajukanta 2004, Lusia 2000) . The heritability estimate is not fixed; differences among groups in amount of genetic variation and/or environmental influences will lead to different estimates of heritability. The principal study design for estimating heritability relies on the comparison of monozygotic and dizygotic twins. Since monozygotic twins share 100% and dizygotic twins 50% of their genes, it is to be expected that if a genetic component for the CAD phenotype exists, it would be more likely seen in monozygotic rather than dizygotic twins. Indeed, Zdravkovic *et al* compared both monozygotic and dizygotic twins in a large (36-year follow-up) Swedish twin study, providing a 38% to 57% estimate of heritability for CAD (Zdravkovic et al. 2002). In the Framingham study (Schildkraut et al. 1989) a family history of CAD, cerebral vascular incidents or peripheral arterial disease was associated with a 2.4-fold increased risk of CAD in men and a 2.2-fold increased risk in women. In the Interheart study (Yusuf et al. 2004), having a family history of CAD resulted in a 1.45-fold increased risk when corrected for other risk factors. Moreover, the Prospective Cardiovascular Münster (PROCAM) study (Cooper, Miller & Humphries 2005) , reported that a family history of myocardial infarction (MI) was an independent risk factor for CAD. All these estimates led to the conclusion that family history is a major risk factor for CAD. A summary of the heritability estimates among studies is show in **Table 1.2.**

Phenotype	Heritability	References
CAD		
Acute myocardial infarction	0.56	Nora et al 1980
Mortality from CAD	0.53-0.57 (men)	Zdravkovic et al 2002
	0.58 (women)	Wienke et al 2001
Coronary artery calcification	0.42	Peyster et al 2002
Atherosclerosis		
Carotid artery atherosclerosis	0.21-0.64	Xiang et al 2002, Fox et al 2003, Swan et al 2003, North et al 2002, Hunt et al 2002

Table 1.2 Heritability of atherosclerosis related phenotypes (Taken from Sayols-Baixeras et al. 2014) .

1.2.2 Monogenic forms of CAD

The genetic contribution to CAD is predominantly polygenic, however, there are several Mendelian causes of disease, which have contributed to our understanding of CAD pathophysiology. Linkage studies of rare monogenic disorders are able to identify the disease associated gene by focusing on the co-segregation of genetic markers (DNA markers of known chromosomal location) and the disease phenotype that occur in a Mendelian mode of inheritance within a family. Once the locus is mapped, fine mapping can be performed to narrow down the region, enabling one to clone and sequence the gene to identify the responsible mutation. The mutations found in those genes are rare variants characterised by high penetrance (the mutation is both adequate and sufficient to induce the disease) and low allele frequency (<1%). Although CAD is a multifactorial disease there have been cases where single gene mutations have been identified and are sufficient to induce the phenotype of CAD under an autosomal dominant or autosomal recessive mode of inheritance. Familial Hypercholesterolemia (FH) is the most common among the disorders that cause elevated levels of LDL-cholesterol. It is inherited in an autosomal dominant mode and is associated with CAD. Classical linkage analysis in FH patients identified causal mutations in 3 genes *LDLR*, *PCSK9* and *APOB* (Soutar, Naoumova 2007). Other autosomal recessive monogenic disorders associated with CAD are Tangier and sitosterolaemia disease, both conditions of which involve mutations within ATP binding cassette (ABC) transporter genes. Tangier disease is associated with a mutation in the *ABC1* gene and is characterised by a marked reduction in plasma HDL, deposition of sterol in macrophages, and early atherosclerosis (Bodzioch et al. 1999). Mutations in the *ABCG5* and *ABCG8* genes cause sitosterolaemia, which is another disorder characterised by abnormal intestinal absorption (hyper absorption) of both cholesterol and plant-derived cholesterol-like molecules, such as sitosterol (Lee et al. 2001).

1.2.3 Polygenic forms of CAD

The vast majority of the genetic variants (SNPs, single nucleotide polymorphisms) that influence predisposition to polygenic CAD generally have low effect sizes and high allele frequency (>5%). In contrast to single gene mutations which are sufficient to cause the disease, SNP effects are low with each SNP contributing only 5% to 10% of the susceptibility to the CAD phenotype (**Figure 1.5**). Individually the SNPs do not cause disease, instead an additive combination of multiple SNPs and environmental factors result in the development of CAD.

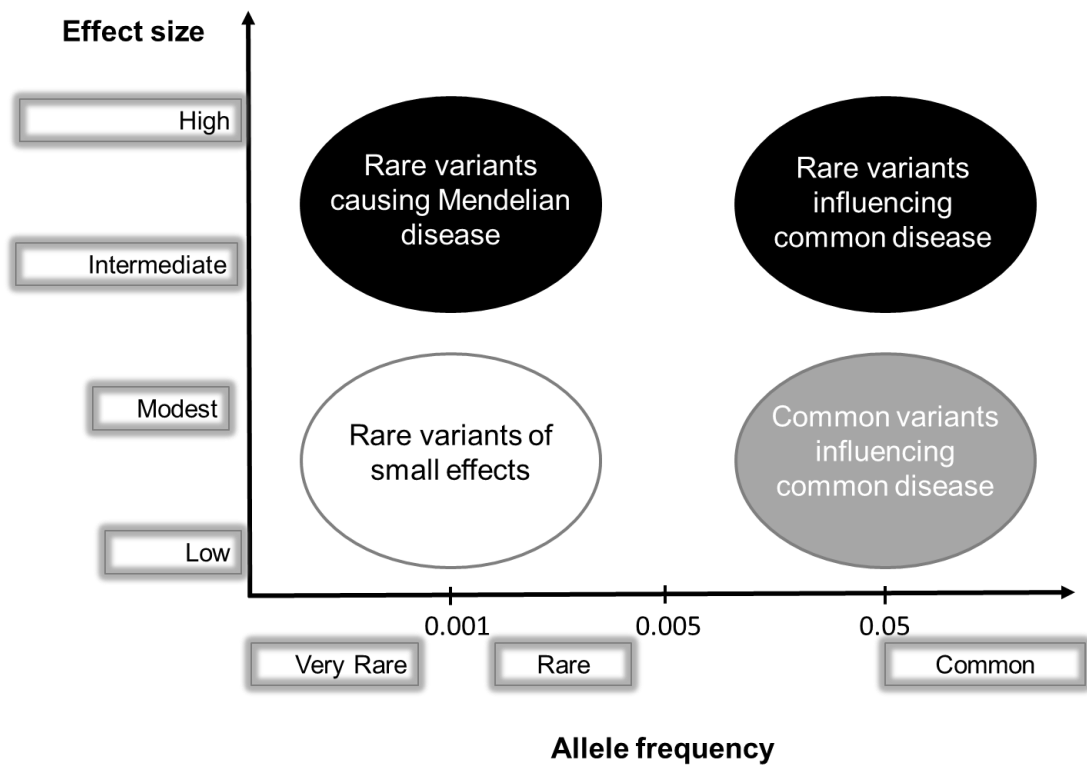


Figure 1.5 Low and high frequency variants and disease susceptibility

Rare variants responsible for Mendelian diseases are characterised by high penetrance and low allele frequencies and are identified mainly by linkage studies. Common variants with high allele frequencies but low effect size are contributing to susceptibility of common diseases and are mainly identified by GWAS. Only a few examples exist for rare variants with high effect sizes

influencing common diseases. Rare variants of low effect size are very hard to be identified by genetic means (Adapted from McCarthy et al. 2008) .

1.2.4 Linkage studies for polygenic CAD forms

Linkage studies have been mainly used for the identification of rare gene mutations in Mendelian disorders. Non-parametric methods of linkage analysis have however been utilised in order to map susceptibility factors of complex disorders. Rather than requiring parameters such as mode of inheritance, gene frequencies and penetrance, non-parametric linkage compares affected relatives, looking for chromosomal regions that are shared more often than would be expected to have occurred by chance (Strachan, Andrew 2011). Early non-parametric linkage studies determined genetic factors by genome wide scanning of microsatellites (short tandem repeat sequences). This required the recruitment of hundreds of families, particularly sibling pairs with MI or CAD. The aim was to identify co-segregation patterns between a chromosomal marker and the disease by looking at around 400 microsatellite markers distributed evenly in the genome and subsequent fine mapping in order to identify the causal genes. Mapping was conducted with the assumption that a nearby gene is in Linkage disequilibrium (LD) with the chromosomal marker. 'LD is the non-random association of alleles at two or more loci on a chromosome and results in the greater co-occurrence of two genetic markers on the same chromosome in a population than would be expected for independent markers' (Padmanabhan et al. 2010). A number of studies were undertaken recruiting families from different countries. Although chromosomal regions were identified by this method the studies all reported varying results with no overlapping genomic regions; Finland (2q21.2-22 and Xq23-26), Germany (14q32.2), Iceland (13q12-13), US (1p34-36,3q13 and 5q31) and UK (2p11, 17p11-17q21) (Pajukanta et al. 2000, Broeckel et al. 2002, Helgadottir et al. 2004, Hauser et al. 2004, Farrall et al. 2006, Samani et al. 2005). Two genes were however identified from these original linkage studies and subsequent fine mapping; *ALOX5AP* and *MEF2A* from the US and Icelandic studies.

1.2.5 CAD Candidate gene studies

Candidate gene studies have been at the forefront of genetic association studies identifying risk variants linked to complex polygenic CAD forms. These studies, which may include members of an affected family or unrelated cases and controls, can be performed relatively quickly and may allow the identification of disease associated genetic variants with small size effects. The candidate gene approach requires the selection of genes that have previously been linked to disease and thus come with prior knowledge about gene function. Following selection of the variants within the candidate gene the SNPs are genotyped in affected (cases) and non-affected individuals (controls). Subsequent identification of the disease associated SNPs is achieved by comparing occurrences in cases versus controls. Several studies have been undertaken since 1990 to identify genetic susceptibility to CAD through the candidate gene approach. One of the most recent examples identified disease associated variants by examining 103 genes in a joint family-based and case control study. This study confirmed disease associations for genes previously linked to High density lipoprotein (HDL), LDL, triglycerides, Apolipoprotein B (APOB) and adiponectin traits as well as identifying two new gene associations linked to HDL cholesterol (Paré et al. 2007). The main findings of candidate gene studies as reviewed by Franchini *et al* are shown in **Table 1.3** (Franchini, Peyvandi & Mannucci 2008) . The candidate gene approach has revealed some loci with significant and convincing effects on atherosclerosis such as *Apolipoprotein E (APOE)*, *LDLR* and *Proprotein convertase subtilisin/kexin type 9 (PCSK9)* (Humphries, Morgan 2004, Cohen et al. 2006, Song, Stampfer & Liu 2004) .

First author, year	Study design	No. of cases/controls	Clinical event	Gene polymorphisms associated with CAD	OR (95% CI)
Yamanda, 2002	Case-control	2819/2242	MI	Connexin 37 C1019T, PAI-1 4G-668/5G, Stromelysin-1 5A- 1171/6A	1.4 (1.1-1.6) 1.6 (1.2-2.1) 4.7 (2.0-12.2)
McCarthy, 2004	Case-control	325/418	MI	THBS2 THBS4 PAI-2	0.38 (0.14-1.01) 2.22 (0.93-5.28) 2.35 (0.90-6.12)
Song, 2004	Meta-analysis	15,492/32,965 (48 studies)	CAD	Apolipoprotein E ϵ_4	1.42 (1.26-1.61)
Ye, 2006	Meta-analysis	66,155/91,307 (191 studies)	CAD	Factor V G1691A Prothrombin G20210A PAI-1 4G-668/5G	1.17 (1.08-1.28) 1.31 (1.12-1.52) 1.06 (1.02-1.10)
Zwicker, 2006	Case-control	1425/1425	MI	THBS1 N700S	1.4(1.1-1.8) (heterozygotes) 1.9 (1.9-3.3) (homozygotes)

Table 1.3 Main findings of CAD candidate genes studies (Taken from Franchini, Peyvandi & Mannucci 2008).

The major drawback, however, of candidate genes studies is that they have only yielded a limited number of genes with weak associations that could not be replicated between studies. This was attributed to various reasons such as genotyping errors, lack of statistical power due to low sample size, population stratification occurring when studying unrelated individuals and heterogeneity of the coronary artery disease phenotype in the subjects studied. The most limiting factor of this type of study is, however, that candidate gene studies are hypothesis driven and are based on the assumption that the genes chosen are mechanistically relevant. By design, these studies do not identify novel genes and pathways that associate with disease.

The majority of the issues related to identifying the genetic cause of CAD was resolved with the advent of large-scale genome-wide association studies. These studies led to a break-through in the identification of genetic loci that contribute to CAD and other complex diseases.

1.2.6 Genome wide association studies (GWAS)

GWAS are hypothesis-free association studies that recruit unrelated but ethnically similar subjects and compare the DNA variation frequency of the two groups. The principal of this method relies on massive scanning of the entire genome (millions of genetic variants are read using SNP array) looking for associations between common DNA sequence variations and the phenotype of interest. This was only feasible after the publication of the Human Genome Project (Sachidanandam et al. 2001, Lander et al. 2001) and the HapMap project, which comprises the human genome variation and the haplotype structure across different populations (International HapMap Consortium 2003 2003). These studies along with high-throughput genotyping technology became the catalyst for GWAS. In 2007 the Wellcome Trust Case Control Consortium conducted a GWAS, which examined 2,000 individuals for each of 7 major diseases (type1 and type 2 diabetes, hypertension, Crohn's disease, rheumatoid arthritis, bipolar disorder and CAD) and a shared set of 3,000 controls. This approach successfully identified 24 independent associations for bipolar disorder, 1 for CAD, 9 for Crohn's disease, 3 for rheumatoid arthritis, 7 for type 1 diabetes and 3 for type 2 diabetes (Burton et al. 2007). GWAS have been informative in identifying loci implicated in predisposition of common diseases like the ones mentioned above as well as others such as prostate and breast cancer.

1.2.6.1 CAD GWAS

The first CAD GWAS were published in 2007 and identified an association between chromosome 9p21.3 and increased risk of disease (Samani et al. 2007, McPherson et al. 2007, Helgadottir et al. 2007). Many subsequent GWAS with increasing numbers of cases and controls have been undertaken and identified multiple genetic loci associated with MI and CAD (Clarke et al. 2009, Erdmann et al. 2009, Ripatti et al. 2010, IBC 50K CAD Consortium 2011). The CARDIoGRAM consortium performed a meta-analysis, which identified 13 new loci associated CAD in addition to confirming 10 of the 12 previously published loci (Schunkert et al. 2011) and a second meta-analysis by the C4D consortium identified a further five loci (Peden et al. 2011). In 2013, CARDIoGRAMplusC4D Consortium performed a further meta-analysis bringing the total of CAD associated loci to 46 (Deloukas et al. 2013). The largest and most complete collection of variants associated with CAD was recently reported by Nikpay *et al* (2015), which performed a meta-analysis of 185 thousand CAD cases and controls, interrogating 6.7 million common (Minor allele frequency (MAF) >0.05) as well as 2.7 million low frequency ($0.005 < \text{MAF} < 0.05$) variants. This analysis confirmed most of the known CAD loci and identified 10 additional loci, bringing the total number to 56 (Nikpay et al. 2015) (**Figure 1.6**). An important finding from these studies is that only around one third of the loci associate with traditional cardiovascular risk factors such as cholesterol levels and blood pressure and most of the loci do not contain genes with known roles in cardiovascular disease. By identifying the affected gene and understanding the causal mechanisms novel pathways that contribute to disease pathology will be identified and offer the potential for new treatments for disease.

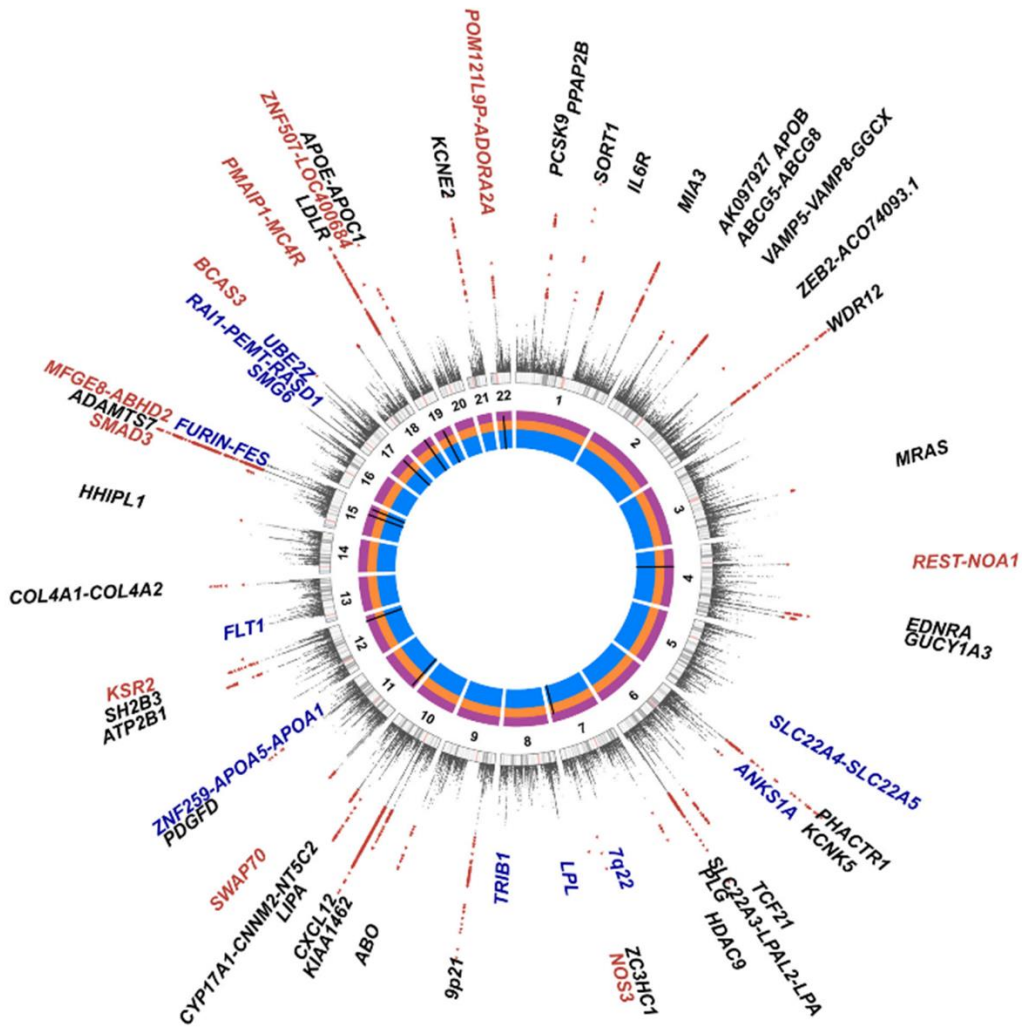


Figure 1.6 Circular Manhattan plot summarising the CAD associated loci
 Representative circular Manhattan plot summarising the findings from the 1000 Genomes CAD association study. The meta-analysis replicated the already known loci, which are depicted in black and have identified 10 novel, depicted in red. Those in blue are the loci with nominal significance ($P < 0.05$) from the same meta-analysis. Genome-wide significant variants ($P < 5 \times 10^{-8}$) are indicated by red triangles (Taken from Nikpay et al 2015).

1.2.6.2 Functional analysis of GWAS loci

Following the identification of genome-wide significant loci the next challenge is to link the disease associated variants to specific genes and the cellular processes that are affected. The process of moving from a disease associated genetic variant to a biological mechanism requires several steps. First, the causal variant needs to be identified and its effects on gene function characterised. The disease associated SNP and its proxy variants that are in high LD need to be investigated for potential functional effects such as protein-coding changes or disruption of regulatory elements and association with gene expression (eQTLs, expression quantitative trait loci). Second, the candidate causal gene needs to be characterised in order to understand its role at the molecular and cellular level. This will most often be based on prior knowledge related to gene function and experimentation using cell models. Third, the gene needs to be investigated in whole organisms to confirm a role in disease pathogenesis.

There are well-defined mouse atherosclerosis models, which allow the investigation of CAD associated genes *in vivo*. These mouse models were developed more than two decades ago and have been used to examine the effects of gene knockout or overexpression of hundreds of candidate genes in atherosclerosis (Pasterkamp et al. 2016). The two major mouse atherosclerotic backgrounds are *ApoE* and *Ldlr* knockouts (Zhang et al. 1992, Ishibashi et al. 1994b). These genes together with several others that affect atherosclerosis in mice such as *ABO* (Voyiaziakis et al. 1998) and *LPL* (Wilson et al. 2001) have been found to associate with CAD in GWAS.

1.2.6.3 14q32.2 CAD associated locus

One of the CAD associated loci identified through GWAS is the 14q32.2 risk locus. The CARDIoGRAM Consortium identified the common variant rs2895811 (allele frequency 0.43) on chromosome 14 as associated with CAD in 2011 (Schunkert et al. 2011). The effect size is 7% per risk allele and the locus does not associate with traditional CAD risk factors.

The variant and all of the SNPs in high LD fall in *Hedgehog interacting protein like 1 (HHIPL1)* (**Figure 1.7**). *HHIPL1* encodes a protein of unknown function but is predicted to be involved Hedgehog signalling because of sequence homology with the Hedgehog interacting protein (HHIP) (Katoh, Katoh 2006). The only previous study of *HHIPL1* was a bioinformatic analysis of the HHIP family of proteins. It should be noted that in the study by Katoh and Katoh the HHIP proteins have slightly different names to their current nomenclature; HHIP was referred to as HHIP1, *HHIPL1* was named HHIPL2 and HHIPL2 was called HHIPL3 (Katoh, Katoh 2006).

There are no eQTLs linking *HHIPL1* expression, however, the lead SNP has been reported to have associate with expression of *YY1*, which is located ~500kb away from the CAD locus (Benjamin et al. 2012, Brænne et al. 2015), It should be noted that this was a borderline association ($P=0.002$) and was not taken forward for replication in the original study. A SNP in high LD with the CAD lead variant does cause a non-synonymous change in *HHIPL1* (Schunkert et al. 2011), however, it isn't known if this is the causal variant.

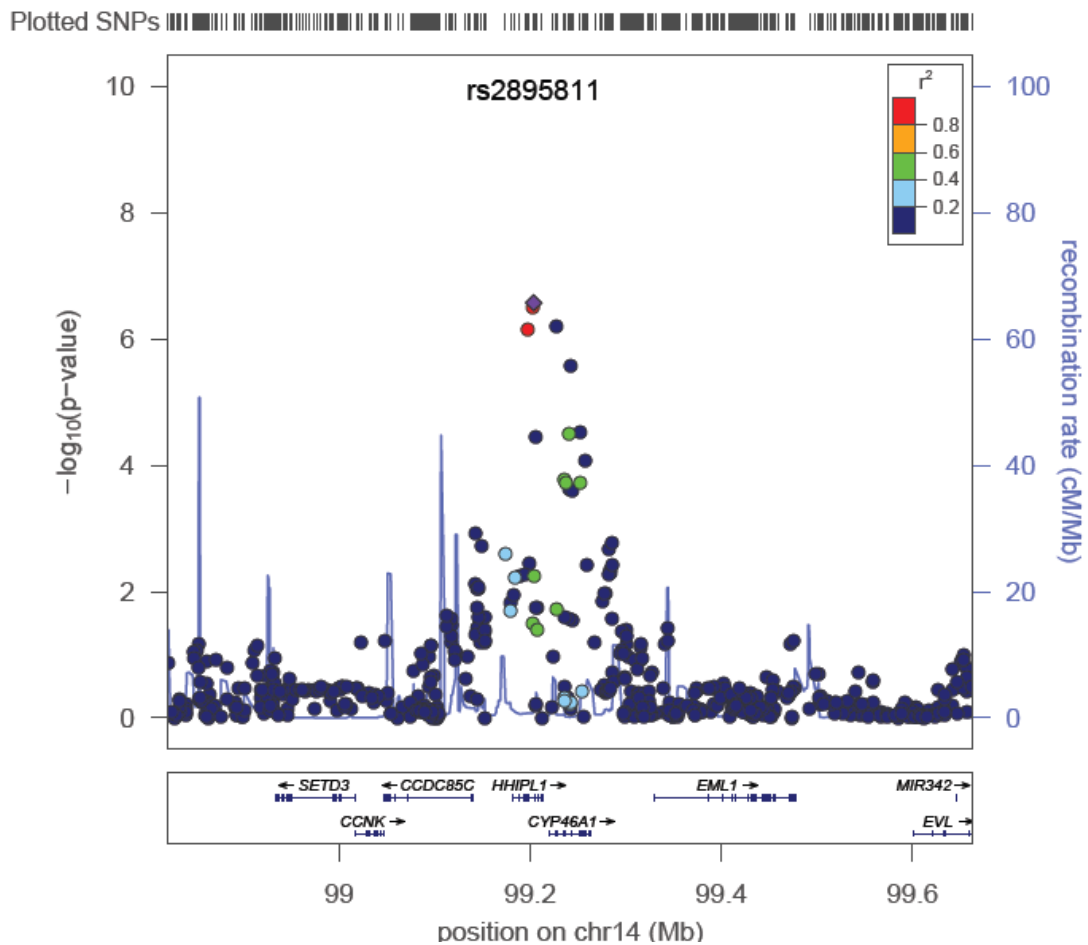


Figure 1.7 Regional association plot for the 14q32.2 CAD locus

The y-axis shows $-\log_{10} P$ values calculated from a logistic regression model, the x-axis plots SNPs by chromosomal position. The disease associated SNP (rs2895811) shown in purple triangle ($P= 1.14 \cdot 10^{-10}$) and all the SNPs in high LD with it fall in the novel *HHPL1* gene. SNPs are colour coded according to their linkage with the lead SNP. Nearby genes on chromosome 14 are *CYP46A1*, *CCDC85C*, *EML1*, *CNK*, *SETD3*, *EVL*, *MIR342*. (Taken from Schunkert et al. 2011) .

1.3 Hedgehog signalling

The Hedgehog pathway (Hh) was originally identified by Nüsslein-Volhard & Wieschaus in 1980, when they performed a mutagenesis screen in *Drosophila melanogaster* and isolated and characterised mutant larvae with defective cuticle formation. One of the mutations was named hedgehog (Hh) because it caused the denticles to be disorganised giving the larvae the appearance of a hedgehog (Christiane Nüsslein-Volhard, Wieschaus 1980). Further investigation revealed that Hh encoded a secreted protein that regulates embryonic patterning in adjacent cells. Hh homologues have subsequently been identified in vertebrates and found to have a similar developmental regulatory role. Vertebrate orthologues were identified in *Mus musculus* (mouse), *Danio rerio* (zebrafish), and *Gallus gallus* (chicken) in 1993 (Echelard et al. 1993, Krauss, Concordet & Ingham 1993, Riddle et al. 1993, Chang et al. 1994) human homologues were described shortly afterwards (Roelink et al. 1995, Marigo et al. 1995). Three Hh genes exist in vertebrates named Sonic hedgehog (*SHH*), Indian hedgehog (*IHH*) and Desert Hedgehog (*DHH*). These genes encode for secreted signalling proteins that act in a concentration gradient dependent manner. Hh proteins undergo post-translational modifications and auto-cleavage, which regulate Hh activity and dispersal from secreting cells to target tissues. In brief these modifications include auto-catalytic cleavage of the C-terminus (Lee et al. 1994), followed by covalent attachment of cholesterol to the amino-terminal peptide and further palmitoylation by the acyltransferase skinny hedgehog (SKI) at the N-terminus (Porter, Young & Beachy 1996b, Pepinsky et al. 1998, Chamoun et al. 2001). Once Hh is dually lipid-modified it is associated with the cell membrane as a monomer until it is released by the surface receptor Dispatched (DISP) (Burke et al. 1999, Tukachinsky et al. 2012, Creanga et al. 2012) (**Figure 1.8 A 1**). Alternatively, cholesterol modified Hh proteins can form soluble multimers that are released from the cell membrane (Chen et al. 2004, Ramsbottom, Pownall 2016) (**Figure 1.8 A 2**). Another route of secretion for Hh proteins is through packing in membranous exovesicles (Parchure et al. 2016). Signal transduction is initiated at the recipient cell surface after binding of the Hh ligand to its receptor Patched (PTCH) (Marigo et al. 1996a). Upon binding of Hh to PTCH, its inhibitory effect on Smoothed (SMO) is attenuated and SMO becomes constitutively active (Marcel Van,

Ingham 1996). Activation of SMO triggers a complex process regulating the activation or repression of Glioma associated transcription factors (GLI) transcription factors. Vertebrates have three GLI transcription factors (GLI1, GLI2, GLI3), which are modulated by phosphorylation, proteolysis and cleavage. GLI1 and GLI2 are thought to function as activators, but GLI2 may also be cleaved to a repressor form, whilst GLI3 is thought to harbour repressor action only (Peter J King, Leonardo Guasti & Ed Laufer 2008, Ruiz 1999) (**Figure 1.8 B&C**). In the absence of Hh, PTCH represses the co-receptor SMO resulting in suppression of gene transcription by the inhibitory GLI proteins (Bijlsma et al. 2006, Corcoran, Scott 2006).

In the late 1990s, Chuang and colleagues conducted a biochemical screen in order to identify novel modulators of Hh signal transduction. They created alkaline phosphatase tagged fusion proteins for Shh, Ihh and Dhh and used these to screen a cDNA expression library (isolated from mouse limb bud). They identified a cDNA clone that promoted cell-surface binding of all three Hh fusion proteins. The isolated cDNA encoded HHIP, a membrane associated protein that binds each of the Hh proteins with the same affinity as Ptch1 and acts as an antagonist of Hh signalling (**Figure 1.8 C**) (Chuang, McMahon 1999). More recently, HHIP was found to also function as a secreted protein and exert its effect on Hh signalling in a non-cell-autonomous manner (Kwong, Bijlsma & Roelink 2014). Crystal structures of HHIP in complex with SHH and DHH have also been solved and the Hh binding requirements of HHIP have been determined through biophysical and mutagenesis studies (Bishop et al. 2009).

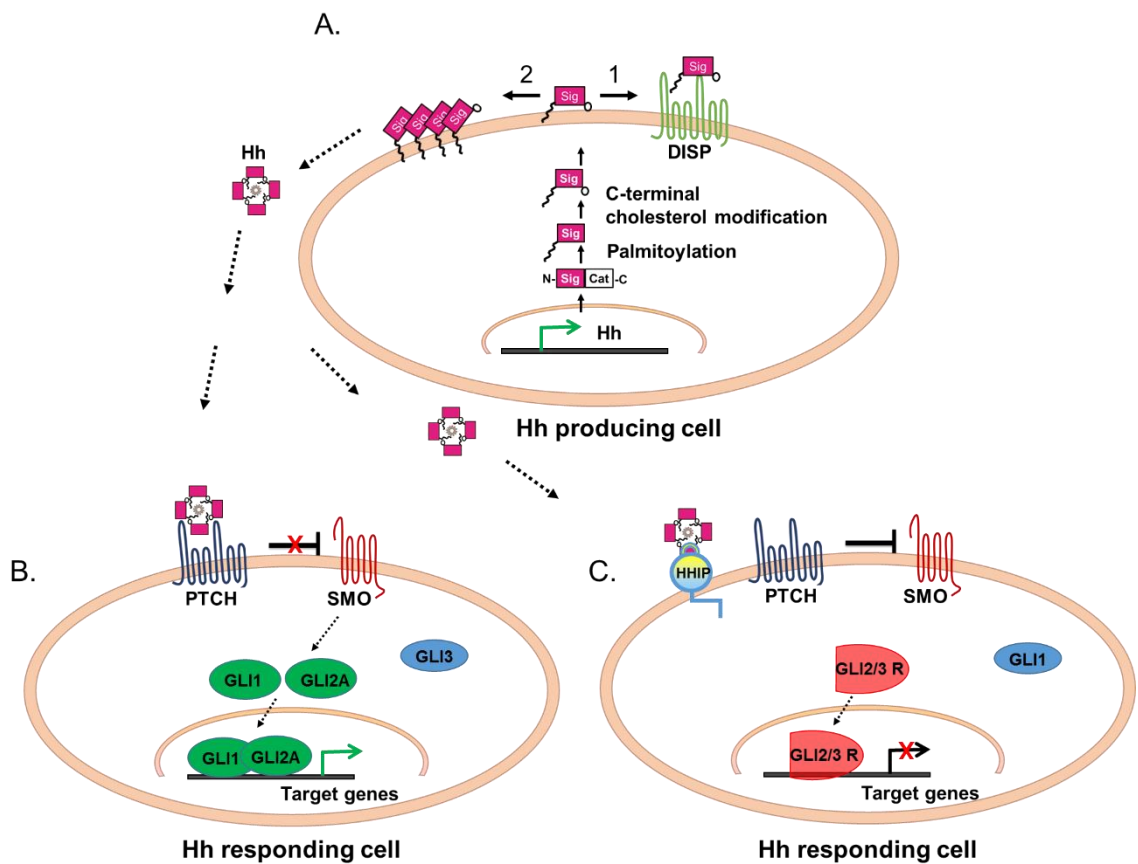


Figure 1.8 Simplified vertebrate Hedgehog signalling pathway

A) Precursor forms of Hh proteins undergo autocatalytic cleavage of the C-terminus followed by dual lipid modifications by SKI in the producing cell. Modified Hh proteins either bind to the DISP membrane receptor as monomers (1) or form multimers, which are released from the cell membrane (2). B) Hh proteins spread in the extracellular space and bind to the PTCH receptor of the recipient cell. Upon binding the inhibitory effect of PTCH to SMO is alleviated and SMO activates downstream signalling, resulting in activation and translocation of GLI1 and full length GLI2 (GLI2A) into the nucleus, whereas GLI3 is retained in the cytoplasm. GLI1 and GLI2 induce transcription of target genes, including Hh pathway molecules such as GLI 1, PTCH1 and HHIP. C) In the absence of Hh proteins or in the presence of the antagonist HHIP, SMO is inactive. Protein modifications lead to truncated repressor forms GLI2 and GLI3

(GLI2/3R), which translocate in the nucleus and sequester gene transcription. At the same time GLI1 is sequestered at the cytoplasm.

1.3.1 Hh pathway and cell behaviour

The core Hh pathway components are evolutionarily conserved between invertebrates and vertebrates and the pathway is an essential regulator of organogenesis and body patterning (Wicking, Smyth & Bale 1999, Ingham, McMahon 2001) . It mainly exerts its functions through regulation of cell growth, cell differentiation, cell proliferation and cell migration during embryonic development (Bale 2002, Bijlsma, Peppelenbosch & Spek 2006) . In adult life it is required for the survival and proliferation of several tissue progenitor cells and the maintenance of adult stem cells in a range of tissues from the hair follicle to the haematopoietic system (Briscoe, Thérond 2013, Beachy, Karhadkar & Berman 2004)

1.3.2 Hh target genes

The target genes of Hh signalling are primarily involved in regulation of cell proliferation, cell survival and cell fate specification. Among those genes are several components of the Hh pathway itself, including PTCH, GLI1, GLI3 (Marigo et al. 1996b, Marigo, Tabin 1996) and HHIP (**Figure 1.8 B&C**). The expression of these genes, which is not observed in the absence of Hh ligand, acts as a marker for active signalling transduction (Ahn, Joyner 2004, Vokes et al. 2007). Many more Hh target genes have been identified by gene expression microarrays and include genes involved in cell cycle regulation, cell adhesion, cell migration, and apoptosis (Bijlsma, Spek & Peppelenbosch 2004, Ingram et al. 2002, Yoon et al. 2002, Hochman et al. 2006) . Hh signalling also acts cooperatively with other signalling pathways such as Notch, Wnt and Hippo, in the regulation of gene expression and cell phenotype. In addition, Hh has been shown to coordinate the expression of essential cardiovascular pathways and processes including angiogenic genes such as vascular endothelial growth factor (Vegf) and angiopoietin 1 and 2 (Ang-1, Ang-2) (Pola et al. 2001, Lee, Moskowitz & Sims 2007) .

1.3.3 Non-canonical Hh signalling

Alternative signalling pathways, which overlap with Hh signalling processes, have also been identified (Bijlsma, Spek 2010). One such non-canonical pathway involves transforming growth factor-beta (TGF-beta) proteins, which directly induce the expression of GLI1 and GLI2 independently of PTCH1/SMO (Dennler et al. 2007). K-RAS signalling has also been shown to mediate Hh activation through GLI1 expression again independently of SMO in human pancreatic ductal adenocarcinoma (Nolan-Stevaux et al. 2009). In this study GLI1 expression was decoupled from the upstream Shh-Ptch-Smo signalling and instead regulated through a combination of TGF-beta and KRAS. This was shown to be necessary for survival and phenotypic transformation of pancreatic cancer cells. Other studies identified a transcription independent Hh signalling cascade (Bijlsma et al. 2008a, Bijlsma et al. 2007). Here, Hh signalling acts through arachidonic acid metabolites to induce rearrangement of the cytoskeleton and promote cell migration in a Gli-independent manner.

The non-canonical signalling pathways are of particular interest when considering paradoxical Hh pathway activity, for example in ischemia studies (discussed below in section 3.1.2).

1.3.4 Hedgehog signalling in human diseases

Given the regulatory effects of the Hh pathway on crucial developmental stages of different tissues and the wide range of molecules participating in this signalling cascade it is not surprising that disruption of the pathway causes diverse abnormal phenotypes. Mutations in components of the Hh pathway can result in either up- or downregulation of the pathway with the majority of phenotypes being developmental congenital syndromes including malformations of the limbs, face, brain or even multi-organ syndromes. Dysregulation of the pathway is also associated with various cancers. A summary of the resultant phenotypic defects due to disruption of Hh signalling is shown in **Table 1.4** below. Hh signalling has been implicated in cardiovascular disease although this is mainly in rodent models with little direct evidence in humans (described in section 3.1.2).

Disease	Body parts affected	Gene	Mutation type/ mechanism of action
Holoprosencephaly	Brain	SHH	Loss of function
Holoprosencephaly	Brain	PTCH	Gain of function
Grieg cephalopolysyndactyly	Limbs, head, face	GLI3	Loss of function
Pallister-Hall syndrome	Multiple (hypothalamic hamartoma, pituitary dysfunction, central polydactyly, and visceral malformations)	GLI3	Dominant negative
Postaxial polydactyly type 3	Hand and foot deformities	GLI3	Partial loss of function
VACTERL	Multiple (atresia, cardiac defects, tracheo-esophageal fistula, renal anomalies, and limb abnormalities)	?GLI2 and GLI3	Mouse model with loss of function of GLI2 and GLI3
Smith-Lemli-Opitz syndrome	Multiple (distinctive facial features, microcephaly), intellectual disability and behavioural problems)	DHCR7	Failure to add cholesterol adduct to SHH
Gorlin syndrome	Skin, nervous system, eyes, endocrine system, and bones (most common skin cancer)	PTCH	Loss of function
Sporadic basal cell carcinoma	As above	PTCH	Loss of function
Sporadic basal cell carcinoma	As above	SMO	Gain of function
Sporadic medulloblastoma	Brain, CNS (cancer)	PTCH	Loss of function
Glioblastoma	Brain, CNS (cancer)	GLI1	Amplification

Table 1.4 Mutations in the Hh signalling pathway in human disease (Adapted from Bale 2002) .

1.4 Mouse models

1.4.1 Mutagenesis strategies in mouse

Genetic manipulation of model organisms is a very informative way of interrogating the function of novel genes. Among model organisms the mouse offers particular advantages for the study of human biology and disease due to similarity in development, body patterning and physiology. The mouse has been targeted by mutagenesis for almost 100 years. In the 1920s X-rays were observed to induce mutations in the offspring of irradiated animals (Little, Bagg 1923, Muller 1927). Subsequently, large-scale screening of irradiated mice was performed in the 1950s and 60s. However, radiation is not a particularly efficient method of inducing mutations. Although mutations are much more frequent than those that occur naturally the frequency is still quite low. Also, the mutations, which are generated, are likely to be deletions, be restricted to certain portions of the genome and result in recessive phenotypes (Thomas, Lamantia & Magnuson 1998). More recently chemically induced mutagenesis using the alkylating agent *N*-ethyl-*N*-nitrosourea (ENU) was employed (Russell et al. 1982, Russell et al. 1979). ENU induces single base-pair substitutions by transferring its ethyl group to oxygen or nitrogen radicals in DNA resulting in mispairing and base-pair substitution. ENU induces mutation much more frequently than radiation and because it generates point mutations it results in a greater range of mutant types such as loss-of-function mutations, gain-of-function mutations, viable hypomorphs of lethal complementation groups and antimorphs (Justice et al. 1999). Induction of mutations by radiation or chemical methods is a random process and is normally used in phenotype based screens. Linkage mapping is used to link a phenotype of interest to the genetic change responsible (Justice et al. 1999)

Over the past 20 or so years genetically driven approaches have become the method of choice for generating mouse models (Gossler et al. 1989, Hicks et al. 1997, Skarnes et al. 1995). Gene trapping involves the integration of a selectable marker or reporter into the genome of mouse embryonic stem (ES) cells by the use of certain retroviruses (Amsterdam 2003, Amsterdam et al. 1997, Qi, Lin & Fan 2004). If the gene trap vector inserts within a gene body, it

is likely to lead to loss-of-function mutations. As with the radiation and chemical methods described above gene trap mutagenesis is a random process, however, as the targeted gene can be identified easily through sequencing it has essentially been employed in a gene-first rather than phenotype-first approach with banks of ES cells carrying gene trap mutations for most mouse genes available from resources such as the International Gene Trap Consortium (IGTC) (Guan et al. 2010). Gene trapping mutagenesis, though, is limited to gene knockout only, and relies on spontaneous mutagenesis events. In contrast gene targeting allows for more accurate and wide gene modifications.

Gene targeting in mouse genome through homologous recombination in ES cells is the one of the most accurate and versatile ways to alter a gene sequence and therefore dissect gene function.

Targeted mutagenesis was first performed in mouse ES cells in the early 1980s (Evans, Kaufman 1981, Martin 1981, Smithies et al. 1985, Thomas, Capecchi 1987). The process requires the introduction of a desired alteration into a targeting cassette, which shares homology to the target genome, and following delivery (usually by electroporation) into the host ES cell recombines with the genome by homologous recombination (HR). Homologous recombination is a naturally occurring process in response to DNA damage (Takata et al. 1998). Conventional targeting vectors consist of positive selectable marker (usually Neomycin, neo) and a negative selectable marker such as thymidine kinase (Mansour, Thomas & Capecchi 1988, Valenzuela et al. 2003) . The use of selectable markers is required for the enrichment of successfully targeted ES cells as HR and correct integration of the targeting cassette occur at relatively low frequencies. Figure 1.9 shows deletion of a genomic region through homologous recombination.

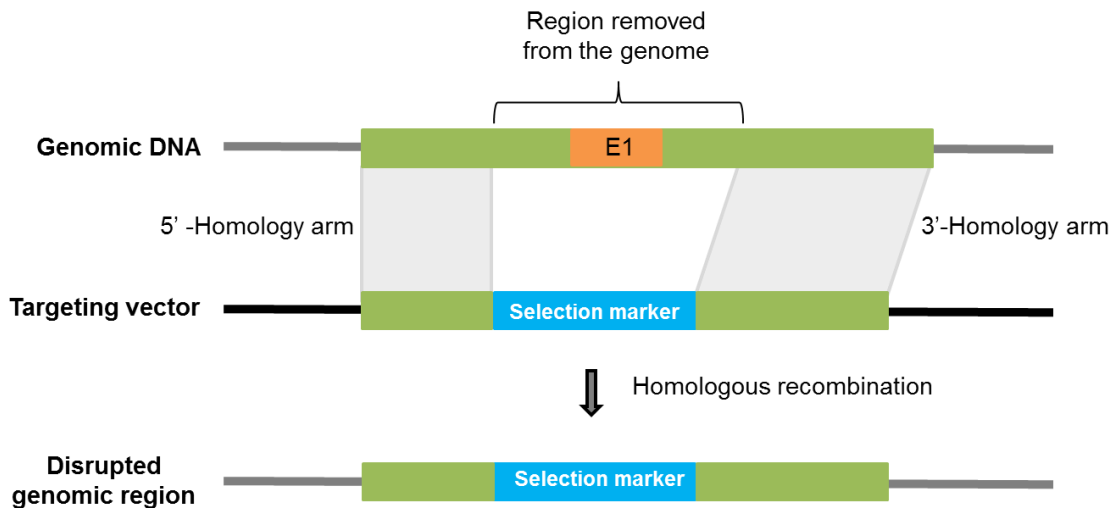


Figure 1.9 Gene targeting through homologous recombination

Schematic representation of a genomic region deletion using HR in ES cells. It is common practice to use a targeting vector that consists of a selectable marker cassette. The cassette will be inserted in the gene sequence that is flanked by the homology arms of the gene, leading to deletion of this sequence. E1: exon 1.

1.4.1.1 Large scale gene targeting

After the completion of the sequencing of the human and mouse genome (Lander et al. 2001, Mouse Genome Sequencing Consortium et al. 2002) large-scale collaborative efforts have been established in order to target all mouse genes through a combination of gene trapping and gene targeting to provide experimental models to investigate gene function. The Knockout Mouse Project (KOMP) (Austin et al. 2004) and the IGTC (Skarnes et al. 2004) were initiated in order to knock out all the mouse genes and provide a publicly available resource of mutant mouse ES cells. Since the establishment of KOMP there has been a significant effort around the world to organise mouse knockout projects, such as the European Conditional Mouse Mutagenesis Program (EUCOMM) (Auwerx et al. 2004) and the North American Conditional Mouse Mutagenesis project (NorCOMM). In order to avoid complexity and overlapping efforts all the above knockout projects merged to form the International

Knockout Mouse Consortium (IKMC) (Collins et al. 2007). The main aims of the IKMC (as summarised by Rosen *et al.*) have been to (1) generate conditional mutations in each protein-coding gene in ES cells, (2) introduce a *lacZ* (β -galactosidase) reporter to allow gene expression of the endogenous tagged locus to be assessed, (3) standardise phenotyping of the resource and (4) create a companion resource of Cre driver lines to enable spatial and temporal control of gene inactivation (Rosen, Schick & Wurst 2015). The combined gene targeting and gene trapping approaches of the IKMC have targeted more than 18,500 genes, most of which (>13,500) have been generated by the EUCOMM/EUCOMMTOOLS and KOMP-CSD consortia, which are successor programmes of the EUCOMM and KOMP respectively (Rosen, Schick & Wurst 2015). The international mouse phenotyping consortium (IMPC) works in concert with the IKMC to provide primary phenotyping information for all of the targeted lines. To date, the IMPC has generated more than 4,900 mutant mouse lines from targeted ES cells supplied by IKMC for primary phenotyping (<http://www.mousephenotype.org>).

1.4.2 Mouse models of atherosclerosis

There are many animal models that have been used for atherosclerosis studies including relatively large animals such as nonhuman primates, swine, hamster, rats and rabbits. Currently the most commonly used species is the mouse. The major advantages of the mouse for the study of atherogenesis rely on the rather low cost of purchase and maintenance, ease of breeding, ease of genetic manipulation, and the ability to monitor atherogenesis in a judicious time frame. Moreover, the availability of numerous inbred mouse strains with different susceptibility to atherosclerosis manifestation allows the identification of genes involved in the determination of sensitivity or resistance to atherosclerosis (Getz, Reardon 2012). Most of the wild type inbred mice are not susceptible to atherosclerosis indeed they are quite resistant to it (C3H is the most resistant) with only exception the C57BL/6J strain (Paigen et al. 1987a, Dansky et al. 1999, Shi et al. 2000). This resistance to atherosclerosis is mainly attributed to the fact mice naturally have high levels of Hdl and relatively low steady-state concentrations of Vldl and Ldl. Moreover, mice do not express cholesteryl ester

transfer protein (CETP), a plasma protein that has gained much interest as a potential target for atheroprotection in humans (Getz, Reardon 2006, Getz, Reardon 2012). Mice therefore need to be primed for atherosclerosis development, either by introducing an atherogenic diet or by using a genetically predisposed atherosclerosis strain (or a combination of both). One such atherogenic diet is the 'Paigen diet' (1.25% cholesterol, 0.5% cholic acid, 15% fat), which is a high fat diet that was used to cause atherosclerosis in wild type mice (Paigen et al. 1985) and also to examine the sensitivity of different strains of wild-type mice to atherosclerosis (Paigen 1995). Mice on a 'Paigen diet' exhibit only small lesions at 4 to 5 months and unphysiologically high cholesterol. Moreover, the diet was shown to promote inflammation through NK-kB activation (Liao et al. 1993) and so is generally now avoided unless the use of cholic acid is specifically required. The most widely-used high-fat diet for atherosclerosis experiments is the so-called Western-type diet, which was first described by Plump *et al.* This diet consists of 21% fat by weight, 0.15% cholesterol and no cholic acid and so is more physiologically accurate to the composition of an average American diet than the Paigen diet (Plump et al. 1992).

1.4.2.1 Genetically modified atherosclerosis mouse models

Creation of mice that are genetically predisposed to atherosclerosis focused on manipulating lipoprotein metabolism and thereby genes that regulate this process. The genes that were targeted for this purpose were *Apoe* and *Ldlr*. *Apoe* is a glycoprotein primarily synthesised in the liver but also in the brain and other tissues both in humans and mice. It localises on the surface of all lipoprotein particles except Ldl and serves as a ligand for two different hepatic receptors; the Ldlr, and the chylomicron remnant receptor. Thus it mediates the uptake of *Apoe*-containing lipoprotein particles by the liver (Getz, Reardon 2009). In 1992 two different groups generated *Apoe* deficient mice by gene targeting in ES cells by HR (J A Piedrahita et al. 1992, Plump et al. 1992). Homozygous *Apoe* deficient mice (*Apoe*^{-/-}) were presented with 5 folds' increase in plasma cholesterol levels, two-fold increase in triglycerides levels and decrease in Hdl. Mice naturally have elevated Hdl and lower Ldl compared to humans and it was found that the *Apoe*^{-/-} model caused a significant shift in

plasma lipoproteins from Hdl to Vldl (**Figure 1.9 & 1.10**). Despite the differences in the lipid profile between humans and mice the *ApoE*^{-/-} mice have similar disease progression to those of *APOE* deficient humans (Jawien, Nastalek & Korbut 2004)

Unable to gain third party permission

Figure 1.10 Plasma cholesterol levels in *ApoE*^{-/-} mice

Representative cholesterol concentrations in lipoprotein fraction of wild type and *ApoE*^{-/-} mice after fast phase liquid chromatography (FPLC) (Taken from Jaiwen, Nastalek & Korbut 2004).

A year later Ishibashi *et al.* created a different atherosclerosis mouse model. This model involved the deletion of the *Ldlr* gene again by targeting ES cells (Ishibashi *et al.* 1993). The Ldlr is a hepatic membrane bound receptor, which has high affinity for the apolipoprotein B100 (Apo B-100) present in the outer layer of the Ldl and for ApoE, which is present in the intermediate density lipoproteins (IDL) particles in humans and mice (Twisk *et al.* 2000). The binding results in endocytosis of IDL and LDL particles by the liver and thus maintenance of the plasma cholesterol levels. *Ldlr* deficient mice (*Ldlr*^{-/-}) show a more modest lipoprotein abnormality compared to the *ApoE*^{-/-} when they are fed normal diet (chow) (**Figure 1.11**). *ApoE*^{-/-} and *Ldlr*^{-/-} are the most well characterised atherosclerosis mouse models. *ApoE*^{-/-} mice are able to develop atherosclerosis even when fed normal diet in contrast to *Ldlr*^{-/-} mice, which show only modest signs of atherosclerosis on normal diet (Nakashima *et al.* 1994, Ma *et al.* 2012). The *Ldlr*^{-/-} model is however very responsive to high fat diet and develop large atherosclerotic lesions, as described when fed with high cholesterol diet (Ishibashi *et al.* 1994b, Plump *et al.* 1992, Kowala *et al.* 2000).

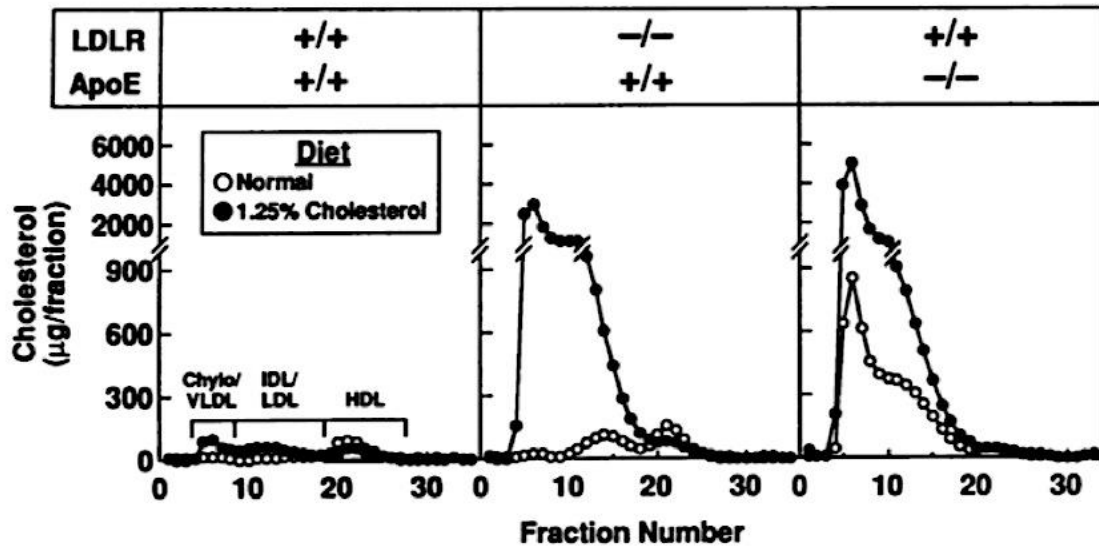


Figure 1.11 Plasma cholesterol levels in *Apoe*^{-/-} and *Ldlr*^{-/-} mice

Representative concentrations in lipoprotein fractions of wild type, *Apoe*^{-/-} and *Ldlr*^{-/-} mice after FPLC. There is a significant increase in total cholesterol levels when mice are fed high cholesterol diet (Adapted from Ishibashi et al. 1994b) .

1.4.2.2 Atherosclerosis pathophysiology in mice

One of the main differences between mouse and human atherosclerosis is the anatomical regions as to where lesions form. In both humans and mice lesions form in distinct vascular regions subject to turbulent blood flow such as the arterial branches and curvatures. In humans, lesions occur more frequently in the coronary arteries, carotids and peripheral vessels such as the iliac artery and in mice more frequently in the aortic root, aortic arch and innominate artery (Getz, Reardon 2012). Figure 1.12 A shows the typical distribution of atherosclerotic plaques in *Apoe*^{-/-} and *Ldlr*^{-/-} mouse models. Large plaques are present at the aortic root, the curvature of the aortic arch and the innominate artery. Smaller plaques form throughout the thoracic aorta and the arterial branching sites (Vanderlaan, Reardon & Getz 2004) .

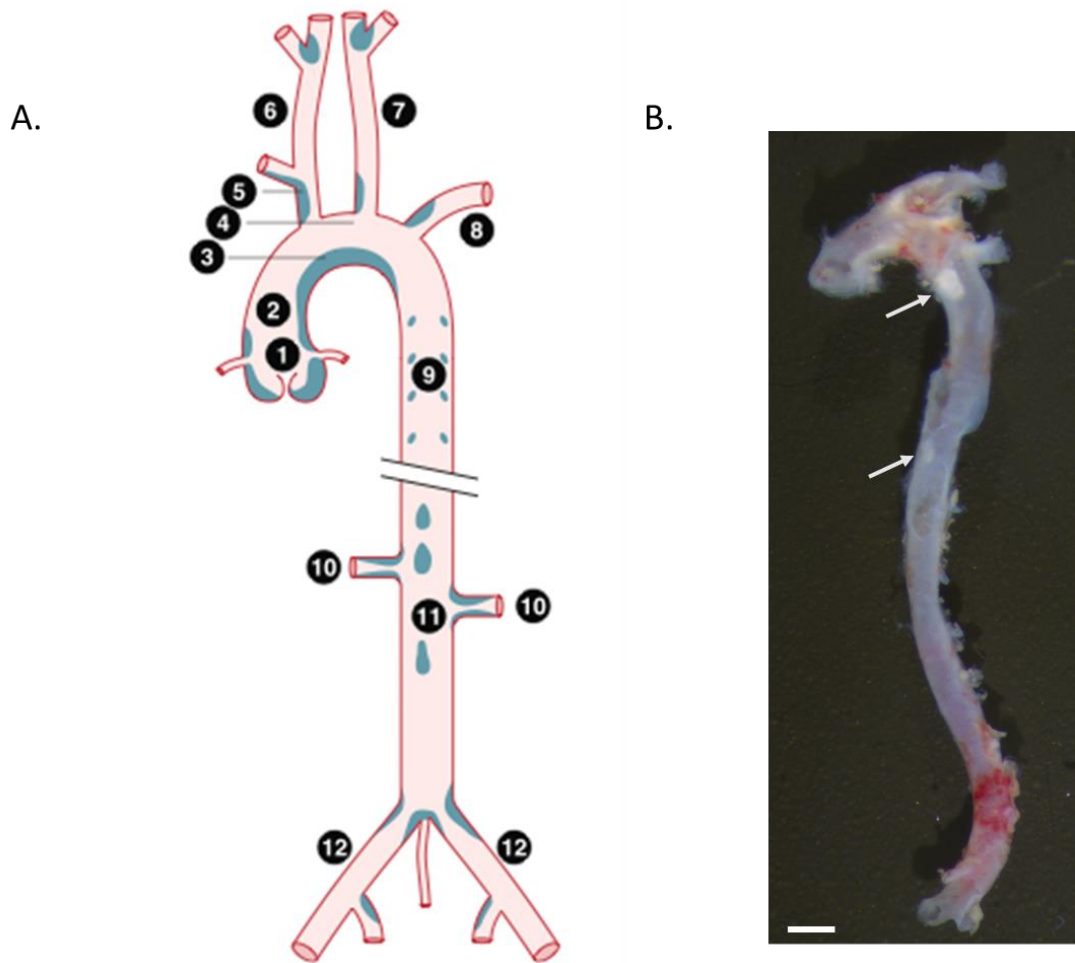


Figure 1.12 Distribution of atherosclerotic lesions in the major mouse arterial vasculature

A) The distribution of atherosclerotic lesions is depicted in the aorta of *Ldlr*^{-/-} mice fed high fat diet. Plaques are distributed across the; 1 aortic root; 2 ascending aorta; 3 lesser curvature of aortic arch; 4 greater curvature of aortic arch; 5 innominate artery; 6 right common carotid artery; 7 left common carotid artery; 8 left subclavian artery; 9 thoracic aorta; 10 renal artery; 11 abdominal aorta as well as 12 iliac artery. Lesions preferentially develop at arterial branches and curvatures (Adapted from Vanderlaan et al 2003). B) Microscopic observation of the aorta from an *Apoe*^{-/-} mouse fed chow diet reveals lesion formation in the aortic arch curvature and the thoracic region (white arrows). Scale bar=1mm.

Since the generation of the hyperlipidemic strains (*Apoe*^{-/-} and *Ldlr*^{-/-}) there have been systematic studies, which describe the atherosclerosis progression in these mice and its manipulation through feeding of different diets such as the 'western diet'.

The morphological features of early stages of atherosclerotic lesions in mice are very similar to their human counterpart and so can be classified according to the American Heart Association staging system (stages I-IV) (described in section 1.1.1) (Stary et al. 1995) (**Table 1.4**).

Unable to gain third party permission

Table 1.5 Atherosclerosis progression in *Apoe*^{-/-} and *Ldlr*^{-/-} mice

The table summarises the disease stages and timetable for lesion development in both *Apoe*^{-/-} and *Ldlr*^{-/-} mice showing that *Apoe*^{-/-} progress more rapidly and beyond stage IV. N/A Not applicable (Taken from Whitman 2004) .

Much of the knowledge regarding the details of cellular and molecular signalling during atherogenesis relies mainly on histological observations of human atherosclerosis as well as in *vitro* data. Similar findings have also been found in mouse atherosclerosis models. For example, extensive examination and description of the atherosclerotic lesions of all stages throughout the arterial tree has been performed for the *Apoe*^{-/-} mouse model by Nakashima *et al.* (Nakashima et al. 1994). Whitman *et al.* has reviewed the process of atherogenesis in *Apoe*^{-/-} and *Ldlr*^{-/-} mouse models in relation to human atherosclerosis and has divided disease development in early lesion development and late lesion development (Whitman 2004) . Early lesion development, which describes stages I to III involve the activation

of the immune system. Indeed, in arteries of healthy teenagers' infiltration of monocytes and T lymphocytes at sites susceptible to atherosclerosis have been observed suggesting that atherosclerosis is a chronic disease which begins in childhood but may become clinically irrelevant until many decades later (Ross 1999, Whitman 2004). The features of early stage lesions in mice are very similar to those in humans. These lesions are characterised by accumulation of lipoproteins and immune cells mainly T-cells and macrophages (Roselaar, Kakkanathu & Daugherty 1996), and a small number of B-cells and dendritic cells (Zhou, Hansson 1999, Bobryshev et al. 2001). As with humans there is significant evidence that accumulation of plasma derived lipoproteins in the arterial wall can initiate cell specific reactions that trigger mouse atherosclerosis (Getz 1990). Once in the tunica intima lipoproteins are captured by matrix components and become oxidised, which was shown to be chemoattractant for monocytes *in vitro* (Quinn et al. 1987). When monocytes migrate in to the intima they differentiate into macrophages, which uptake modified lipoproteins via their scavenger receptors and become ester-enriched foam cells (Nicholson et al. 2001, Boullier et al. 2001). The generation and accumulation of numerous ester-enriched foam cells forms a cell mass, which is commonly termed as fatty streak. Fatty streak lesions are common in both *Apoe*^{-/-} and *Ldlr*^{-/-} mice (**Figure 1.13 A**). These lesions can further progress to stage IV, which are considered advanced because they are characterised by extracellular lipid accumulation, known as lipid core (**Figure 1.13 B**). The lipid core is the result of the consolidation of distinct lipid pools that begin to collect in stage III lesions. When the lipid core undergoes an increase in fibrous tissue, a 'cap' containing smooth muscle cells surrounded by connective tissue is created and the lesion are labelled stage V (**Figure 1.13 C**). Sometimes however distinguishing between stage IV and V is not possible because both stages comprise similar components, therefore they are both known as fibrous plaques (Whitman 2004). Lesion IV and V have clinical relevance in humans because they can rupture and cause fissures, haematomas and/or thrombosis leading to morbidity. Although stage IV and V develop in *Apoe*^{-/-} mice after prolonged feeding with atherogenic diet it is not clear yet if they rupture. Stage VI lesions, which are lesions IV or V containing a haematoma or thrombus (**Figure 1.13 D**), have only been reported in the innominate and carotid artery of *Apoe*^{-/-} mice (Zadelaar et

al. 2005, Rosenfeld et al. 2000, Clarke et al. 2006, Clarke et al. 2008, von der Thusen et al. 2002). Development of stage V lesions in *Ldlr*^{-/-} mice is under debate because there is no histological evidence of the presence of a fibrous cap (Ishibashi et al. 1994a) (**Table 1.4**)

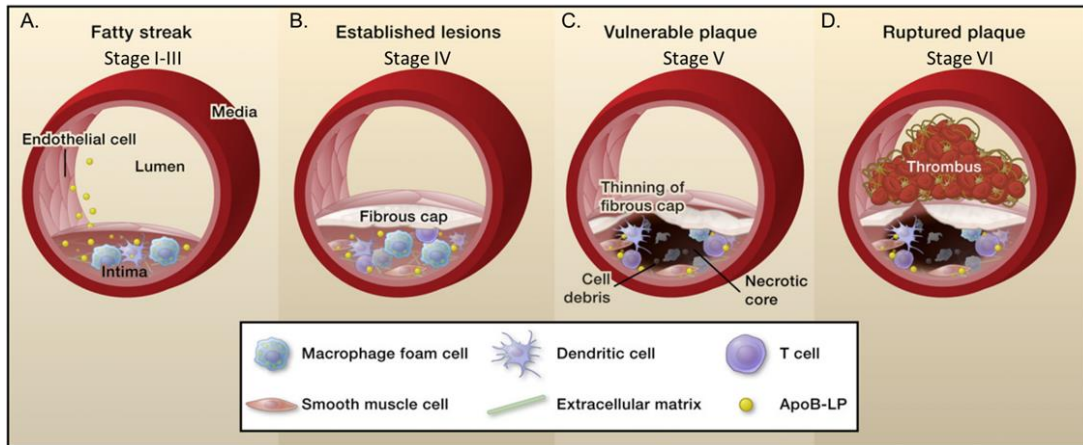


Figure 1.13 Progression of mouse atherosclerotic lesions

A) Early stages of the disease (I-III) are characterised by infiltration of ApoB-containing lipoproteins (ApoB-LP) in the tunica intima and subsequent recruitment of blood cells such as monocytes, T cells and dendritic cells in the vessel wall. Differentiated monocytes to macrophages uptake oxidised ApoB-LP and become foam cells creating fatty streaks. B) Subsequent extracellular lipid accumulation leads to the creation of a lipid core, which is further populated by SMCs. Deposition of connective tissue by SMCs creates a fibrous cap at the top of the lipid core. Lesions at this point are classified as stage IV. C) Further disease progression to stage V is characterised by cell apoptosis creating a necrotic core. D) Vulnerable lesions are prone to rupture exposing the thrombogenic material into the arterial lumen. However, this stage is questionable in mice (Adapted from Moore, Tabas 2011) .

1.5 Hypothesis

GWAS have identified an association between variants on chromosomal 14q32.2 and CAD. The lead SNP and all the SNPs in high LD fall within a region coding for an uncharacterised protein termed HHIPL1. The study will use *in vitro* and *in vivo* models to investigate the hypothesis that;

HHIPL1 is a novel component of the Hh signalling pathway and is the causal gene for CAD at the 14q32.2 locus.

1.6 Aims of the thesis

The aims of the study are to;

- Determine whether HHIPL1 is involved in Hh signalling
- Explore the expression and function in cardiovascular cells and atherosclerosis relevant cell processes.
- Investigate if knockout of Hhip1 affects disease in mouse models of atherosclerosis.

2 Materials and Methods

2.1 Cell biology

2.1.1 Cell maintenance

2.1.1.1 Human embryonic kidney cells

Human embryonic kidney cells (HEK293, ATCC CRL-1573) were cultured at 37°C and 5% CO₂ in Dulbecco Modified Eagle Medium (DMEM) [additives: 10% Fetal Calf Serum (FCS, Invitrogen), 1% penicillin/streptomycin (PAA)] until 60-80 % confluent. Upon confluency, the waste medium was discarded and the tissue fragments and cell monolayer were washed with phosphate buffered saline (PBS). The adherent cells were detached with 5x Trypsin/EDTA (1:2 dilution of 10x Trypsin/EDTA in PBS). 2ml of Trypsin/EDTA was added for every 75cm² for 2-5 minutes (min) at 37°C, until cells detached from the plastic surface. 10mL of complete medium was added to inactivate the trypsin. The trypsinized surface was washed with PBS, and also placed into the centrifuge tube. After centrifugation at 300 g for 5 min, the supernatant was discarded, and the cell pellet was re-suspended in the appropriate volume of pre-warmed medium. Cells that reached 80% confluency were diluted at a 1:12 ratio.

2.1.1.2 Human aortic smooth muscle cells

Human aortic smooth muscle cells (HASMC, Invitrogen) were cultured at 37°C and 5% CO₂ in Medium 231 (GIBCO/Invitrogen) supplemented with 5% Smooth Muscle Growth Supplement (SMGS, GIBCO/Invitrogen) and 1% penicillin/streptomycin until 60-80 % confluent. Cells were split as described in section 2.1.1.1. Cells that reached 80% confluency were diluted at a 1:3 ratio.

2.1.1.3 Cell cryopreservation

Cells were trypsinized as described in section 2.1.1.1. After centrifugation the supernatant was discarded. The cell pellet was resuspended at a density between 8-40 x 10⁵ cells in cryoprotectant solution (50% complete medium, 40% FCS and 10% dimethyl sulfoxide, DMSO) and transferred to cryovials. The cells were stored overnight at -80°C, and subsequently transferred to a liquid nitrogen tank for long term storage.

2.1.1.4 Cell revival from liquid nitrogen

Qryovials containing cells were transferred from the liquid nitrogen and thawed in a 37°C water bath. The vial contents were added to 12 mL of full media in a T75 flask and left undisturbed for two days. The medium was then replaced with fresh. Cells were subcultured when confluency was observed (as described in section 2.1.1.1).

2.1.2 Cell transfection methods

2.1.2.1 Lipofectamine based transfection

HEK293 cells were appropriately seeded in a 6-well plate in order to reach 80% confluency after 24 hours. Cells were transfected using Lipofectamine LTX (Invitrogen). For each reaction a master mix containing 500µl OPTIMEM, 5µl PlusReagent and 2.5µg plasmid DNA was prepared and incubated for 5 mins at room temperature. 15µl of Lipofectamine LTX was then added to the above master mix and incubated for 15 mins at room temperature. Following incubation, the master mix was added by gentle agitation to each well. The media was replaced 24 hours post-transfection with DMEM containing no serum for downstream western blot analysis.

2.1.2.2 Electroporation

HEK 293 cells were also transfected by electroporation. For each reaction 1×10^6 cells were used. The cell number was determined by a haemocytometer. For this purpose, 10µl of cell suspension was mixed with 10µl of 0.4% Trypan Blue (Fisher scientific) solution and onto a haemocytometer to perform cell count and determine cell viability. The appropriate volume of media containing 1×10^6 cells was centrifuged at 300 g for 5 mins. The supernatant was discarded and the cells were resuspended in 1mL of serum free and antibiotic free Opti-MEM medium (Invitrogen). Cells were further washed twice in Opti-MEM. After the third wash cells were resuspended in 100µl Opti-MEM containing 10µg of plasmid DNA (5 µg of each plasmid when co-transfection was performed). The cell suspension was mixed gently by tapping the cuvette without creating foam and dispensed into 2mm gap electroporation cuvettes (EC-002S NEPA). The cuvette was placed into the CU500 cuvette chamber and the electroporation

was performed using the NEPAGene21 electroporator according to the parameters shown in **Table 2.1**. The electroporated cells were then added to 2mL of full DMEM (6-well format) and cultured for 24 hours. For downstream analysis medium was changed to 1mL of serum free DMEM 24 hours post transfection.

Plasmid	Set Parameters											
	Poring Pulse						Transfer Pulse					
	V	Length (ms)	Interval (ms)	No.	D. Rate (%)	Polarity	V	Length (ms)	Interval (ms)	No.	D. Rate (%)	Polarity
HHIPL1-FLAG	125	2.5	50	2	10	+	20	50	50	5	40	+/-
HHIPL1-GFP	125	5	50	2	10	+	20	50	50	5	40	+/-
HHIPL1-FLAG +SHH-GFP	125	2.5	50	2	10	+	20	50	50	5	40	+/-
HHIPL1-FLAG+ pGFP(ev)	125	2.5	50	2	10	+	20	50	50	5	40	+/-
SHH- GFP+ pcDNA(ev)	125	2.5	50	2	10	+	20	50	50	5	40	+/-

Table 2.1 Electroporation parameters for HEK293 cells

2.1.2.3 Reverse transfection of siRNA

HASMC were treated with two different siRNAs (Qiagen) against HHIPL1 as well as a combination of them. As a positive control for the transfection efficiency a cell death control siRNA (AllStars HS cell death control siRNA, Qiagen) was transfected to HASMC. The target sequence of each siRNA is presented in **Table 2.2**. HASMC were seeded so that they reached 60% confluency at the day of siRNA transfection. 22-30x10⁴ cells in a volume of 2mL media per well of a 6-well plate were used for each reaction. For each well a mastermix containing 6.25µl of siRNA (20µM) diluted in 250µl of Opti-MEM was prepared and added to each well. Additionally, 250µl of Opti-MEM and 5µl of Lipofectamine RNAiMAX reagent (Invitrogen) was added per well. The lipid and siRNA complexes were incubated for 15 mins at room temperature. Following incubation 2 mL of cells were added per well. Cells were placed back in the incubator for downstream analysis.

NCBI Reference sequence	siRNA Name	Target sequence
		Sense strand Antisense strand (5'-3')
NM_00112728	Hs_KIAA1822_1	GCGCATCGACGTGGACCGTAA GCAUCGACGUGGACCGUAATT UUACGGUCCACGUCGAUGCGC
NM_001127258	Hs_HHIPL1_2	ACCCAGGGCTATGCCAATAAT CCAGGGCUAUGCCAAUAAUTT AUUAUUGGCAUAGCCCUGGGT

Table 2.2 siRNA target sequences.

Hs_KIAA1822_1=siRNA1, Hs_HHIPL1_2= siRNA2

2.1.3 Behavioural assays

2.1.3.1 Migration assay (scratch assay)

HASMC were transfected with siRNAs as described in section 2.1.2.3 and left to reach more than 90% confluency in Medium 231 supplemented with 5% SMGS (GIBCO/Invitrogen) (no migration stimulus was added), which usually required 24-48 hours post transfection in a 6-well plate. Upon confluency, a 200 μ l pipette tip was used to make a scratch the length of the well. The angle of the tip was held at approximately 30 degrees, in order to keep the scratch width limited. Cells were washed with pre-warmed media and were placed to the incubator. Three positions were set along the scratch (**Figure 2.1**, red circles) and imaged for up to 12 hours. Images of the three different scratch positions were acquired using the EVOS xl core Microscope (Advanced Microscopy Group) every two hours.

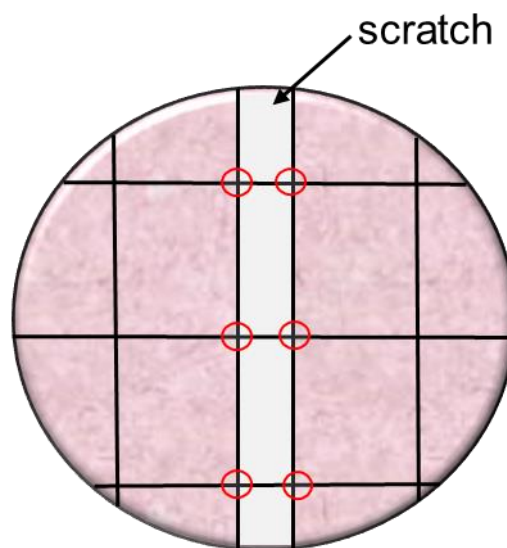


Figure 2.1 Schematic representation of scratch assay

Scratch was monitored every two hours for up to 12 hours at the marked regions (red circles).

2.1.3.2 Image analysis of migration assay

Cell images for migration assays were taken using the EVOS xl core Microscope (Advanced Microscopy Group). In order to calculate the percentage of cell coverage at the scratch area a quantification protocol written by Dr Ir K.R. Straatman was performed in ImageJ software. Cell coverage was monitored at three different regions of the scratch. Each sample was performed in duplicates and each experiment was repeated three times. Cell coverage was measured at 4, 8 and 12 hours post-scratch.

2.1.3.3 Proliferation assay

HASMC were transfected with siRNAs as described in section 2.1.2.3 and were incubated in Medium 231 supplemented with 5% SMGS (GIBCO/Invitrogen) (no proliferation stimulus was added), for 24 hours post transfection without disturbing them. After the cells have recovered from transfection they were trypsinised (section 2.1.1.1) and were counted with the use of a haemocytometer. The proliferation assay was performed in a 96-well plate. Each sample was plated in triplicates at a 2,500 cell density. Three regions across each well were photographed using the EVOS xl core Microscope (Advanced Microscopy Group) at 0, 24, 48 and 72 hours after plating.

2.1.3.4 Image analysis of proliferation assay

Cell count of three random regions of each well was obtained every 24 hours using the manual count plug in of the ImageJ software. Each sample was performed in triplicates and each experiment was repeated three times. The cell count was normalized to the average cell count of all samples at 0 hours' time point.

2.1.4 Cell imaging

2.1.4.1 HEK293 fixation and staining

HEK293 cells were transfected with HHIPL1-GFP plasmid according to the electroporation conditions shown in **Table 2.1** and cultured in full media in a 6-well plate with coverslips placed in the base. 48 hours post transfection the medium was aspirated and the cells were fixed in 4% (w/v) paraformaldehyde (PFA) in PBS for 10 min at room temperature. PFA was removed and the cells

were washed in PBS for 2 min. Cells were then permeabilised with 0.2% Triton-X in PBS for 2 min. Triton-X was discarded and cells were washed again with PBS for 2min. Nuclei were stained with 4',6-diamidino-2-phenylindole (DAPI dilactate, Invitrogen) diluted 1:5000 in PBS for 5 min in the dark. After incubation with DAPI cells were washed three times with PBS, 2 min each. The coverslips carrying the adherent cells were carefully detached from the bottom wells using forceps and placed on microscope slide that had been precoated with fluoreshield mounting medium (Abcam). Cells were visualised by an Olympus FV1000 confocal microscope with assistance provided by Kees Straatman (University of Leicester Advanced Imaging Facility).

2.2 Protein methods

2.2.1 Western blotting

2.2.1.1 Cell lysate protein preparation

Following lipofectamine transfection (section 2.1.2.1), HEK293 cultured surfaces were washed twice in PBS and cells were collected by scraping using a plastic cell scraper. The cells were centrifuged at 6,000 rpm for 5 min and any residual PBS removed. The cells were then resuspended in 100µl HEPES lysis buffer (50mM HEPES ph 7.4, 50mM KCl, 1mM EGTA, 1mM MgCl₂, 1mM NaF) containing 1X phosphatase inhibitors cocktail (10X phoSTOP, Roche). Lysates were incubated on ice for 30 min followed by centrifugation at 13,000 rpm for 5 min. The protein containing supernatant was then collected. 11µl of protein sample was added to 5µl NuPAGE LDS (4X Invitrogen) sample buffer, and 4µl DTT (0.1M) and the mixture was incubated at 70°C for 10 min. Proteins were then either stored in -80°C or immediately subjected to SDS polyacrylamide gel electrophoresis as described in section 2.2.1.3.

2.2.1.2 Concentration of conditioned media

Conditioned media was subjected to protein precipitation using trichloroacetic acid (TCA, Sigma Aldrich). An equal volume of 20% TCA was added to conditioned media, incubated on ice for 30 min and centrifuged at 13,000 rpm for 15min at 4°C. Following centrifugation, the supernatant was removed and

300µl of cold acetone was added to the pellet. Samples were centrifuged again at 13,000 rpm for 15min at 4°C, supernatant was removed and the pellet was dried at 95°C for 10 min. The pellet was then dissolved in a total volume of 20µl containing 5µl NuPAGE LDS (4X Invitrogen) sample buffer, 4µl DTT (0.1M) and 11µl ultra-pure H₂O, followed by incubation at 70°C for 10 min. Proteins were then either stored at -80°C or subjected to SDS polyacrylamide gel electrophoresis (as described in section 2.2.1.3).

2.2.1.3 SDS page

The protein containing samples (18µl) were resolved on pre-cast polyacrylamide NuPAGE Novex 10% Bis-Tris gels (Invitrogen). The gel was run for 50 min at 200V in 1x MOPS buffer (Invitrogen). 5µl of Seebule Plus prestained (Invitrogen) molecular weight marker was run alongside the samples.

2.2.1.4 Protein transfer

Following electrophoresis, the samples were transferred to a nitrocellulose membrane by wet-transfer using the XCell II Blot module (Novex, Invitrogen), in 1X Novex Tris-Glycine Transfer buffer (Invitrogen) containing 10% Methanol. Proteins were transferred for 70 mins at 30V at room temperature.

2.2.1.5 Immunoblotting

Following transfer, the membranes were incubated in blocking buffer containing 4% non-fat milk in PBS+0.1% Tween 20 (PBST) for one hour with gentle rocking. After blocking, membranes were incubated with primary antibody appropriately diluted in blocking buffer overnight at 4°C (see **Table 2.3**). The membranes were then washed three times in PBST for 5 min with agitation followed by incubation with the secondary antibody appropriately diluted in blocking buffer for one hour at room temperature (see **Table 2.3**). The membranes were then washed again with PBST three times. For protein detection membranes were incubated in 1mL Amersham ECL Western blotting detection reagent (GE Healthcare life sciences) for 5 min and imaged using the ImageQuant LAS 4000 (GE Healthcare life sciences) system.

2.2.2 Immunoprecipitation (IP)

HEK293 cells were co-transfected with three different plasmid combinations; HHIPL1-FLAG and SHH-GFP, HHIPL1-FLAG and pGFP empty vector or SHH-GFP and pcDNA3.1 empty vector by electroporation as described in section 2.1.2.2. Plasmid description is provided in section 2.5.1. For one IP reaction 1×10^6 transfected cells (one 9.5 cm² well) in 1mL of media were used. 24 hours post transfection the medium was changed to serum free medium and cells were incubated overnight.

2.2.2.1 Cell lysate protein extraction

48 hours post transfection the medium was aspirated and the cultured surfaces were washed twice in 1mL PBS. Cells were collected by scraping using a plastic cell scraper and centrifuged at 500 g for 3 min at 4°C in order to remove residual PBS. The cell pellet was resuspended in a total volume of 70µl of lysis buffer (10mM Tris/Cl pH 7.5; 150mM NaCl; 0.5mM EDTA; 1% TritonX) containing 1X of each inhibitor (7X protease inhibitor cocktail and 10X phosphatase inhibitors, Roche) and incubated on ice for 30 mins. The suspension was then sonicated following three cycles of 30sec at 50% amplitude with 1 min ice incubation in between the cycles. Cell lysates were centrifuged at 17,000 g for 10 mins at 4°C. The protein containing supernatant was removed to a pre-cooled Eppendorf and 300µl of dilution buffer (10mM Tris/Cl pH 7.5; 150mM NaCl; 0.5mM EDTA) were added.

2.2.2.2 Conditioned media protein preparation

48 hours post transfection conditioned media were collected and centrifuged at 17,000g for 7 mins at 4°C to remove any cell debris. 530µl of the cleared supernatant was transferred to a pre cooled Eppendorf and 100µl of protease inhibitor cocktail (7X cOmplete, Roche) as well as 70µl of phosphatase inhibitors (10X PhoSTOP, Roche) were added.

2.2.2.3 GFP_Trap® _A beads equilibration.

GFP_Trap® _A (Chromotek) were vortexed briefly. For one immunoprecipitation reaction 25µl of slurry was used. In order to equilibrate the beads, the slurry was pipetted into 500µl of ice cold dilution buffer and

centrifuged at 2,500 g for 2min at 4°C. The supernatant was discarded and the wash was repeated twice.

2.2.2.4 Protein binding

50µl of cell lysates and conditioned media was saved for western blotting analysis (referred to as input sample, IN). The remaining protein sample was added to the equilibrated beads. The samples were tumbled end-over-end on a wheel for 2 hours at 4°C. After protein binding the samples were centrifuged at 2,500g for 2 min at 4°C and the remaining supernatant was discarded. The pellet was washed in 500µl ice-cold dilution buffer three times and the supernatant was removed. In order to elute the proteins bound to the beads the pellet was resuspended in 1X NuPAGE LDS (4X Invitrogen) sample buffer and 20mM DTT to a total volume of 50µl by H₂O. The suspension was boiled for 10 min at 95 °C and was subjected to western blotting. The IN sample was also prepared for western blotting. 27.5µl of input protein was added to 12.5µl of NUPAGE LDS (4X Invitrogen) sample buffer and 10 µl of DTT (0.1M) followed by incubation at 70 °C for 10 mins.

2.2.2.5 Western blotting of IP samples

Following immunoprecipitation 18µl of IN or IP sample from section 2.2.2.4 was resolved on 10% polyacrylamide NuPage BisTris precast gels (Invitrogen) as described in section 2.2.1.3. Protein transfer on a nitrocellulose membrane was performed (as described in section 2.2.1.4) and the membranes were reciprocally stained with appropriately diluted anti-FLAG and anti-GFP primary antibodies (see **Table 2.3**) (as described in section 2.2.1.5).

Primary	Host Species	Supplier	Use	Titration
Anti-FLAG peptide/dykdddk (clone M2)	Mouse	Sigma Aldrich (F3165)	WB	1:3000
Anti-GFP peptide (clone GF28R)	Rabbit	Thermo Scientific (MA5-15256)	WB	1:1000
Secondary	Host Species	Supplier	Use	Titration
Anti-mouse IgG (horseradish/peroxidase conjugated)	Sheep	Amersham (NA931)	WB	1:5000
Anti-rabbit IgG (horseradish/peroxidase conjugated)	Donkey	Amersham (NA934)	WB	1:5000

Table 2.3 Primary and secondary antibodies used for western blotting (WB).

2.3 Molecular biology

2.3.1 RNA isolation from mouse tissue

Mouse tissues were collected and transferred to 1ml of RNA $later$ to be stored long term at -20°C. Total RNA was extracted from tissues using the RNeasy Mini Kit Plus (Qiagen) and a modified protocol. Briefly 15-20 mg of tissues were lysed in 900 μ l QIAzol Lysis Reagent using a rotor-stator homogeniser followed by addition of 100 μ l gDNA Eliminator Solution. Aortic tissue homogenisation was performed by placing the tissue in ice-cold tubes prefilled with ceramic beads (Peflab) and 450 μ l of QIAzol Lysis Reagent. The tubes were then placed in a Precellys 24/24 dual homogeniser (Peflab) and the tissue was lysed for 20 sec at 5000 rpm. After lysis the remaining 450 μ l of QIAzol Lysis Reagent was added to the homogenate. At this stage, all samples had 180 μ l of chloroform added to the tube followed by centrifugation at 12,000 g for 15 min at 4°C. The aqueous phase was then transferred to an RNeasy spin column and centrifuged at 10,000 g for 15 sec. The eluate was discarded and 350 μ l of Buffer RWT was added to the column. Following centrifugation at >8,000 g for 15 s 10 μ l of DNase I stock solution in 70 μ l Buffer RDD was added to the column and incubated for 15 min at room temperature. The column was centrifuged at 10,000 g for 15sec for the two first washes and for 2min after the last RPE wash. The column was then transferred to a fresh collection tube. 30 μ l of RNase free water added and the RNA was eluted by centrifugation at 10,000 g for 1min.

The eluted RNA was quantified using the Nanodrop ND-8000 spectrophotometer (Labtech). Measurements were taken at 260, 230 and 280nm. RNA purity and concentration was calculated from these values using the 260/280 and 230/280 ratios.

2.3.2 RNA isolation from cells

Total RNA was extracted using the RNeasy Plus Mini Kit (Qiagen) and a modified protocol. A maximum of 1×10^7 cells were harvested by trypsinisation and subsequent centrifugation at 17,000 g for 5 min. 350 μ l of RLT buffer (containing 0.001% β -mercaptoethanol in RLT buffer) was added to cell pellet and vortexed for 30sec. The lysate was then transferred to a QIAshredder

(Qiagen) column and centrifuged at 13,000 g for 2 min and the column was discarded. The flow through was transferred to a gDNA eliminator column (Qiagen) and centrifuged for 30 sec at >8,000g. The supernatant was retained and a volume of 70% ethanol was added to the filtrate. The filtrate was transferred to an RNeasy spin column (700ul at a time) and centrifuged for 15 sec at >8,000g. The flow through was discarded. 350µl of RW1 buffer was then added to the column and centrifuged for 15 sec at >8,000 g and again the flow through was discarded. A master mix of 10µl of DNase and 70µl of RDD buffer was then added to the column and incubated for 15 sec at room temperature. A further 350µl of RW1 buffer was added and spun for 15 sec at >8,000g. The flow through was discarded and 500µl of RPE buffer was added to the column followed by centrifugation at 8,000 g for 15 sec. The last step was repeated and the flow through was discarded. A final centrifugation at full speed (17,000 g) for 1 min was performed in order to dry the membrane. The RNeasy spin column was placed in a new collection tube and 30µl of RNase free water was added and spun at 8,000g in in order to elute the RNA.

The eluted RNA was quantified using the Nanodrop ND-8000 spectrophotometer (Labtech). Measurements were taken at 260, 230 and 280nm. RNA purity and concentration was calculated from these values using the 260/280 and 230/280 ratios.

2.3.3 cDNA synthesis

cDNA (complementary DNA) was generated from RNA using the sensiFAST cDNA Synthesis Kit (BIOLINE) according to manufacturer's instructions. Where possible the input amount of RNA was 900ng for all the samples. For aortic arch and thoracic aorta derived RNA the input amount was 400ng and 350ng respectively, due to low RNA yield. In brief each reaction was prepared on ice and required nµl of RNA, 4µl of 5x TransAmp buffer, 1µl of Reverse transcriptase and DNase/RNase free water up to 20µl. A reaction without reverse transcriptase was used as a control for genomic contamination. The mixture was incubated in a thermal cycler under the following conditions. 25°C for 10 min (primer annealing), 45°C for 15 min (reverse transcription) followed by 85°C for 5 min (enzyme inactivation).

2.3.4 Genomic DNA isolation

Mouse ear snips taken for identification purposes were used for DNA extraction. 70µl of 0.05M NaOH was added to each sample and incubated at 95°C for 15 min. The samples were left to cool to room temperature. 7µl of 1M Tris (pH7.5) was then added to each sample. Samples were stored at 4°C until needed.

2.3.5 DNA gel extraction and sequencing

In order to verify the amplified products corresponded to human HH1PL1 and mouse Hhip1, Sanger sequencing was performed. For this purpose, the PCR products were electrophoresed on 1% agarose gel and the subsequent band were excised from the gel under a UV lamp and DNA was. The DNA was then extracted from the gel using the GeneJET Gel Extraction Kit (Thermo scientific) according to the manufacturer's instructions. DNA concentration was determined using a NanoDrop 8000 spectrophotometer. Sequencing was performed by the Protein Nucleic Acid Chemistry Laboratory (PNAACL) of the University, using sequencing primers (0.4ng/µl) described in section 2.3.6 (**Table 2.4**). The sequences were analysed using the CHROMAS software.

2.3.6 Primer design

Mouse *Hhip1* primers for RT-PCR and qPCR were designed based on the sequences published on GenBank or Ensemble using NCBI primer designing tool (<https://www.ncbi.nlm.nih.gov/tools/primer-blast/>). *Hhip1* genotyping primers were provided by KOMP. Primer sequences for the housekeeping genes (*B2m*, *Rpl4*, *36b4*) were published by Erbilgin *et al* (2013) or requested directly from the authors. *Ldlr* (Stock number: 002207) and *ApoE* (Stock number: 002052) genotyping primers were provided by the Jackson laboratory. Human *HH1PL1* primers were designed based on the sequences published on GenBank or Ensemble using the Primer3 (<http://bioinfo.ut.ee/primer3/>) software. Primer sequences for the housekeeping gene *PSMB4* were kindly provided by Dr. Veryan Codd in the department.

The cloning primers were designed based on the published sequences of the human *HH1PL1* and *SHH* (GenBank) and the instructions provided by the Protein Expression laboratory of the University (PROTEX). The same principal

applies to all cloning and requires three steps. First the vector backbone was chosen. Then a 5' vector homology region for forward and reverse primers was provided by PROTEX according to the family vector chosen. The last step required the design of the insert homology region at the end of each vector homology region. The insert homology region was 15-25 bp (longer if AT rich, shorter if GC rich) ensuring that 8bp at the 3' end were unique and the last nucleotide at this end was either an A or T. Moreover, the stop codon was omitted from the reverse insert homology sequence.

The sequencing primers were designed according to the desired read length. In cases where only the start and the end of the gene sequence was required the primers annealing to the vector homology ends were provided by PROTEX. In cases where the entire length of the gene was sequenced the primers were designed using the Primer 3 tool and the published gene sequences (**Table 2.4**).

NCBI Reference sequence	Gene	Species	Primer name (Sequence 5'-3')	Product length (bp)	Annealing temperature	Use
NM_001044380	Hedgehog interacting protein like-1(Hhip1)	Mouse	ODA1: ACTTCATGTCCACGGGTGTT ODA2: CTCCTCACCTTCACCTGAGC	127	55°C	RT-PCR/qPCR/Sequencing
NM_001127258	Hedgehog interacting protein like-1(HHIPL1)	Human	ODA3: GGGAGCTGTACTTCATGTGCG ODA4: CGGGATGAACTTTTCTTTGG	197	55°C	qPCR
NM_001127258	Hedgehog interacting protein like-1(HHIPL1)	Human	ODA5: ACTTCATGTGCGACAGGGGAG ODA6: TGGGCACAAAGGGGATGAG	150	57 °C	RT-PCR/sequencing
NM_002796.2	Proteasome subunit beta 4 (PSMB4)	Human	ODA7: GCTGATGGAGAGAGCTTCCT ODA8: GAACGGGCATCTCGGTAGTA	203	58 °C	RT-PCR/qPCR

NM_009735	Beta-2 microglobulin (B2m)	Mouse	ODA9: GCAGGTTCAAATGAATCTTCAGAGCAT ODA10: TACGTAACACAGTTCCACCCGCCTC	264	55°C	qPCR
NM_007475.5	Ribosomal protein, large, P0 (36b4)	Mouse	ODA11: TGAAGCAAAGGAAGAGTCGGAGGA ODA12: AAGCAGGCTGACTTGTTGCTTTG	91	55°C	qPCR
NM_024212	Ribosomal protein L4 (Rpl4)	Mouse	ODA13: CGCAACATCCCTGGTATTACT ODA14: ACTTCCGAAAGCACTCTCCG	115	55°C	RT- PCR/qPCR
NP_414878.1	Beta-D- galactosidase (lacZ)	Escherichi a coli	ODA15: ACTCTGGCTCACAGTACGCGT ODA16: CAGCGTTCGACCCAGGCGT	350	59°C	RT-PCR
NM_001044380	Hedgehog interacting protein like-1(Hhip1)	Mouse	ODA17: CCAACATGGTAGGACTGACTAGGGC ODA18: TGCCTGCCTTCTATCATCCATTTGC	531	55°C	Genotyping (wild type allele)

NM_001044380	Hedgehog interacting protein like-1(Hhip1)	Mouse	ODA19: GGGATCTCATGCTGGAGTTCTTCG ODA20: TGCCTGCCTTCTATCATCCATTTGC	509	50°C	Genotyping (knockout allele)
NM_001252658	Low density lipoprotein receptor (Ldlr)	Mouse	ODA21: CCATATGCATCCCCAGTCTT ODA22: AATCCATCTTGTTCAATGGCCGATC ODA23: GCGATGGATACACTCACTGC	multiple	55 °C	Genotyping (Knockout and mutant allele)
NM_009696	Apolipoprotein-e (ApoE)	Mouse	ODA24: GCCTAGCCGAGGGAGAGCCG ODA25: GCCGCCCGACTGCATCT ODA26: TGTGACTTGGGAGCTCTGCAGC	multiple	55 °C	Genotyping (Knockout and mutant allele)
N/A	HHIPL1-GFP	Human seq insert	ODA27: ATTGCTTCCACCCAGC ODA28: CTCCTCGAACTTGTTCTGGCC ODA29: CAACATGTGGCGCTGCTC ODA30: GACGATGTGCGCTGCGCG ODA31: TTCCTGGCACAGCAGGTC	N/A	N/A	Sequencing
N/A	HHIPL1-FLAG	Human seq insert	ODA32: CCACCCGGCTGATGTTCA ODA33: ACTGCTTCCCTTACCTGCTG ODA34: AACCAGCCTCAAACCACAAC ODA35: GTCCACCTCCTCGAACTTGT ODA36: CACACGTTGGCAAGTCG ODA37: CCTGTCGACATGAAGTACAGC	N/A	N/A	Sequencing

N/A	SHH-GFP	Human seq insert	Provided by PROTEX	N/A	N/A	Sequencing
N/A	HHIPL1-GFP	Human seq insert	ODA38:CTACCGGACTCAGATCTCGAGATGGCCCGGGCCAG GGCCGGGGCGCT ODA39:TACCGTCGACTGCATGAATTCAGGTCGGGGTTCT GGTGGCT	N/A	N/A	Cloning
N/A	HHIPL1-FLAG	Human seq insert	ODA40:ACCCAAGCTTGGTACCATGGCCCGGGCCAGGGCC GGGGCGCT ODA41:AAAATACAGTTCTCGAGCAGGTCGGGGTTCTGGT GGCT	N/A	N/A	Cloning
N/A	SHH-GFP	Human seq insert	ODA42:CTACCGGACTCAGATCTCGAGATGCTGCTGCTGGC GAGATGTCT ODA43:TACCGTCGACTGCATGAATTCGCTGGACTTGACCG CCAT	N/A	N/A	Cloning

Table 2.4 Primer sequences.

Shown are the NCBI gene reference number, the sequences for each primer pair, the length of the PCR product and the optimal annealing temperatures. The purpose of each primer pair is also indicated. Seq: sequence, N/A: not applicable

2.3.7 Genotyping of *Hhip1* transgenic mice

Two PCR reactions were performed upon genomic DNA previously extracted (section 2.3.4). The first reaction detected the *Hhip1* wild type allele whilst the second reaction detected the knockout allele. Each reaction was performed as detailed in **Table 2.5**.

Component	Volume (μ l)
Genomic DNA	1
MyTaq DNA polymerase (5u/ μ l, Bioline)	0.5
MyTaq reaction buffer (5X Bioline)	5
Forward primer (10 μ M)	1
Reverse primer (10 μ M)	1
Ultra-pure H ₂ O	16.5
Total	25

Table 2.5 PCR recipe for *Hhip1* genotyping.

For detection of wild type and knockout *ApoE* and *Ldlr* allele two PCR reactions were performed using a *Taq* polymerase master mix (1.1 X ReddyMix, Thermo scientific). Each reaction was performed as detailed in **Table 2.6**.

Component	Volume (µl)
ReddyMix reagent (1.1X Thermo scientific)	15
Forward primer (10µM)	1
Reverse primer (10µM)	1
Total: 15µl of the above master mix + 1µl genomic DNA	16 µl

Table 2.6 PCR recipe for *Ldlr* and *ApoE* genotyping.

Primer pair details for all PCRs described above are shown in **Table 2.7**. All reactions were incubated in a thermal cycler (G-Storm GS4, G-Storm, UK) according to the conditions shown in the **Table 2.7**. PCR products were visualised by electrophoresis in a 1% agarose gel and the ladder used was the PCR Sizer 100 bp DNA Ladder (Norgen)

Gene/ Primer name	Taq Polymerase	PCR (profile)
<i>Hhip1</i> (wild type allele) ODA17/ODA18	MyTaq, Bioline	94°C 5min; 35 cycles {94°C 15s, 55°C 30s, 72°C 40s} 72°C 5 min
<i>Hhip1</i> (knockout allele) ODA19/ODA20	MyTaq, Bioline	94°C 1min; 35 cycles {94°C 30s, 50°C 30s, 72°C 1min} 72°C 10 min
<i>Apoe</i> ODA24/ODA25/ODA26	ReddyMix, Thermo scientific	95°C 1min; 35 cycles {95°C 30s, 55°C 30s, 72°C 30s} 72°C 10 min
<i>Ldlr</i> ODA21/ODA22/ODA23	ReddyMix, Thermo scientific	95°C 1min; 35 cycles {95°C 30s, 55°C 30s, 72°C 30s} 72°C 10 min

Table 2.7 PCR conditions for genotyping.

2.3.8 Reverse Transcription PCR (RT-PCR)

RT-PCR was performed using a *Taq* polymerase master mix (2X ReddyMix, Thermo scientific). Each reaction was performed as described below in **Table 2.8**.

Component	Volume (μ l)
ReddyMix reagent (1.1X Thermo scientific)	15
Forward primer (10 μ M)	1
Reverse primer (10 μ M)	1
Total: 15 μ l of the above master mix + 1 μ l cDNA (45ng/ μ l)	16

Table 2.8 RT-PCR recipe using ReddyMix polymerase.

Alternatively, RT-PCR was performed using a different *Taq* polymerase. For each reaction a master mix was prepared as described below in **Table 2.9**.

Component	Volume (μ l)
cDNA (45ng/ μ l)	1
MyTaq DNA polymerase (5u/ μ l, Bioline)	0.1
MyTaq reaction buffer (5X Bioline)	4
Forward primer (10 μ M)	1
Reverse primer (10 μ M)	1
Ultra-pure H ₂ O	12.9
Total	20

Table 2.9 RT-PCR recipe using MyTaq polymerase.

Primer pair details for all RT-PCRs described above are shown in **Table 2.10**. All reactions were incubated in a thermal cycler (G-Storm GS4, G-Storm, UK) according to the conditions shown in **Table 2.10**. PCR products were visualised by electrophoresis in a 1% agarose gel and the ladder used was the PCR Sizer 100bp DNA Ladder (Norgen)

Gene (Primer name)	Taq Polymerase	RT-PCR (profile)
<i>HHIPL1</i> (ODA5/ODA6)	ReddyMix, Thermo scientific	95°C 1min; 35 cycles {95°C 15s, 57°C 30s, 72°C 40s} 72°C 10 min
<i>PSMB4</i> (ODA7/ODA8)	MyTaq, Bioline	95°C 1min; 40 cycles {95°C 15s, 58°C 15s, 72°C 30s} 72°C 10 min
<i>Hhip1</i> (ODA1/ODA2)	ReddyMix, Thermo scientific	95°C 1min; 35 cycles {95°C 30s, 55°C 30s, 72°C 30s} 72°C 10 min
<i>Rpl4</i> (ODA13/ODA14)	ReddyMix, Thermo scientific	95°C 1min; 35 cycles {95°C 30s, 55°C 30s, 72°C 30s} 72°C 10 min

Table 2.10 RT-PCR conditions for each gene.

2.3.9 Quantitative-PCR (qPCR)

2.3.9.1 Standard curve analysis

For all different primer pairs, a melt curve analysis was performed initially and the PCR products were also electrophoresed on a 1% agarose gel.

For standard curve analysis, a 2- fold dilution series was used to obtain 6 different template concentrations starting from 150ng. The linear range of each reaction was calculated by plotting the number of cycles (Ct values) against the Log_{10} of the template concentration. The line of regression was calculated to determine the linearity of the data (known as R^2), an R^2 value greater than 0.98 indicated good linearity. The slope of the standard curve was also used to determine the amplification efficiency of the reaction. A standard curve slope of -3.32 indicates a PCR reaction with 100% efficiency, according to the formula $E = (10^{-1/\text{slope}} - 1) \times 100$ (Smith et al. 2006). A concentration that fell within the middle of the linear range was used for downstream analysis (see **Table 2.11**). The standard curves of the housekeeping genes and the gene of interest were compared in order to assure that the efficiency of all the reactions was similar. Moreover, a melt curve was performed in order to check the specificity of the primers and the presence of one product only. **Figure 2.2** shows a representative example of a standard curve and melt curve, in this case for *Rpl4* gene.

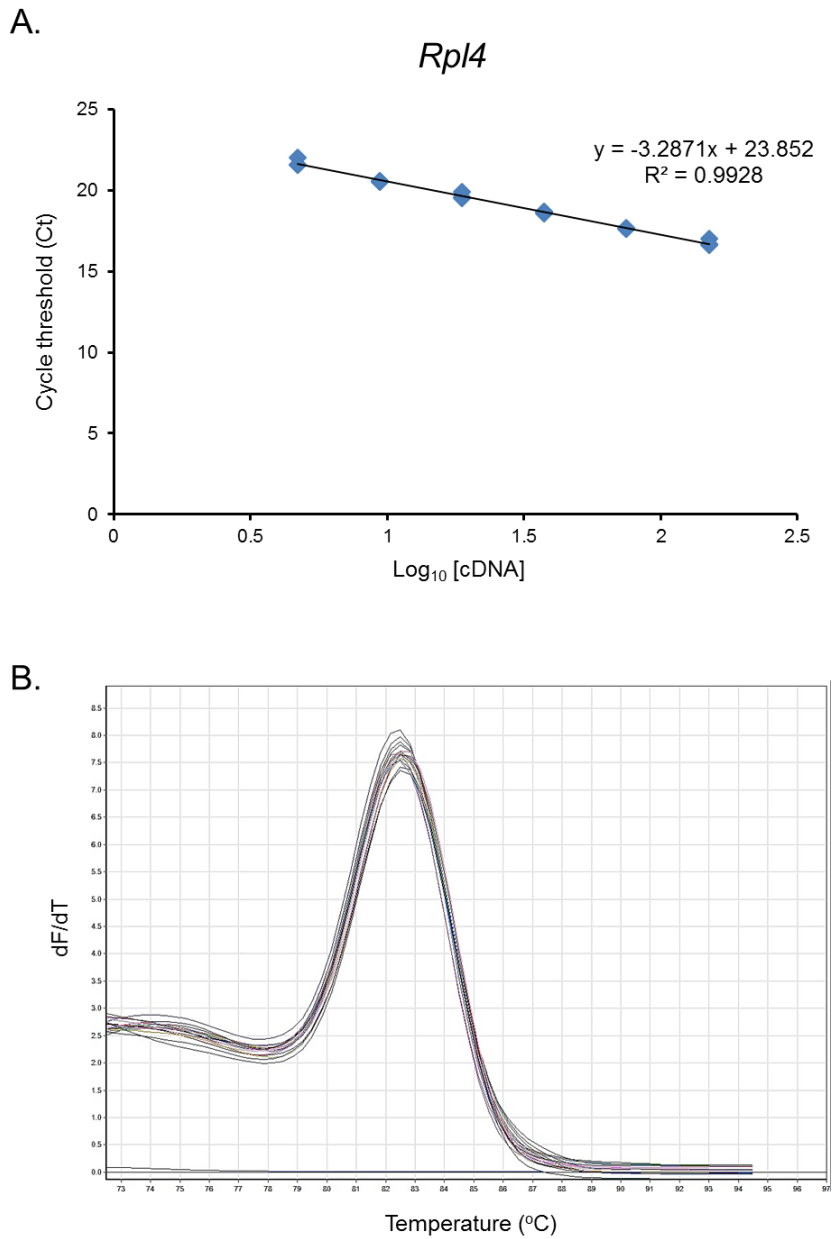


Figure 2.2 *Rpl4* standard curve and melt curve

A) Standard curve for qPCR analysis of a 2-fold dilution series using primers for the mouse housekeeping *Rpl4* quantification. The slope is -3.2871 and the linear correlation coefficient is 0.9928. B) Melt curve profile of the *Rpl4* gene shows only one amplification peak indicative of a specific product.

2.3.9.2 qPCR conditions

The SensiMix SYBR No-Rox (BIOLINE) master mix containing the SYBR Green I dye, dNTPs, stabilisers and enhancers was used for qRT-PCR. All reactions were performed using the Rotor-Gene system (Qiagen). Each reaction contained 12.5µl SensiMix SYBR No-Rox (2X), the appropriate amount of each primer and cDNA and water up to a total volume of 25µl (see **Table 2.11**). All reactions were conducted in triplicates.

Gene (Primer name)	cDNA concentration	Primer concentration	qPCR (profile)
<i>HHIPL1</i> (ODA5/ODA6)	20ng	600nM	3 step; 40 cycles {95°C 15s, 55°C 15s, 72°C 30s}
<i>PSMB4</i> (ODA7/ODA8)	20ng	600nM	3 step; 40 cycles {95°C 15s, 58°C 15s, 72°C 30s}
<i>Hhip1</i> (ODA1/ODA2)	40ng	600nM	3 step; 40 cycles {95°C 15s, 55°C 15s, 72°C 30s}
<i>Rpl4</i> (ODA13/ODA14)	15ng	300nM	3 step; 40 cycles {95°C 15s, 55°C 15s, 72°C 30s}

Table 2.11 qPCR conditions for each gene

Shown are the optimal primer concentration, cDNA template concentration and the qPCR profile for each gene.

All the reactions were incubated in a Rotor-Gene according to the general conditions shown in **Table 2.12**. Melt curve analysis was performed collecting all fluorescence values from 72°C to 95°C, rising by one degree each time.

Temperature	Time	Notes	Cycles
95°C	15 sec	Dissociation	40
x°C	15 sec	Primer annealing	
72°C	30 sec	Elongation (acquiring to Cycling A)	
Collect endpoint fluorescence value			

Table 2.12 qPCR cycling conditions.

Comparative quantitation was performed using the Rotor-Gene software. This method is based on the amplification efficiency of each reaction. Therefore, the efficiency for each individual sample was calculated based on the rate of fluorescence change and the mean efficiency across the run. The software determines a “take off” value (start of the exponential phase), thus avoiding potential bias being introduced when manually setting a threshold for Ct. The slope of the line from the take off point until the end of the exponential amplification was used the amplification efficiency. For each reaction an appropriate sample was set as calibrator and in order to correct for variation in starting amount all samples were normalised to housekeeping genes.

2.3.9.3 Housekeeping gene validation

Three mouse housekeeping genes were tested; Beta-2 microglobulin (*B2m*), ribosomal protein, large, P0 (*36b4*) and ribosomal protein L4 (*Rpl4*) (Erbilgin et al. 2013) The expression of all three genes was tested in a panel of different tissues under different experimental conditions. Conditions assessed include expression in *Apoe*^{-/-} mice verses age matched wild types and *Hhip1*^{-/-} mice

verses wild type littermates. The amplification efficiency of all three housekeeping genes was compared in *ApoE*^{-/-} mice verses age matched wild types and *Hhip1*^{-/-} mice verses wild type and it was found that *Rpl4* was the most stably expressed gene across all experimental conditions. This was also confirmed using the Normfinder algorithm (Andersen, Jensen & Orntoft 2004) . The human *PSMB4* was previously validated in the laboratory.

2.4 Microbiology

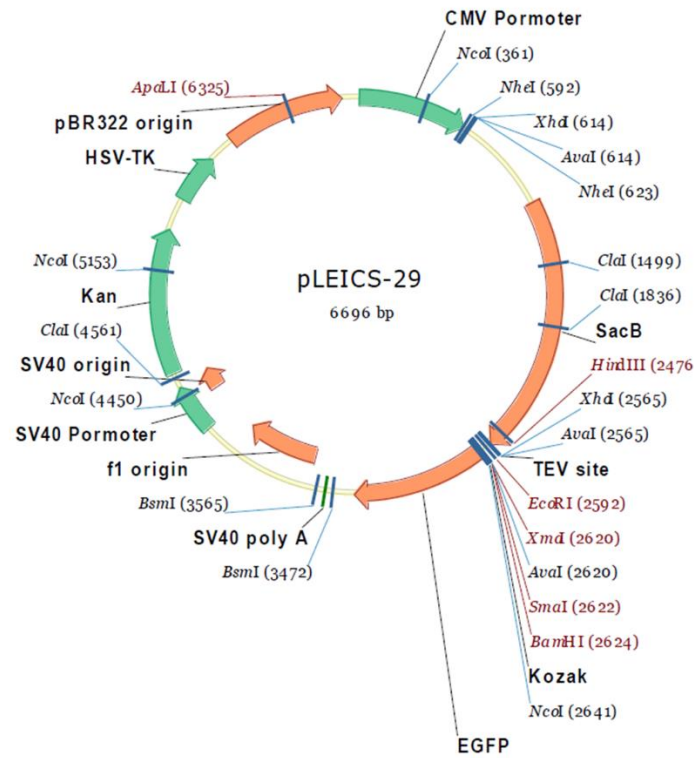
2.4.1 Plasmid cloning

Full-length human *HHIPL1* cDNA (Genscript, NM_001127258) was cloned by ligation independent cloning into two different plasmid vectors by PROTEX at the University of Leicester, using primers described in section 2.3.6. The first plasmid vector contained a C-terminal GFP-tag sequence (pLEICS-29) (**Figure 2.3 A**), whilst the second contained a c-terminal FLAG-tag sequence (pLEICS-49) (**Figure 2.3 B**).

Full-length human *SHH* (pANT7_cGST plasmid, HsCD00005768, DNASU). was cloned into pLEICS-29 by PROTEX using primers described in section 2.3.6.

pLEICS-29/HHIPL1, pLEICS-49/HHIPL1 and pLEICS-29/SHH plasmids are referred to as HHIPL1-GFP, HHIPL1-FLAG and SHH-GFP respectively.

A.



B.

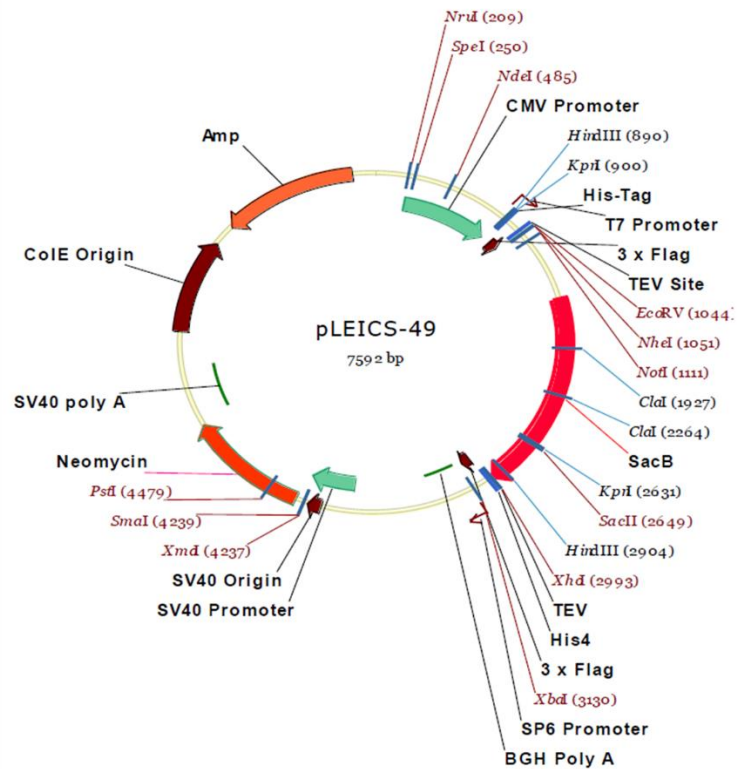


Figure 2.3 Plasmid maps used for HHIPL1 and SHH cloning

The full length of HHIPL1 was cloned in both vectors (A&B) whereas SHH was cloned in pLEICS-29 (B).

2.4.2 Bacterial plasmid transformation

Each of HHIPL1-GFP, HHIPL1-FLAG and SHH-GFP plasmids were transformed into DH5 α *E. coli* cells (BioLine) by combining 50 μ l of DH5 α cells with ~200ng of plasmid DNA. The sample was mixed gently, and incubated on ice for 30 min. Then, the sample was heated at 42°C for 45 seconds on a heat block, followed by 2 min on ice. 100 μ l of 2.5% sterile Luria Broth (LB, Sigma Aldrich) media in water was added and the sample was incubated at 37°C in a shaking incubator (200 rpm) for 1 hour. 100 μ l of transformed cells were plated on LB agar (2.5% LB, 1.5% agar, Difco, 0.1mg/ml ampicillin or 0.5mg/ml kanamycin, Sigma Aldrich) plates and incubated at 37°C overnight. Following this, a single colony was picked and cultured in 5ml LB media supplemented with 0.1mg/ml ampicillin or 0.5mg/ml kanamycin in universal tubes overnight. A glycerol stock was taken from one of the tubes for long-term storage of the transformed bacteria by combining 600 μ l 100% glycerol with 400 μ l of culture and storing at -80°C. The remaining culture was used for plasmid preparation using the Qiaprep spin miniprep kit (Qiagen), according to the manufacturer's instructions. DNA concentration was determined using a NanoDrop 8000 spectrophotometer. Eluted plasmid was stored at -20°C.

2.4.3 Plasmid Midiprep extraction

For larger scale plasmid extraction, a single colony was inoculated into a 10 mL LB/selective antibiotic and cultured at 37°C in a shaking incubator (200 rpm) overnight (16-21 hours). 200-500 μ l (depending on whether the plasmid is of low or high copy number) of the starting culture was inoculated into a 100mL LB/selective antibiotic and cultured at 37°C in a shaking incubator (200 rpm) overnight (16-21 hours). Subsequent plasmid extraction was performed with the PureYield™ Plasmid Midiprep System (Promega) according to the manufacturer's instructions. DNA concentration was determined using a NanoDrop 8000 spectrophotometer. Eluted plasmid was stored at -20°C.

2.4.4 Plasmid sequencing

Plasmids were sequenced by PNAFL at the University of Leicester, using primers (0.4ng/μl) described in 2.3.6 (**Table 2.4**). The sequences were analysed using the CHROMAS software.

2.5 Animal preparations

2.5.1 Animal model

All work involving animals was performed under under Project Licence 60/4332. A genetically altered mouse strain was generated from ES cells (*Hhip1*^{tm1a(KOMP)Wtsi}) purchased from The Knock Out Mouse Project (KOMP). All work reported here has been carried out on mice carrying the knock out first allele (*Hhip1*^{tm1a(KOMP)Wtsi}) which will now be referred to as *Hhip1*^{-/-}.

2.5.2 Mouse husbandry

Mouse husbandry was undertaken according to the Home Office Code of Practice for the Housing and Care of Animals Bred, Supplied or Used for Scientific Purposes. Mice were identified by the genotyping of ear snips (section 2.3.6.1) and the following breeding pairs set up to obtain the experimental genotypes;

- *Hhip1*^{+/-};*[*gene*]^{-/-} x *Hhip1*^{+/-};*[gene]*^{-/-}
 - *Hhip1*^{-/-};*[gene]*^{+/-} x *Hhip1*^{-/-};*[gene]*^{+/-}
 - *Hhip1*^{+/+};*[gene]*^{+/-} x *Hhip1*^{+/+};*[gene]*^{+/-}
- **[gene]*: *Ldlr* or *ApoE*

Western diet (IPS ltd) contained 19.8% fat, 18% protein, 6.7% fiber, 51.3% carbohydrates, 0.15% cholesterol. Mice of the same genotype and sex were housed together when on study.

2.5.3 Non invasive blood pressure measurement

Mouse holders were put into the cages at least 24 hours before blood pressure measurement in order for the mice to acclimitise. Conscious mice were then placed into the holders and the blood pressure measured using CODA-4.0 equipment (Kent Scientific Corporation, Connecticut, USA) according to the manufacturers instructions. This system involves placing a cuff on the animal's tail to occlude the bloodflow where upon deflation, a Volume Pressure Recording (VPR) sensor, placed distal to the occlusion cuff, records the blood pressure. The sensor measures six parameters simultaneously: systolic blood pressure, diastolic blood pressure, mean blood pressure, heart pulse rate, tail blood volume, and tail blood flow (Malkoff 2005). A standard program of 5 acclimitisation cycles followed by 15 cycles of measurements (with 5 sec between cycles and a deflation time of 15 sec) was used. The CODA system contains an algorithm that detects unexpected VPR readings due to mouse movement and rejects these as measurements; a mouse was deemed to have been successfully measured if the system had 'accepted' the results from at least 10 cycles. Mice were rejected where the systolic blood pressure standard deviation was greater than 30.

2.5.4 Mouse termination

At the end of the atherosclerosis study, mice were terminated by exsanguination (vena cava bleed) under isoflurane anaesthesia. The legislated procedure (under Project Licence 60/4332) was performed by the animal unit staff and death was also confirmed by cervical dislocation.

2.6 Tissue dissection

2.6.1 *En face* preparation of the aorta

The thoracic aorta was removed from the mouse and fixed overnight in 4% (w/v) PFA in PBS. Minor branches were cut off and the adventitia was removed. The aorta was then opened longitudinally along the inner curvature of the arch and down the length of the aorta. In order to obtain a flat preparation a second incision was made along the outer curvature of the arch. All the above

dissection was performed under a stereo DM80 Leica microscope.

2.6.2 Aortic root preparation

To separate the heart from the aorta the anterior aspect of the heart was placed toward the operator and the aorta was cut 2mm away from the point at which it emerged from the heart tissue. A scalpel was then used in order to cut away 70% of the ventricular tissue leaving the upper part of the heart intact. The dissected aortic roots (see section 2.7.1) were embedded cut side down

2.7 Histology

2.7.1 Tissue preparation (frozen)

All tissues to be prepared for frozen sectioning were placed into Peel-A-Way tissue moulds (Fisher), cut side down and immersed in cryoprotective compound, (OCT-optimal cutting temperature compound, Thermo scientific). The tissue was then snap frozen in a dry ice- ethanol bath and then placed at -80°C until required.

2.7.2 Sectioning of frozen samples

All embedded frozen samples were sectioned at 10µm and collected onto polysine slides (Fisher Scientific). In particular, 10µm thick aortic root sections were collected from the appearance of the aortic sinus (identified by the appearance of aortic cusps (**Figure 2.4**), which was deemed point zero. From here every section was collected and sequentially placed on 10 polysine slides. This was repeated nine times in order to obtain 900µm of aortic length. Ultimately 90 sections were collected onto 30 slides and each slide carried 3 sections with 100µm intervals (**Figure 2.5**) (Daugherty, Whitman 2003). All sections were stored at -80°C until further analysis. For downstream plaque composition analysis 3 slides (spanning ≈900µm) carrying 3 sections each were used. For example for ORO analysis slides 90-390-690 were used.

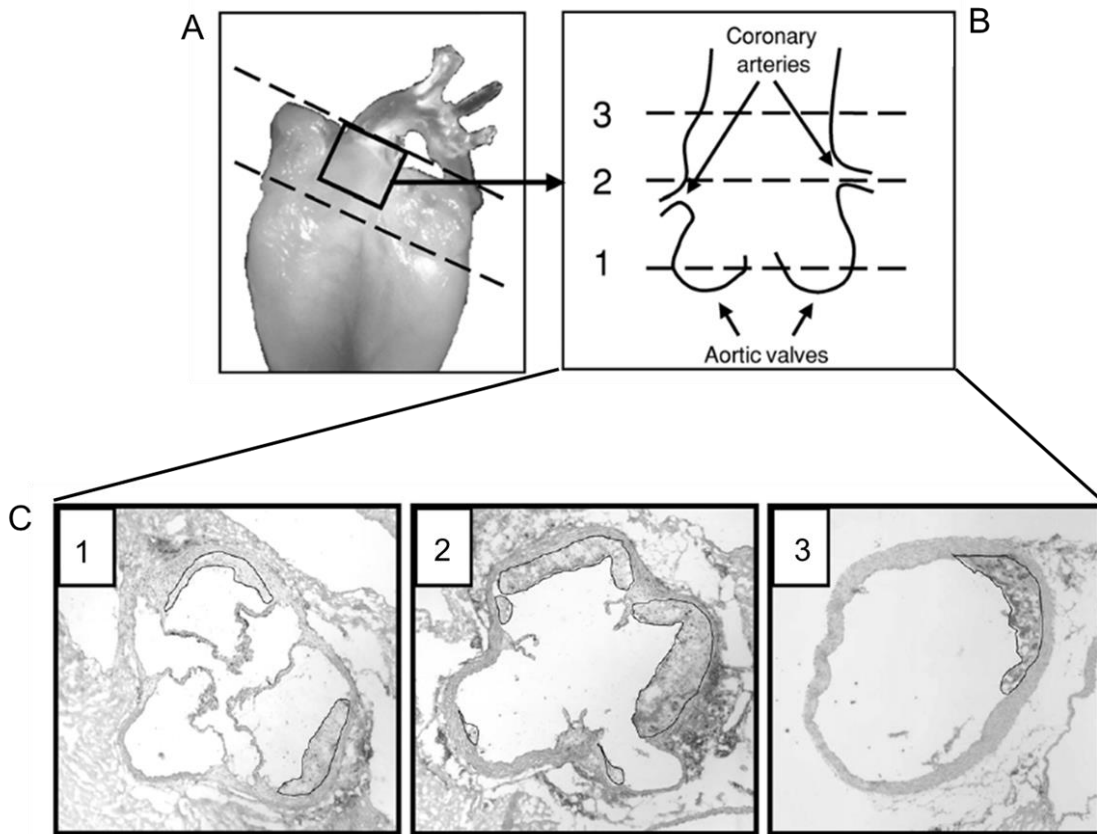


Figure 2.4 Schematic representation of the aortic root orientation and sectioning

A) During gross dissection, the heart was cut as indicated by dotted lines. B) Diagrammatic representation of the aortic root. The dotted lines correspond to the labelled 1, 2 and 3 in (C) (Adapted from Daugherty, Whitman 2003).

Aortic root sectioning

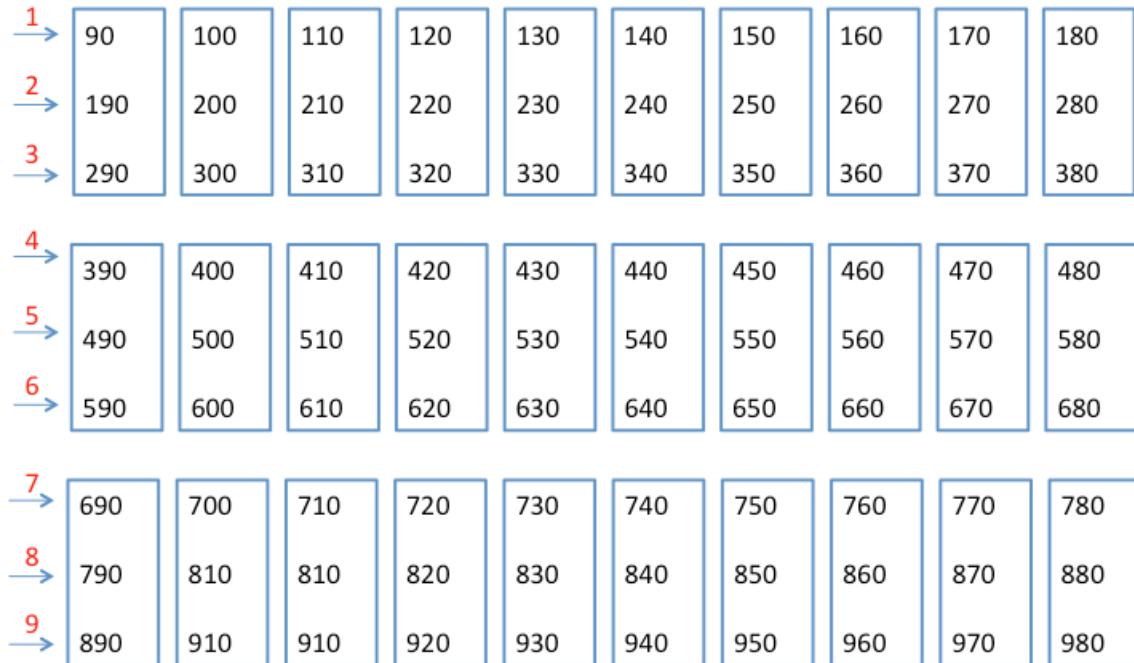


Figure 2.5 Schematic representation of aortic root sectioning

90 aortic root sections (10µm thick) were obtained from zero time point (90) up to a region in the ascending aorta. Numbering in red indicates the nine sequential cycles of tissue collection.

2.7.3 Oil Red O (ORO) staining of the aorta

Following en face preparation the aorta (section 2.6.1) was stained with Oil Red O. Aortas were briefly rinsed in water and incubated in 60% isopropanol for 2 min. Following this, aortas were incubated in 60% ORO [100% ORO Sigma (1g in 100 mL 99% isopropanol) diluted in H₂O]. Stained aortas were then pinned out on a Sylgard® coated petri dish using entomological pins. Aorta images were taken using a DM800 Leica microscope and the percentage of aortic area stained red (aortic area stained red/whole aorta size) was calculated using the LAS V 4.0 software.

2.7.4 X-gal staining of frozen sections

Slides carrying frozen sections were dried at room temperature for 20 min slides and then fixed in 2% formaldehyde in phosphate buffered saline (PBS pH 7.2) containing 0.2% glutaraldehyde for 5 min. After fixation slides were washed 3 times in x-gal wash buffer (0.1% deoxycholate – 0.02% Nonidet P-40 – 0.05% bovine serum albumin (BSA)). The slides were then placed in x-gal containing solution (5mM potassium ferrocyanide ($[\text{Fe}(\text{CN})_6]^{4-}$), 5mM potassium ferricyanide ($[\text{K}_3\text{Fe}(\text{CN})_6]^{6-}$) and 1mg/ml x-gal (Fisher) diluted in (DMSO, Sigma Aldrich) and incubated overnight at 37°C. Stained slides were dehydrated in serial ethanol dilutions. 70% ethanol for 10 min followed by two washes in 90% ethanol for 10min each and two washes in 100% ethanol for 10min. Slides were cleared twice in 100% xylene (Fisher) for 10 min each and mounted with DPX (Sigma Aldrich).

2.7.5 Immunohistochemical staining of frozen sections for β -galactosidase

Slides carrying frozen sections were dried at room temperature for 20 min slides and then fixed in cold acetone for 10 mins at -20°C. Slides were dried at 10 min at room temperature and washed twice in PBS. Endogenous peroxidase activity was blocked for 10 min in 0.3% H_2O_2 in methanol. Slides were then washed for 5 mins in PBS and tissue was marked with pap pen. Blocking in 10% goat serum (+0.5% Triton-X) was performed for an hour at room temperature. Following blocking slides were incubated with primary chicken polyclonal anti- β -gal (Abcam) diluted 1:1000 in 4% serum at 4°C in a humidified chamber overnight. The slides were then washed in PBS three times (10 min each) and incubated with secondary biotinylated anti-chicken (Vector labs) diluted 1:500 in 4% serum for 30 min at room temperature. The slides were then washed again in PBS and incubated with horseradish streptavidin-peroxidase ready to use (Vector laboratories) for 30 min. The sections were again washed three times in PBS (10 min each) before being incubated with 200 μl of 3,3'-diaminobenzidin (DAB) (Vector laboratories) and left for no more than 5 min. The DAB was washed away with water and the slides counterstained in haematoxylin (Gill No. 2, Sigma Aldrich) for 30 seconds. After counterstaining serial ethanol

dehydration steps consisting of 10 mins in 70% ethanol, 10 mins in 90% and 10 mins at 100% followed by two xylene (Fisher) washes 10 mins each were performed. Finally, the sections were mounted with DPX. Images were acquired using a DM2500 Leica microscope.

2.7.6 Immunohistochemical staining of frozen sections (MOMA-2 and α -SMA)

Slides carrying frozen sections were dried at room temperature for 20 min slides and then fixed in cold acetone for 10 mins at -20°C. Slides were dried for 20 min at room temperature. Endogenous peroxidase activity was blocked for 10 min in 0.3% H₂O₂ in methanol at room temperature. Slides were then washed for 5 mins in PBS pH 7.5 and tissue was marked with pap pen. Blocking in 2.5% goat serum (Vector Laboratories) for both MOMA-2 and alpha smooth muscle actin (α -SMA) was performed for an hour at 23°C. Blocking buffer was drained off and slides were incubated with primary antibody appropriately diluted in 2.5% goat serum at 4°C in a humidified chamber overnight (see **Table 2.13**). Slides were then rinsed three times in PBS, 5 mins each. Slides were then incubated with the appropriate secondary horseradish peroxidase conjugated antibody (see **Table 2.13**) at 23°C for 30 min. Three PBS washes were then performed and 200 μ l of DAB (Vector laboratories) for no more than 5 min was applied to the slides. After primary antibody incubation the manufacturer's protocol was followed for visualisation. The DAB was washed away with water and the slides counterstained in haematoxylin (Gill No. 2, Sigma Aldrich) for 30 seconds. After counterstaining serial ethanol dehydration steps consisting of 10 mins in 70% ethanol, 10 mins in 90% and 10 mins at 100% followed by two xylene (Fisher) washes 10 mins each were performed. Finally, the sections were mounted with DPX (Lamb, Thermo scientific). Images were acquired using a DM2500 Leica microscope.

For all immunohistochemistry described above tissue incubation without primary and without secondary antibody was performed as a negative controls in order to check specificity of the antibodies.

Primary antibody	Host Species	Supplier	Titration	Secondary antibody	Supplier	Titration	Use
β -galactosidase (polyclonal)	Chicken	Abcam (ab9361)	1:1000	Biotinilated anti-chicken	Vector laboratories (BA-9010)	1:500	IHC-Fr
Intracellular antigen of macrophages and monocytes (MOMA-2 clone)	Rat	BIORAD (MCA519G)	1:250	ImmPRESS HRP anti-Rat IgG Peroxidase	Vector Laboratories (MP-7444)	Ready to use	IHC-Fr
Alpha smooth muscle actin (a-SMA) (polyclonal)	Rabbit	Abcam (ab5694)	1:500	ImmPRESS HRP anti-Rabbit IgG Peroxidase	Vector Laboratories (MP-7451)	Ready to use	IHC-Fr

Table 2.13 Primary and secondary antibodies used for immunohistochemistry

Shown are the primary antibodies, host species, titration and the corresponding secondary antibodies.

IHC-Fr: Immunohistochemistry frozen.

2.7.7 ORO staining of frozen sections

Slides carrying frozen sections were dried at room temperature for 20 min and fixed in 4% (w/v) PFA for 10 min at room temperature. Slides were then immersed in 60% isopropanol for 1-2 mins followed by incubation in 60% ORO [100% ORO, Sigma (1g in 100 mL 99% isopropanol) diluted in H₂O] for an hour at room temperature. Excess of ORO was washed away in running water for 5 mins. Water was drained off and the slides were mounted with aqueous mounting medium (BioGenex). Images were acquired using a DM2500 Leica microscope.

2.7.8 Masson's trichrome staining for frozen sections

Collagen staining was performed using the Masson's Trichrome kit (Sigma-Aldrich). Slides carrying frozen sections were dried at room temperature for 20 min and fixed in 4% (w/v) PFA for an hour at room temperature. In order to intensify the colours slides were incubated in Bouin's solution (Sigma-Aldrich) over night at room temperature. Slides were then washed for 10 min in running water and rinsed in deionized water (ddH₂O). Equal parts of Weigert's Hematoxylin solutions A and B (Sigma-Aldrich) were mixed and applied to the slides for 5min, for nuclei staining. Slides were washed under warm running tap water for 10 min to remove excess of Hematoxylin, followed by ddH₂O rinsing. For cytoplasm staining slides were incubated in Fuchsin solution for 5 min. Three washes in ddH₂O were then performed and slides were incubated for 5 min in Phosphotungstic/Phosphomolybdic solution (1 volume of each solution in 2 volumes of ddH₂O). Following this, slides were stained for 5 min with Aniline Blue Solution to stain collagen in blue. Slides were then washed three times in ddH₂O and incubated for 2 min in 1% glacial acetic acid. Two ddH₂O washes were performed and slides were dehydrated in serial ethanol dilutions including 70% for 1 min, 90% for 1 min, 100% for 1 min and finally cleared in 100% xylene (Fisher) for 5 min. Slides were then mounted with DPX (Lamb, Thermo scientific). Images were acquired using a DM2500 Leica microscope and the percentage of aortic area stained blue (aortic area stained blue divided by the whole aorta size) was calculated using the LAS V 4.0 software.

2.7.9 Image analysis and quantification of histological sections

All histological slides were visualized under a DM2500 Leica microscope and the percentage of staining for ORO, MOMA-2 and α -SMA was quantified using the ImageJ software and macro algorithms for each staining (kindly written by Dr Ir K.R. Straatman, Senior Experimental Officer Advanced Imaging Facility). The main principle applied to all staining analyses required the quantification of staining amount by pixel analysis and subsequent normalisation by the aorta size.

2.8 Statistical analysis

All data from experiments was analysed in both GraphPad Prism 6.00 (GraphPad software Inc.) and Microsoft Excel. Microsoft Office Excel was also used to generate graphs. Results are shown as mean \pm Standard Deviation (SD) unless otherwise stated. SD was chosen as it shows the variation in the individual samples.

2.8.1 *In vitro* data

Statistical significance of the data was assessed by a Student's t-test assuming normal data distribution. In HASMCs migration and proliferation assays, paired t-tests were used to compare the percentage cell coverage (wound area covered by cells) in cells treated with siRNA vs. cells treated with non targeting siRNA control (NTC). A *P*-value <0.05 was considered statistically significant.

2.8.2 *In vivo* data

For atherosclerosis studies, unpaired Student t-tests were used to compare percent lesion area of aorta (*en face*) or actual lesion area (aortic roots) of *Hhpl1*^{-/-} animals to control *Hhpl1*^{+/+} animals for each hyperlipidemic background separately. For lesion compositional analysis unpaired Student t-tests were also used to compare percent of cellular component coverage in *Hhpl1*^{-/-} and *Hhpl1*^{+/+} animals. For *Hhpl1* expression study (qPCR data) one-way Analysis of Variance (ANOVA), was used to compare more than two groups, followed by post-hoc tests (unpaired t-tests).

All values reported in this thesis derived from parametric analysis assuming normal data distribution. However, non-parametric Mann–Whitney test and non-parametric ANOVA (Kruskal -Wallis) were also performed to confirm significant results. A *P*-value <0.05 was considered statistically significant.

Power calculations were used to determine the number of mice per group using the mean SD of the two groups, 80% power and *P*-value ≤ 0.05 . The effect size was estimated from the mean difference between controls and experimental groups.

2.9 *In silico* analysis

2.9.1 Protein domain prediction

For prediction of HHIPL1 protein domains, the reference sequence (Q96JK4.2) from UniProtKB/Swiss-Prot was used for analysis. For prediction of signal peptide sequences and their cleavage sites the *SignalP 4.1* Server (Nielsen et al. 1997, Petersen et al. 2011) (<http://www.cbs.dtu.dk/services/SignalP/>) was used. The *TMHMM 2.0* Server (Sonnhammer, von Heijne & Krogh 1998) (<http://www.cbs.dtu.dk/services/TMHMM/>) was also used for prediction of transmembrane helices.

2.9.2 Protein alignment

Protein sequences for human and mouse HHIP, HHIPL1 and HHIPL2 were obtained from Ensembl and aligned using the CLUSTAL OMEGA alignment tool (<http://www.ebi.ac.uk/Tools/msa/clustalo/>). The MView tool was used to generate the alignment figure (<http://www.ebi.ac.uk/Tools/msa/mview/>).

3 *In vitro* investigation of HHIPL1

3.1 Introduction

GWAS have identified variants at chromosome 14q32 that are associated with CAD. The variants fall within the uncharacterised gene *HHIPL1*, a sequence paralogue of *HHIP*, which encodes a known antagonist of the Hh signalling pathway. Hh signalling is a well-studied developmental pathway, which is implicated in a number of different diseases. Here, the main aim is to investigate *HHIPL1* protein function and test whether it acts through the Hh pathway.

3.1.1 Hh signalling in vasculature maintenance

In addition to its role in the development of the vasculature during embryogenesis (described in section 4.1.2) Hh-mediated angiogenic signalling is essential for the maintenance of adult vasculature. Hh signalling is also reactivated during postnatal vascular repair processes in pathological conditions such as myocardial ischemia, tissue regeneration and inflammation (Mooney et al. 2015). A requirement for Hh signalling during the maintenance of normal coronary vasculature has been demonstrated in adult mice (Lavine, Kovacs & Ornitz 2008). *Shh* was shown to be expressed in fibroblasts in adult heart tissue whereas the target *Ptch1* gene was transcribed in cardiomyocytes and SMCs. The study of *Smo* deficient mice proved that the Hh pathway is responsible for the integrity of coronary vasculature. These mice demonstrated ventricular dilation, increased mortality and reduced fractional shortening (Lavine, Kovacs & Ornitz 2008). The underlying mechanism was deemed to be dependent on cardiac dysfunction and hypoxia (due to reduced vascular density), which resulted in cell death and fibrosis. Moreover, Morrow and colleagues (2009) showed that Hh signalling coordinates expression of Notch target genes via VEGF-A in adult human and rat SMC. Activation of the Hh pathway by SHH (recombinant SHH and/or SHH plasmid) enhanced SMC proliferation and survival and increased the levels of *VEGF-A* and *Hrt-3* (Notch signalling target). These effects were reversed by cyclopamine mediated inhibition of Hh signalling and by inhibition of the Notch pathway (Morrow et al. 2009). In another study, liver derived Shh carrying microparticles promoted changes in angiogenic gene expression in hepatic sinusoidal endothelial cells

(Witek et al. 2009). Shh has also been shown to induce the expression of smooth muscle cell-related markers such as alpha-smooth muscle actin (α -SMA), desmin and myocardin, as well as basement membrane components during the formation of microvessel-like structures in human bone regeneration and vascularisation implicating Hh signalling in blood vessel maturation (Dohle et al. 2011).

3.1.2 Hh signalling in vascular disease

A phenomenon commonly seen in disease pathogenesis is the re-expression of developmental gene regulatory networks (Redmond et al. 2011). The upregulation of Hh signalling following injury has been investigated *in vivo* using mouse models as well as *in vitro* using haemopoietic and vascular cell models. Pola *et al* (2001) demonstrated a role for Shh in angiogenesis in adult tissue following ischemic injury. Exogenous administration of Shh protein in a hind limb ischemia model resulted in enhanced expression of angiogenic genes such as *Ang* and *Vegf* in interstitial fibroblasts resulting in rescue of the limb. The same study also showed that embryonic and adult fibroblasts in culture treated with Shh exhibited upregulated *Ptch* and increased expression of all three isoforms of *Vegf* as well as *Ang1* and *Ang2* (Pola et al. 2001, Lee, Moskowitz & Sims 2007) . In a later study, the same group reported postnatal Shh-induced revascularization and muscle regeneration after induction of hind limb ischemia (Pola et al. 2003). Addition of a Shh inhibitory antibody had a detrimental effect on capillary density and blood flow, due to reduced expression of angiogenic factors, showing that endogenous Shh production in response to ischemia is a physiologically relevant phenomenon. Similar Shh activation was also found in retinal angiogenesis in a retinal ischemia mouse model. Shh promoted physiological angiogenesis and pathophysiological neovascularisation upstream of *Vegf*, which was attenuated by inhibition of Hh signalling with cyclopamine (Surace et al. 2006). Another Hh protein has also been reported to have a major role in ischemia-induced angiogenesis and muscle repair. In this study induction of hindlimb ischemia in *Dhh* deficient mice resulted in impaired limb perfusion. *Dhh* was shown to promote peripheral nerve survival in the ischemic muscle and ultimately maintained the pool of nerve-derived proangiogenic

factors (Renault et al. 2013). Subsequently, the role of Hh signalling in myocardial infarction was also investigated. In rat models of diabetic neuropathy, treatment with Shh protein induced arteriogenesis and restoration of nerve function, suggesting a potential therapeutic role of exogenous Shh (Kusano et al. 2004). The same group investigated the effect of intramyocardial gene transfer of naked DNA encoding human SHH upon the recovery from acute and chronic myocardial ischemia in adult rats. It was found that the Hh signalling pathway was upregulated in fibroblasts and cardiomyocytes resulting in elevated neovascularization and reduced fibrosis and cardiac apoptosis (Kusano et al. 2005). A potential role for Shh during intimal hyperplasia was also been proposed by a different group, which demonstrated that Shh/Gli2 signalling induces arterial vascular SMC (VSMC) proliferation via the Rb/E2F (G(1) cyclin-retinoblastoma axis) pathway during restenosis in both human VSMCs and in a model of mouse restenosis (Li et al. 2010).

Hh signalling has also been reported to be responsive to mechanical loading *in vitro* and to control vascular development *in vivo*. Morrow *et al.* (2007) investigated the role of cyclic strain and pulsatile flow in relation to Hh signalling and growth of adult rat VSMCs in culture. SMCs exposed to cyclic strain and pulsatile flow showed significant decrease in proliferation and increased apoptosis and down regulation of Hh signalling. Treatment with recombinant SHH rescued this effect. This is a significant finding suggesting that biomechanical strain can modulate Hh and thus could be of great importance during arterial remodelling and atherogenesis *in vivo* (Morrow et al. 2007). PTCH-1 was also shown to mediate low flow-induced neointimal hyperplasia via regulation of Notch pathway (Redmond et al. 2013). Inhibition of PTCH-1 either by cyclopamine in human coronary arterial SMC (subjected to low pulsatile flow) or by perivascular delivery of siRNA *in vivo* (in a mouse model of ligation injury) resulted in reduced Notch expression, attenuated SMC proliferation and reduced vascular remodelling.

There is less evidence regarding a direct role for Hh signalling in atherosclerosis. Beckers *et al.* (2007) reported an increase in atherosclerosis in an *Apoe*^{-/-} atherosclerotic mouse model following treatment with the inhibitory Shh antibody (5E1). An increase in the total plaque area in the aortic arch was

concluded to be due to elevated oxidised Ldl uptake in macrophages in a scavenger receptor-mediated manner. Consistent with this result was the observation that activation of the Hh signalling cascade by recombinant Shh caused decreased Ldl uptake, whereas anti-Hh treatment resulted in decreased plasma cholesterol levels. This study suggested that Hh signalling is re-initiated in atherosclerotic plaques and controls plasma lipid levels and atherosclerosis development and progression (Beckers et al. 2007). A later study investigated the status of Hh pathway activity in both human healthy vessels and atherosclerotic plaques (Queiroz et al. 2012). This investigation reported constitutively active Hh signalling in healthy vessels characterised by high mRNA expression levels of the Hh pathway targets *PTCH1* and *GLI1*. *PTCH1* and *GLI1* mRNA expression positively correlated with the expression levels of *IHH* and *DHH*. In contrast, substantial levels of Hh ligand expression were detected in human atherosclerotic plaques but *PTCH1* and *GLI1* levels were low suggesting the existence of an inhibitory mechanism in atherosclerotic plaques.

The findings outlined above are all examples of how the known signalling components and target genes of the pathway mediate Hh signalling during disease. In addition, a small number of studies have identified paradoxical Hh pathway activity, which is reminiscent of the non-canonical pathways (similar to those described in section 3.1.3). *Gli3* heterozygous null mice were reported to have myocardial ischemia, elevated fibrosis, diminished ventricular output and decreased neovascularization compared with wild type littermates (Renault et al. 2009). It was shown that Gli3 induced angiogenesis through Akt and MAP kinase pathways and promoted the transcription of angiogenic proteins (e.g Vegf, and Pdgf), while not affecting known Hh pathway target genes. This outcome was unexpected as Gli3 was believed to be a suppressor of the Hh pathway target genes (Renault et al. 2009). The finding that a supposed transcription suppressor protein of the Hh pathway could in fact comprise Hh-stimulatory action was in agreement with a study from Bijlsma *et al* (2008b). Cyclopamine-mediated inhibition of the pathway resulted in improvement of myocardial ischemia in a mouse model. The beneficial outcome was dependent on reduced fractional shortening, stroke volume and ejection fraction induced by

ischemia- reperfusion and did not affect vascularisation (Bijlsma et al. 2008b). The authors concluded that Hh may possess a dualistic action in cardiac ischemia, in which elevated exogenous levels are capable of tissue repair, whereas endogenous Hh seems to worsen the effect on the coronary artery disease outcome (Bijlsma, Spek 2010).

3.2 Results

3.2.1 *In silico* analysis of HHIPL1

HHIP is a secreted Hh antagonist that consists of an N-terminal signal peptide, a frizzled-like fold, a β -propeller, two epidermal growth factor (EGF) domains and a C-terminal membrane anchor (**Fig 3.1 A**) (Bosanac et al. 2009, Kwong, Bijlsma & Roelink 2014) . HHIPL1 shares 22% sequence identity with HHIP (**Fig 3.1 B**). The sequence homology is restricted to the frizzled-like fold and the β -propeller, which contains the Hh interacting region. Across the Hh interacting region the sequence identity between the two proteins is 43%. HHIPL1 does not contain EGF domains, instead protein domain prediction using SMART identifies a C-terminal scavenger receptor domain.

In silico analysis was also carried out using *TMHMM 2.0* (Sonnhammer, von Heijne & Krogh 1998) (<http://www.cbs.dtu.dk/services/TMHMM/>) and *SignalP 4.1* (Nielsen et al. 1997, Petersen et al. 2011)(<http://www.cbs.dtu.dk/services/SignalP/>). *SignalP 4.1* is a bioinformatics server able to predict the presence and location of signal peptides and cleavage sites in amino acid sequences. Signal peptides control the entry of many eukaryotic and prokaryotic proteins in to the secretory pathway and are found in secreted proteins and proteins of the plasma membrane, lysosomes, endosomes and other organelles of the secretory pathway. The signal sequences are approximately 6-20 amino acids long and often located at the N-terminus of the precursor protein. At the end of the signal sequence of secreted proteins there is an amino acid sequence which is recognised by signal peptidases and cleaved off while the protein translocates through the membrane (von Heijne 1990, Gierasch 1989, Rapoport 1992). The

SignalP 4.1 tool is able to predict signal peptide sequences and their cleavage sites. Using the HHIPL1 reference sequence (Q96JK4.2) from UniProtKB/Swiss-Prot the presence of a signal peptide and its cleavage site was investigated. The three main outcomes of this bioinformatics analysis are; (1) the *C-score*, which refers to cleavage site score and tends to be high at the position immediately after the cleavage site, (2) the *S-score*, which distinguishes the presence of signal peptides from the mature part of the protein and from proteins without signal peptides, and (3) the *Y-score* which is a combined outcome of the *C* and *S* score and a better predictor of a cleavage site. In addition, the tool provides a discrimination score (*D score*), which distinguishes between signal and non-signal peptides. HHIPL1 has high scores for all measurements (>0.5) suggesting the presence of a signal peptide (**Figure 3.2 A**). Non-secreted proteins would have very low scores for all the *SignalP* output measurements (close to 0.1). This signal peptide was predicted to be located at amino acid position 5 with a cleavage site at amino acid position 20.

TMHMM 2.0 is a bioinformatics tool that predicts the location and orientation of alpha helices in membrane-spanning proteins based on a hidden Markov model. The main outputs of this analysis are the number of predicted transmembrane helices (TMH), the number of expected amino acids in the TMH as well as the probability of the existence of a TMH. Using the HHIPL1 reference sequence (Q96JK4.2) from UniProtKB/Swiss-Prot and the THMM2.0 it was found that HHIPL1 lacks a TMH and is very likely to be located outside the cell (**Figure 3.2 B**).

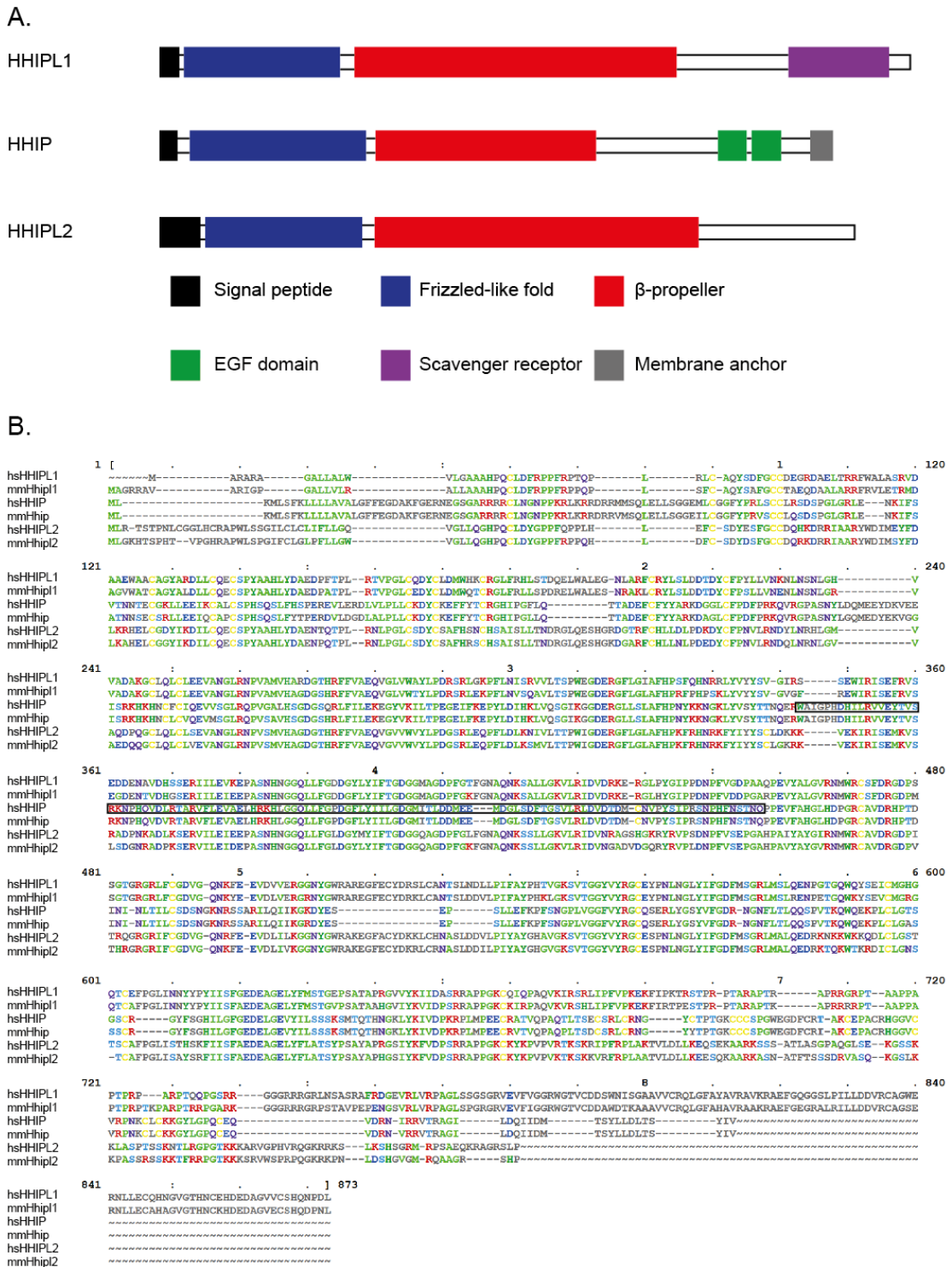


Figure 3.1 HHIP protein family

A) Schematic representation of human HHIPL1, HHIP and HHIPL2 protein domains. B) Comparison of human and mouse HHIPL1, HHIP and HHIPL2 proteins. Human and mouse HHIP proteins were aligned according to amino acids in their sequences conserved between them. Amino acids are colour coded based on their physicochemical properties. (:) Indicates conservation

between groups of strongly similar properties. (·) Indicates conservation between groups of weakly similar properties. The numbers at the right of the alignment indicate the position in the sequence. The hedgehog interacting domain of human HHIP is boxed. hs: human, mm: mouse.

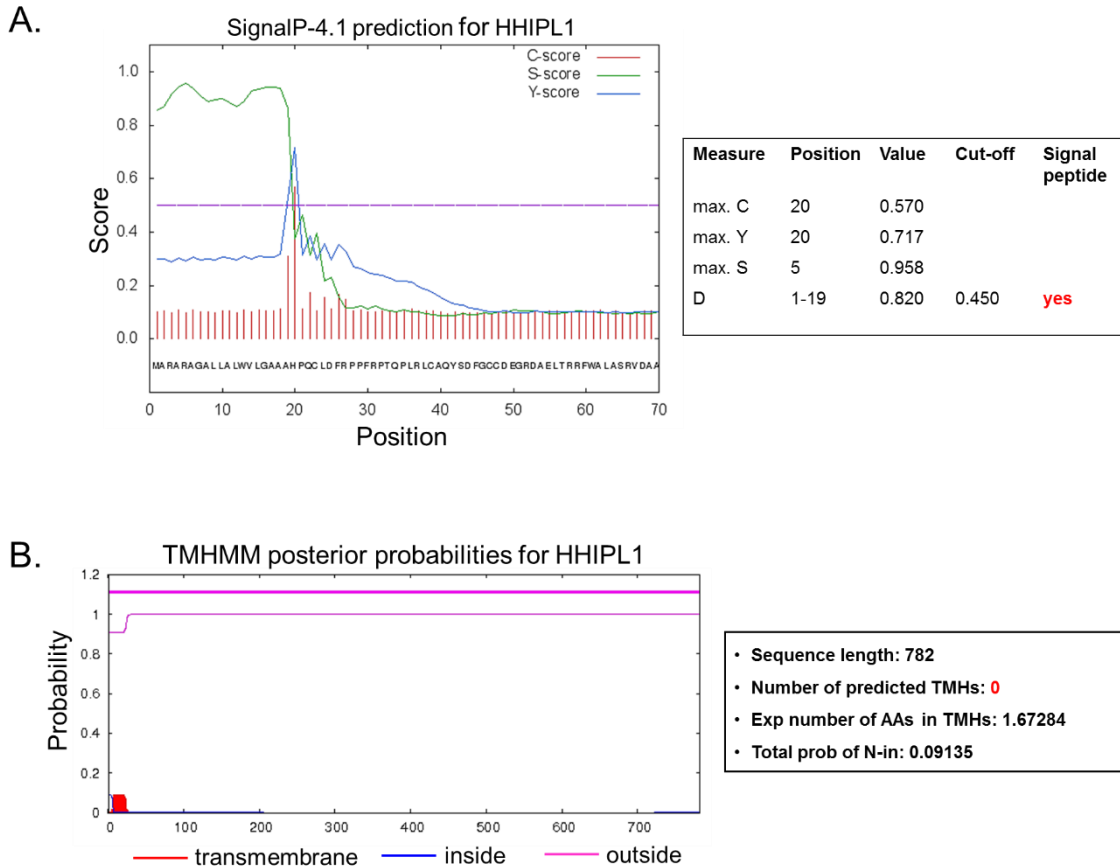


Figure 3.2 *In silico* prediction of HHIPL1 localisation

A) Graphical output of the SignalP 4.1 server, which predicted the presence of a signal peptide and its cleavage sites for HHIPL1. Shown in the table are the values of three different scores, C, Y, S and D, their positions in the amino acid sequence as well as the prediction of a signal peptide. B) Graphical output of the TMHMM 2.0 server, which predicted the lack of a transmembrane domain (posterior probability for such a domain is very low, N-in=0.09). Shown in the table are the sequence length, the number of predicted TMH, the number of expected amino acids (AA) in the TMHs and the probability for the transmembrane domain (N-in).

3.2.2 *In vitro* investigation of HHIPL1 cellular localisation

To confirm that HHIPL1 is secreted its cellular localisation was investigated in HEK293 cells, which do not express *HHIPL1* endogenously (RT-PCR, data not shown). Full-length *HHIPL1* cDNA obtained from Genscript (NM_001127258) was cloned into the pLEICS-29 plasmid, which contains a C-terminal GFP tag (section 2.4.1), to generate a HHIPL1-GFP mammalian expression construct and confirmed by sequencing. The HHIPL1-GFP plasmid was transfected into HEK293 cells using a NEPA21 electroporator. Cells were fixed in 4% PFA 48 hours post transfection and stained with DAPI for nuclei visualisation. Cells were imaged using a confocal microscope and GFP fluorescence was seen in cellular compartments likely to be the Endoplasmic reticulum (ER) and Golgi apparatus (**Figure 3.3 A**). No fluorescence was seen at the cell surface suggesting that HHIPL1 is not associated with the cell membrane.

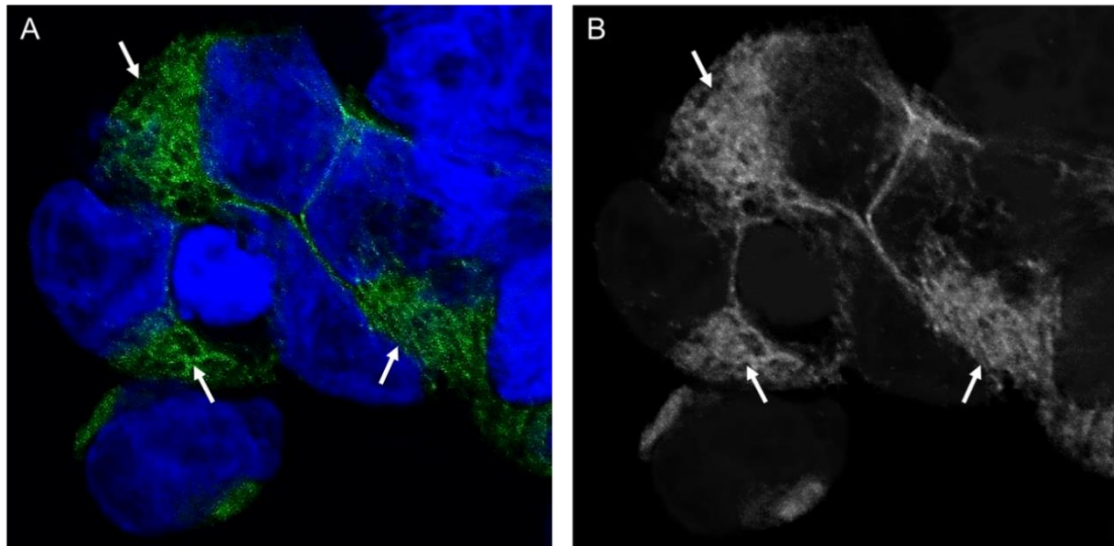


Figure 3.3 Subcellular localisation of HHIPL1

A) Representative confocal images of HEK 293 cells expressing HHIPL1-GFP (green) protein and stained with DAPI (blue). Cellular localisation is consistent with ER and Golgi (white arrows). No staining was observed at the cell surface.

B) Image from (A) depicted in inverted colours.

Next, HHIPL1 localisation was investigated by western blotting. Full-length *HHIPL1* cDNA was cloned into pLEICS-49 plasmid, which contains a C-terminal FLAG tag, as described in section 2.4.1 and confirmed by sequencing. The HHIPL1-FLAG plasmid was transfected into HEK293 cells using Lipofectamine LTX and cell lysates and conditioned media were collected 48-hour post-transfection. Conditioned media was concentrated by TCA precipitation. Proteins were separated by SDS-PAGE electrophoresis followed by western blotting and HHIPL1-FLAG detected using anti-FLAG antibody. HHIPL1-FLAG was seen at the expected size in both cell lysates (**Figure 3.4 lane 1**) and conditioned media (**Figure 3.4 lane 3**) confirming it is a secreted protein. Cell lysates and conditioned media from HEK293 cells transfected with an empty GFP plasmid vector were used as a negative control (**Figure 3.4 lane 2 and 4**).

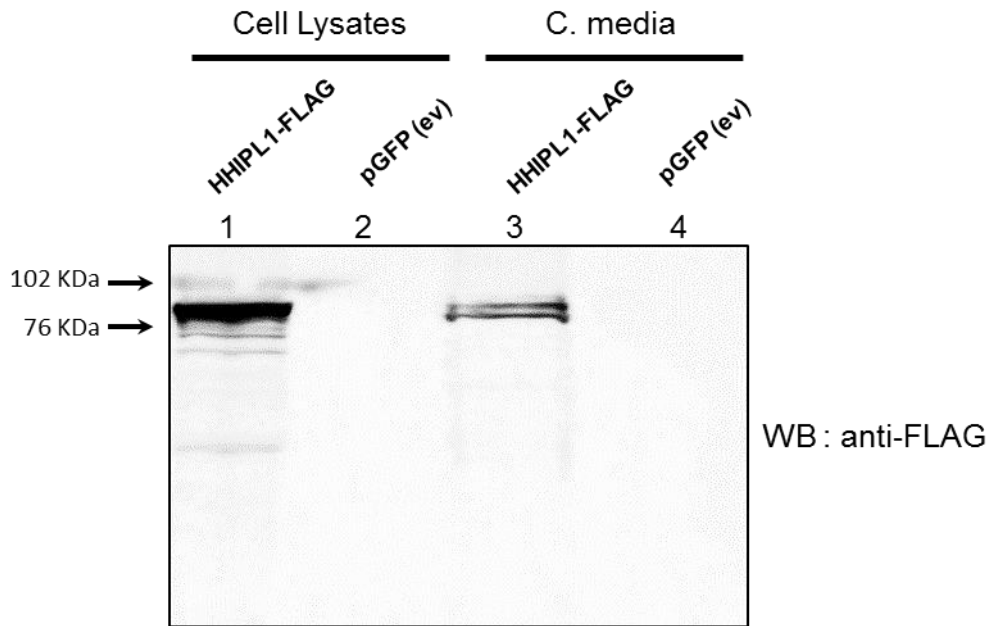


Figure 3.4 Detection of HH1PL1 in conditioned media

Representative western blotting of HEK 293 cells expressing HH1PL1-FLAG protein. Protein containing cell lysates and conditioned media were separated by SDS-PAGE and immunoblotted with anti-FLAG. HEK293 cells transfected with empty GFP plasmid vector (pGFP (ev)) were used as a negative control. HH1PL-FLAG fusion is associated with cell lysates (Lane 1) and conditioned media (Lane 3).

3.2.3 Analysis of HHIPL1-SHH interaction

To determine if HHIPL1 interacts with Hh proteins immunoprecipitation (IP) was performed. HEK293 cells were co-transfected by electroporation with HHIPL1-FLAG and SHH-GFP plasmids (full-length *SHH* cDNA was imported from DNASU and cloned into pLEICS-29, section 2.4.1) or empty vector controls. Cell lysates and conditioned media were collected and then immunoprecipitated with GFP-trap beads. Both HHIPL1-FLAG and SHH-GFP fusion proteins were detected in the immunoprecipitated samples from both cell lysates (**Figure 3.5 A lane 2**) and conditioned media (**Figure 3.5 B lane 2**) indicating HHIPL1 and SHH interact. HEK293 cells transfected with HHIPL1-FLAG and pGFP empty vector (pGFP (ev)) served as a negative control. In this sample HHIPL1-FLAG was only present in the input (**Figure 3.5 A lane 3**) and not in the immunoprecipitated sample (**Figure 3.5 A lane 4**). HHIPL1 was not detected in the input sample from conditioned media possibly due to low input HHIPL1 concentration (**Figure 3.5 B lane 3**). Cells transfected with SHH-GFP and pCDNA3.1 empty vector (pCDNA (ev)) were included as controls. SHH-GFP was detected in the IP sample (**Figure 3.5 B lane 6**) but due to low concentration in conditioned media was not detected in the input sample (**Figure 3.5 B lane 5**).

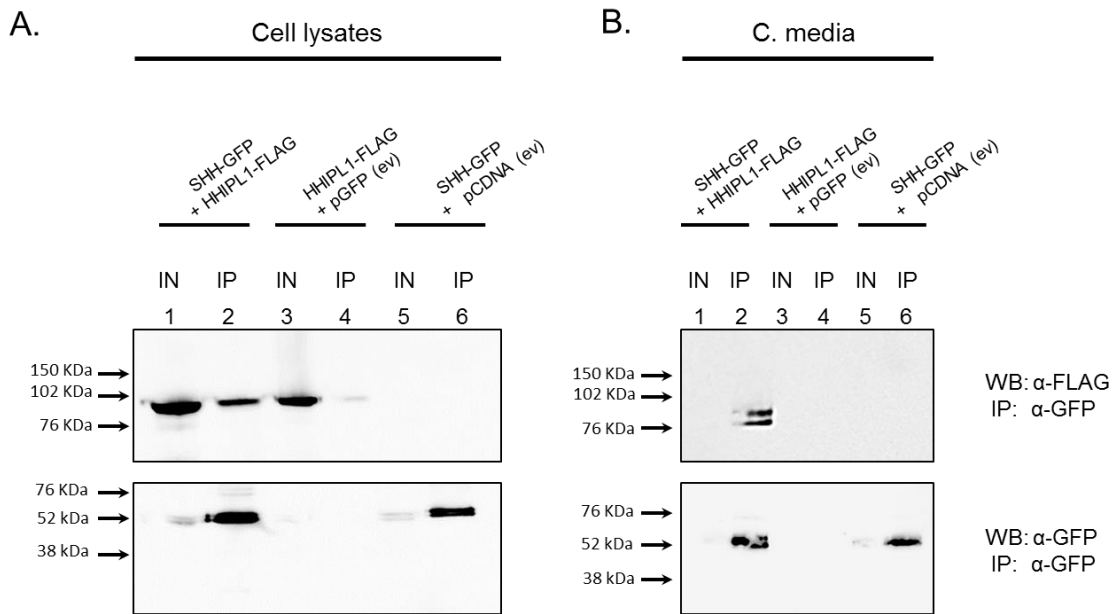


Figure 3.5 HHIPL1 interacts with SHH

Immunoprecipitation from HEK293 cell lysates (A) and conditioned media (B). Lanes 1-2; HEK293 cells co-transfected with SHH-GFP and HHIPL-FLAG plasmids. Lane 3-4; HEK293 cells co-transfected with HHIPL1-FLAG and pGFP (ev) serving as negative control for the IP. Lane 5-6; HEK293 cells co-transfected with SHH-GFP and pCDNA (ev), used as a positive control for SHH-GFP IP.

Upper panel: shows western blot of proteins with anti-FLAG antibody,

Lower panel: shows western blot of proteins with anti-GFP antibody

IN= sample before immunoprecipitation

IP= sample after immunoprecipitation with anti-GFP beads

3.2.4 Investigation of *HHIPL1* expression in vessel wall cells

The expression of *HHIPL1* was investigated in primary human endothelial cells (Human Umbilical Vein Endothelial Cells, HUVEC) and primary HASMCs. For this purpose, cDNA derived from these cells was amplified with *HHIPL1* primers by PCR and the products were visualised by agarose gel electrophoresis. cDNA synthesis reactions without Reverse transcriptase enzyme (NRT) were included as negative controls for genomic contamination. *HHIPL1* expression was detectable in HASMCs but not in HUVECs (**Figure 3.6 A**). The housekeeping gene *PSMB4* was used as a loading control for the amount of input RNA (**Figure 3.6 B**). In order to confirm the amplified product corresponded to *HHIPL1* gene, the resultant band was excised from the gel and confirmed by sequencing.

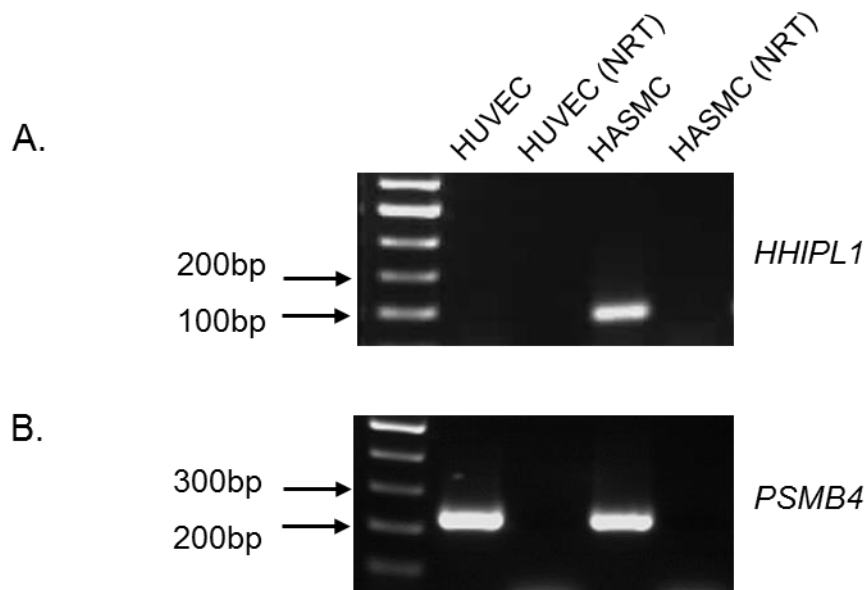


Figure 3.6 *HHIPL1* expression in HASMC

A) *HHIPL1* expression was investigated in HUVECs and HASMCs by RT-PCR and was only detected in HASMC. B) *PSMB4* housekeeping gene was used as a loading control.

3.2.5 Investigation of the effect of *HHIPL1* knockdown on HASMC behaviour

3.2.5.1 *HHIPL1* siRNA mediated knockdown in HASMC

Having detected expression of *HHIPL1* in HASMCs, the effect of *HHIPL1* knockdown on atherosclerosis relevant cell processes was investigated. Two different siRNAs were used to target *HHIPL1* individually and in combination. A non-targeting siRNA (NTC) was used as a negative control and an siRNA which leads to cell-death was used to confirm transfection efficiency. Primary HASMCs were cultured as described in section 2.1.1.2 and all experiments were performed at similar passages (between passage 3 and 6). 50nM of each siRNA was transfected using Lipofectamine RNAiMAX and cells were collected 24, 48 and 72 hours post-transfection. The cell death controls showed almost 100% cell death by 48-hours post transfection suggesting efficient transfection of siRNA (**Figure 3.7**).

RNA was extracted from cells at 24, 48 and 72 hours and knockdown of *HHIPL1* confirmed by qPCR. *HHIPL1* expression was found to be reduced by 72%-84% for siRNA1, 92-96% for siRNA2 and 85-92% for both siRNAs (**Figure 3.8**). Knockdown of *HHIPL1* was retained over 72 hours.

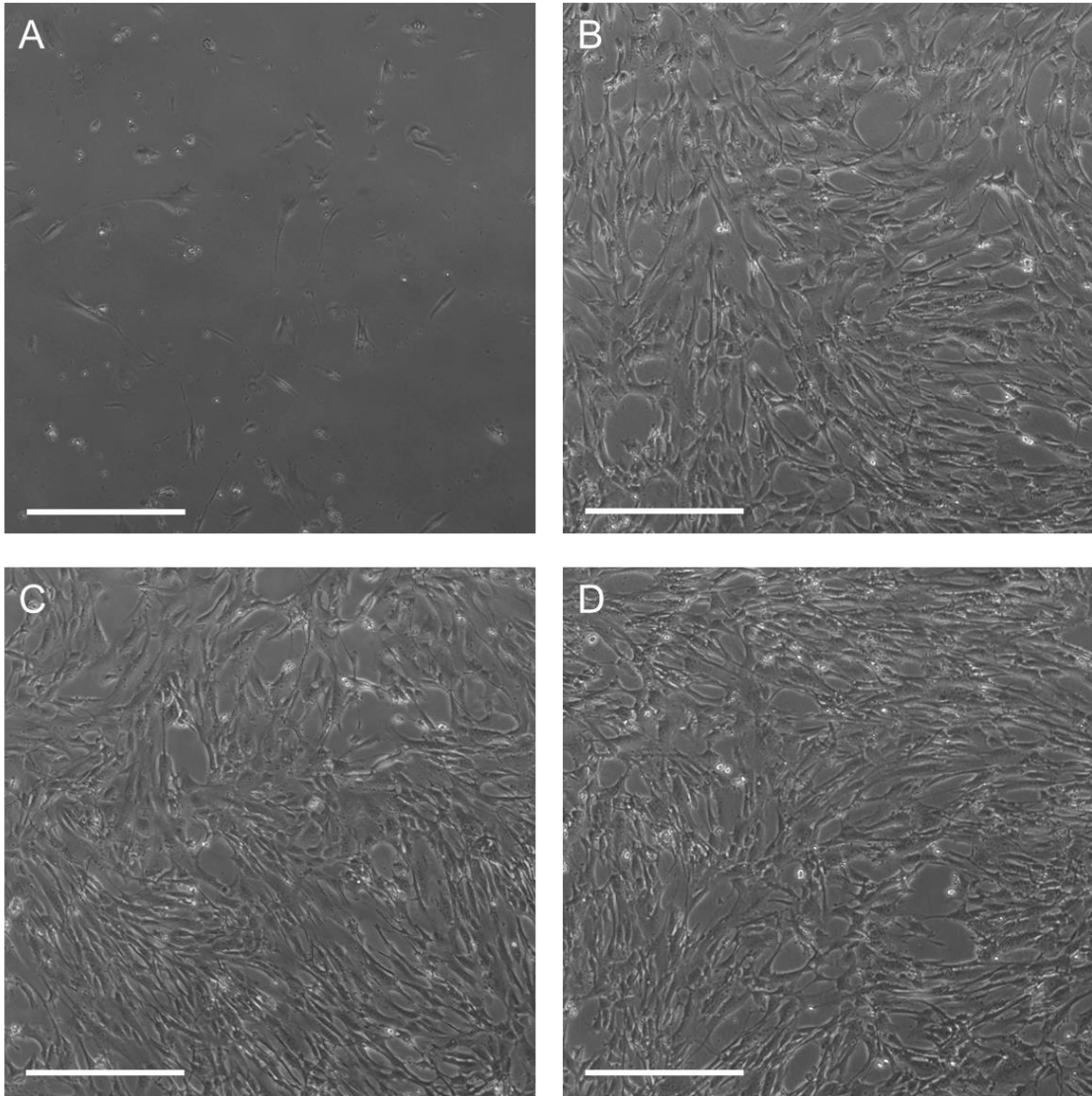


Figure 3.7 HASMC siRNA transfection

Representative images of HASMC 48 post siRNA transfection. Shown are cells transfected with cell death control siRNA (A), NTC siRNA (B), siRNA 1 against *HHIPL1* (C) and siRNA 2 against *HHIPL1* (D). Scale bars= 500µm

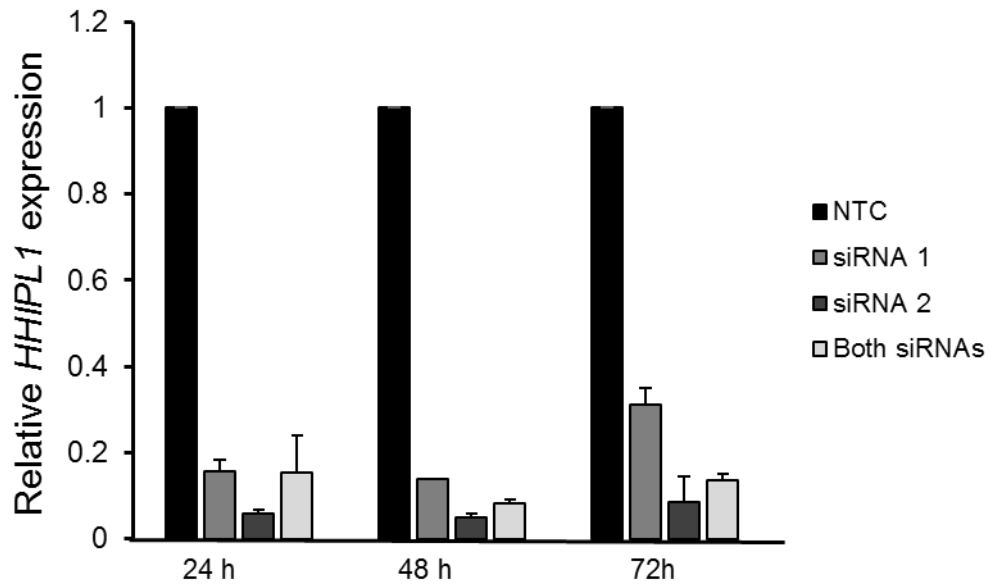


Figure 3.8 Relative *HHPL1* expression after siRNA treatment

HHPL1 expression was reduced by 72-96% when compared to NTC and the effect was retained over 72 h. All values were normalised to the NTC values at each time point. Error bars= SD (n=3).

3.2.5.2 Effect of *HHIPL1* knockdown on HASMC proliferation

During atherogenesis SMCs proliferate and migrate from the media to the intima. First, the effect of *HHIPL1* knockdown on HASMC proliferation was investigated. HASMCs were transfected with the two siRNAs targeting *HHIPL1* or the NTC siRNA and left to recover for 24 hours post transfection. 2,500 cells were then seeded in a 96 well plate in triplicate wells. Three images were taken of each well and the cell number was counted. Interestingly cells transfected with siRNA1, siRNA2 or both siRNAs were found to have a significant reduction (siRNA1 $P=0.04$, siRNA2 $P=0.03$, both siRNAs $P=0.03$) of 30-40% in relative cell number at 72 hours compared to the non-targeting control (NTC). Cells treated with both siRNAs also showed a significant reduction in cell count at 24 ($P=0.03$) and 48 hours ($P=0.04$) (**Figure 3.9**).

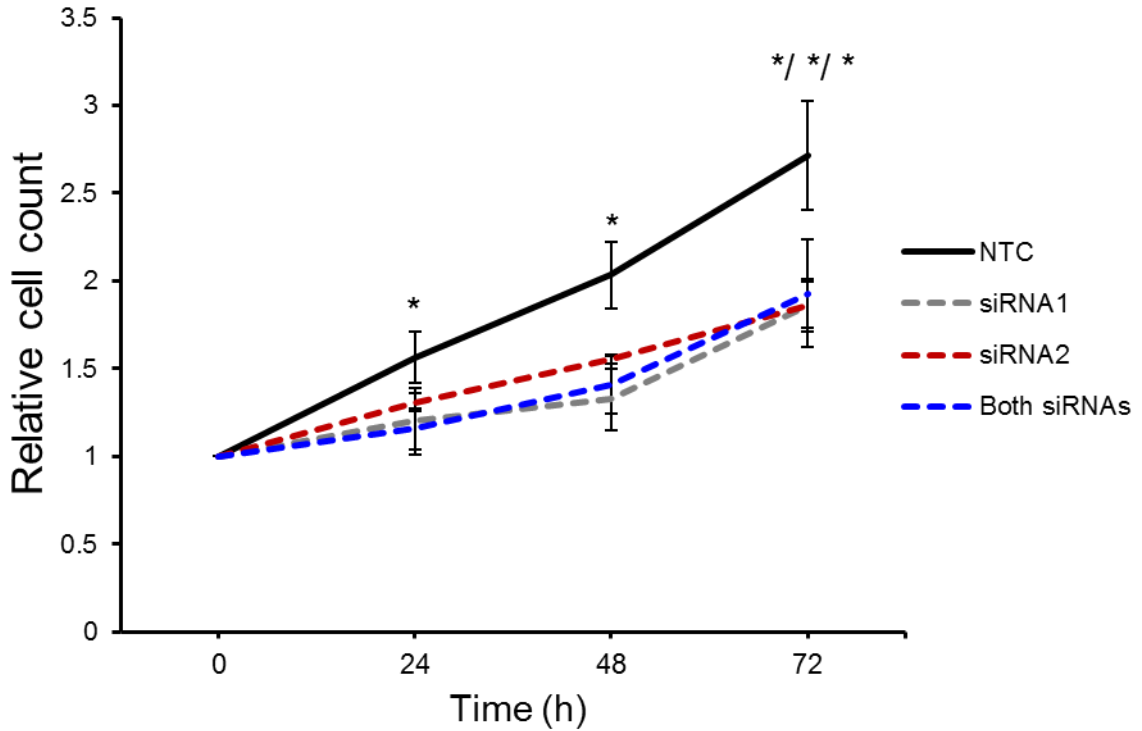


Figure 3.9 HASMC proliferation following *HHIPL1* knockdown

Relative cell count was measured for cells treated with siRNA1, siRNA2 or both siRNAs. Values were normalised to the average cell count at 0h time point. Samples were compared with NTC at each time point; both siRNAs at 24h (paired t test, $P=0.03$), 48h (paired t test, $P=0.04$) and 72h ($P=0.03$); siRNA1 at 72h ($P=0.04$) and siRNA2 at 72h ($P=0.03$). Statistical significance was tested using paired Students t-test * $P \leq 0.05$. Error bars= SEM (n=4).

3.2.5.3 Effect of *HHIPL1* knockdown on HASMC migration

Next, the effect of *HHIPL1* knockdown on HASMC migration was investigated using a wound healing (scratch) assay. HASMC were transfected with both *HHIPL1* siRNAs or NTC siRNA negative control. Cells were seeded at high density in a 6-well plate in duplicates and 48 hours post transfection a scratch was created in the centre of each well using a pipette tip. The scratch was then imaged in 3 positions over a 12-hour period. Cell migration was measured according to the percentage of the wound (scratch) area covered by cells (referred to as cell coverage) (**Figure 3.10**). In cells transfected with siRNA2 and both siRNAs it was found that migration (% cell coverage) was significantly reduced by 17% and 19% respectively ($P=0.037$ and $P=0.02$) compared to NTC treated cells at 8 hours (**Figure 3.11**). In cells transfected with both siRNAs migration was also reduced by 27% ($P=0.038$) at 12 hours.

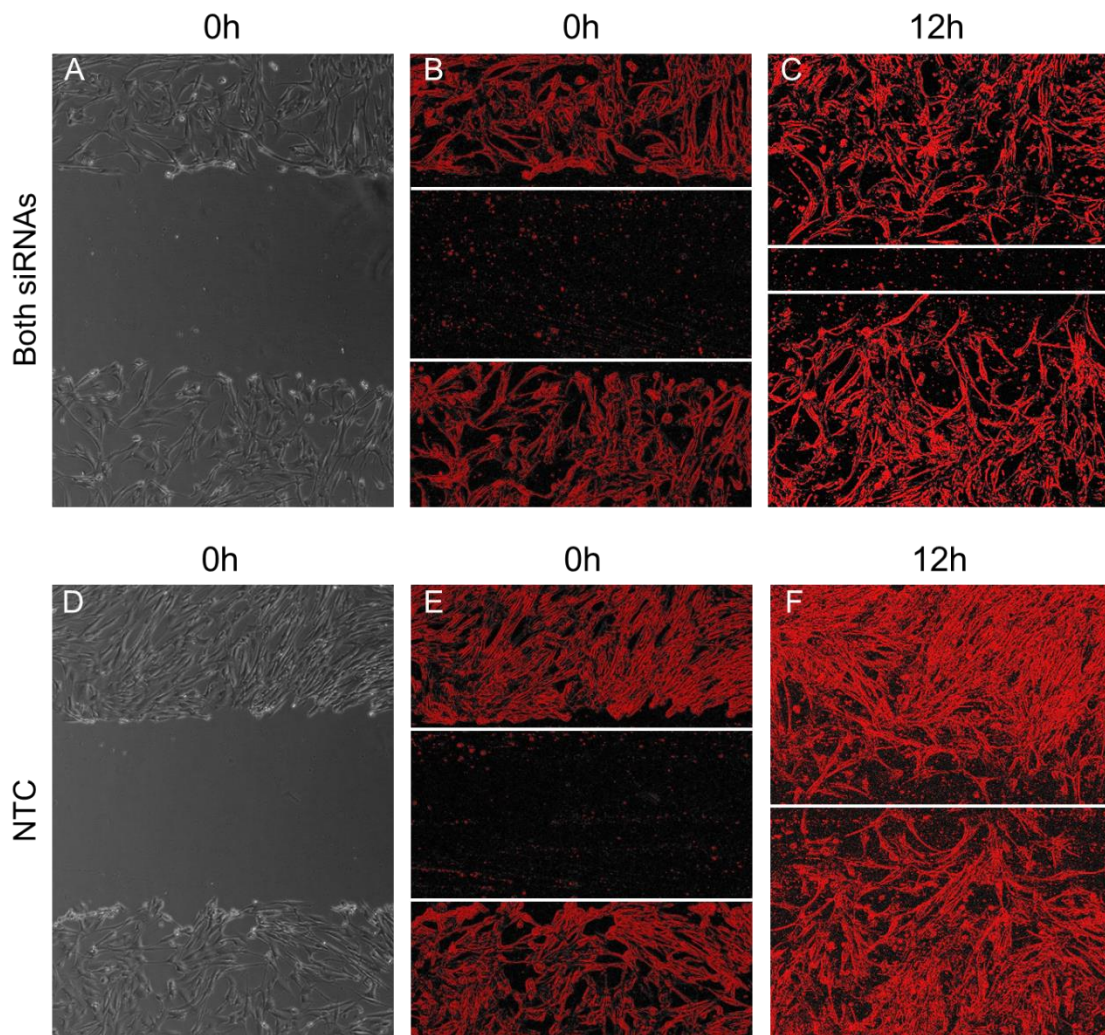


Figure 3.10 Representative wound healing images in HASMCs

A/D) Representative images of the wound created on confluent monolayers of HASMCs at 0 hours. Image J software analysis detected the cell covered area (red) of the original images at 0 hours (B/E) and at 12 hours (C/F). Images A-C refer to HASMCs treated with both siRNAs and images D-F refer to HASMCs treated with NTC. Magnification 4X.

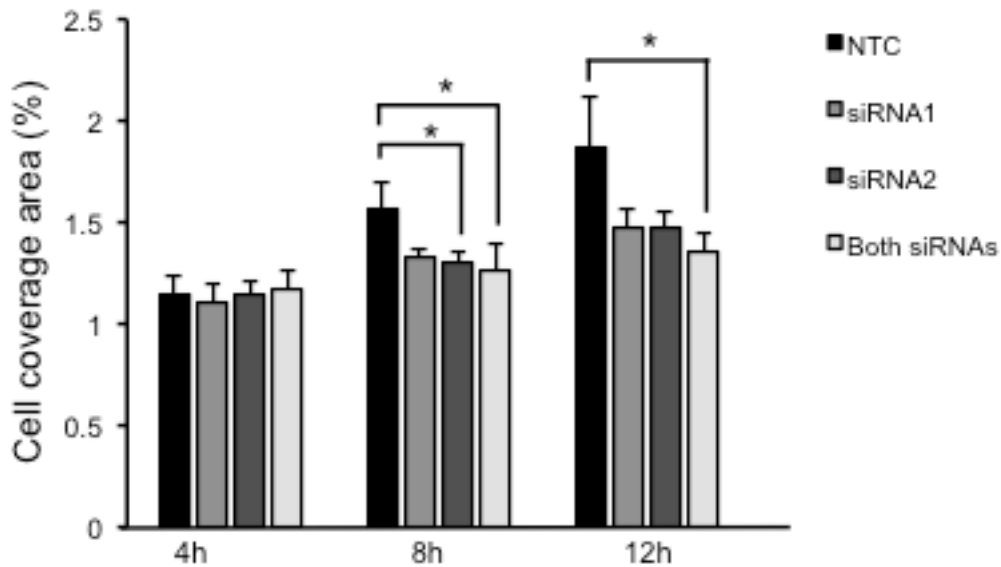


Figure 3.11 HASMC migration following *HHIPL1* knockdown

The migration rate of HASMC over 12 hours was calculated based on the cell coverage. In cells treated with siRNA1 and both siRNAs migration was reduced by 17% (paired t test, $P=0.037$) and 19% (paired t test, $P=0.02$) respectively at 8 hours. Similarly, at 12 hours in cells transfected with both siRNAs migration was reduced by 27% (paired t test, $P=0.038$). Statistical significance was tested using paired Students t-test. * $P \leq 0.05$, Error bars=SD (n=3).

3.3 Discussion

Here, HHIPL1 was shown to be a secreted protein which interacts with SHH, the main ligand of the Hh signalling. Analysis of *HHIPL1* expression in vessel wall cell types showed that it is present in HASMCs and knockdown resulted in reduced migration and proliferation.

Sequence comparison between HHIPL1 and HHIP family members *in silico* revealed that HHIPL1 retains the hedgehog interacting domain that has been well characterised in HHIP. HHIP is the only member of the protein family that had previously undergone functional analysis and acts as both a membrane associated and secreted antagonist of Hh signalling (Kwong, Bijlsma & Roelink 2014, Chuang, McMahon 1999) . Analysis of HHIPL1 cellular localisation using *in silico* prediction and *in vitro* experimentation showed that it does not have a transmembrane domain and is not at the cell surface and is a secreted protein. Based on sequence conservation it was predicted that HHIPL1 would directly interact with Hh proteins of which SHH is the best characterised. Immunoprecipitation from the cell lysates and conditioned media of transiently transfected cells confirmed that the two proteins interact and provides experimental evidence supporting the hypothesis that HHIPL1 acts through the Hh pathway. The findings of this project support a role for HHIPL1 in the Hh pathway, however further investigation is required in order to identify how HHIPL1 modulates Hh signalling. This can be addressed by looking at expression levels of downstream target genes (GLI1/PTCH1), which indicate active Hh signalling. By looking at expression levels of these genes in relation to altered HHIPL1 levels (ether overexpression or knockdown) it would be feasible to conclude how HHIPL1 modulates signal transduction. Similar immunoprecipitation experiments can also be conducted with the other Hh proteins, DHH and IHH in order to examine whether HHIPL1 is able to bind these. As HHIPL1 is not retained in the cell membrane it raises question about how it exerts it functions in the extracellular space. A combination of *in vivo* experiments in chicken neural tube and *in vitro* cultured cells suggested that the secreted form of HHIP moves towards the Shh gradient and inhibits the Shh signalling in a non-cell autonomous manner and control which cells are Shh

responsive (Kwong, Bijlsma & Roelink 2014) . It will be interesting to determine whether HHIPL1 acts in a similar manner.

Protein sequence analysis also predicts that HHIPL1 has a scavenger receptor domain at its C terminus. The other HHIP family members lack this domain. Scavenger receptor domains are found in the receptor proteins that recognise modified LDL and mediate uptake of oxidised and acetylated LDL by macrophages and SMCs (described in section 1.1.1). It is not clear if HHIPL1 is able to perform a similar function although this would appear to be an unlikely role for a secreted protein. Nevertheless, characterisation of the requirement of the HHIPL1 scavenger receptor domain on HHIPL1 function is needed. It is known that Hh ligands undergo various lipid modifications, which govern their cellular release, range of signalling and signalling potency (Grover et al. 2011). These modifications involve covalent attachment of cholesterol and palmitate at the C-terminus of the protein (Porter, Young & Beachy 1996a) . The hydrophobic properties of these two lipid moieties promote the formation of the soluble multimeric Hh complexes, which are secreted by the producing cell (Feng et al. 2004, Daniela Panáková et al. 2005). Given that HHIPL1 carries a scavenger receptor, which might be capable of binding cholesterol particles, it would be interesting to examine if interaction between HHIPL1 and SHH is mediated by the scavenger receptor.

Down-regulation of *HHIPL1* resulted in primary HASMCs reduced cell proliferation and migration. Hh signalling is a known regulator of SMC proliferation and migration (Morrow et al. 2007, Morrow et al. 2009, Redmond et al. 2013, Fu et al. 2006, Yao et al. 2014). It would be interesting to investigate the interplay between HHIPL1 and SHH in the context of SMC phenotype and to determine if HHIPL1 exerts its effect as a positive or negative regulator of Hh signalling.

3.4 Conclusion

HHIPL1 is a secreted protein, which interacts with SHH and regulates atherosclerosis relevant cell processes in HASMCs. This is the first functional investigation of HHIPL1 and further studies are required in order to determine

its exact role in Hh signalling and whether it's through this pathway that it exerts its regulation on HASMC phenotype.

4 Validation and characterisation of a *Hhip1* knockout mouse model

4.1 Introduction

The knockout mouse has been a widely used animal model for investigating genes involved in human disease. In the past decade large-scale gene targeting has been performed by international consortia with the aim of generating models for all mouse genes. To date, more than 18,500 genes - including *Hhip1* - have been knocked out in mice through a combination of gene targeting and gene trapping (Rosen, Schick & Wurst 2015) . Here, the generation and validation of a *Hhip1* knockout construct imported from the KOMP will be described together with the breeding and phenotypic investigation of *Hhip1* knockout mice. In addition, *Hhip1* expression at mRNA and protein level will be investigated.

4.1.1 KOMP mutagenesis strategy

KOMP generates knockout alleles by insertion of a 'Knockout-first conditional' targeting vector in C57BL/6N embryonic stem cells (Pettitt et al. 2009, Skarnes et al. 2011). *Hhip1* is among the genes targeted using the knockout-first conditional approach. This mutagenesis approach was first described by Testa *et al.* (2004) and is in essence a combination of gene trapping and gene targeting. The knockout first comprises a targeting cassette inserted into an early intron of an intact gene. A splice acceptor (sA) in the cassette captures the RNA transcript and an efficient polyadenylation signal (pA) truncates the transcript so that the gene is not transcribed into mRNA downstream of the cassette, producing a knockout at the RNA processing level. The knockout-first allele also includes a *lacZ* reporter in-frame with the preceding exon, which can be used to assess target gene expression pattern (Testa et al. 2004) (**Figure 4.1 A**)

The knockout first cassette also includes two flippase recognition target (FRT) sequences either sides of the cassette along with flanking *loxP* sites (locus of crossover (x) in P1 bacteriophage). This design allows the conversion of the knockout first allele to a conditional allele through the expression of flippase (FLP) recombinase in either ES cells or by breeding knockout first mice with transgenic FLP expressing mice (**Figure 4.1 B**). The FLP recombinase induces recombination between the two FRT sequences removing the knockout first

allele. The conditional allele can be further converted into a true knockout. The presence of *loxP* sites either side of a critical exon allows the deletion of the exon via Cre recombination. The choice of the critical exon is based on the principal that the removal of the exon will delete an essential part of the encoded protein or cause a frameshift and result in a non-functional truncated protein (Gu et al. 1994). Excision of the critical exon can be spatio-temporally directed by crossing with a mouse, which expresses Cre recombinase under the control of cell-type specific or inducible promoter (Nagy et al. 1998, Meyers, Lewandoski & Martin 1998) (**Figure 4.1 D**). The same principal of *loxP*/Cre recombination can be applied directly to the knockout first allele to generate a true knockout allele (**Figure 4.1 C**).

The use of a conditional knockout addresses the limitation of developmental abnormalities or lethality, which is common among conventional knockout models.

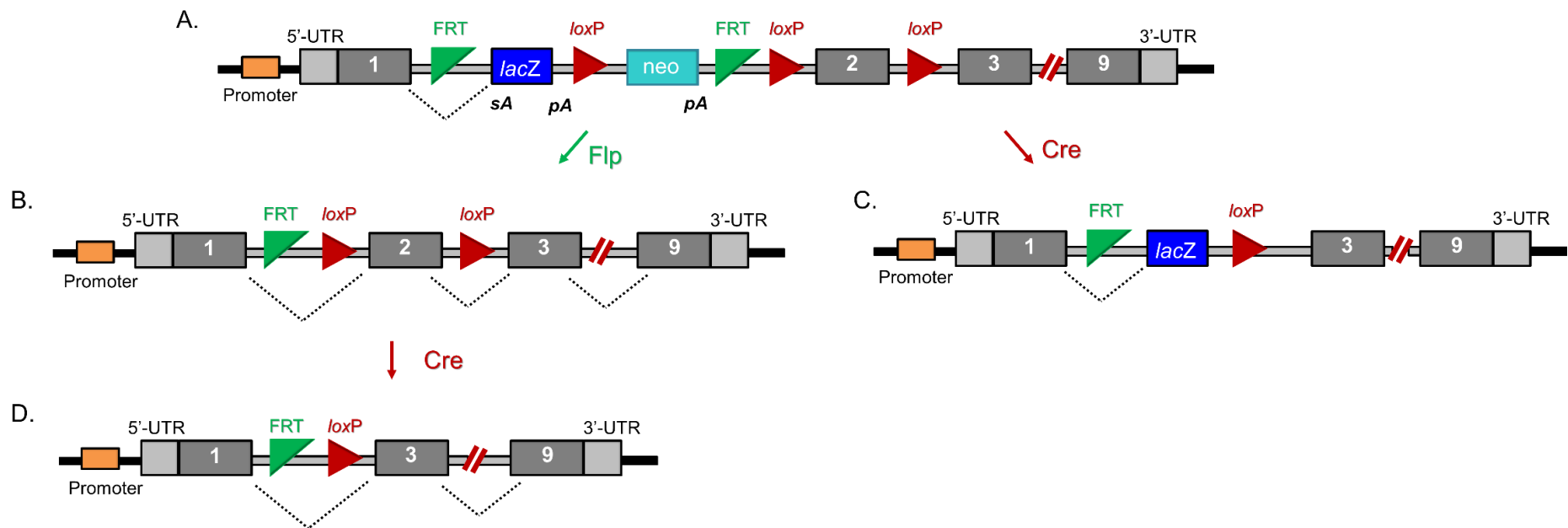


Figure 4.1 *Hhip1* knock out first allele and possible allele variants

Schematic representation of *Hhip1* knockout first allele variations. A) Shown is the initial unmodified allele, knockout first (*Hhip1*^{tm1a(KOMP)Wtsi}), which is predicted to generate a null allele through splicing (sA) to a *lacZ* element, which is present in the targeting cassette. B) A conditional allele is generated by removal of the gene-trapping elements (sA, pA) by crossing with a FLP recombinase expressing mouse, which reverts the allele to current wild type version. C) Alternatively the knockout first allele can be crossed with a Cre expressing strain, which will remove the DNA elements flanked by *loxP* sites. D) The conditional allele (B) can be further modified by Cre recombination, upon which the critical exon, in this case exon 2, is excised creating a truncated protein that is subject to mediated decay by the cell. This is a safe knockout variation of the gene. Schematic representation not in scale.

4.1.2 Hh mouse models

Results from previous work in chapter 3 support a role for HHPL1 in Hh signalling. As described in chapters 1 and 3 Hh signalling is a well-conserved pathway that regulates morphogenesis of a wide range of tissues and organs during development and is reactivated in a number of different diseases. The genes encoding the Hh ligands were first identified through a mutagenesis screen for mutations that disrupt larval body plan in *Drosophila* (Christiane Nüsslein-Volhard, Wieschaus 1980) and disruption of the hedgehog pathway in mice and humans results in similar developmental defects reflecting the conserved function of the pathway. Ingham *et al.* (2001) provided a comprehensive review of the tissues that are dependent on Hh signalling (Ingham, McMahon 2001). There are only a few parts of the mammal body that are not affected by the Hh pathway. Hh signalling, regulates cell fate, cell proliferation and cell maintenance in different cell types and is dependent on the concentration of the three vertebrate secreted homologs Shh, Ihh and Dhh (Krauss, Concordet & Ingham 1993, Riddle *et al.* 1993) . There are distinct molecular responses to different thresholds of the secreted morphogens that give rise to various body parts.

Hh signalling is a crucial regulator of a wide range of tissues in vertebrates such as the limbs and somites, the nervous system, the cardiovascular system and others. It is known that the notochord and the floor plate produce essential signals for the formation of the neural tube whereas the zone of polarizing activity has been suggested to regulate the anterior polarity in the limb. Expression of *Shh* in these three key signalling centres of the embryo (notochord, floor plate and the zone of polarizing activity) served as evidence for Hh implication in neural tube and limb formation (Ingham, McMahon 2001). Additionally, ectopic expression of *Shh* in the mouse (as well as in other species; zebra fish, frog, fish, and chick) further supported the initial evidence that Shh regulates ventral polarity in the neural tube and anterior–posterior polarity in the limb (Riddle *et al.* 1993, Chang *et al.* 1994). Evidence for Shh involvement in the central nervous system (CNS) through signalling in the neural tube was proposed by the study of *Shh* mutant mice. *Shh* gene targeted disruption caused defective development of axial structures such as the notochord and floorplate as well as abnormalities including absence of distal

limbs and cyclopia (Chiang et al. 1996). Moreover, downregulation of the pathway in homozygous null *Ptch1* mutants was shown to cause neural tube defects (open and overgrown neural tubes) and subsequent death during embryogenesis (Goodrich et al. 1997). Members of the Gli transcription factors have been also implicated in mouse development. For example, *Gli1/Gli2* double homozygous mutants have extreme CNS and lung defects (Park et al. 2000). Not only mutations in the Hh morphogens but also disruption of the signalling have an effect in the development of the embryo. Chuang *et al.* showed that inhibition of the pathway by overexpression of *Hhip* in the cartilage, where *Ihh* controls growth, results in a shorter skeleton of the mouse embryo (Chuang, McMahon 1999). Dysregulation of the Hh signalling has also been investigated during lung development. In *Hhip* mutant mouse embryos Hh signalling was upregulated resulting in severe defective branching and morphogenesis in the lung. Loss of *Hhip* expression was also associated with absent *fibroblast growth factor 10 (Fgf10)* expression from the mesenchyme, where secondary lung branching initiates, suggesting Hh signalling acts upstream *Fgf10* during lung morphogenesis (Chuang, Kawcak & McMahon 2003) .

The above are just a few examples indicating the importance of Hh signalling in mouse development. Mutations in almost all the components of the Hh pathway in mouse are associated with developmental phenotypes. A summary of the Hh genes and the associated defective phenotypes is shown in **Table 4.1**.

Included in the many tissues and organs regulated by Hh signalling is the cardiovascular system. Mouse studies have identified Hh components as key regulators of vascular development in the aorta, coronary vessels and yolk sac (Redmond et al. 2011, Yamagishi et al. 2003) and several Hh mouse models have cardiovascular defects. One of the earliest functions of Hh signalling in mouse hemato-vascular system development was revealed by inhibition of *Ihh* in the endoderm which caused failure to activate hematopoiesis and vasculogenesis in the adjacent epiblast (Dyer et al. 2001). Similarly, *Ihh* and *Smo* null murine yolk sacs failed to develop beyond a primitive vascular plexus and did not progress to the angiogenic stage of development, confirming a role for Hh pathway in yolk sac angiogenesis (Byrd et al. 2002). The role of *Shh* in

blood vessel development was studied by Vokes *et al* (2004), where they showed through several lines of evidence that endodermal derived Shh is an important regulating factor of blood vessel assembly and tubulogenesis in mouse embryos (Steven A. Vokes *et al.* 2004). Shh was also shown to mediate migration of progenitor endothelial cells from bone marrow and the subsequent capillary formation of mature endothelial cells, confirming that endothelial cells are direct targets of Hh signalling (Kanda *et al.* 2003). The role of the Hh pathway has also been investigated in relation to other essential developmental pathways. Lawson *et al.* (2002) provided evidence that the Hh pathway stimulates formation of the zebrafish aorta by acting upstream of the Vegf and Notch pathway (Lawson, Vogel & Weinstein 2002) . This signalling hierarchy was subsequently confirmed in a mouse model that utilised *Smo* and *Ptch* mutant embryos to show that Hh signalling co-coordinates Vegf and Notch signalling to pattern the developing vascular system (Coultas *et al.* 2010). Moreover, studies in mouse embryos revealed that Fgf induces expression of *Shh* in the epicardial layer of the heart between embryonic days E11.5-13.5, which results in upregulation of Vegf and Ang-2 in the myocardium promoting the development of coronary vessels in the subepicardial space and within the myocardium (Lavine, Ornitz 2007). A summary of the cardiovascular phenotypes of various Hh mouse mutants is shown in **Table 4.1**.

Gene	Developmental phenotype	Cardiovascular phenotype
Shh	Heterozygotes: Limb and bone abnormalities Homozygotes: embryonic lethality before E12	<ul style="list-style-type: none"> •Abnormal vasculogenesis •Morphological defects in heart, pulmonary artery & vein, arteries •Abnormal outflow tract development
Ihh	Homozygotes: Lethal before or shortly after birth. Chondrocyte and osteoblast defects	<ul style="list-style-type: none"> •Yolk sac vasculature defects
Dhh	Male infertility, abnormal nervous system development	No phenotype
Gli1	No phenotype	No phenotype
Gli2	Embryonic lethality at E18.5. Homozygotes: Skeletal malformations, lung defects, nervous system abnormalities, absent foregut and floorplate	No phenotype
Gli3	Heterozygotes: Limb and digit malformations Homozygotes: Perinatal lethality, craniofacial and digit defects	<ul style="list-style-type: none"> •Abnormal vein and myocardium morphology •Haemorrhage at E14
Ptch1	Heterozygotes: Large, brain neuron abnormalities, hindlimb defects Hypomorphic mutants: Reproductive defects Homozygotes: Embryonic lethality at E10 due to neural tube defects	<ul style="list-style-type: none"> •Abnormal heart development
Ptch2	Male homozygotes (gene disruption): Haematopoietic and immune system defects, skin defects	No phenotype
Smo	Homozygotes: Mid-gestation lethality. Neural tube and gut defects	<ul style="list-style-type: none"> •Morphological defects in arteries, myocardium, pericardium •Abnormal heart looping and outflow tract development •Haemorrhage •Abnormal blood circulation •Yolk sac vasculature defects
Hhip	Homozygotes: Lethal shortly after birth due to respiration failure. Lung, spleen and pancreas defective morphogenesis	No phenotype
Disp1	Homozygotes: Neural tube, forelimbs and craniofacial defects	<ul style="list-style-type: none"> •Abnormal heart looping •Pericardial edema

Sufu	Targeted disruption: Mid-gestation lethality, neural tube defects, incomplete embryo turning, abnormal somite development	<ul style="list-style-type: none"> •Abnormal cardiac looping •Morphological defects in coronary artery •Haemorrhage
Cdon	Homozygotes: Craniofacial defects, usually dies before weaning	<ul style="list-style-type: none"> •Morphological defects in blood vessels •Haemorrhage

Table 4.1 Hh mouse models and phenotypes (Data sourced by mouse genome informatics database, MGI).

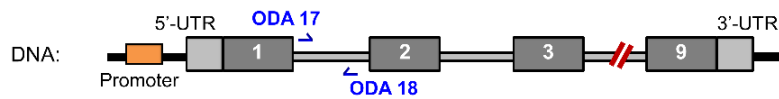
4.2 Results

4.2.1 Validation of *Hhip1* knockout first construct

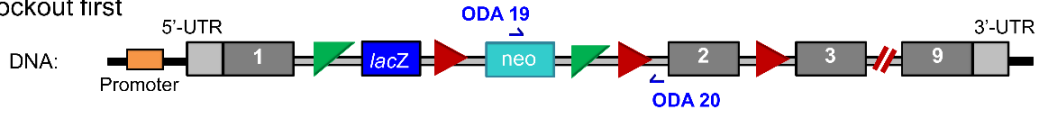
Mouse ES cells that carry the *Hhip1* knockout first construct (*Hhip1*^{tm1a(KOMP)Wtsi}) were imported from KOMP into the animal facility at the University of Leicester. Injection of the ES cells into a blastocyst followed by transfer into a pseudopregnant mother gave rise to chimeric mice (performed by the animal facility). Following germline transmission by crossing to C57BL/6J mice, further backcrossing was performed in order to obtain a more homogenous genetic background (up to 7 generations, N7). The resultant *Hhip1* knockout out first mice, referred to as *Hhip1*^{-/-} were viable with no signs of abnormalities.

For the identification of mutant and wild type littermates a genotyping technique was developed targeting specific regions of the gene. Two PCR reactions were conducted on genomic DNA to confirm which animals carried the knock out first version of the allele. The first PCR reaction includes a primer pair (ODA17/ODA18) designed to anneal to the endogenous sequence on either side of the exogenous construct and so will only generate a PCR product from the wild type allele (the PCR product is too large to successfully amplify when the exogenous DNA of the knockout first allele is present) (**Figure 4.2 A**). The second PCR reaction includes a primer (ODA19/ODA20) designed to anneal to the Neo cassette, hence confirming the presence of the knockout first allele (**Figure 4.2 B**).

A) Wild type



B) Knockout first



C)

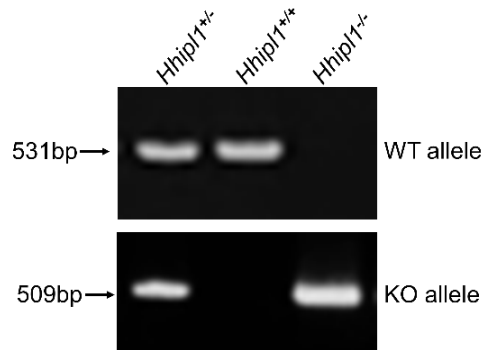
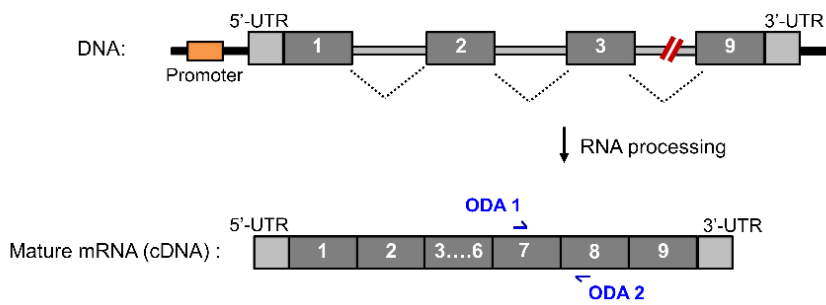


Figure 4.2 Genotyping of *Hhip1* transgenic mice

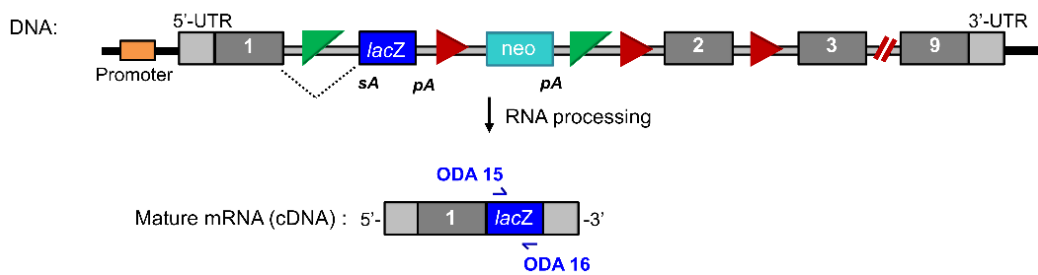
A) One primer pair (ODA17/ODA18) was designed to target the wild type sequence of the *Hhip1* gene on either side of the construct, producing a band of 531 bp when the wild type allele was present. B) The second primer pair (ODA19/ODA20) targeted the Neo cassette that is part of the exogenous DNA introduced into the knockout first allele. C) Agarose gel shows the PCR products of three different genotypes *Hhip1*^{+/-}, *Hhip1*^{+/+} and *Hhip1*^{-/-}. Green triangles: FRT sites, Red triangles: *loxP* sites, UTR: untranslated region.

The *Hhip1* knockout first allele contains a targeting cassette driven by the endogenous *Hhip1* promoter and acts as a knockout at the RNA level due to the presence of a *sA* upstream of a *lacZ* reporter, which is followed by stop sequences *pA* sequences. This allele version can be converted to a conditional allele via Flp recombination and then subsequently to a null allele via Cre recombination (**Figure 4.1**). Figure 4.3 A and B show the *Hhip1* wild-type and knockout first alleles and the expected mRNA products. To confirm that *Hhip1* is not expressed from the knock out first version of the allele, RNA was extracted from a *Hhip1*^{-/-} mouse and compared to that of a wild type littermate. Two RT-PCRs were conducted (**Figure 4.3 C**); the first was designed to amplify exons seven to eight of the endogenous *Hhip1* mRNA (ODA1/ODA2), which should be present in the wild type mouse and absent in the knock out mouse, since these exons are downstream of the targeted region. The second RT-PCR targeted the *lacZ* region of the targeting cassette (ODA15/ODA16), which should be present in the knockout mouse.

A) Wild type



B) Knockout first



C)

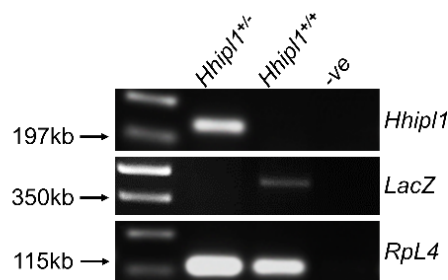


Figure 4.3 Validation of the knockout construct

Schematic representation of the wild type (A) and the Knockout first alleles (B) at the DNA level along with the resultant mRNA products. Primers (ODA1/ODA2) were designed to amplify exon seven to eight and hence confirm the presence of the wild type allele whilst primers (ODA15/ODA16) were used to amplify the *lacZ* gene. C) Agarose gel shows the RT-PCR products of *Hhip1*^{-/-} and *Hhip1*^{+/+} mouse tissue. *Rpl4* housekeeping gene was used as a loading control. Green triangles: FRT sites, Red triangles: *loxP* sites.

4.2.2 Phenotypic characterisation of *Hhip1*^{-/-} mouse

Mice were monitored for signs of sub-viability at all stages. Homozygous null mice (*Hhip1*^{-/-}) were born in the expected Mendelian frequency and there were no losses peri- or postnatally. The mice were weighed weekly and showed no difference in weight in comparison to controls (**Figure 4.4 A&B**). Additionally, the mice were monitored for any signs of dysmorphology but nothing of note was observed.

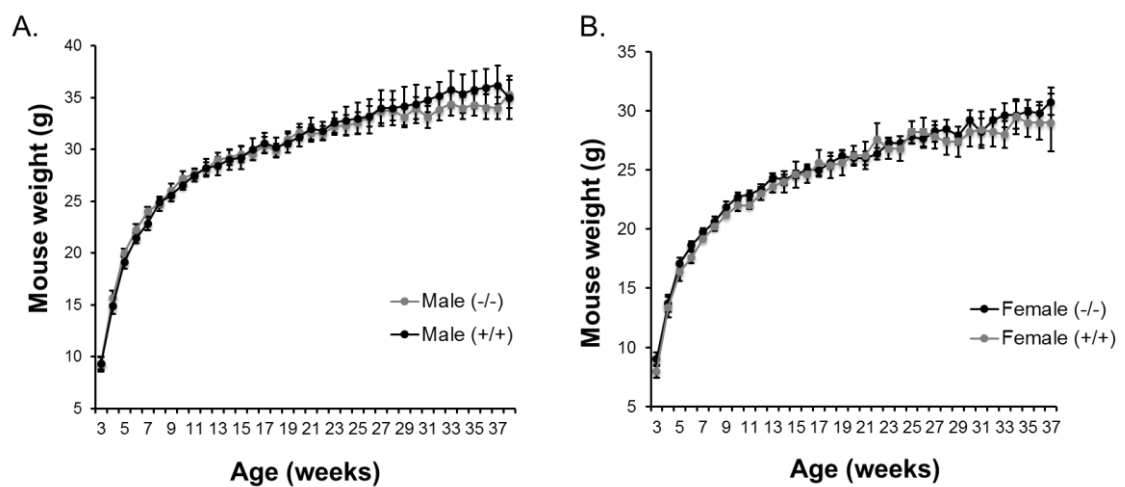


Figure 4.4 *Hhip1*^{-/-} mouse weights

Mice were weighed weekly. The first measurement was taken after weaning (3 weeks old) and the last when they were ≈ 10 months old. A) No difference was observed in either *Hhip1*^{-/-} or *Hhip1*^{+/+} male mice ($n=7$ *Hhip1*^{+/+} vs $n=9$ *Hhip1*^{-/-}, $P>0.05$) and the same was found for female mice ($n=5$ *Hhip1*^{+/+} vs $n=11$ *Hhip1*^{-/-}, $P>0.05$) (B). Statistical significance was tested using unpaired Students t-test.

4.2.3 Analysis of *Hhip1* expression in mouse tissues

To investigate the expression of *Hhip1* in a panel of tissues, RNA was isolated from an *ApoE*^{-/-} mouse and the subsequent cDNA was subjected to RT-PCR. *Hhip1* was detected in the majority of the tissues investigated. *Rpl4* was used as a loading control (**Figure 4.5**).

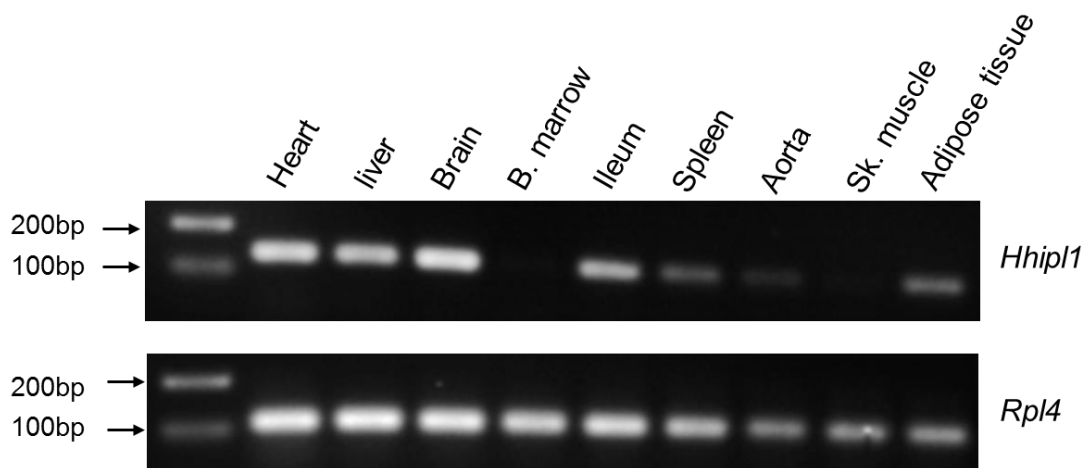


Figure 4.5 *Hhip1* expression in mouse

Expression of *Hhip1* was assessed in a panel of 9 different mouse tissues by RT-PCR. *Hhip1* is expressed in all tissues except bone marrow and skeletal muscle. *Rpl4* was used as loading control.

4.2.4 Histological examination of *Hhip1* expression

RT-PCR provided some indication as to which mouse tissues express *Hhip1* at mRNA level. In order to determine the specific *Hhip1* expression pattern, histochemical analysis of *Hhip1*^{-/-} and *Hhip1*^{+/+} tissue was undertaken, utilizing the *lacZ* reporter. As described in section 4.1.3 *lacZ* is spliced in-frame after *Hhip1* exon 1 and is under the control of the *Hhip1* promoter. Therefore, *lacZ* activity was used as an indirect method of assessing *Hhip1* localisation. The tissues that expressed *Hhip1* at the mRNA level were subjected to histochemical X-gal staining (**Figure 4.6 - 4.8**). When β -galactosidase enzyme is present it hydrolyses X-gal substrate producing a blue chromogenic precipitate. Therefore, knockout tissue was expected to comprise staining whilst wild type derived tissue served as a negative control. Stomach, which endogenously expresses β -galactosidase (Bolon 2008) acted as a positive control (**Figure 4.6**). Significant difficulty was experienced in detecting staining for the majority of the tissues examined. Expression was detected in the coronary septal artery (**Figure 4.7**) and brain (**Figure 4.8**), however, the level of staining was weak and not reproducible.

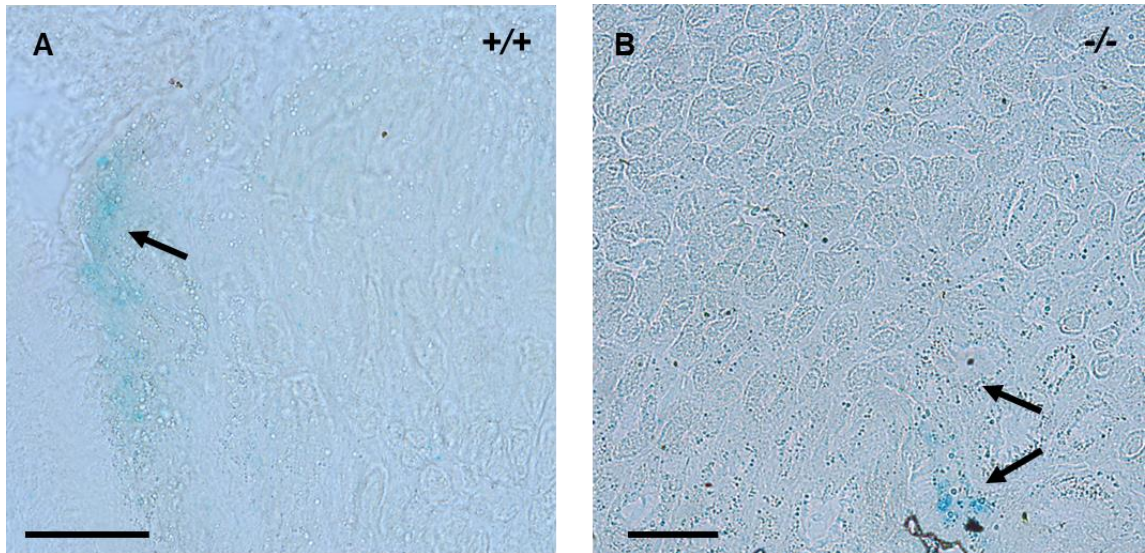


Figure 4.6 Endogenous β -galactosidase in stomach frozen slides

Detection of β -galactosidase activity (black arrows) by x-gal staining in frozen sections of *Hhpl1*^{+/+} (A) and *Hhpl1*^{-/-} stomach (B), at the level of gastric glands. Scale bars=50 μ m.

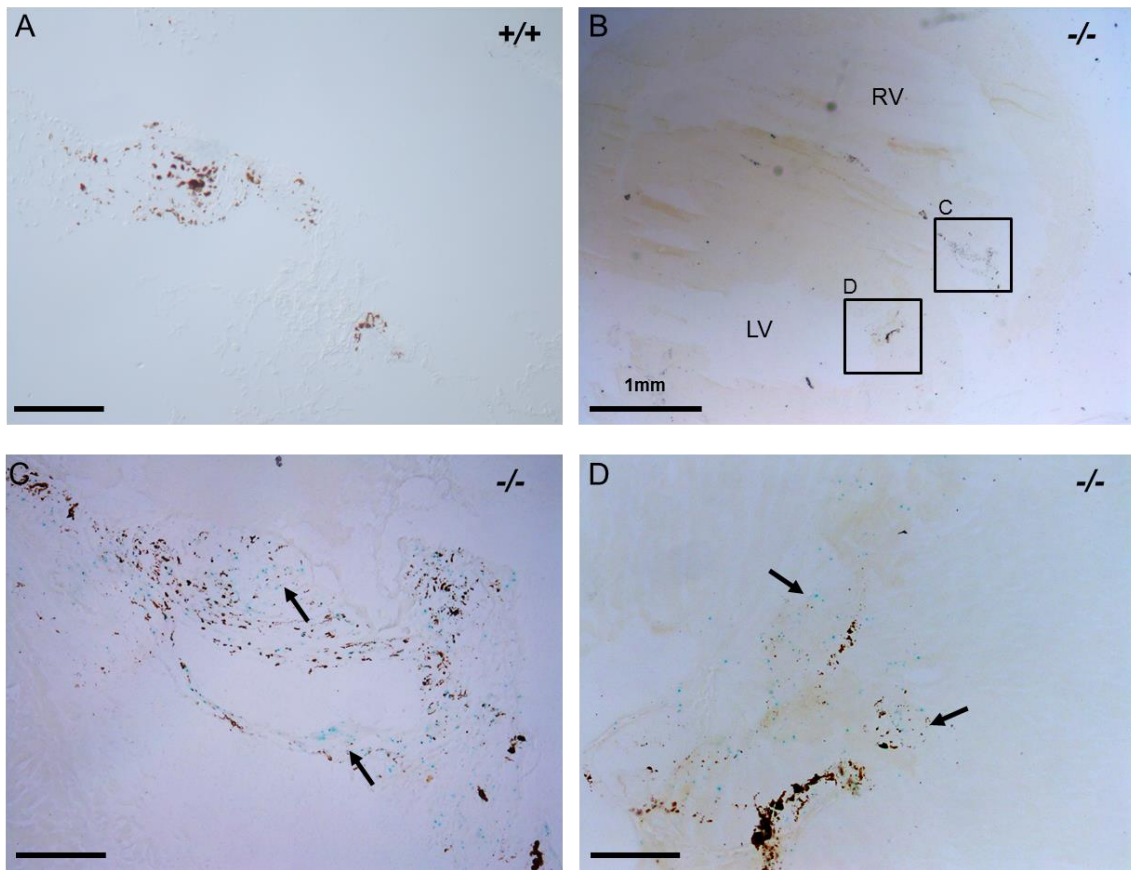


Figure 4.7 *Hhip1* expression in heart vasculature

A) Representative image of *Hhip1*^{+/+} heart frozen section at the level of coronary septal artery, where no β -galactosidase was detected. B) Detection of β -galactosidase activity by x-gal staining in frozen sections of a *Hhip1*^{-/-} heart at the level of coronary septal artery. Images (C) and (D) are higher magnifications of the regions shown in (B). Positive staining indicated by black arrows. Scale bars=100 μ m unless otherwise stated. RV: right ventricle, LV: left ventricle.

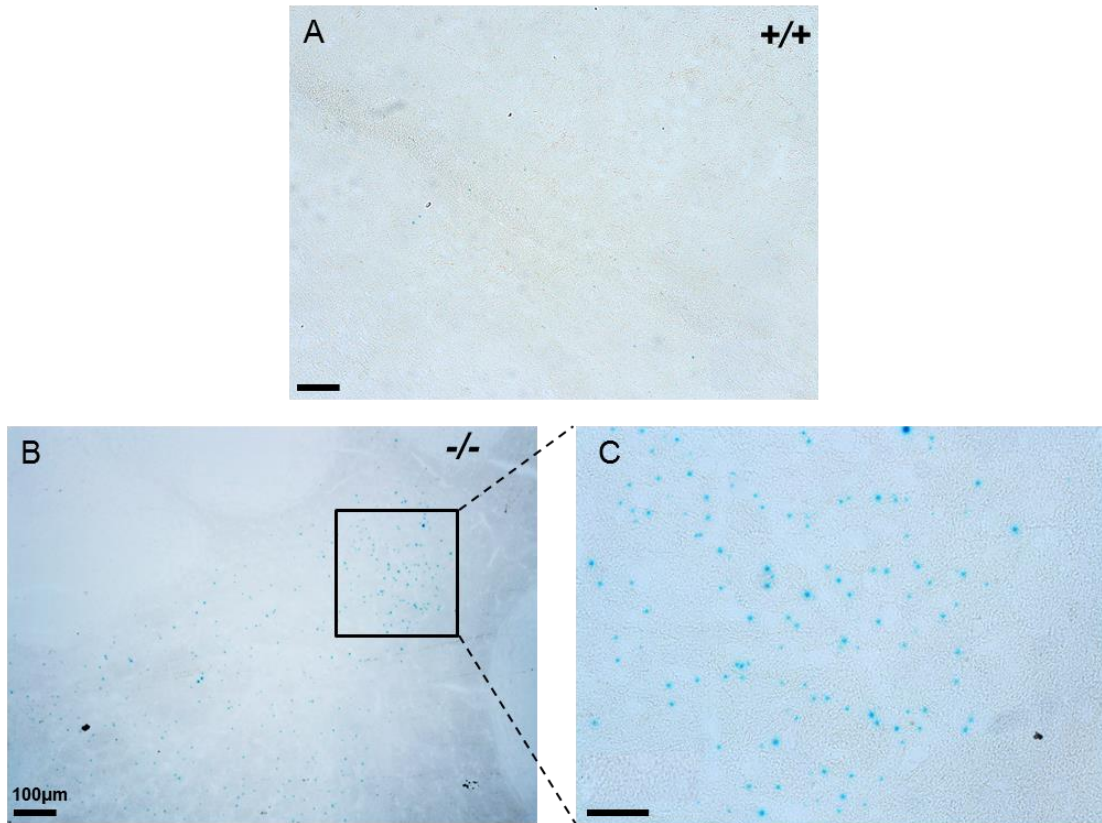


Figure 4.8 *Hhip1* expression in brain

A) Representative image of a frozen section from *Hhip1*^{+/+} brain, which comprised no x-gal staining. B) Detection of β -galactosidase activity in frozen sections of *Hhip1*^{-/-} brain. Image in (C) is a higher magnification of the region shown in (B). Scale bars=50 μ m unless otherwise stated.

In an attempt to overcome the difficulty in detecting *lacZ* expression various immunohistochemical approaches were followed. Immunohistochemical staining was expected to amplify the *lacZ* signal, since it relies on a tertiary structure detection method. The target antigenic signal is amplified by conjugating enzyme or fluorophores to secondary antibodies or avidin/streptavidin, which then binds to the biotinylated secondary antibody. The immunohistochemical approaches performed included the use of two different anti β -galactosidase antibodies both in frozen and paraffin sections as well as two secondary detection methods. The first detection system was a one-step protocol (Impress peroxidase polymer detection) from Vector laboratories, which is based on micropolymer technology and subsequent peroxidase-dependent detection. The second system involved a two-step protocol (Envision system) from DAKO (Agilent pathology solutions) based on a unique enzyme-conjugated polymer backbone, which also carries secondary antibody. Despite multiple efforts and optimization β -galactosidase staining was not detected in tissue from *Hhip1*^{-/-} animals. Stomach always produced positive staining suggesting the protocols were efficiently detecting β -galactosidase (**Figure 4.9**).

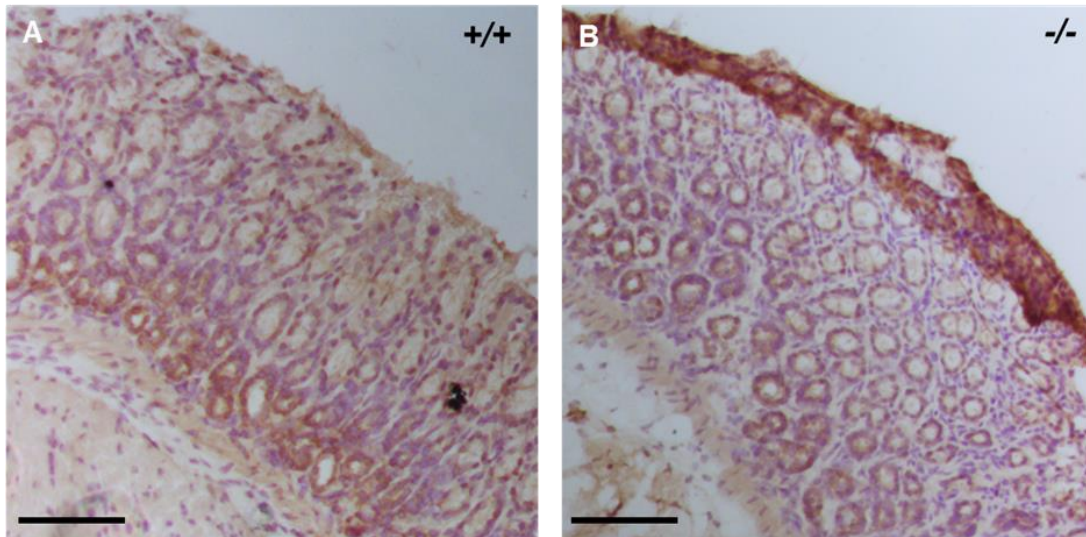


Figure 4.9 Endogenous β -galactosidase expression in stomach

Detection of β -galactosidase by immunohistochemistry. Interaction of the secondary horseradish peroxidase (HRP) conjugated antibody with DAB substrate produced brown staining. Detection of endogenous β -galactosidase activity in frozen sections of both *Hhip1*^{+/+} (A) and *Hhip1*^{-/-} stomach (B). Scale bars=100 μ m.

4.3 Discussion

Here, the generation of *Hhip1* knockout mice (which carry the knockout first *Hhip1*^{tm1a(KOMP)Wtsi} allele) were generated from ES cells imported from the KOMP repository. The lack of expression of *Hhip1* exons 7 and 8, which are downstream of the knockout first targeting cassette, in *Hhip1*^{-/-} animals confirmed that the knockout first is a non-expressive form of the allele. *Hhip1*^{-/-} mice were born at the expected Mendelian ratio and no fertility issues were identified. In addition, no overt phenotypic abnormalities were observed in these mice. The IMPC provides phenotypic data for *Hhip1* knockout mice and similarly to the above observations they report no significant differences in any of the tissues except for a small increase in tibia length in *Hhip1* null animals (<http://www.mousephenotype.org/data/genes/MGI:1919265>). Further analysis, would be required in order to exclude any minor phenotypic effects.

As described earlier (section 4.1.4), Hh signalling is a key regulator of development and it was shown through several Hh mouse models that up or downregulation can cause major phenotypes. Data from chapter 3 support a role for HH1PL1 in Hh signalling so the absence of phenotype in the knockout animals is somewhat surprising. The absence of a phenotype could be explained by functional redundancy in signalling components, where other members of the protein family (such as HHIP or HH1PL2) counteract for loss of HH1PL1. Similar redundancy is seen with *Gli1* and *Gli2*. *Gli1* homozygous knockout mice and *Gli2* heterozygous mice are both phenotypically normal, however *Gli1* homozygotes that are also heterozygous for *Gli2* die soon after birth with multiple developmental defects (Park et al. 2000).

Expression of *Hhip1* was detected in the majority of mouse tissues investigated by RT-PCR, however, no antibody was available to assess *Hhip1* expression at the protein level. Instead, in an attempt to more specifically characterise the expression pattern of *Hhip1* two different approaches including enzymatic (x-gal) and immunohistochemical (anti β -galactosidase) analysis were followed to assess the expression of the *lacZ* reporter. From the tissues that were examined by X-gal staining (heart, liver, brain, ileum, spleen, fat, aorta) only brain and septal artery showed any staining. The septal artery is only present in mice and is analogous to the human left anterior descending artery (Kumar et

al. 2005, Hu et al. 2005). For both staining approaches stomach was used as a positive control as it is known it comprises endogenous β -galactosidase activity (Bolon 2008). Immunohistochemical staining efficiently detected endogenous β -galactosidase activity in stomach, however detection of β -galactosidase in other tissues was negative. The failure to detect *lacZ* expression in mice carrying a knockout first mutation has been reported by the Sanger Institute Mouse Genetics Project (MGP), the major contributor of the IMPC, which generates knockout mouse lines using ES cells by EUCOMM and KOMP (White et al. 2013). Tuck *et al.* (2015) recently reported the *lacZ* expression in 424 knockout first lines. 4% of the lines examined showed complete absence of expression, 25.2% showed limited tissue expression, 24.8% localised expression and 46% were broadly expressed (Tuck et al. 2015). In another study *lacZ* expression was investigated in 313 mutant mouse lines with ~20% showing no specific staining (West et al. 2015). Further investigation will be required to identify the normal expression of *Hhip1*. *In situ* hybridization would allow the identification of *Hhip1* expression at the RNA level and allow the specific cell types, which express *Hhip1* to be identified. In addition, the generation of an antibody that recognizes mouse Hhip1 protein would allow further characterisation of expression and would be required to properly identify the localization of the secreted protein.

4.4 Conclusion

In conclusion, *Hhip1*^{-/-} mice were generated from ES cells carrying the knockout first allele (*Hhip1*^{tm1a(KOMP)Wtsi}). Knockout was validated at the DNA and RNA level. Knock-out mice are viable and phenotypically normal. Because of this, the knock-out first *Hhip1*^{-/-} mice were considered suitable for use in an atherosclerosis study without the need to generate either a “true” or tissue specific conditional knock-out.

5 Investigation of *Hhip1* in mouse models of atherosclerosis

5.1 Introduction

Mouse models have been used for more than 30 years to study the effects of gene knockout, overexpression and drug treatment on the development of atherosclerosis resulting in more than 500 genes being implicated in disease pathogenesis (Stylianou et al. 2012, Pasterkamp et al. 2016). Investigation of the CAD GWAS genes in these mouse models provides a method of confirming whether a gene is involved in atherogenesis. In this chapter the effect of *Hhip1* on atherosclerosis is investigated in two hyperlipidemic mouse strains (*ApoE*^{-/-} and *Ldlr*^{-/-}).

5.1.1 Validation of GWAS loci using mouse models of atherosclerosis

Since 2007 more than 60 loci have been reported to be associated with CAD in humans through GWAS. The ultimate aim of GWAS is the discovery of causal genes at the CAD associated chromosomal regions. This is mainly achieved by exploring the candidate gene function using mouse models of atherosclerosis, which allow the study of the disease within a reasonable time frame. Therefore, mice have proven crucial in understanding the molecular and cellular basis of atherosclerosis. The majority of the studies involve the deletion of the gene of interest (knockout), however some studies over express the gene of interest or modulate its activity through drug treatment. Approximately one third of CAD associated genes have been investigated in mouse atherosclerosis studies (**Table 5.1**), however, in most cases the studies were performed prior to the GWAS as the gene had already been incriminated in cardiovascular disease.

CAD associated locus	Mouse model	Atherosclerosis outcome	Reference
PCSK9	Knockout	Reduced	(Denis et al. 2012)
SORT1	Knockout	Reduced	(Mortensen et al. 2014, Patel et al. 2015)
APOB	huAPOB transgenic	Increased	(Voyiaziakis et al. 1998)
APOE	Knockout	Increased	(Zhang et al. 1992)
LDLR	Knockout	Increased	(Ishibashi et al. 1994b)
ABCG5-ABCG8	huABCG5 & ABCG8 transgenic (liver overexpression)	No effect	(Wu et al. 2004)
GUCY1A3	Knockout	Reduced	(Puimedon et al. 2015)
PLG	Plg knockout/uPa overexpression	Reduced	(Kremen et al. 2008)
HDAC9	Knockout	Reduced	(Cao et al. 2014)
9p21	Deletion of neighbouring genes: Mtap, Cdkn2a, p19Arf and Cdkn2b	<i>Mtap</i> ^{+/-} : increased <i>Cdkn2a</i> ^{+/-} : reduced <i>p19Arf</i> and <i>Cdkn2b</i> : no effect	(Visel et al. 2010)
SH2B3/LNK	Knockout	Increased	(Wang et al. 2016)
ADAMTS7	Knockout	Reduced	(Bauer et al. 2015)
KCNE2	Knockout	Increased	(Lee et al. 2015)
LPL	huLPL (macrophage expression)/ <i>ApoE</i> ^{-/-}	Increased	(Wilson et al. 2001)
APOC1	Knockout/LPS treatment	LPS induced atherosclerosis in <i>Apoc1</i> ^{+/+} but not in <i>Apoc1</i> ^{-/-}	(Westerterp et al. 2007)
eNOS (NOS3)	Knockout	Increased	(Ponnuswamy et al. 2012)
MFGE8	Knockout	Increased	(Ait-Oufella et al. 2007)
CXCL12	C57BL/6 Compound treatment (CXCL12)	Stable lesions without promoting atherosclerosis	(Akhtar et al. 2013)
EDNRA	<i>ApoE</i> ^{-/-} ; <i>Ldlr</i> ^{-/-} Compound treatment (EDNRA inhibition)	Reduced (when chronic inhibition)	(Barton et al. 1998)

TRIB1	Knockout	Increased (heterozygous)	(Arndt, 2015)
FLT1	Knockout	Increased	(Matsui et al. 2014)
Furin	<i>Ldlr</i> ^{-/-} /Hepatic profurin overexpression	Reduced	(Lei et al. 2014)
SMAD	<i>ApoE</i> ^{-/-} ; <i>Ldlr</i> ^{-/-} Compound treatment (Smad 1,2,3 activation by atorvastatin)	Reduced	(Vecerova et al. 2012)

Table 5.1 Investigation of GWAS loci using mouse models of atherosclerosis.

Hu= human

LPS= Lipopolysaccharide

uPa= urokinase type plasminogen activator

5.1.2 Quantitation of atherosclerosis in mouse models

In humans the various modes of assessing the clinical presence of atherosclerosis focus on the lesion size as an indicator of atherosclerosis progression. Similarly, in mouse atherosclerosis studies plaque size is one of the main focuses and is measured in two different ways. One approach involves the quantification of lesion size by *en-face* analysis of the aorta whereas the other method focuses on lesion size in the aortic root. *En face* analysis of the aorta normally includes the arch and thoracic regions and can extend down into the abdominal aorta and was first described by Tangiral *et al.* (Tangirala, Rubin & Palinski 1995) . The *en face* method involves the isolation of the required regions of the aorta, which is then cut longitudinally in order to expose the intimal surface. The lesions are then defined by ORO staining, which stains neutral triglycerides and lipids. *En face* analysis provides lesion coverage information without taking into account the thickness of the plaque.

The second approach is examination of the aortic root, which was the first described method for measuring lesion size (Paigen et al. 1987b). In brief, this method relies on sequential tissue sectioning from the origin of the aortic valves towards the ascending aorta. Following sectioning, the lesion area within the root is defined by ORO staining. Analysis of the aortic root provides information about whether the lesions are expanding in thickness and/or laterally and hence it is considered more accurate than *en face* analysis.

While lesion size continues to be an important indicator of atherosclerosis progression, it is clear that the clinical manifestation of atherosclerosis occurs due to plaque rupture and subsequent thrombosis, which is dependent upon lesion composition. Defining the cellular components is also important, especially when the effect of a gene is investigated as it could affect a cellular pathway rather than the overall disease progression. Identification of the main components of a lesion is achieved by histochemical and immunohistochemical staining of cross sections of the aortic root. The major components analysed for this purpose are lipids, macrophage/monocytes, SMCs and collagen (Lu, Rateri & Daugherty 2007) .

5.1.3 Atherosclerosis study design

There are few major factors that need to be taken into account when designing an atherosclerosis study. These mainly include the stimulus for atherosclerosis development (choice of hyperlipidemic strain and diet), the study duration and the gender of the animals.

As discussed above *Apoe*^{-/-} and *Ldlr*^{-/-} are the most well described mice for which the disease progression is known. For the purpose of this study both *Apoe*^{-/-} and *Ldlr*^{-/-} mice on a C57BL/6 background were examined as *Hhip1* was a novel gene and so its impact upon atherosclerosis development could not be predicted. Consequently, if *Hhip1* was reducing atherosclerosis it was postulated that its effect would be more obvious on an *Apoe*^{-/-} background where the disease is more advanced whereas if it was acting in the opposite direction it would be easier to detect this effect on an *Ldlr*^{-/-} background where the disease is less advanced. A combination of the appropriate hyperlipidemic background and treatment with atherogenic diet is common practice for accelerating disease progression. Western diet is the most commonly used diet in atherosclerosis studies because it mimics the average dietary composition consumed by humans in Western world.

The duration of the study is another factor that needs to be taken into consideration. The majority of such studies investigate lesions that are being defined at a single time interval dictated either by the age or mouse or by the atherosclerosis stimulus. This can provide accurate information only if the extent of disease affected by a manipulation is either unaltered or constant but

there is however the possibility that the manipulation has only a transient effect in which case this effect could be missed if only late disease stages are studied (Daugherty, Rateri 2005).

As far as gender factor is concerned it is unclear how gender affects atherosclerosis outcome. Some studies suggest female mice develop lesions to a greater extent (Paigen et al. 1987a, Tangirala, Rubin & Palinski 1995, Smith et al. 2010) compared to male but this was not consistent in other studies (Nelson et al. 2007, Marsh et al. 1999, Li et al. 2000). However most of the studies conclude that the atherosclerosis outcome can be gender-dependent and suggest that it should be taken into account when designing atherosclerosis studies (Surra et al. 2010, Daugherty, Rateri 2005).

5.2 Results

5.2.1 Investigation of *Hhip1* expression in atherosclerosis

To gain further insight regarding *Hhip1* in atherosclerosis, its expression was investigated in the aortic arch and the thoracic aorta of an atherosclerotic mouse model. *Apoe*^{-/-} mice develop atherosclerotic lesions on a chow diet with increasing disease severity corresponding to mouse age (**Figure 5.1 A**) (Nakashima et al. 1994). Mice were therefore collected between 6 and 48 weeks of age and two distinct aortic regions were dissected for RNA extraction; the aortic arch which is the site most susceptible to lesion development and the middle third of the thoracic aorta which is more resistant to disease (**Figure 5.1 B&C**).

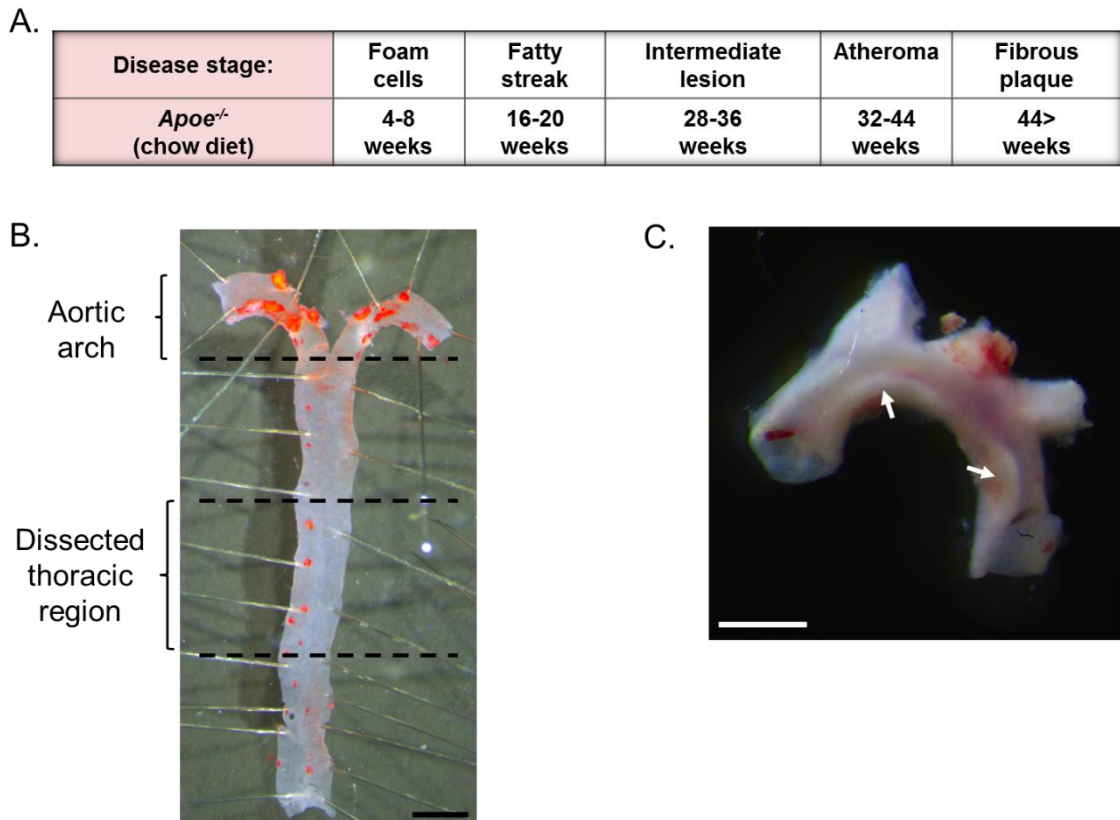


Figure 5.1 Aortic sites included in the expression study

A) Table shows the correlation between disease stages and mouse age in *Apoe*^{-/-} mice fed chow diet. B) Longitudinal section through the inner curvature of the aortic arch down the diaphragm of an 18 weeks old *Apoe*^{-/-} mouse. Lesions depicted in red after ORO staining are mostly localised in the aortic arch. Black dotted lines show the sites of dissection. Scale bar =2mm C) Microscopic observation of atherosclerotic lesions localised at the arch (white arrows). Scale bar = 1mm.

Additionally, in order to control for any ageing effect on *Hhip1* expression C57BL/6 mice of 6, 24 and 48 weeks of age were examined. *Hhip1* expression was determined by qPCR in relation to *Rpl4* housekeeper control. *Hhip1* expression was significantly increased across the different time-points (ANOVA $P=0.0004$) in the aortic arch of *Apoe*^{-/-} mice with an increase in expression of almost three-fold by the end of the study (**Figure 5.2 A**). Post-hoc comparisons to the 6-week time-point showed a significant increase in expression at 32 ($P=0.001$), 40 ($P=0.002$) and 48 weeks ($P=0.01$). No differences in *Hhip1* expression were detected in the aortic arch across the aged C57BL/6 mice (**Figure 5.2 B**), indicating that the increase seen in the aortic arch of *Apoe*^{-/-} mice is disease related rather than age related. In contrast to the increased expression in the aortic arch there was a moderate decrease in *Hhip1* expression in the thoracic aorta (ANOVA $P=0.02$) (**Figure 5.2 C**). Further post-hoc comparisons to the 6-week time-points showed a modest but significant decrease in expression at 24 ($P=0.03$), 32 ($P=0.004$) and 40 weeks ($P=0.02$), whereas no difference was observed in *Hhip1* expression of C57BL/6 mice (**Figure 5.2 D**).

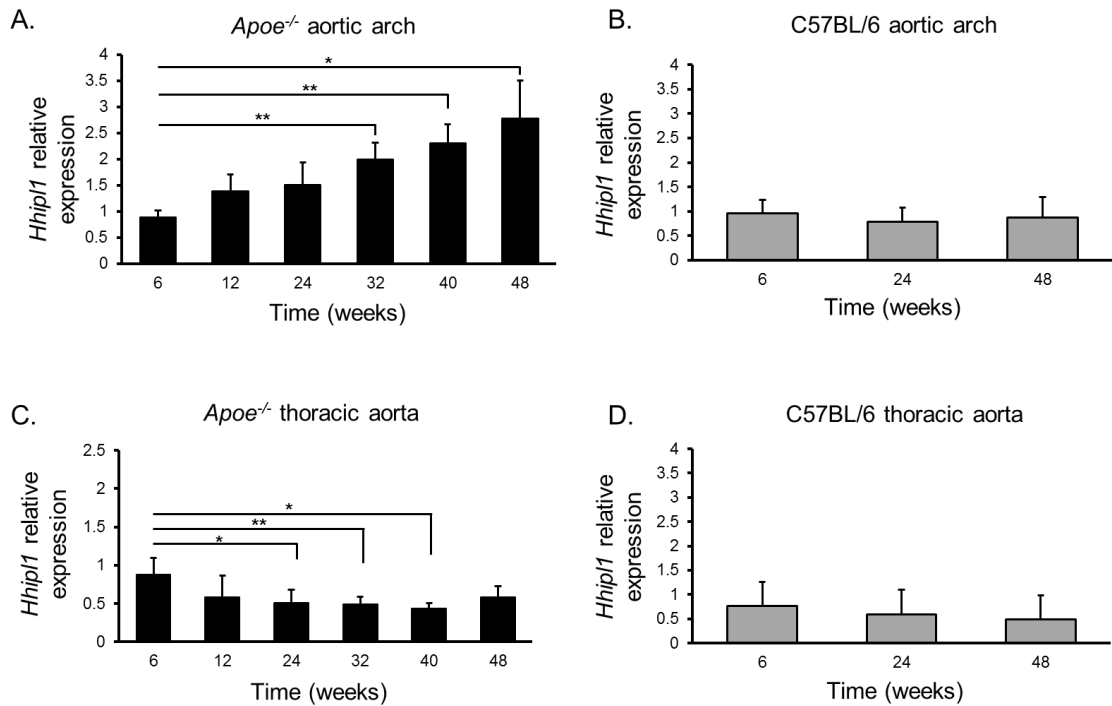


Figure 5.2 *Hhip1* expression pattern during atherosclerosis progression

A) Increased expression of *Hhip1* was detected in the aortic arch of *Apoe*^{-/-} mice (n=3-6 mice/ group, 6 vs 32 $P=0.001$, 6 vs 40 $P=0.002$, 6 vs 48 $P=0.01$, one-way ANOVA $P=0.0004$). B) No difference in *Hhip1* expression in the aortic arch of wild type mice was observed. C) Decreased expression was observed in the thoracic aorta of *Apoe*^{-/-} mice between 24 and 40 weeks when compared with 6 weeks (n=3-6 mice/group, 6 vs 24 $P=0.03$, 6 vs 32 $P=0.004$, 6 vs 40 $P=0.02$, one-way ANOVA $P=0.02$). D) No change in *Hhip1* expression was observed at the thoracic aorta of aged wild type mice. Expression was normalised to *Rpl4*. * $P\leq 0.05$, ** $P\leq 0.01$, *** $P\leq 0.001$

5.2.2 *Hhip1*^{-/-} mouse atherosclerosis study

Having confirmed a relationship between *Hhip1* expression and atherosclerosis progression I went on to directly test whether *Hhip1* is involved in disease pathogenesis in two mouse models of atherosclerosis. For this purpose, mice carrying the *Hhip1* knockout first construct (chapter 4) were backcrossed to C57BL/6 mice for 6 generations (N6) in order to obtain a more homogeneous genetic background. These mice were then crossed to *Apoe*^{-/-} and *Ldlr*^{-/-} atherosclerosis mouse strains. Double male knockouts (KO) referred to as *Hhip1*^{-/-}; *Apoe*^{-/-} and *Hhip1*^{-/-}; *Ldlr*^{-/-} were investigated in comparison to littermates wild-type for *Hhip1*, referred to as *Hhip1*^{+/+}; *Apoe*^{-/-} and *Hhip1*^{+/+}; *Ldlr*^{-/-}. The PCR genotyping strategy to identify wild type or knockout *Hhip1* allele was described in chapter 4 (section 4.2.1) and is shown in **Figure 5.3 A&B**. Genotyping for both the *Ldlr* and *Apoe* alleles was performed using a PCR able to detect both the wild-type and mutant versions. There are three different outcomes for each PCR design indicating either the presence of a wild type band, a mutant band or the presence of two bands for a heterozygous genotype (**Figure 5.3 C&D**).

In order to accelerate disease progression in double KO mice and wild type controls for *Hhip1*, mice were fed 'western-diet' for 12 weeks from 6 weeks of age (**Figure 5.4**).

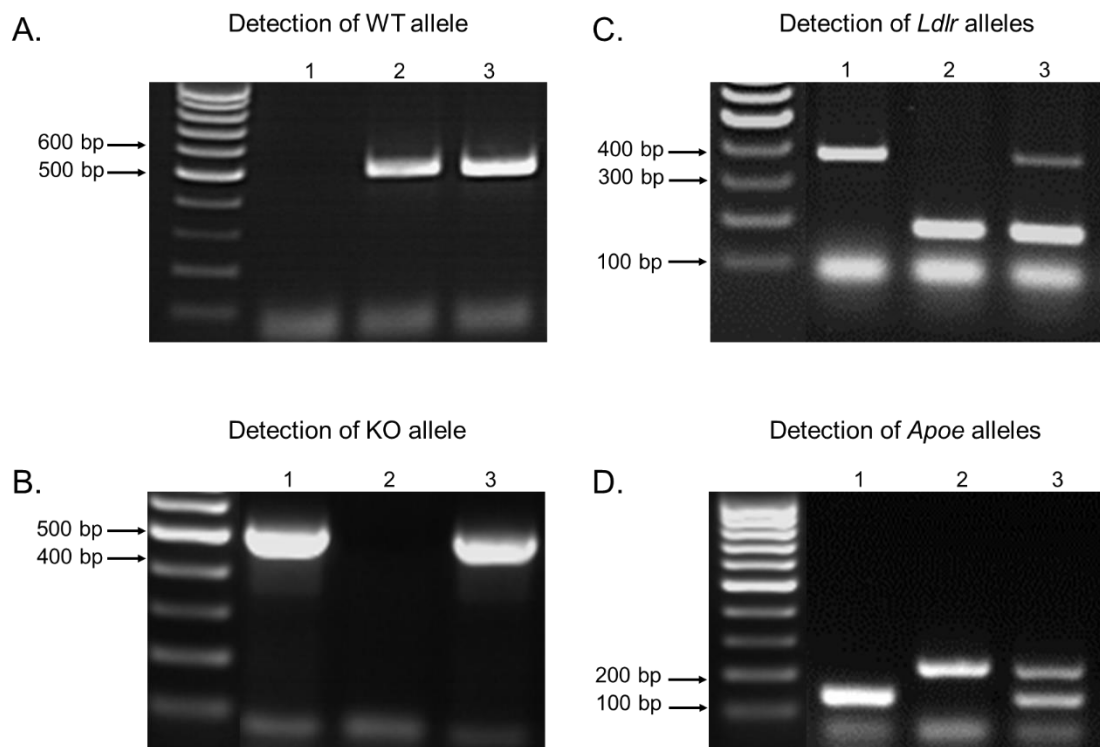


Figure 5.3 Representative mouse genotypes

Gel shows the PCR products of *Hhip1* wild type (WT) (A) allele and KO allele (B) (Lane1: *Hhip1*^{-/-}, Lane 2: *Hhip1*^{+/+}, Lane 3: *Hhip1*^{+/-}). C) PCR outcomes for *Ldlr* allele (Lane1: *Ldlr*^{-/-}, Lane 2: *Ldlr*^{+/+}, Lane 3: *Ldlr*^{+/-}) and *Apoe* allele (D) (Lane1: *Apoe*^{+/+}, Lane 2: *Apoe*^{-/-}, Lane 3: *Apoe*^{+/-}).

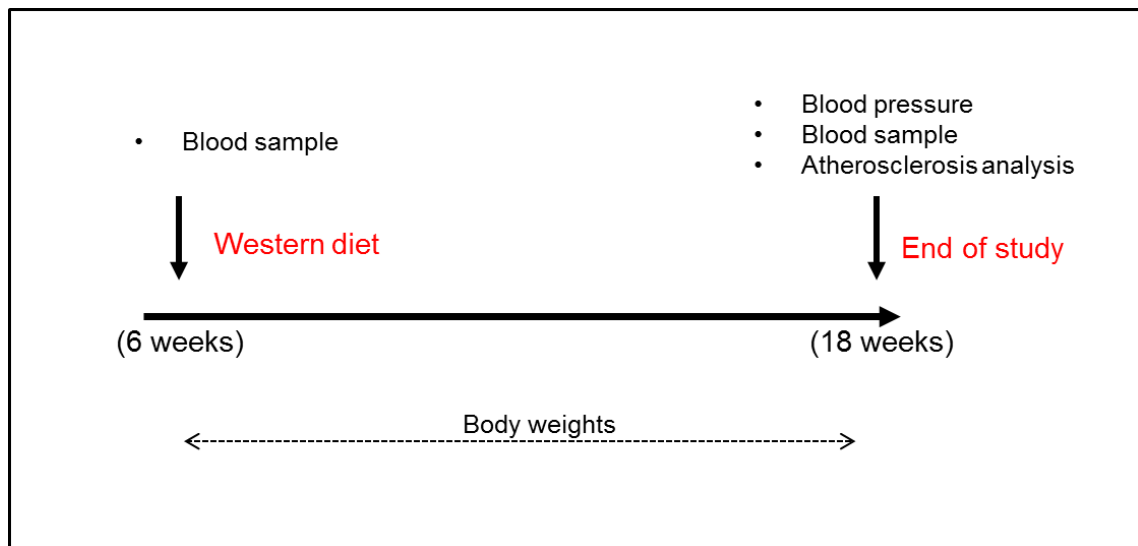


Figure 5.4 Atherosclerosis study design

The diagram shows the experimental design of the atherosclerosis study. All genotype groups (*Hhpl1*^{-/-};*Ldlr*^{-/-} and *Hhpl1*^{-/-};*Apoe*^{-/-} as well as wild type littermates for *Hhpl1*) were fed western diet for 12 weeks. Mouse weights were monitored weekly during the study and blood pressure measurements were obtained at the endpoint. Blood samples were collected before the start and at the end of the study, for future lipid analysis. Mice were sacrificed at 18 weeks of age and atherosclerosis progression was assessed.

5.2.3 Assessment of body weight and blood pressure in *Hhpl1*^{-/-} mice

Blood pressure and body weight were measured to determine whether *Hhpl1* knockout influences traditional cardiovascular disease risk factors. Body weight was measured weekly through the study and no difference was found between *Hhpl1*^{+/+};*Ldlr*^{-/-} and *Hhpl1*^{-/-};*Ldlr*^{-/-} (**Figure 5.5 A**) or *Hhpl1*^{+/+};*Apoe*^{-/-} and *Hhpl1*^{-/-};*Apoe*^{-/-} (**Figure 5.5 B**).

Blood pressure was measured using non-invasive VPR sensor technology, which involves an occlusion tail cuff as part of the procedure. There was no difference in either systolic or diastolic blood pressure in *Hhpl1*^{-/-};*Ldlr*^{-/-} or *Hhpl1*^{-/-};*Apoe*^{-/-} mice compared to wild-type controls (**Figure 5.6**).

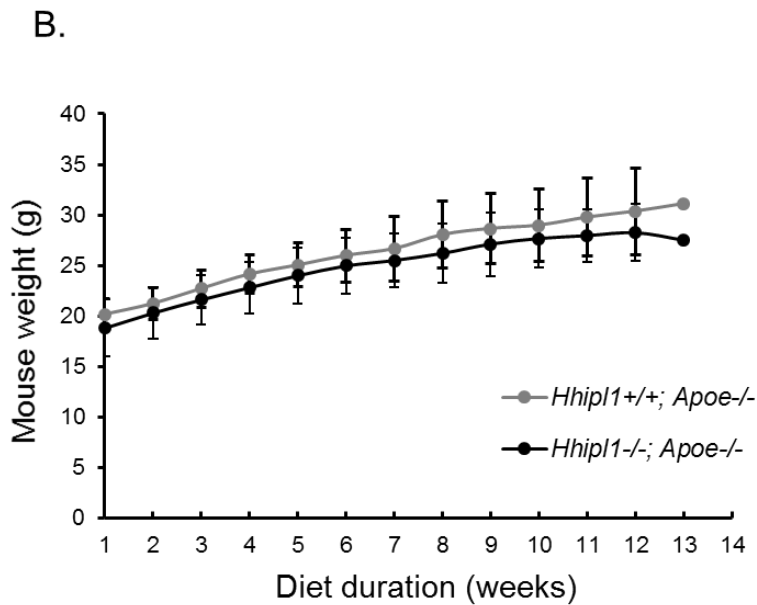
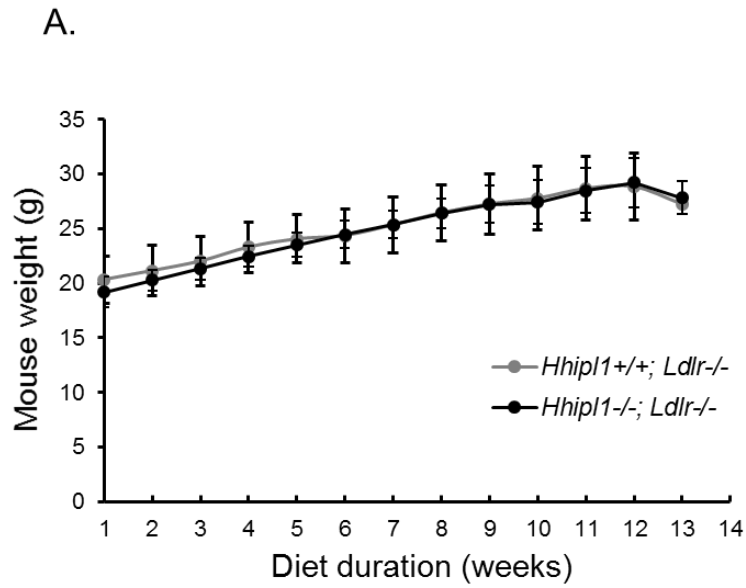


Figure 5.5 Mouse weights during western-diet treatment

Body weight was monitored weekly during the western diet treatment. No difference was observed in either *Ldlr*^{-/-} (n=18 vs n=19, $P>0.05$) (A) or *Apoe*^{-/-} backgrounds (n=19 vs n=17, $P>0.05$) (B). Statistical significance was tested using unpaired Students t-tests.

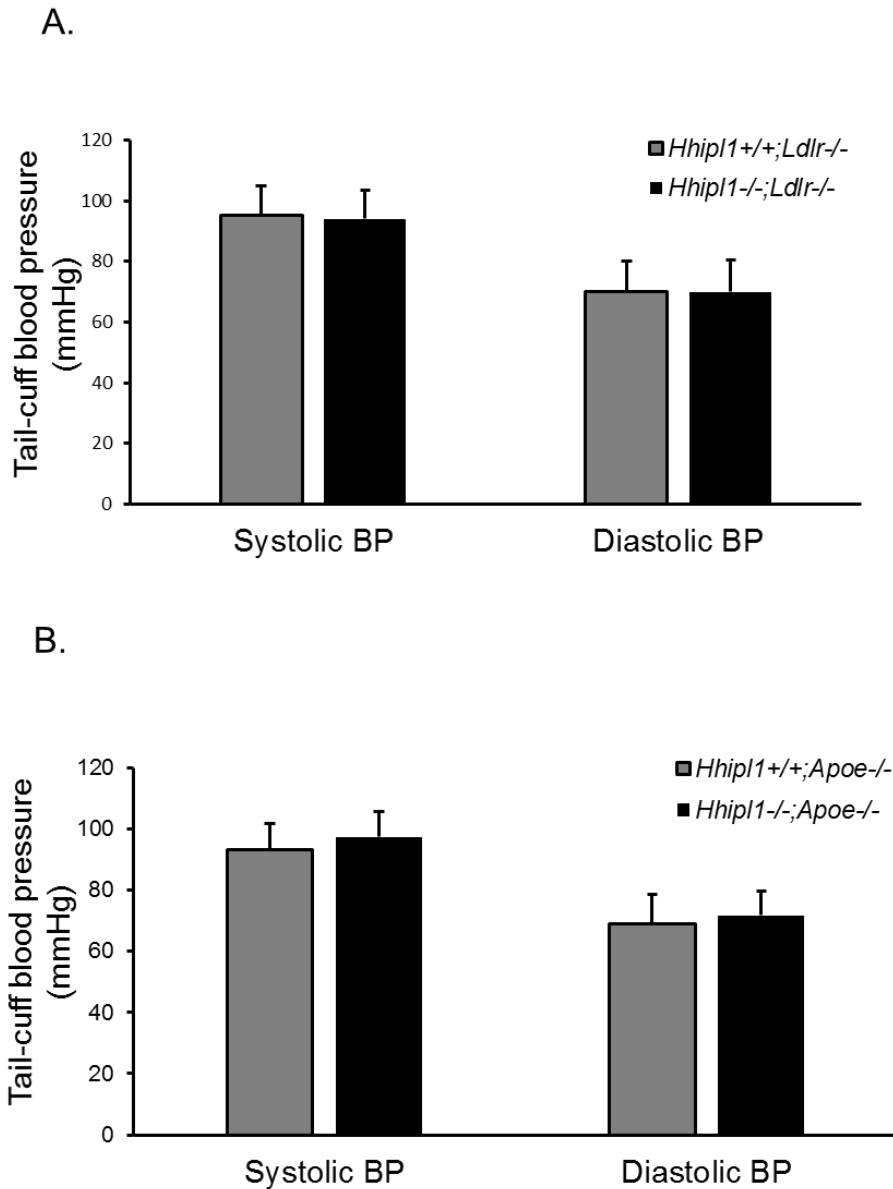


Figure 5.6 Blood pressure assessment

Blood pressure was measured by tail cuff VPR technology. No differences were observed in either systolic or diastolic blood pressure in *Ldlr*^{-/-} (n=15, $P>0.05$) (A) or *Apoe*^{-/-} (n=19 vs n=17, $P>0.05$) backgrounds (B). Statistical significance was tested using unpaired Students t-tests.

5.2.4 Quantitation of atherosclerosis in *Hhip1*^{-/-} mice

Atherosclerosis progression was assessed in both the entire aorta (excluding the abdominal region) by *en face* preparation and the aortic root by cross sectioning. Both anatomical regions were included in the analysis in order to obtain information about lesion coverage and thickness (described in section 5.1.4). For the *en face* analysis aortas were freshly isolated and the intimal area was exposed by creating a longitudinal cut. ORO staining was performed in order to visualise atherosclerotic lesions. Following staining, the aortas were imaged using a stereo microscope and plaque area was calculated and normalised to the total aorta size using the LAS V 4.0 imaging software. *Hhip1*^{-/-}; *Ldlr*^{-/-} mice exhibited a significant reduction of 56% (± 29) ($P=5 \times 10^{-6}$) in lesion area compared to the *Hhip1*^{+/+}; *Ldlr*^{-/-} littermate controls (**Figure 5.7 A&B**). In concordance with the above finding *Hhip1*^{-/-}; *Apoe*^{-/-} mice had a 53.4% (± 25) reduction ($P=0.0002$) in lesion area compared to *Hhip1*^{+/+}; *Apoe*^{-/-} controls (**Figure 5.8 A&B**).

Serial aortic root sections were collected (9 sections/mouse, spanning a 900 μ m stretch of the aortic root) and stained with ORO staining. The aortic root lesions were defined by positive ORO staining and lesion area was calculated and normalised to the total aorta size using the ImageJ software. *Hhip1*^{-/-}; *Ldlr*^{-/-} mice exhibited a 35% ($\pm 15\%$) reduction in lesion area ($P=0.002$) compared to controls (**Figure 5.7 C&D**). *Hhip1*^{-/-}; *Apoe*^{-/-} mice showed a non-significant reduction in lesion size of 11% (± 22) ($P=0.4$) (**Figure 5.8 C&D**).

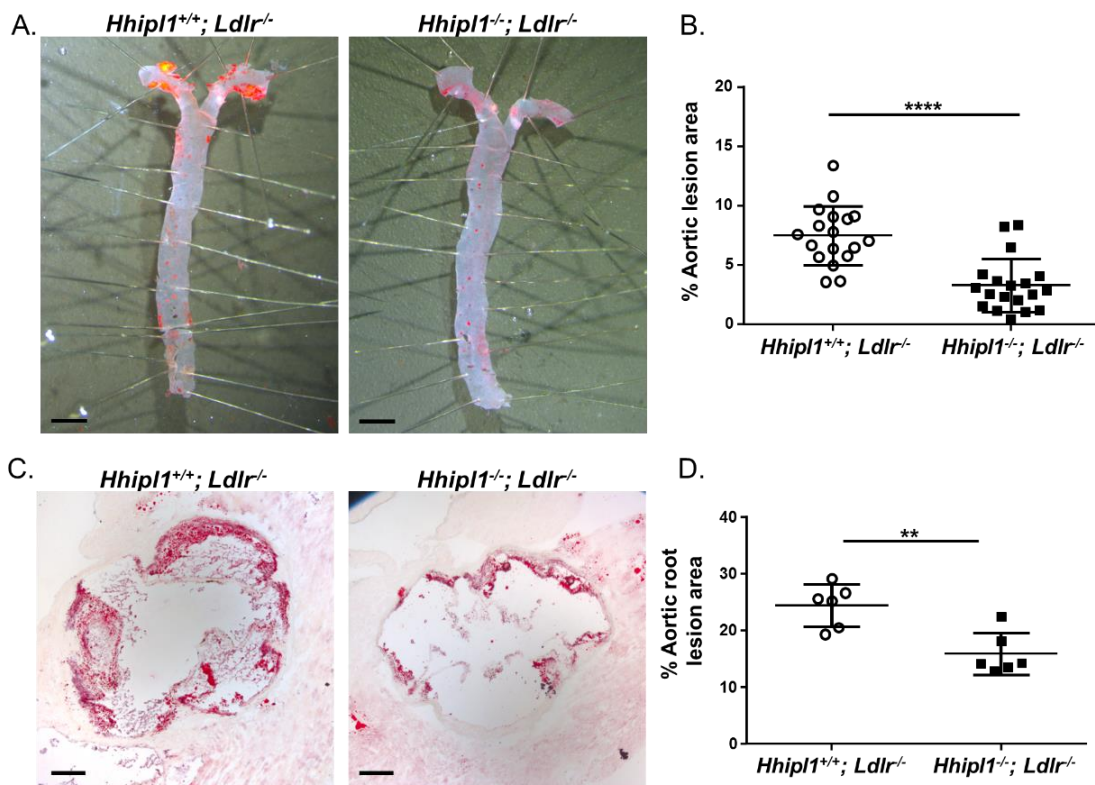


Figure 5.7 Quantification of atherosclerotic lesions in *Hhip1*; *Ldlr*^{-/-}A) Representative microphotographs of *en face* preparation of aortas from *Hhip1*^{-/-}; *Ldlr*^{-/-} and *Hhip1*^{+/+}; *Ldlr*^{-/-} mice stained with ORO (red). B) After 12 weeks on western diet atherosclerotic lesion areas were significantly attenuated in the double KO (n=18 vs n=19, $P= 5 \times 10^{-6}$) Scale bars=2mm. C) Representative microphotographs of aortic root sections from *Hhip1*^{-/-}; *Ldlr*^{-/-} and *Hhip1*^{+/+}; *Ldlr*^{-/-} mice stained red with ORO. D) Quantification of lesion area was performed on the entire length of the aortic root using 9 sections per mouse, showing a significant reduction in atherosclerotic lesion in *Hhip1*^{-/-}; *Ldlr*^{-/-} mice (n=6, $P=0.0027$). Statistical significance was tested using unpaired Students t-tests. ** $P \leq 0.01$, *** $P \leq 0.001$. Scale bars=200 μ m.

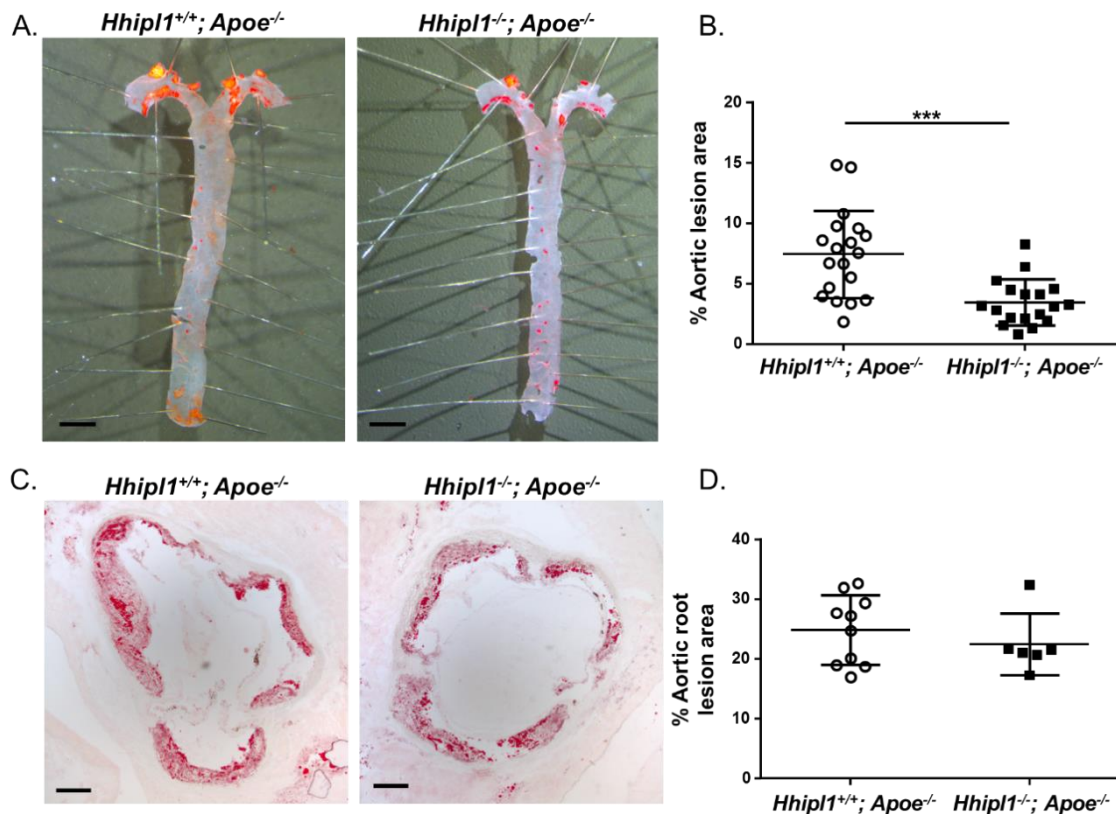


Figure 5.8 Quantification of atherosclerotic lesions in *Hhip1*; *Apoe*^{-/-}

A) Representative microphotographs of *en face* preparation of aortas from *Hhip1*^{-/-}; *Apoe*^{-/-} and *Hhip1*^{+/+}; *Apoe*^{-/-} mice stained with ORO (red). B) After 12 weeks on western diet atherosclerotic lesion areas were significantly attenuated in the double KO (n=18 vs n=19, $P=0.0002$) Scale bars=2mm. C) Representative microphotographs of aortic root sections from *Hhip1*^{-/-}; *Apoe*^{-/-} and *Hhip1*^{+/+}; *Apoe*^{-/-} mice stained with ORO (red). D) Quantification of lesion area was performed on the entire length of the aortic root using 9 sections per mouse. A non-significant reduction in lesion area was observed in the double KO (n=10 vs n=6, $P=0.4$). Statistical significance was tested using unpaired Students t-tests. *** $P\leq 0.001$. Scale bars=200 μ m.

5.2.5 Compositional analysis of atherosclerotic lesions in *Hhip1*^{-/-} mice

While lesion size is the first indicator of disease development, the composition analysis of lesions gives useful insight about the disease development, plaque stability and the potential cell-type specific effects. Given the complexity of the disease process it is important to gather as much information as possible about the cellular components that contribute to lesion morphology. The aortic root is the most common region for examining the morphology. Therefore the main components of aortic root lesions from the *Hhip1*;*Ldlr* and *Hhip1*;*ApoE* double KO mice as well as the relevant *Hhip1* littermate controls were characterised. Serial aortic root sections were obtained (9 sections/mouse) and assessed for lipids by ORO staining and collagen by Masson's Trichrome staining. Additionally, IHC was performed for macrophage (MOMA-2) and SMC markers (α -SMA) (**Figure 5.9, 5.10 & 5.11**). Image analysis for lesion component coverage (as a percentage of the total lesion area) revealed a 46% (\pm 20%) ($P=0.0036$) reduction in cells stained positive for α -SMA in *Hhip1*^{-/-}; *Ldlr*^{-/-} lesions compared to controls (**Figure 5.9 C&G**) and similarly 47% (\pm 20%) ($P=0.001$) reduction in *Hhip1*^{-/-}; *ApoE*^{-/-} mice (**Figure 5.10 C&G**). In addition, there was a non-significant reduction in collagen content in the plaques of both *Hhip1*^{-/-}; *Ldlr*^{-/-} and *Hhip1*^{-/-}; *ApoE*^{-/-} mice ($P=0.07$ for *Hhip1*^{-/-}; *Ldlr*^{-/-}, $P=0.08$ for *Hhip1*^{-/-}; *ApoE*^{-/-}) (**Figure 5.9 & 5.10 D&H**). The percentage of lipids within the plaque was not altered for the *Ldlr*^{-/-} background but a borderline difference was observed on the *ApoE*^{-/-} background. The lipid difference seen on the *ApoE*^{-/-} background, however, was not powered according to statistical analysis and therefore it was not considered convincing (**Figure 5.10 A&E**). The macrophage content was the same for both double KO mice and controls on both hyperlipidemic backgrounds (**Figure 5.9 B&F** and **Figure 5.10 B&F**). Overall *Hhip1* deficiency was associated with a reduction in lesion size in both *Hhip1*^{-/-}; *Ldlr*^{-/-} and *Hhip1*^{-/-}; *ApoE*^{-/-} mice. The lesions in double KO mice were characterised by reduced SMC content and by a trend towards a reduction in collagen, which could be explained by the SMC deficiency.

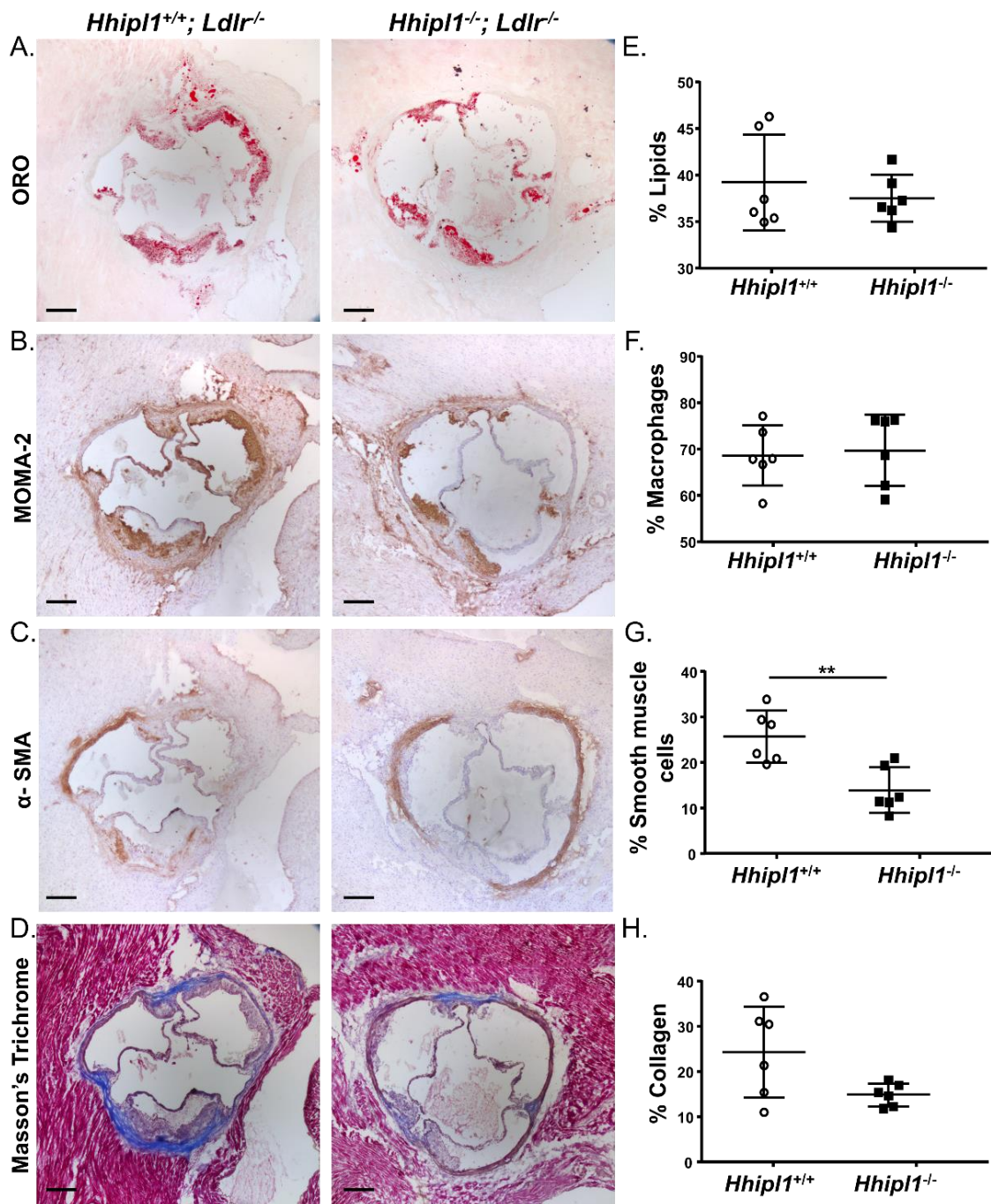


Figure 5.9 Compositional analysis of *Hhip1*;*Ldlr*^{-/-} atherosclerotic lesions
 Representative photomicrographs of atherosclerotic lesion components. ORO staining for lipids, (A), anti-MOMA-2 staining for macrophages (B), anti- α -SMA staining for SMCs (C) and Masson's Trichrome for collagen (D) were performed in aortic root sections from *Hhip1*^{-/-};*Ldlr*^{-/-} and *Hhip1*^{-/-};*Ldlr*^{+/+} mice fed western-diet for 12 weeks (n=6/group). The percentage coverage of lipids (E), macrophages (F), SMCs (G) and collagen (H) was quantified by the average of 9 serial sections per mouse and was normalised to lesion area. After 12 weeks

on western diet the SMC content was significantly reduced by ≈ 2 fold in double KOs ($n=6$, $P=0.0036$). Collagen content was altered in the same direction as SMCs. Macrophage and lipid content remained constant for both genotypes. Statistical significance was tested using unpaired Students t-tests. ** $P \leq 0.01$. Scale bars=200 μ m.

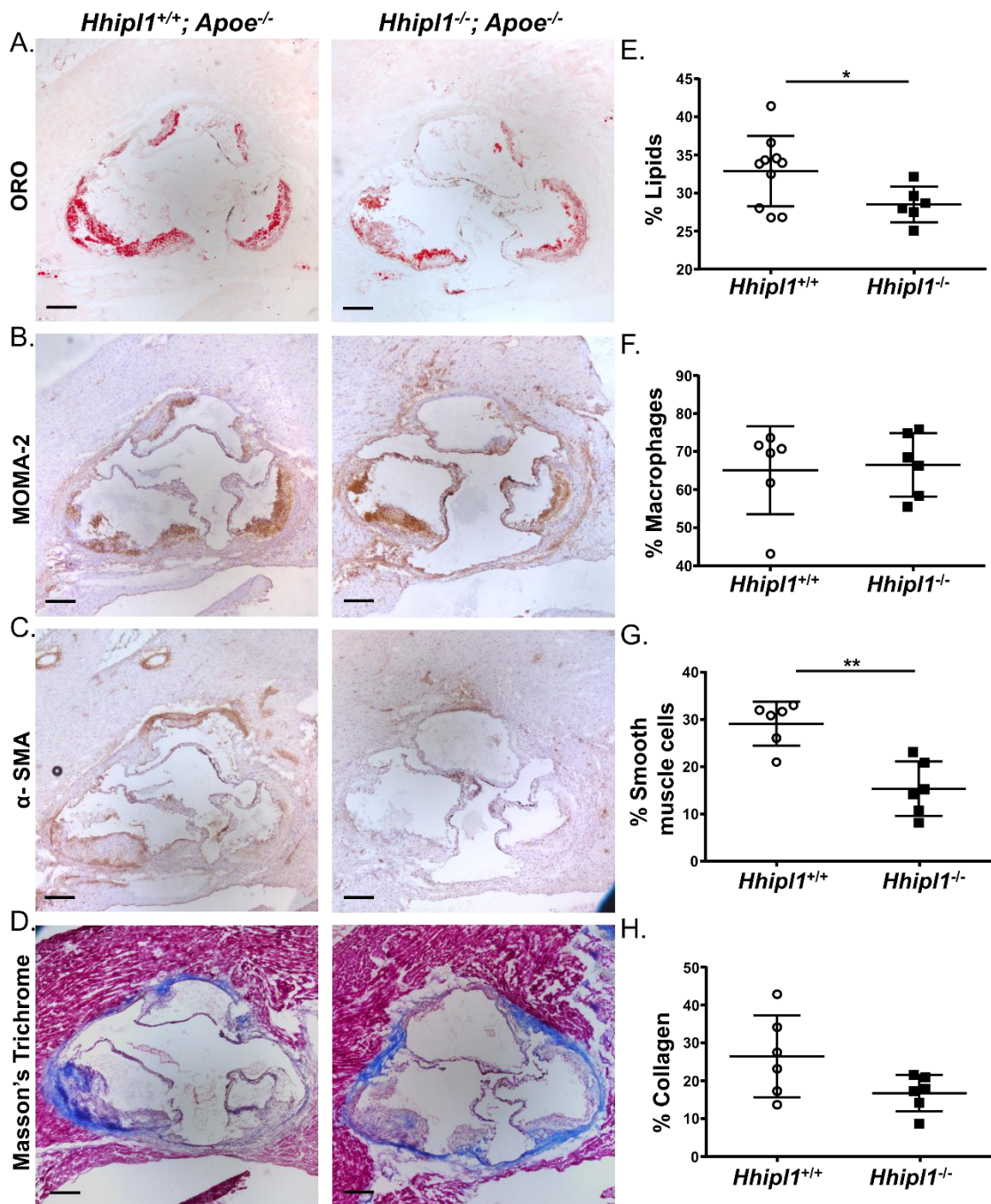


Figure 5.10 Compositional analysis of *Hhip1*;*ApoE*^{-/-} atherosclerotic lesions

Representative photomicrographs of atherosclerotic lesion components. ORO staining for lipids, (A), anti-MOMA-2 staining for macrophages (B), anti- α -SMA staining for SMCs (C) and Masson's Trichrome for collagen (D) were performed in aortic root sections from *Hhip1*^{-/-}; *Ldlr*^{-/-} and *Hhip1*^{-/-}; *Ldlr*^{+/+} mice fed western-diet for 12 weeks (n=6/group). The percentage coverage of lipids (E), macrophages (F), SMCs (G) and collagen (H) was quantified by the average of

9 serial sections per mouse and was normalised to lesion area. After 12 weeks on western diet the SMCs content was significantly reduced by ≈ 2 fold in double KOs ($n=6$, $P=0.001$). Collagen content was altered in the same direction as SMCs. Macrophage content remained constant for both genotypes, whereas lipid content was reduced in *Hhip1*^{-/-}; *ApoE*^{-/-} but the effect was not highly significant ($n=10$ vs $n=6$, $P=0.049$) (E). Statistical significance was tested using unpaired Students t-tests. * $P \leq 0.05$, ** $P \leq 0.01$. Scale bars=200 μ m.

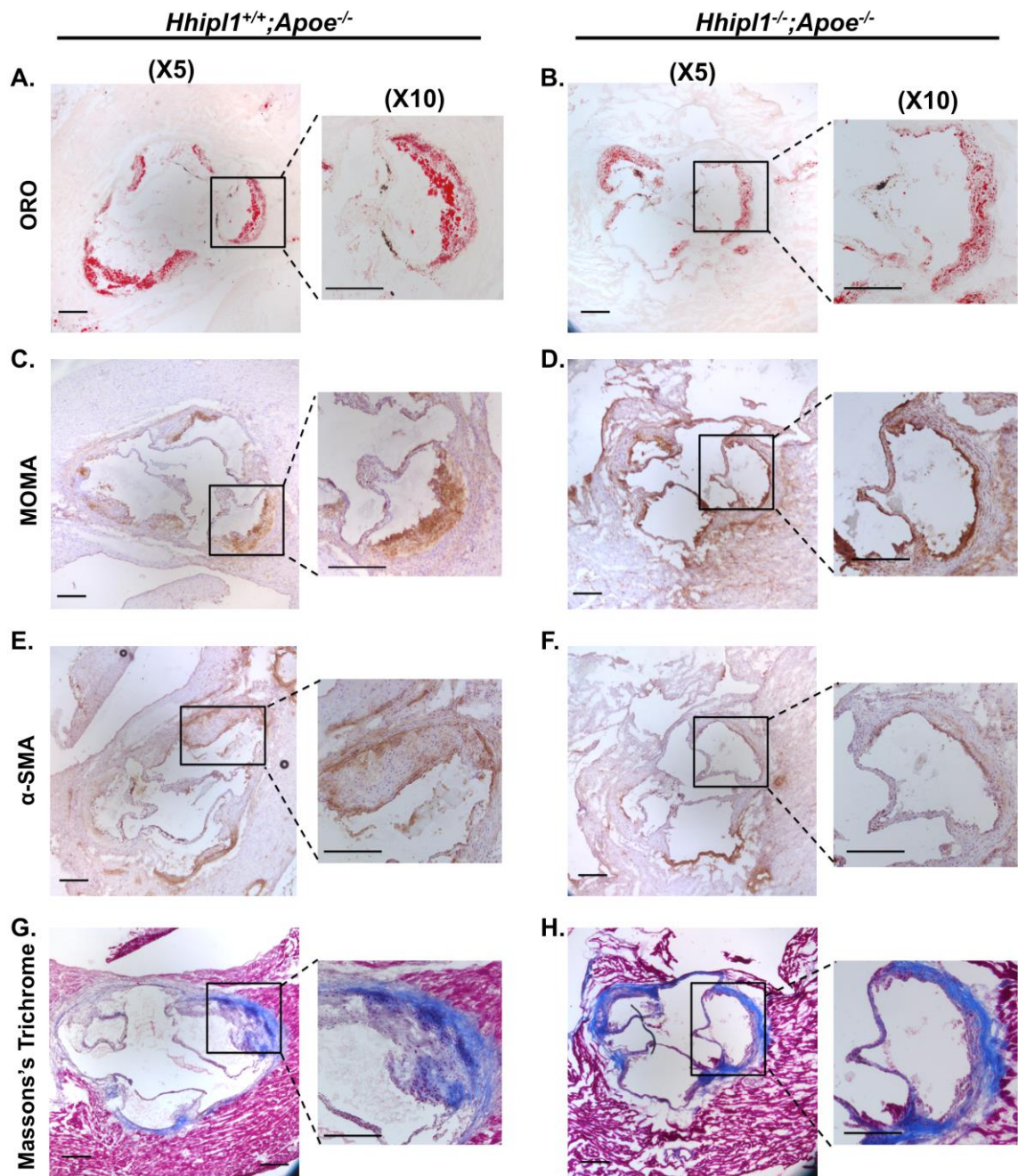


Figure 5.11 Cellular staining of *Hhip1*;*ApoE*^{-/-} atherosclerotic lesions

Higher magnification images (10X) illustrate the cellular and molecular composition of *Hhip1*^{-/-}; *ApoE*^{-/-} and *Hhip1*^{+/+}; *ApoE*^{-/-} lesions. Lipid content is shown in (A&B), macrophages in (C&D), SMCs in (E&F) and collagen in (G&H). Scale bars=200µm.

5.3 Discussion

The results described in this chapter demonstrate that knockout of *Hhip1* in mouse causes a pronounced reduction in atherosclerosis providing strong evidence that human *HHIPL1* is the causal gene at the 14q32 CAD risk locus.

Hhip1 implication in atherosclerosis was studied in two mouse hyperlipidemic models. Whole-body *Hhip1* KO mice were obtained and bred onto both the *Ldlr*^{-/-} and *ApoE*^{-/-} mouse strains. After 12 weeks of treatment with atherogenic diet (western-diet), double KO mice (*Hhip1*^{-/-};*Ldlr*^{-/-} and *Hhip1*^{-/-};*ApoE*^{-/-}) exhibited significantly smaller atherosclerotic lesions both at the aorta and at the aortic root in comparison to controls. The observation that *Hhip1* deficiency was associated with reduced atherosclerosis suggests that *Hhip1* is potentially pro-atherogenic and it could therefore be a therapeutic target. In order to evaluate *Hhip1* as a potential therapeutic agent, however, it is necessary to define more of its properties in relation to disease progression. The results described here refer to complete loss of *Hhip1*. Investigation of *Hhip1* heterozygous mice would provide information regarding any gene dosage effect and whether haploinsufficiency of *Hhip1* results in reduced atherosclerosis. An intermediate effect on lesion development would make *HHIPL1* a more promising potential clinical target. It would also be important to investigate *Hhip1* deficiency in female mice to eliminate any gender effects.

The effect of *Hhip1* on atherosclerosis relevant cell types is also important in order to define even further its origin and how it contributes to the disease pathogenesis. Therefore the cellular composition of aortic root lesions from *Hhip1*^{-/-};*ApoE*^{-/-} and *Hhip1*^{-/-};*Ldlr*^{-/-} in comparison to *Hhip1* wild type littermates was investigated. Histological analysis confirmed that *Hhip1*^{-/-};*ApoE*^{-/-} and *Hhip1*^{-/-};*Ldlr*^{-/-} exhibited lesions of significantly reduced size compare to the control mice. Double KO lesions were characterised by significantly less SMCs and a non-significant reduction in collagen content. The lipid and macrophage profile of these lesions was not altered. These data suggest that *Hhip1* is proatherogenic and that its deficiency is beneficial since plaques are smaller. The characteristics of *Hhip1*^{-/-} lesions (low levels of SMC and collagen) are in fact typical of earlier stage lesions (Doran, Meller & Mcnamara 2008, Stary 2000, Nakashima et al. 1994) and so it could be postulated that loss of *Hhip1*

is delaying atherosclerosis progression. However, more investigation is needed in order to give a definitive answer, which would inform potential therapeutic strategies targeting HHPL1 in humans. One way to address this is to examine *Hhip1*^{-/-} lesions at a later time point such as at 18 weeks for example, when lesions are predicted to be beyond stage IV (**Table 5.2**). It could be anticipated that these lesions will either be no more advanced than those seen after 12 weeks of western diet (i.e the development of atherosclerosis is halted) or the lesions will have continued to advance (i.e. disease progression is slowed). An additional approach could also be to conditionally knock out *Hhip1* in adult mice after the atherosclerosis process has initiated in order to provide information on whether atherosclerosis pathogenesis can be stopped or even recede. This would be feasible by utilising the inducible Cre/*loxP* recombination system of the *Hhip1* knockout first construct.

In order to draw a conclusion, however, about whether loss of *Hhip1* exerts a beneficial effect on atherosclerosis outcome or not, plaque vulnerability should also be taken into account. Loss of SMCs results in a thinner fibrous cap, which is consistent with plaque rupture. SMC content nevertheless is not the only contributing factor to this issue. Macrophages were shown to promote vulnerability by secreting metalloproteinases that degrade the ECM (New et al. 2013) and a large necrotic core was reported to impose a greater risk of rupture (Virmani et al. 2006). Other characteristics of a vulnerable lesion is spotty calcification, expansive remodelling preserving the lumen, neovascularization, plaque haemorrhage and adventitial/perivascular inflammation (Bentzon et al. 2014). In the present study *Hhip1* deficiency was only associated with loss of SMC and reduced collagen and no changes in lipid or macrophage content were seen. This suggests that *Hhip1* deficiency does not meet all the criteria for a vulnerable plaque.

As discussed above *Hhip1* deficiency was associated with reduced SMC content in plaques, suggesting that *Hhip1* regulates SMC content in the lesions. *In vitro* data from HASMCs described in chapter 3 (section 3.2.5) revealed that *HHPL1* knockdown caused reduced migration and proliferation of these cells. Thus, it is reasonable to conclude that the reduction in SMC observed in *Hhip1*^{-/-} mice could be due to *Hhip1* regulatory effect on migration and proliferation of these cells. Additionally, there are other processes that determine SMC density

during atherosclerosis, such as apoptosis, phenotypic switching and senescence (Bennett, Sinha & Owens 2016) , on which *Hhip1* could also have an effect.

Detection of SMC was achieved by the use of α -SMA, which is a standard marker expressed by SMC. This cell type undergoes phenotypic switching, which includes a decrease in SMC markers such as smooth muscle cell myosin heavy chain (MYH11), 22-kDa SMC lineage-restricted protein (SM22⁺/tagln), α -SMA, smoothelin, and others (Laura et al. 2015, Feil et al. 2014, Gomez et al. 2013). Moreover, other cells of myeloid origin such as macrophages can express SMC markers in plaques and act as SMC-like cells (Allahverdian et al. 2014). Thereby, the use of more markers could provide information about the origin of SMC present in *Hhip1* atherosclerotic plaques.

In line with the atherosclerosis study is further evidence obtained from a gene expression study, which also suggests a role for *Hhip1* in disease development. *Hhip1* expression pattern was investigated during disease progression in an *Apoe*^{-/-} mouse model fed chow diet. Having studied a range of differently aged mice in order to resemble the entire disease process it was found that expression of *Hhip1* was significantly increased in the aortic arch of *Apoe*^{-/-} mice but it did not change in aged C57BL/6 wild type mice. This finding suggests that changes in *Hhip1* levels are caused by disease progression rather than ageing and that *Hhip1* is actively involved in atherosclerosis. *In vitro* data from chapter 3 shows that *HHIPL1* is expressed in SMCs and the results in this chapter show that *Hhip1* knockout causes reduced SMC content in atherosclerotic plaques making this the likely source of *Hhip1* expression. However, it is unclear whether the changes in *Hhip1* levels in plaques is due to altered expression in SMCs or a result of differences in proportion of SMCs (as a result of proliferation, migration and migration) in lesions.

The expression of *Hhip1* was also investigated in the thoracic aorta, which is more resistant to atherosclerosis development (no plaques were observed in the study animals, data not shown). In contrast to the findings in the aortic root *Hhip1* expression was lower in the thoracic aorta of *Apoe*^{-/-} mice compared to wild-type controls. This could possibly be attributed to one or two different factors; endothelial shear stress (ESS) or embryonic origin of SMCs. Atherosclerotic lesions predominantly form in regions of low ESS such as the

outer waist of bifurcations or the inner curve of arteries, whereas regions of moderate/physiological and high ESS are generally protected such as linear arterial segments (thoracic aorta). ESS is 'the tangential stress due to the friction of the flowing blood on the endothelial surface of the arterial wall' (Wentzel et al. 2012) and has been reported both in humans and mice. It is suggested by different studies that high ESS is atheroprotective and that endothelial cells in regions of high ESS express various atheroprotective genes, and downregulate pro-atherogenic ones, leading to stability and quiescence. On the contrary in regions where low ESS occurs endothelial cells upregulate the expression of proatherogenic genes and suppress that of protective genes (Chatzizisis et al. 2007, Brooks, Lelkes & Rubanyi 2002, Chen et al. 2001, Traub, Berk 1998) . Consequently, *Hhip1* upregulation in the aortic arch, where ESS is low, and concomitant downregulation in the thoracic aorta (physiological ESS) suggests that *Hhip1* is a proatherogenic gene. Other studies propose that ESS modulates SMC gene expression exerting an atheroprotective phenotype on the vessel wall (Chiu et al. 2004). Disturbed blood flow and subsequent low ESS was also shown to influence mitogenic activities in a shear level-dependent manner affecting SMC density and migration. Shear stress was inversely correlated with the cell density in this study (Liu et al. 2003a, Liu et al. 2003b). Taking into account the studies it is also possible that the transcription levels were also affected by SMC density.

Another factor that has been suggested to influence disease susceptibility and gene expression at distinct vascular regions is embryonic origin of VSMCs at these sites. Lineage tracing studies have shown that different regions in the aorta comprise VSMCs of different embryonic origin. For example, VSMCs in the ascending aorta and the arch, are derived from neural crest, whereas the descending aorta is predominantly derived from somatic precursors (Majesky 2007). Moreover, these lineage-specific VSMCs even though phenotypically similar they respond differently to risk factors and have different requirements to disease associated transcription factors, hence they show variable disease susceptibility (Bennett, Sinha & Owens 2016) .

5.4 Conclusion

In conclusion, this study provides the first experimental evidence that *Hhip1* is a causal gene in the 14q32.2 locus identified as part of CAD GWAS. It has been shown *in vivo* that *Hhip1* is pro-atherogenic and may promote progression and complications of the disease by regulating SMCs content and accelerating atherosclerosis progression.

6 Discussion

Over the last decade large-scale genetic association studies have identified more than 56 loci that associate with increased risk of CAD (Samani et al. 2007, Clarke et al. 2009, IBC 50K CAD Consortium 2011, Schunkert et al. 2011, Nikpay et al. 2015). The disease associated variants identified are generally common (allele frequency > 5%) with low to moderate effect size (the majority have less than 10% increased risk per allele). What is remarkable about these loci is that only a third of them are associated with conventional risk factors for cardiovascular disease and many of the disease associated variants are near genes without a known role in cardiovascular function. By characterising the function of these genes and identifying the pathways through which the genetic variants exert their effects might permit the development of new diagnostic and therapeutic strategies for CAD.

A major challenge in interpreting the GWAS findings and drawing conclusions about their biological relevance is the identification and characterisation of the causal gene at each disease associated locus. The disease associated variants at the chromosome14q32 locus fall within the *HHIPL1* gene, which encodes a previously uncharacterised homologue of a Hh signalling antagonist (Schunkert et al. 2011). However, there is no other evidence, such as eQTLs, linking the disease associated variants to *HHIPL1* or other genes at the 14q32 locus.

In this study, using a combination of *in vitro* and *in vivo* models *HHIPL1* was found to be a secreted SHH interacting protein that modulates SMC phenotype and promotes atherosclerosis. *In vivo*, *Hhip1*^{-/-} mice showed that *Hhip1* deficiency causes significant protection from western-diet induced atherosclerosis in two hyperlipidemic mouse models. There is also change in the phenotype of the atherosclerotic plaques which have reduced SMC content compared with controls. *In vitro* data provides the first functional evidence for a role of *HHIPL1* in the Hh pathway and also revealed that *HHIPL1* regulates proliferation and migration of HASMC. Together, these data strongly support *HHIPL1* as the causal gene at the 14q32 CAD risk locus.

ES cells carrying a *Hhip1* knockout first construct were purchased from the KOMP repository. These were used to generate chimeric mice from which germline transmission onto a C57BL/6 background was achieved. Unlike with

many of the published Hh mouse models, *Hhip1*^{-/-} mice were viable with no obvious phenotypic abnormalities. *Hhip1* was found to be broadly expressed across a panel of mouse tissues including in the aorta and the heart, both of which are relevant tissues with regard to atherosclerosis. In an attempt to gain more information about the cellular origin of Hhip1, its localisation was investigated in *Hhip1*^{-/-} tissues, using a *lacZ* reporter under the control of the *Hhip1* promoter. Detection of *lacZ*, however, proved inconclusive as of the tissues that were examined (heart, liver, brain, ileum, spleen, fat, aorta) only brain was found to have reproducible staining with some occasional staining also observed in the septal artery in the heart. The IMPC found a lack of *lacZ* expression in other KOMP knockout mouse lines. Of the 424 knockout first lines examined 4% showed complete absence of expression, 25.2% limited tissue expression and 24.8% localised expression (Tuck et al. 2015). In another study *lacZ* expression was investigated in 313 mutant mouse lines with ~20% showing no specific staining (West et al. 2015).

In order to undertake an atherosclerosis study, the *Hhip1*^{-/-} mice were crossed to the well-studied *Apoe*^{-/-} and *Ldlr*^{-/-} strains. Hyperlipidemic strains are required, as wild type mice do not spontaneously manifest atherosclerosis (Getz, Reardon 2006, Getz, Reardon 2012). The double KO *Hhip1*^{-/-};*Apoe*^{-/-} and *Hhip1*^{-/-};*Ldlr*^{-/-} male mice and the relevant controls (*Hhip1*^{+/+};*Apoe*^{-/-} and *Hhip1*^{+/+};*Ldlr*^{-/-}) were then fed western diet to further accelerate disease progression. After 12 weeks of receiving the western diet it was found that loss of *Hhip1* resulted in reduction of more than 50% in atherosclerotic lesions in the aortic arch and thoracic aorta, on both hyperlipidemic backgrounds by *en face* analysis. This reduction was also observed in the aortic root. Compositional analysis of the atherosclerotic lesions showed that *Hhip1*^{-/-};*Apoe*^{-/-} and *Hhip1*^{-/-};*Ldlr*^{-/-} plaques did not differ in lipid and macrophage content when compared to the wild type controls. They did however; contain significantly reduced SMC content and a reduced (although not statistically significant) amount of collagen. These findings clearly suggest that Hhip1 plays a role in atherosclerosis development and acts through SMCs. The data suggests that loss of Hhip1 has a beneficial outcome in atherosclerosis development and that it could be a potential therapeutic target. There are however several questions that need to

be answered in order to define how HHPL1 might be targeted. It will be important to identify the disease stage at which *Hhip1* starts to have an effect on disease progression. Gaining information about a possible disease-stage-specific effect will help identify the appropriate time frame at which *Hhip1* could be therapeutically targeted. Knocking out *Hhip1* after the atherosclerosis process has initiated would provide information on whether the pathogenesis of atherosclerosis can be halted or even recede. This could be investigated by utilising the inducible Cre//oxP recombination element of the *Hhip1* knockout first construct. Gene dosage should also be taken into consideration, as in the present study, only complete loss of *Hhip1* was investigated. By studying heterozygous animals, it would be possible to determine if haploinsufficiency of *Hhip1* is also beneficial with regard to atherosclerosis progression. This would provide essential information for the potential use of future therapeutic agents and their efficacy.

Hhip1 expression was also investigated in two aortic regions of *Apoe*^{-/-} mice; the aortic arch, which is the most atherosclerosis susceptible segment of the aorta and the thoracic aorta. In an effort to cover the entire range of atherosclerosis disease stages mice between 6 and 48 weeks of age were included in the study. *Hhip1* expression was significantly increased with disease burden in the aortic arch of *Apoe*^{-/-} mice. The change in expression could either be a result of altered gene expression in cells such as SMC or due to changing cell content. Additional histochemical analysis of plaques for *Hhip1* localisation is needed in order to identify its cellular origin and thus clarify its role in the process of atherosclerosis.

HHPL1 is a paralogue of the Hh antagonist HHIP (Katoh, Katoh 2006). The Hh signalling pathway plays an essential regulatory role during embryonic development and patterning and in adult cell homeostasis. It performs a fundamental role in the development of many tissues and organs, including the cardiovascular system. Hh signalling is also reactivated in several diseases, however, evidence supporting a role in atherosclerosis is quite limited. The HHIP protein family comprises HHIP, HHPL1 and HHPL2 and is conserved in vertebrates. Prior to this investigation, only HHIP had been studied experimentally. HHIP was initially described as a membrane associated protein

able to interact with each of the three Hh ligands and inhibit Hh signalling. More recently, HHIP has been shown to also be secreted into the extracellular space and regulate Hh signalling in a non-cell autonomous manner (Kwong, Bijlsma & Roelink 2014, Chuang, McMahon 1999) . Analysis of HHIP1 cellular localisation by *in silico* prediction and *in vitro* experimentation showed that it is a secreted protein and is not present at the cell surface. The full-length HHIP1 protein shares 21% sequence identity with HHIP whilst the Hh interacting region shows 43% identity between the two proteins. Immunoprecipitation from the cell lysates and conditioned media from transiently transfected cells confirmed that HHIP1 can directly bind SHH. Further investigation regarding its regulatory role in Hh signalling will be required to determine whether HHIP1 is a functional homologue of HHIP or if it regulates the Hh pathway in some other way. It would be particularly interesting to investigate whether the HHIP1 scavenger receptor domain is involved in the modulation of Hh signalling or if it points to another HHIP1 function. Transcriptional targets of the pathway include the GLI proteins as well as the HHIP and the PTCH, hence studying the expression levels of these genes in relation to HHIP1 will give insight about the role of HHIP1 in the pathway. It would also be of interest to work out if HHIP1 is a target of the Hh pathway as is the case with other components of the pathway. This could be addressed by inhibition of the pathway with either cyclopamine or the monoclonal 5E1 antibody, which binds all Hh ligands, and subsequent investigation of the expression levels of HHIP1. Moreover, additional immunoprecipitation experiments can be conducted in order to examine whether HHIP1 can also bind DHH and IHH as HHIP. All the above are experiments that will give a mechanistic insight about HHIP1

The observed reduction in plaque size and SMC content in *Hhip1*^{-/-} mice is supported by experiments in HASMCs. Expression analysis of cardiovascular cell-types showed that *HHIP1* is expressed by HASMCs but not HUVECs. Therefore, the role of HHIP1 in HASMCs was assessed by siRNA knockdown. Migration and proliferation are the two main processes SMCs undergo during atherosclerosis development. Down-regulation of *HHIP1* resulted in reduced proliferation and migration of HASMCs, suggesting a regulatory role for HHIP1 in these disease related processes. Hh signalling has previously been shown to

regulate SMC proliferation and migration. The majority of the studies demonstrated a role for Hh signalling in SMC proliferation and migration following either upregulation of the pathway with recombinant SHH and/or inhibition with cyclopamine or monoclonal antibody 5E1 (Morrow et al. 2007, Morrow et al. 2009, Yao et al. 2014, Wang et al. 2010). The data presented in this study suggests that HHIPL1, like SHH, promotes SMC proliferation and migration, suggesting that HHIPL1, at least in this context, isn't acting as an antagonist in its modulation of Hh signalling and that further investigation into the interplay between HHIPL1 and SHH in the regulation of SMC phenotype is required.

In order to truly understand how *HHIPL1* contributes to the development of atherosclerosis in humans it will be necessary to investigate how the disease associated variants affect HHIPL1 function. The lead variant, rs2895811, and the majority of its high LD proxies fall in non-coding regions of the *HHIPL1* gene. One variant, rs7158073, causes a valine to alanine change at amino acid position 692 within the predicted scavenger receptor domain and the functional effects of this variant need to be verified experimentally. No association between the CAD associated variants and *HHIPL1* expression has been reported, however there are a limited number of studies with gene expression data from relevant cardiovascular tissues and cell types.

The development of non-invasive methods for treating patients suffering from coronary artery disease is an ongoing field of research with the identification and validation of new CAD associated genes potentially aiding the design of new therapies. For example, *PCSK9*, which contains common variants associated with CAD, is one such gene that has subsequently been therapeutically targeted. A monoclonal antibody (alirocumab) to PCSK9 has been developed and studied in phase two and three clinical trials (Stroes et al. 2014, Lepor, Kereiakes 2015). It was shown to significantly lower patients' LDL levels by 45-62% with a high safety profile and was approved by the FDA (US Food and Drug Administration) and the European Medicines Agency in 2015 for the treatment of adults with hypercholesterolemia (Jones et al. 2016, Roth 2016). The vast majority of the GWAS identified genes, however have not yet been clinically targeted. Grover *et al* have undertaken an *in silico* analysis for

the identification of novel therapeutic targets for CAD from GWAS data in which they have integrated known drug data from three drug databases with predicted candidate CAD genes and found that 30% of the predicted candidate genes could serve as novel therapeutic targets, and 14% of the retrieved drugs are potential novel therapeutics for CAD. The novel therapeutics reported included both FDA-approved drugs and drugs currently in clinical trials (Grover et al. 2015). Having shown in this present study that deletion of *Hhip1* has atheroprotective effects in mice, having also provided the first evidence for a role of HHPL1 in the Hh pathway and the fact that HHPL1 is a secreted protein, it is likely that HHPL1 and the Hh pathway in general are promising therapeutic targets for CAD. Several Hh inhibitors have previously reached phases -1-2- in clinical trials, but have predominantly focussed upon cancer (Redmond et al. 2011). As far as CAD is concerned, strategies under consideration include the use of Hh agonists (including the actual Hh proteins), Hh gene transfer and small molecule agonists (Redmond et al. 2011). An issue to consider, however, are the reported dualistic effects of Hhs in that during ischemic conditions high exogenous Hh levels are able to repair tissue damage, whereas endogenous Hh seems to aggravate coronary artery disease (Bijlsma, Spek 2010, Redmond et al. 2011). Any detrimental effects of manipulating the Hh pathway must also clearly be taken into consideration such as carcinogenic effects and potential disruption in the homeostasis of adult vasculature given the importance of Hh signalling in this process (Morrow et al. 2007).

Overall Hh signalling is a promising signalling pathway in terms of the development of CAD. Elucidating as many components of this pathway as possible such as HHPL1 and establishing their potential role in the Hh signalling could provide new drug targets for cardiovascular disease.

6.1 Study limitations

The present study has provided evidence showing *Hhip1* deficiency is beneficial in mouse atherosclerosis and that it potentially acts through Hh signalling to regulate HASMCs proliferation and migration. Nevertheless there are some limitations to this study, which preclude a more definitive answer

about the function of HHIPL1. First detection of Hhip1 protein expression in *Hhip1*^{-/-} mouse tissue was unsuccessful due to unreliable *LacZ* reporter and the lack of an antibody against Hhip1. Therefore lack of Hhip1 protein localisation data made it impossible to identify its cellular origin and potential action area. Next, evidence regarding the effect of Hhip1 deletion on circulating lipids and monocyte levels is required in order to further investigate Hhip1 role on other CAD risk factors. However, no association with traditional risk factors and HHIPL1 was reported in humans (Schunkert et al. 2011). *In vitro* data from HASMCs showed that HHIPL1 regulates proliferation and migration but this was not investigated *in vivo*. Analysis of Hhip1 effect on these cellular processes in mouse *Hhip1*^{-/-} derived VSMCs would be necessary to confirm the *in vitro* data. Another important consideration when interpreting HHIPL1 function is the lack of human evidence. As mentioned earlier there are no eQTLs linking the disease associated variants to *HHIPL1* expression in human tissue, therefore we are yet unable to facilitate translation of our mouse findings into human therapeutics. In conclusion further *in vitro* analysis is needed in order to understand how HHIPL1 modulates (direction of action) Hh signalling and give a more precise answer regarding its molecular mechanism.

6.2 Future work

The work, which will be required to further define the molecular function of HHIPL1 and the precise mechanism of action in atherosclerosis, is summarised here.

Investigation of:

- HHIPL1 regulatory role in Hh signalling *in vitro*
- How the disease associated variants affect HHIPL1 function
- The functionality of the HHIPL1 scavenger receptor
- *HHIPL1* role in other cardiovascular relevant cell types
- Hhip1 protein localisation in mouse tissue
- Hhip1 effect on proliferation of SMCs *in vivo*
- Disease stage specific effect of Hhip1 on mouse atherosclerosis
- *Hhip1* haploinsufficiency effect on atherosclerosis outcome

6.3 Conclusion

In this study, *HHIPL1* was investigated as a candidate causal gene at the chromosome 14q32 CAD associated locus. HASMCs express *HHIPL1*, which encodes a secreted protein that interacts with SHH, the main ligand of the Hh signalling pathway. Knockdown of *HHIPL1* expression resulted in reduced SMC proliferation and migration, two important processes during the development of atherosclerotic plaques. In atherosclerosis mouse models *Hhip1* expression was found to increase with disease burden and *Hhip1* knockout caused a substantial decrease in plaque size. The findings confirm the identity of a novel atherosclerosis gene and provide a potential target for therapeutic intervention.

7 References

Ahn, S. & Joyner, A.L. 2004, "Dynamic changes in the response of cells to positive hedgehog signaling during mouse limb patterning", *Cell*, vol. 118, no. 4, pp. 505-516.

Ait-Oufella, H., Kinugawa, K., Zoll, J., Simon, T., Boddaert, J., Heeneman, S., Blanc-Brude, O., Barateau, V., Potteaux, S., Merval, R., Esposito, B., Teissier, E., Daemen, M.J., Leseche, G., Boulanger, C., Tedgui, A. & Mallat, Z. 2007, "Lactadherin deficiency leads to apoptotic cell accumulation and accelerated atherosclerosis in mice", *Circulation*, vol. 115, no. 16, pp. 2168-2177.

Akhtar, S., Gremse, F., Kiessling, F., Weber, C. & Schober, A. 2013, "CXCL12 promotes the stabilization of atherosclerotic lesions mediated by smooth muscle progenitor cells in Apoe- deficient mice", *Arteriosclerosis, Thrombosis, and Vascular Biology*, vol. 33, no. 4, pp. 679.

Allahverdian, C., Sima, Chehroudi, M., A., Mcmanus, A., B., Abraham, A., T. & Francis, A., G. 2014, "Contribution of Intimal Smooth Muscle Cells to Cholesterol Accumulation and Macrophage- Like Cells in Human Atherosclerosis", *Circulation*, vol. 129, no. 15, pp. 1551-1559.

Amsterdam, A., Yoon, C., Allende, M., Becker, T., Kawakami, K., Burgess, S., Gaiano, N. & Hopkins, N. 1997, "Retrovirus-mediated insertional mutagenesis in zebrafish and identification of a molecular marker for embryonic germ cells", *Cold Spring Harbor symposia on quantitative biology*, vol. 62, pp. 437-450.

Amsterdam, A. 2003, *Insertional mutagenesis in zebrafish*, Hoboken.

Andersen, C.L., Jensen, J.L. & Orntoft, T.F. 2004, "Normalization of real-time quantitative reverse transcription-PCR data: a model-based variance estimation approach to identify genes suited for normalization, applied to bladder and colon cancer data sets", *Cancer research*, vol. 64, no. 15, pp. 5245-5250.

Arndt, L.D., J; Jeromin, F; Thiery, J; Burkhardt; R (2015). Heterozygous deficiency of Tribbles homolog-1 gene (Trib1) increases atherosclerotic lesions in ApoE-knockout mice. 12. Jahrestagung Deutsche Vereinte Gesellschaft für Klinische Medizin und Laboratoriumsmedizin e.V. (DGKL) P068.

Austin, C.P., Battey, J.F., Bradley, A., Bucan, M., Capecchi, M., Collins, F.S., Dove, W.F., Duyk, G., Dymecki, S., Eppig, J.T., Grieder, F.B., Heintz, N., Hicks, G., Insel, T.R., Joyner, A., Koller, B.H., Lloyd, K.C., Magnuson, T., Moore, M.W., Nagy, A., Pollock, J.D., Roses, A.D., Sands, A.T., Seed, B., Skarnes, W.C., Snoddy, J., Soriano, P., Stewart, D.J., Stewart, F., Stillman, B., Varmus, H., Varticovski, L., Verma, I.M., Vogt, T.F., von Melchner, H., Witkowski, J., Woychik, R.P., Wurst, W., Yancopoulos, G.D., Young, S.G. & Zambrowicz, B. 2004, "The knockout mouse project", *Nature genetics*, vol. 36, no. 9, pp. 921-924.

Auwerx, J., Avner, P., Baldock, R., Ballabio, A., Balling, R., Barbacid, M., Berns, A., Bradley, A., Brown, S., Carmeliet, P., Chambon, P., Cox, R., Davidson, D., Davies, K., Duboule, D., Forejt, J., Granucci, F., Hastie, N., de Angelis, M.H., Jackson, I., Kioussis, D., Kollias, G., Lathrop, M., Lendahl, U., Malumbres, M., von Melchner, H., Muller, W., Partanen, J., Ricciardi-Castagnoli, P., Rigby, P., Rosen, B., Rosenthal, N., Skarnes, B., Stewart, A.F., Thornton, J., Tocchini-Valentini, G., Wagner, E., Wahli, W. & Wurst, W. 2004, "The European dimension for the mouse genome mutagenesis program", *Nature genetics*, vol. 36, no. 9, pp. 925-927.

Bale, A.E. 2002, "Hedgehog signaling and human disease", *Annual review of genomics and human genetics*, vol. 3, pp. 47.

Barton, M., Haudenschild, C.C., d'Uscio, L.V., Shaw, S., Munter, K. & Luscher, T.F. 1998, "Endothelin ETA receptor blockade restores NO-mediated endothelial function and inhibits atherosclerosis in apolipoprotein E-deficient mice", *Proceedings of the National Academy of Sciences of the United States of America*, vol. 95, no. 24, pp. 14367-14372.

Bauer, R.C., Tohyama, J., Cui, J., Cheng, L., Yang, J., Zhang, X., Ou, K., Paschos, G.K., Zheng, X.L., Parmacek, M.S., Rader, D.J. & Reilly, M.P. 2015, "Knockout of Adamts7, a novel coronary artery disease locus in humans, reduces atherosclerosis in mice", *Circulation*, vol. 131, no. 13, pp. 1202.

Beachy, P.A., Karhadkar, S.S. & Berman, D.M. 2004, "Tissue repair and stem cell renewal in carcinogenesis", *Nature*, vol. 432, no. 7015, pp. 324-331.

Beckers, L., Lutgens, E., Heeneman, S., Wang, L., Burkly, L.C., Rousch, M.M.J., Davidson, N.O., Gijbels, M.J.J., de Winther, M.P.J. & Daemen, M.J.A.P. 2007, "Disruption of hedgehog signalling in ApoE -/- mice reduces plasma lipid levels, but increases atherosclerosis due to enhanced lipid uptake by macrophages", *The Journal of pathology*, vol. 212, no. 4, pp. 420-428.

Benjamin, P.F., Makino, S., Radhakrishnan, J., Plant, K., Leslie, S., Dilthey, A., Ellis, P., Langford, C., Fredrik, O.V. & Julian, C.K. 2012, "Genetics of gene expression in primary immune cells identifies cell type-specific master regulators and roles of HLA alleles", *Nature genetics*, vol. 44, no. 5, pp. 502.

Bennett, R., M., Sinha, K., S. & Owens, K., G. 2016, "Vascular Smooth Muscle Cells in Atherosclerosis", *Circulation research*, vol. 118, no. 4, pp. 692-702.

Bentzon, F., Jacob, Otsuka, F., Fumiyuki, Virmani, F., Renu & Falk, F., Erling 2014, "Mechanisms of Plaque Formation and Rupture", *Circulation research*, vol. 114, no. 12, pp. 1852-1866.

- Bijlsma, M.F., Borensztajn, K.S., Roelink, H., Peppelenbosch, M.P. & Spek, C.A. 2007, "Sonic hedgehog induces transcription-independent cytoskeletal rearrangement and migration regulated by arachidonate metabolites", *Cellular signalling*, vol. 19, no. 12, pp. 2596-2604.
- Bijlsma, M.F., Peppelenbosch, M.P., Spek, C.A. & Roelink, H. 2008a, "Leukotriene synthesis is required for hedgehog-dependent neurite projection in neuralized embryoid bodies but not for motor neuron differentiation", *Stem cells (Dayton, Ohio)*, vol. 26, no. 5, pp. 1138-1145.
- Bijlsma, M.F., Spek, C.A. & Peppelenbosch, M.P. 2004, "Hedgehog: an unusual signal transducer", *BioEssays : news and reviews in molecular, cellular and developmental biology*, vol. 26, no. 4, pp. 387-394.
- Bijlsma, M.F., Leenders, P.J.A., Janssen, B.J.A., Peppelenbosch, M.P., Ten Cate, H. & Spek, C.A. 2008b, "Endogenous hedgehog expression contributes to myocardial ischemia-reperfusion-induced injury", *Experimental biology and medicine (Maywood, N.J.)*, vol. 233, no. 8, pp. 989-996.
- Bijlsma, M.F., Peppelenbosch, M.P. & Spek, C.A. 2006, "Hedgehog morphogen in cardiovascular disease", *Circulation*, vol. 114, no. 18, pp. 1985-1991.
- Bijlsma, M.F. & Spek, C.A. 2010, "The Hedgehog morphogen in myocardial ischemia-reperfusion injury", *Experimental biology and medicine (Maywood, N.J.)*, vol. 235, no. 4, pp. 447-454.
- Bijlsma, M.F., Spek, C.A., Zivkovic, D., van, d.W., Rezaee, F. & Peppelenbosch, M.P. 2006, "Repression of Smoothed by Patched-Dependent (Pro-)Vitamin D3 Secretion (Repression of Smoothed by Patched)", *PLoS Biology*, vol. 4, no. 8, pp. e232.
- Bishop, B., Aricescu, A.R., Harlos, K., O'Callaghan, C.A., Jones, E.Y. & Siebold, C. 2009, "Structural insights into hedgehog ligand sequestration by the human hedgehog-interacting protein HHIP", *Nature structural & molecular biology*, vol. 16, no. 7, pp. 698-703.
- Blanco-Colio, L.M. 2014, *TWEAK/Fn14 Axis: A Promising Target for the Treatment of Cardiovascular Diseases*, Switzerland.
- Bobryshev, Y.V., Taksir, T., Lord, R.S. & Freeman, M.W. 2001, "Evidence that dendritic cells infiltrate atherosclerotic lesions in apolipoprotein E-deficient mice", *Histology and histopathology*, vol. 16, no. 3, pp. 801-808.
- Bodzioch, M., Orso, E., Klucken, J., Langmann, T., Bottcher, A., Diederich, W., Drobnik, W., Barlage, S., Buchler, C., Porsch-Ozcurumez, M., Kaminski, W.E., Hahmann, H.W., Oette, K., Rothe, G., Aslanidis, C., Lackner, K.J. & Schmitz, G. 1999, "The gene encoding ATP-binding

cassette transporter 1 is mutated in Tangier disease", *Nature genetics*, vol. 22, no. 4, pp. 347-351.

Bolon, B. 2008, "Whole mount enzyme histochemistry as a rapid screen at necropsy for expression of beta-galactosidase (LacZ)-bearing transgenes: considerations for separating specific LacZ activity from nonspecific (endogenous) galactosidase activity", *Toxicologic pathology*, vol. 36, no. 2, pp. 265-276.

Bosanac, I., Maun, H.R., Scales, S.J., Wen, X., Lingel, A., Bazan, J.F., de Sauvage, F.J., Hymowitz, S.G. & Lazarus, R.A. 2009, "The structure of SHH in complex with HHIP reveals a recognition role for the Shh pseudo active site in signaling", *Nature structural & molecular biology*, vol. 16, no. 7, pp. 691-697.

Boullier, A., Bird, D.A., Chang, M., Dennis, E.A., Friedman, P., Gillotte-taylor, K., Hörkkö, S., Palinski, W., Quehenberger, O., Shaw, P., Steinberg, D., Terpstra, V. & Witztum, J.L. 2001, "Scavenger Receptors, Oxidized LDL, and Atherosclerosis", *Annals of the New York Academy of Sciences*, vol. 947, no. 1, pp. 214-223.

Brænne, I., Civelek, M., Vilne, B., Di Narzo, A., Johnson, A.D., Zhao, Y., Reiz, B., Codoni, V., Webb, T.R., Foroughi Asl, H., Hamby, S.E., Zeng, L., Trégouët, D., Hao, K., Topol, E.J., Schadt, E.E., Yang, X., Samani, N.J., Björkegren, J.,L.M., Erdmann, J., Schunkert, H. & Lusi, A.J. 2015, "Prediction of Causal Candidate Genes in Coronary Artery Disease Loci", *Arteriosclerosis, Thrombosis, and Vascular Biology*, vol. 35, no. 10, pp. 2207.

Briscoe, J. & Théron, P.P. 2013, "The mechanisms of Hedgehog signalling and its roles in development and disease", *Nature reviews.Molecular cell biology*, vol. 14, no. 7, pp. 416.

Broeckel, U., Hengstenberg, C., Björn Mayer, Holmer, S., Martin, L.J., Comuzzie, A.G., Blangero, J., Peter Nürnberg, André Reis, Günter A.J. Riegger, Jacob, H.J. & Schunkert, H. 2002, "A comprehensive linkage analysis for myocardial infarction and its related risk factors", *Nature genetics*, vol. 30, no. 2, pp. 210.

Brooks, A.R., Lelkes, P.I. & Rubanyi, G.M. 2002, "Gene expression profiling of human aortic endothelial cells exposed to disturbed flow and steady laminar flow", *Physiological genomics*, vol. 9, no. 1, pp. 27.

Burke, R., Nellen, D., Bellotto, M., Hafen, E., Senti, K., Dickson, B.J. & Basler, K. 1999, "Dispatched, a Novel Sterol- Sensing Domain Protein Dedicated to the Release of Cholesterol-Modified Hedgehog from Signaling Cells", *Cell*, vol. 99, no. 7, pp. 803-815.

Burton, P.R., Samani, N.J., Cummings, F.R., Jewell, D.P., Todd, J.A., Donnelly, P., Barrett, J.C., Davison, D., Easton, D., Evans, D., Leung, H.,

Marchini, J.L., Clayton, D.G., Morris, A.P., Spencer, C.C.A., Tobin, M.D., Attwood, A.P., Boorman, J.P., Cant, B., Everson, U., Hussey, J.M., Jolley, J.D., Knight, A.S., Cardon, L.R., Koch, K., Meech, E., Nutland, S., Prowse, C.V., Stevens, H.E., Taylor, N.C., Walters, G.R., Walker, N.M., Watkins, N.A., Winzer, T., Craddock, N., Jones, R.W., McArdle, W.L., Ring, S.M., Strachan, D.P., Pembrey, M., Breen, G., St Clair, D., Caesar, S., Gordon-Smith, K., Jones, L., Deloukas, P., Fraser, C., Green, E.K., Grozeva, D., Hamshere, M.L., Holmans, P.A., Jones, I.R., Kirov, G., Moskvina, V., Nikolov, I., O'Donovan, M.C., Duncanson, A., Owen, M.J., Collier, D.A., Elkin, A., Farmer, A., Williamson, R., McGuffin, P., Young, A.H., Ferrier, I.N., Ball, S.G., Balmforth, A.J., Kwiatkowski, D.P., Barrett, J.H., Bishop, D.T., Iles, M.M., Maqbool, A., Yuldasheva, N., Hall, A.S., Braund, P.S., Dixon, R.J., Mangino, M., Stevens, S., McCarthy, M.I., Thompson, J.R., Bredin, F., Tremelling, M., Parkes, M., Drummond, H., Lees, C.W., Nimmo, E.R., Satsangi, J., Fisher, S.A., Forbes, A., Ouwehand, W.H., Lewis, C.M., Onnie, C.M., Prescott, N.J., Sanderson, J., Mathew, C.G., Barbour, J., Mohiuddin, M.K., Todhunter, C.E., Mansfield, J.C. & Ahmad, T. 2007, "Genome-wide association study of 14,000 cases of seven common diseases and 3,000 shared controls", *Nature*, vol. 447, no. 7145, pp. 661-678.

Byrd, N., Becker, S., Maye, P., Narasimhaiah, R., St-Jacques, B., Zhang, X., McMahon, J., McMahon, A. & Grabel, L. 2002, "Hedgehog is required for murine yolk sac angiogenesis", *Development (Cambridge, England)*, vol. 129, no. 2, pp. 361.

Cao, J., Q., Rong, S., Shunxing, Repa, S., J., Clair, S., R., Parks, S., J. & Mishra, S., N. 2014, "Histone Deacetylase 9 Represses Cholesterol Efflux and Alternatively Activated Macrophages in Atherosclerosis Development", *Arteriosclerosis, Thrombosis, and Vascular Biology*, vol. 34, no. 9, pp. 1871-1879.

Chamoun, Z., Mann, R.K., Nellen, D., Von Kessler, D.P., Bellotto, M., Beachy, P.A. & Basler, K. 2001, "Skinny hedgehog, an acyltransferase required for palmitoylation and activity of the hedgehog signal", *Science (New York, N.Y.)*, vol. 293, no. 5537, pp. 2080.

Chang, D.T., López, A., Von Kessler, D.P., Chiang, C., Simandl, B.K., Zhao, R., Seldin, M.F., Fallon, J.F. & Beachy, P.A. 1994, "Products, genetic linkage and limb patterning activity of a murine hedgehog gene", *Development (Cambridge, England)*, vol. 120, no. 11, pp. 3339.

Chatzizisis, Y.S., Coskun, A.U., Jonas, M., Edelman, E.R., Feldman, C.L. & Stone, P.H. 2007, "Role of Endothelial Shear Stress in the Natural History of Coronary Atherosclerosis and Vascular Remodeling: Molecular, Cellular, and Vascular Behavior", *Journal of the American College of Cardiology*, vol. 49, no. 25, pp. 2379-2393.

Chen, B.P., Li, Y.S., Zhao, Y., Chen, K.D., Li, S., Lao, J., Yuan, S., Shyy, J.Y. & Chien, S. 2001, "DNA microarray analysis of gene expression in

endothelial cells in response to 24- h shear stress", *Physiological genomics*, vol. 7, no. 1, pp. 55.

Chen, M., Li, Y., Kawakami, T., Xu, S. & Chuang, P. 2004, "Palmitoylation is required for the production of a soluble multimeric Hedgehog protein complex and long- range signaling in vertebrates", *Genes & development*, vol. 18, no. 6, pp. 641.

Chiang, C., Litingtung, Y., Lee, E., Young, K.E., Jeffrey, L.C., Westphal, H. & Beachy, P.A. 1996, "Cyclopia and defective axial patterning in mice lacking Sonic hedgehog gene function", *Nature*, vol. 383, no. 6599, pp. 407.

Chiu, J., Chen, L., Chen, C., Lee, P. & Lee, C. 2004, "A model for studying the effect of shear stress on interactions between vascular endothelial cells and smooth muscle cells", *Journal of Biomechanics*, vol. 37, no. 4, pp. 531-539.

Christiane Nüsslein-Volhard & Wieschaus, E. 1980, "Mutations affecting segment number and polarity in *Drosophila*", *Nature*, vol. 287, no. 5785, pp. 795.

Chuang, P.T. & McMahon, A.P. 1999, *Vertebrate Hedgehog signalling modulated by induction of a Hedgehog-binding protein*.

Chuang, P., Kawcak, T. & McMahon, A.P. 2003, "Feedback control of mammalian Hedgehog signaling by the Hedgehog- binding protein, Hip1, modulates Fgf signaling during branching morphogenesis of the lung", *Genes & development*, vol. 17, no. 3, pp. 342.

Clarke, M.C., Figg, N., Maguire, J.J., Davenport, A.P., Goddard, M., Littlewood, T.D. & Bennett, M.R. 2006, "Apoptosis of vascular smooth muscle cells induces features of plaque vulnerability in atherosclerosis", *Nature medicine*, vol. 12, no. 9, pp. 1075-1080.

Clarke, M.C., Littlewood, T.D., Figg, N., Maguire, J.J., Davenport, A.P., Goddard, M. & Bennett, M.R. 2008, "Chronic apoptosis of vascular smooth muscle cells accelerates atherosclerosis and promotes calcification and medial degeneration", *Circulation research*, vol. 102, no. 12, pp. 1529-1538.

Clarke, R., Peden, J.F., Hopewell, J.C., Kyriakou, T., Goel, A., Heath, S.C., Parish, S., Barlera, S., Franzosi, M.G., Rust, S., Bennett, D., Silveira, A., Malarstig, A., Green, F.R., Lathrop, M., Gigante, B., Leander, K., de Faire, U., Seedorf, U., Hamsten, A., Collins, R., Watkins, H., Farrall, M. & PROCARDIS Consortium 2009, "Genetic variants associated with Lp(a) lipoprotein level and coronary disease", *The New England journal of medicine*, vol. 361, no. 26, pp. 2518-2528.

Cohen, J.C., Boerwinkle, E., Mosley, T.H. & Hobbs, H.H. 2006, "Sequence variations in PCSK9, low LDL, and protection against coronary heart disease", *The New England journal of medicine*, vol. 354, no. 14, pp. 1264.

Collins, F.S., Finnell, R.H., Rossant, J. & Wurst, W. 2007, "A new partner for the international knockout mouse consortium", *Cell*, vol. 129, no. 2, pp. 235.

Cooper, J.A., Miller, G.J. & Humphries, S.E. 2005, "A comparison of the PROCAM and Framingham point-scoring systems for estimation of individual risk of coronary heart disease in the Second Northwick Park Heart Study", *Atherosclerosis*, vol. 181, no. 1, pp. 93-100.

Corcoran, R.B. & Scott, M.P. 2006, "Oxysterols stimulate Sonic hedgehog signal transduction and proliferation of medulloblastoma cells", *Proceedings of the National Academy of Sciences of the United States of America*, vol. 103, no. 22, pp. 8408-8413.

Coultas, L., Nieuwenhuis, E., Anderson, G.A., Cabezas, J., Nagy, A., Henkelman, R.M., Hui, C.C. & Rossant, J. 2010, "Hedgehog regulates distinct vascular patterning events through VEGF-dependent and -independent mechanisms", *Blood*, vol. 116, no. 4, pp. 653-660.

Creanga, A., Glenn, T.D., Mann, R.K., Saunders, A.M., Talbot, W.S. & Beachy, P.A. 2012, "Scube/ You activity mediates release of dually lipid-modified Hedgehog signal in soluble form", *Genes & development*, vol. 26, no. 12, pp. 1312.

Dai, G., Kaazempur-Mofrad, M.R., Natarajan, S., Zhang, Y., Vaughn, S., Blackman, B.R., Kamm, R.D., Garcia-Cardena, G. & Gimbrone, M.A., Jr 2004, "Distinct endothelial phenotypes evoked by arterial waveforms derived from atherosclerosis-susceptible and -resistant regions of human vasculature", *Proceedings of the National Academy of Sciences of the United States of America*, vol. 101, no. 41, pp. 14871-14876.

Daniela Panáková, Sprong, H., Marois, E., Thiele, C. & Eaton, S. 2005, "Lipoprotein particles are required for Hedgehog and Wingless signalling", *Nature*, vol. 435, no. 7038, pp. 58.

Dansky, H.M., Charlton, S.A., Sikes, J.L., Heath, S.C., Simantov, R., Levin, L.F., Shu, P., Moore, K.J., Breslow, J.L. & Smith, J.D. 1999, "Genetic background determines the extent of atherosclerosis in ApoE-deficient mice", *Arteriosclerosis, Thrombosis, and Vascular Biology*, vol. 19, no. 8, pp. 1960-1968.

Daugherty, A. & Whitman, S.C. 2003, "Quantification of atherosclerosis in mice", *Methods in molecular biology (Clifton, N.J.)*, vol. 209, pp. 293-309.

Daugherty, A. & Rateri, D.L. 2005, "Development of experimental designs for atherosclerosis studies in mice", *Methods (San Diego, Calif.)*, vol. 36, no. 2, pp. 129-138.

Davies, M.J., Richardson, P.D., Woolf, N., Katz, D.R. & Mann, J. 1993, "Risk of thrombosis in human atherosclerotic plaques: role of extracellular

lipid, macrophage, and smooth muscle cell content", *British heart journal*, vol. 69, no. 5, pp. 377-381.

Dawber, T.R., Meadors, G.F. & Moore, F.E., Jr 1951, "Epidemiological approaches to heart disease: the Framingham Study", *American Journal of Public Health and the Nation's Health*, vol. 41, no. 3, pp. 279-281.

Dawber, T.R., Moore, F.E. & Mann, G.V. 1957, "Coronary heart disease in the Framingham study", *American Journal of Public Health and the Nation's Health*, vol. 47, no. 4 Pt 2, pp. 4-24.

Deloukas, P., Goldstein, B.A., Amouyel, P., Stirrups, K., König, I.R., Cazier, J., Johansson, A., Hall, A.S., Lee, J., Willer, C.J., Chambers, J.C., Esko, T., Kanoni, S., Folkersen, L., Goel, A., Grundberg, E., Havulinna, A.S., Ho, W.K., Hopewell, J.C., Eriksson, N., Kleber, M.E., Kristiansson, K., Lundmark, P., Willenborg, C., Lyytikäinen, L., Rafelt, S., Shungin, D., Strawbridge, R.J., Thorleifsson, G., Tikkanen, E., Van Zuydam, N., Voight, B.F., Waite, L.L., Zhang, W., Farrall, M., Ziegler, A., Absher, D., Altshuler, D., Balmforth, A.J., Barroso, I., Braund, P.S., Burgdorf, C., Claudi-Boehm, S., Cox, D., Dimitriou, M., Assimes, T.L., Do, R., Doney, A.S.F., El Mokhtari, N., Eriksson, P., Fischer, K., Fontanillas, P., Franco-Cereceda, A., Gigante, B., Groop, L., Gustafsson, S., Thompson, J.R., Hager, J., Hallmans, G., Han, B., Hunt, S.E., Kang, H.M., Illig, T., Kessler, T., Knowles, J.W., Kolovou, G., Kuusisto, J., Ingelsson, E., Langenberg, C., Langford, C., Leander, K., Lokki, M., Lundmark, A., McCarthy, M.I., Meisinger, C., Melander, O., Mihailov, E., Maouche, S., Saleheen, D., Morris, A.D., Müller-Nurasyid, M., Nikus, K., Peden, J.F., Rayner, N.W., Rasheed, A., Rosinger, S., Rubin, D., Rumpf, M.P., Schäfer, A., Erdmann, J., Sivananthan, M., Song, C., Stewart, A.F.R., Tan, S., Thorgeirsson, G., van der Schoot, C.E., Wagner, P.J., Wells, G.A., Wild, P.S., Yang, T., CARDIOGENICS Consortium, CARDIoGRAMplusC4D Consortium, Wellcome Trust Case Control Consortium, DIAGRAM Consortium & MuTHER Consortium 2013, "Large-scale association analysis identifies new risk loci for coronary artery disease", *Nature genetics*, vol. 45, no. 1, pp. 25.

Demer, L.L. 2002, "Vascular calcification and osteoporosis: inflammatory responses to oxidized lipids", *International journal of epidemiology*, vol. 31, no. 4, pp. 737-741.

Denis, M., Marcinkiewicz, J., Zaid, A., Gauthier, D., Poirier, S., Lazure, C., Seidah, N.G. & Prat, A. 2012, "Gene inactivation of proprotein convertase subtilisin/ kexin type 9 reduces atherosclerosis in mice.(Report)", *Circulation*, vol. 125, no. 7, pp. 894-901.

Dennler, S., Andre, J., Alexaki, I., Li, A., Magnaldo, T., ten Dijke, P., Wang, X.J., Verrecchia, F. & Mauviel, A. 2007, "Induction of sonic hedgehog mediators by transforming growth factor-beta: Smad3-dependent activation of Gli2 and Gli1 expression in vitro and in vivo", *Cancer research*, vol. 67, no. 14, pp. 6981-6986.

Dohle, E., Fuchs, S., Kolbe, M., Hofmann, A., Schmidt, H. & Kirkpatrick, C.J. 2011, "Comparative study assessing effects of sonic hedgehog and VEGF in a human co-culture model for bone vascularisation strategies", *European cells & materials*, vol. 21, pp. 144-156.

Doran, A.C., Meller, N. & Mcnamara, C.A. 2008, "Role of smooth muscle cells in the initiation and early progression of atherosclerosis", *Arteriosclerosis, Thrombosis, and Vascular Biology*, vol. 28, no. 5, pp. 812.

Dyer, M.A., Farrington, S.M., Mohn, D., Munday, J.R. & Baron, M.H. 2001, "Indian hedgehog activates hematopoiesis and vasculogenesis and can respecify prospective neurectodermal cell fate in the mouse embryo", *Development (Cambridge, England)*, vol. 128, no. 10, pp. 1717.

Echelard, Y., Epstein, D.J., St-Jacques, B., Shen, L., Mohler, J., McMahon, J.A. & McMahon, A.P. 1993, "Sonic hedgehog, a member of a family of putative signaling molecules, is implicated in the regulation of CNS polarity", *Cell*, vol. 75, no. 7, pp. 1417-1430.

Erbilgin, A., Civelek, M., Romanoski, C.E., Pan, C., Hagopian, R., Berliner, J.A. & Lusis, A.J. 2013, "Identification of CAD candidate genes in GWAS loci and their expression in vascular cells", *Journal of lipid research*, vol. 54, no. 7, pp. 1894-1905.

Erdmann, J., Grosshennig, A., Braund, P.S., Konig, I.R., Hengstenberg, C., Hall, A.S., Linsel-Nitschke, P., Kathiresan, S., Wright, B., Tregouet, D.A., Cambien, F., Bruse, P., Aherrahrou, Z., Wagner, A.K., Stark, K., Schwartz, S.M., Salomaa, V., Elosua, R., Melander, O., Voight, B.F., O'Donnell, C.J., Peltonen, L., Siscovick, D.S., Altshuler, D., Merlini, P.A., Peyvandi, F., Bernardinelli, L., Ardissino, D., Schillert, A., Blankenberg, S., Zeller, T., Wild, P., Schwarz, D.F., Tiret, L., Perret, C., Schreiber, S., El Mokhtari, N.E., Schafer, A., Marz, W., Renner, W., Bugert, P., Kluter, H., Schrezenmeir, J., Rubin, D., Ball, S.G., Balmforth, A.J., Wichmann, H.E., Meitinger, T., Fischer, M., Meisinger, C., Baumert, J., Peters, A., Ouwehand, W.H., Italian Atherosclerosis, Thrombosis, and Vascular Biology Working Group, Myocardial Infarction Genetics Consortium, Wellcome Trust Case Control Consortium, Cardiogenics Consortium, Deloukas, P., Thompson, J.R., Ziegler, A., Samani, N.J. & Schunkert, H. 2009, "New susceptibility locus for coronary artery disease on chromosome 3q22.3", *Nature genetics*, vol. 41, no. 3, pp. 280-282.

Eriksson, E.E., Xie, X., Werr, J., Thoren, P. & Lindbom, L. 2001, "Importance of Primary Capture and L- Selectin- Dependent Secondary Capture in Leukocyte Accumulation in Inflammation and Atherosclerosis in Vivo", *The Journal of experimental medicine*, vol. 194, no. 2, pp. 205-218.

Evans, M.J. & Kaufman, M.H. 1981, "Establishment in culture of pluripotential cells from mouse embryos", *Nature*, vol. 292, no. 5819, pp. 154.

Falk, E. 1992, "Why do plaques rupture?", *Circulation*, vol. 86, no. 6 Suppl, pp. III30.

Farrall, M., Green, F.R., Peden, J.F., Olsson, P.G., Clarke, R., Hellenius, M., Rust, S., Lagercrantz, J., Franzosi, M.G., Schulte, H., Carey, A., Olsson, G., Assmann, G., Tognoni, G., Collins, R., Hamsten, A. & Watkins, H. 2006, "Genome- Wide Mapping of Susceptibility to Coronary Artery Disease Identifies a Novel Replicated Locus on Chromosome 17 (Replicated CAD Locus on Chromosome 17)", *PLoS Genetics*, vol. 2, no. 5, pp. e72.

Feil, S., Fehrenbacher, B., Lukowski, R., Essmann, F., Schulze-Osthoff, K., Schaller, M. & Feil, R. 2014, "Transdifferentiation of Vascular Smooth Muscle Cells to Macrophage- Like Cells During Atherogenesis", *Circulation research*, vol. 115, no. 7, pp. 662-667.

Feng, J., White, B., Tyurina, O.V., Guner, B., Larson, T., Lee, H.Y., Karlstrom, R.O. & Kohtz, J.D. 2004, "Synergistic and antagonistic roles of the Sonic hedgehog N- and C- terminal lipids", *Development (Cambridge, England)*, vol. 131, no. 17, pp. 4357.

Franchini, M., Peyvandi, F. & Mannucci, P.M. 2008, "The Genetic Basis of Coronary Artery Disease: From Candidate Genes to Whole Genome Analysis", *Trends in cardiovascular medicine*, vol. 18, no. 5, pp. 157-162.

Fu, J.R., Liu, W.L., Zhou, J.F., Sun, H.Y., Xu, H.Z., Luo, L., Zhang, H. & Zhou, Y.F. 2006, "Sonic hedgehog protein promotes bone marrow-derived endothelial progenitor cell proliferation, migration and VEGF production via PI 3-kinase/Akt signaling pathways", *Acta Pharmacologica Sinica*, vol. 27, no. 6, pp. 685-693.

Getz, G.S. 1990, "The involvement of lipoproteins in atherogenesis. Evolving concepts", *Annals of the New York Academy of Sciences*, vol. 598, pp. 17-28.

Getz, G.S. & Reardon, C.A. 2012, "Animal models of atherosclerosis", *Arteriosclerosis, Thrombosis, and Vascular Biology*, vol. 32, no. 5, pp. 1104-1115.

Getz, G.S. & Reardon, C.A. 2009, "Apoprotein E as a lipid transport and signaling protein in the blood, liver, and artery wall", *Journal of lipid research*, vol. 50, no. Suppl, pp. S156-61.

Getz, G.S. & Reardon, C.A. 2006, "Diet and murine atherosclerosis", *Arteriosclerosis, Thrombosis, and Vascular Biology*, vol. 26, no. 2, pp. 242-249.

Gierasch, L.M. 1989, "Signal sequences", *Biochemistry*, vol. 28, no. 3, pp. 923-930.

Go, A.S., Fox, C.S., Franco, S., Fullerton, H.J., Gillespie, C., Hailpern, S.M., Heit, J.A., Howard, V.J., Huffman, M.D., Kissela, B.M., Kittner, S.J., Mozaffarian, D., Lackland, D.T., Lichtman, J.H., Lisabeth, L.D., Magid, D., Marcus, G.M., Marelli, A., Matchar, D.B., McGuire, D.K., Mohler, E.R., Moy, C.S., Roger, V.L., Mussolino, M.E., Nichol, G., Paynter, N.P., Schreiner, P.J., Sorlie, P.D., Stein, J., Turan, T.N., Virani, S.S., Wong, N.D., Woo, D., Benjamin, E.J., Turner, M.B., Berry, J.D., Borden, W.B., Bravata, D.M., Dai, S., Ford, E.S., on behalf of the American Heart Association Statistics Committee and Stroke Statistics Subcommittee & American Heart Association Statistics Committee and Stroke Statistics Subcommittee 2013, "Heart disease and stroke statistics--2013 update: a report from the American Heart Association", *Circulation*, vol. 127, no. 1, pp. e6-e245.

Gomez, D., Shankman, L.S., Nguyen, A.T. & Owens, G.K. 2013, "Detection of histone modifications at specific gene loci in single cells in histological sections", *Nature methods*, vol. 10, no. 2, pp. 171-177.

Goodrich, L.V., Milenkovic, L., Higgins, K.M. & Scott, M.P. 1997, "Altered neural cell fates and medulloblastoma in mouse patched mutants", *Science (New York, N.Y.)*, vol. 277, no. 5329, pp. 1109-1113.

Göran K Hansson 2005, "MECHANISMS OF DISEASE: Inflammation, Atherosclerosis, and Coronary Artery Disease", *The New England journal of medicine*, vol. 352, no. 16, pp. 1685.

Gossler, A., Joyner, A.L., Rossant, J. & Skarnes, W.C. 1989, "Mouse embryonic stem cells and reporter constructs to detect developmentally regulated genes", *Science*, vol. 244, no. 4903, pp. 463.

Grover, M.P., Ballouz, S., Mohanasundaram, K.A., George, R.A., Goscinski, A., Crowley, T.M., Sherman, C.D. & Wouters, M.A. 2015, "Novel therapeutics for coronary artery disease from genome-wide association study data", *BMC medical genomics*, vol. 8 Suppl 2, pp. S1-8794-8-S2-S1. Epub 2015 May 29.

Grover, V.K., Valadez, J.G., Bowman, A.B., Cooper, M.K. & Treisman, J.E. 2011, "Lipid Modifications of Sonic Hedgehog Ligand Dictate Cellular Reception and Signal Response", *PLoS ONE*, vol. 6, no. 7.

Gu, H., Marth, J.D., Orban, P.C., Mossmann, H. & Rajewsky, K. 1994, "Deletion of a DNA polymerase beta gene segment in T cells using cell type-specific gene targeting", *Science (New York, N.Y.)*, vol. 265, no. 5168, pp. 103.

Guan, C., Ye, C., Yang, X. & Gao, J. 2010, *A review of current large-scale mouse knockout efforts*, Hoboken.

Hauser, E.R., Crossman, D.C., Granger, C.B., Haines, J.L., Jones, C.J.H., Mooser, V., Mcadam, B., Winkelmann, B.R., Wiseman, A.H., Muhlestein, J.B., Bartel, A.G., Dennis, C.A., Dowdy, E., Estabrooks, S., Eggleston, K.,

Francis, S., Roche, K., Clevenger, P.W., Huang, L., Pedersen, B., Shah, S., Schmidt, S., Haynes, C., West, S., Asper, D., Booze, M., Sharma, S., Sundseth, S., Middleton, L., Roses, A.D., Hauser, M.A., Vance, J.M., Pericak-Vance, M. & Kraus, W.E. 2004, "A Genomewide Scan for Early-Onset Coronary Artery Disease in 438 Families: The GENECARD Study", *The American Journal of Human Genetics*, vol. 75, no. 3, pp. 436-447.

Hawe, E., Talmud, P.J., Miller, G.J., Humphries, S.E. & Second Northwick Park Heart Study 2003, "Family history is a coronary heart disease risk factor in the Second Northwick Park Heart Study", *Annals of Human Genetics*, vol. 67, no. Pt 2, pp. 97-106.

Helgadottir, A., Manolescu, A., Thorleifsson, G., Gretarsdottir, S., Jonsdottir, H., Thorsteinsdottir, U., Samani, N.J., Gudmundsson, G., Grant, S.F., Thorgeirsson, G., Sveinbjornsdottir, S., Valdimarsson, E.M., Matthiasson, S.E., Johannsson, H., Gudmundsdottir, O., Gurney, M.E., Sainz, J., Thorhallsdottir, M., Andresdottir, M., Frigge, M.L., Topol, E.J., Kong, A., Gudnason, V., Hakonarson, H., Gulcher, J.R. & Stefansson, K. 2004, "The gene encoding 5-lipoxygenase activating protein confers risk of myocardial infarction and stroke", *Nature genetics*, vol. 36, no. 3, pp. 233-239.

Helgadottir, A., Thorleifsson, G., Manolescu, A., Gretarsdottir, S., Blondal, T., Jonasdottir, A., Jonasdottir, A., Sigurdsson, A., Baker, A., Palsson, A., Masson, G., Gudbjartsson, D.F., Magnusson, K.P., Andersen, K., Levey, A.I., Backman, V.M., Matthiasdottir, S., Jonsdottir, T., Palsson, S., Einarsdottir, H., Gunnarsdottir, S., Gylfason, A., Vaccarino, V., Hooper, W.C., Reilly, M.P., Granger, C.B., Austin, H., Rader, D.J., Shah, S.H., Quyyumi, A.A., Gulcher, J.R., Thorgeirsson, G., Thorsteinsdottir, U., Kong, A. & Stefansson, K. 2007, "A common variant on chromosome 9p21 affects the risk of myocardial infarction", *Science (New York, N.Y.)*, vol. 316, no. 5830, pp. 1491-1493.

Hicks, G.G., Er-Gang Shi, Xuan-Mei Li, Chun-Hua Li, Pawlak, M. & Earl Ruley, H. 1997, "Functional genomics in mice by tagged sequence mutagenesis", *Nature genetics*, vol. 16, no. 4, pp. 338.

Hochman, E., Castiel, A., Jacob-Hirsch, J., Amariglio, N. & Izraeli, S. 2006, "Molecular pathways regulating pro-migratory effects of Hedgehog signaling", *The Journal of biological chemistry*, vol. 281, no. 45, pp. 33860-33870.

Hu, W., Polinsky, P., Sadoun, E., Rosenfeld, M.E. & Schwartz, S.M. 2005, "Atherosclerotic lesions in the common coronary arteries of ApoE knockout mice", *Cardiovascular Pathology*, vol. 14, no. 3, pp. 120-125.

Humphries, S.E. & Morgan, L. 2004, "Genetic risk factors for stroke and carotid atherosclerosis: insights into pathophysiology from candidate gene approaches", *Lancet Neurology*, vol. 3, no. 4, pp. 227-236.

IBC 50K CAD Consortium 2011, *Large-scale gene-centric analysis identifies novel variants for coronary artery disease*, Public Library of Science, United States.

Ingham, P.W. & McMahon, A.P. 2001, *Hedgehog signaling in animal development: paradigms and principles*.

Ingram, W.J., Wicking, C.A., Grimmond, S.M., Forrest, A.R. & Wainwright, B.J. 2002, "Novel genes regulated by Sonic Hedgehog in pluripotent mesenchymal cells", *Oncogene*, vol. 21, no. 53, pp. 8196-8205.

International HapMap Consortium 2003 2003, "The International HapMap Project", *Nature*, vol. 426, no. 6968, pp. 789.

Ishibashi, S., Brown, M.S., Goldstein, J.L., Gerard, R.D., Hammer, R.E. & Herz, J. 1993, "Hypercholesterolemia in low density lipoprotein receptor knockout mice and its reversal by adenovirus-mediated gene delivery", *The Journal of clinical investigation*, vol. 92, no. 2, pp. 883-893.

Ishibashi, S., Goldstein, J.L., Brown, M.S., Herz, J. & Burns, D.K. 1994a, "Massive xanthomatosis and atherosclerosis in cholesterol-fed low density lipoprotein receptor-negative mice", *The Journal of clinical investigation*, vol. 93, no. 5, pp. 1885-1893.

Ishibashi, S., Herz, J., Maeda, N., Goldstein, J.L. & Brown, M.S. 1994b, "The two-receptor model of lipoprotein clearance: tests of the hypothesis in "knockout" mice lacking the low density lipoprotein receptor, apolipoprotein E, or both proteins", *Proceedings of the National Academy of Sciences of the United States of America*, vol. 91, no. 10, pp. 4431-4435.

J A Piedrahita, S H Zhang, J R Hagan, P M Oliver & N Maeda 1992, "Generation of mice carrying a mutant apolipoprotein E gene inactivated by gene targeting in embryonic stem cells", *Proceedings of the National Academy of Sciences of the United States of America*, vol. 89, no. 10, pp. 4471-4475.

Janeway, C.A. & Medzhitov, R. 2002, *INNATE IMMUNE RECOGNITION*.

Jawien, J., Nastalek, P. & Korbut, R. 2004, "Mouse models of experimental atherosclerosis", *Journal of physiology and pharmacology : an official journal of the Polish Physiological Society*, vol. 55, no. 3, pp. 503-517.

Jones, P.H., Bays, H.E., Chaudhari, U., Pordy, R., Lorenzato, C., Miller, K. & Robinson, J.G. 2016, "Safety of Alirocumab (A PCSK9 Monoclonal Antibody) (From 14 Randomized Trials)", *The American Journal of Cardiology*, .

Justice, M.J., Noveroske, J.K., Weber, J.S., Zheng, B. & Bradley, A. 1999, "Mouse ENU mutagenesis", *Human molecular genetics*, vol. 8, no. 10, pp. 1955-1963.

Kanda, S., Mochizuki, Y., Suematsu, T., Miyata, Y., Nomata, K. & Kanetake, H. 2003, "Sonic hedgehog induces capillary morphogenesis by endothelial cells through phosphoinositide 3-kinase", *The Journal of biological chemistry*, vol. 278, no. 10, pp. 8244-8249.

Katoh, Y. & Katoh, M. 2006, "Comparative genomics on HHIP family orthologs", *International journal of molecular medicine*, vol. 17, no. 2, pp. 391.

Kowala, M.C., Recce, R.F., Beyer, S.F., Gu, C.F. & Valentine, M. 2000, *Characterization of atherosclerosis in LDL receptor knockout mice: macrophage accumulation correlates with rapid and sustained expression of aortic MCP-1/JE*.

Krauss, S., Concordet, J.-. & Ingham, P.W. 1993, "A functionally conserved homolog of the Drosophila segment polarity gene hh is expressed in tissues with polarizing activity in zebrafish embryos", *Cell*, vol. 75, no. 7, pp. 1431-1444.

Kremen, M., Krishnan, R., Emery, I., Hu, J.H., Slezicki, K.I., Wu, A., Qian, K., Du, L., Plawman, A., Stempien-Otero, A. & Dichek, D.A. 2008, "Plasminogen mediates the atherogenic effects of macrophage-expressed urokinase and accelerates atherosclerosis in apoE- knockout mice.(MEDICAL SCIENCES)(Author abstract)(Report)", *Proceedings of the National Academy of Sciences of the United States*, vol. 105, no. 44, pp. 17109.

Kumar, D., Hacker, T.A., Buck, J., Whitesell, L.F., Kaji, E.H., Douglas, P.S. & Kamp, T.J. 2005, "Distinct mouse coronary anatomy and myocardial infarction consequent to ligation", *Coronary artery disease*, vol. 16, no. 1, pp. 41.

Kusano, K.F., Kearney, M., Asahara, T., Losordo, D.W., Allendoerfer, K.L., Munger, W., Pola, R., Bosch-Marce, M., Kirchmair, R., Yoon, Y., Curry, C. & Silver, M. 2004, "Sonic Hedgehog Induces Arteriogenesis in Diabetic Vasa Nervorum and Restores Function in Diabetic Neuropathy", *Arteriosclerosis, Thrombosis, and Vascular Biology*, vol. 24, no. 11, pp. 2102-2107.

Kusano, K.F., Tkebuchava, T., Thorne, T., Takenaka, H., Aikawa, R., Goukassian, D., von Samson, P., Hamada, H., Yoon, Y., Silver, M., Eaton, E., Pola, R., Ma, H., Heyd, L., Kearney, M., Munger, W., Porter, J.A., Kishore, R., Losordo, D.W., Murayama, T., Curry, C., Kawamoto, A., Iwakura, A., Shintani, S., Li, M. & Asai, J. 2005, "Sonic hedgehog myocardial gene therapy: tissue repair through transient reconstitution of embryonic signaling", *Nature medicine*, vol. 11, no. 11, pp. 1197-1204.

Kwong, L., Bijlsma, M.F. & Roelink, H. 2014, "Shh-mediated degradation of Hhip allows cell autonomous and non-cell autonomous Shh signalling", *Nature communications*, vol. 5, pp. 4849.

Lander, E.S., Linton, L.M., Birren, B., Nusbaum, C., Zody, M.C., Baldwin, J., Devon, K., Dewar, K., Doyle, M., FitzHugh, W., Funke, R., Gage, D., Harris, K., Heaford, A., Howland, J., Kann, L., Lehoczky, J., LeVine, R., McEwan, P., McKernan, K., Meldrim, J., Mesirov, J.P., Miranda, C., Morris, W., Naylor, J., Raymond, C., Rosetti, M., Santos, R., Sheridan, A., Sougnez, C., Stange-Thomann, Y., Stojanovic, N., Subramanian, A., Wyman, D., Rogers, J., Sulston, J., Ainscough, R., Beck, S., Bentley, D., Burton, J., Clee, C., Carter, N., Coulson, A., Deadman, R., Deloukas, P., Dunham, A., Dunham, I., Durbin, R., French, L., Grafham, D., Gregory, S., Hubbard, T., Humphray, S., Hunt, A., Jones, M., Lloyd, C., McMurray, A., Matthews, L., Mercer, S., Milne, S., Mullikin, J.C., Mungall, A., Plumb, R., Ross, M., Shownkeen, R., Sims, S., Waterston, R.H., Wilson, R.K., Hillier, L.W., McPherson, J.D., Marra, M.A., Mardis, E.R., Fulton, L.A., Chinwalla, A.T., Pepin, K.H., Gish, W.R., Chissoe, S.L., Wendl, M.C., Delehaunty, K.D., Miner, T.L., Delehaunty, A., Kramer, J.B., Cook, L.L., Fulton, R.S., Johnson, D.L., Minx, P.J., Clifton, S.W., Hawkins, T., Branscomb, E., Predki, P., Richardson, P., Wenning, S., Slezak, T., Doggett, N., Cheng, J.F., Olsen, A., Lucas, S., Elkin, C., Uberbacher, E., Frazier, M., Gibbs, R.A., Muzny, D.M., Scherer, S.E., Bouck, J.B., Sodergren, E.J., Worley, K.C., Rives, C.M., Gorrell, J.H., Metzker, M.L., Naylor, S.L., Kucherlapati, R.S., Nelson, D.L., Weinstock, G.M., Sakaki, Y., Fujiyama, A., Hattori, M., Yada, T., Toyoda, A., Itoh, T., Kawagoe, C., Watanabe, H., Totoki, Y., Taylor, T., Weissenbach, J., Heilig, R., Saurin, W., Artiguenave, F., Brottier, P., Bruls, T., Pelletier, E., Robert, C., Wincker, P., Smith, D.R., Doucette-Stamm, L., Rubenfield, M., Weinstock, K., Lee, H.M., Dubois, J., Rosenthal, A., Platzer, M., Nyakatura, G., Taudien, S., Rump, A., Yang, H., Yu, J., Wang, J., Huang, G., Gu, J., Hood, L., Rowen, L., Madan, A., Qin, S., Davis, R.W., Federspiel, N.A., Abola, A.P., Proctor, M.J., Myers, R.M., Schmutz, J., Dickson, M., Grimwood, J., Cox, D.R., Olson, M.V., Kaul, R., Raymond, C., Shimizu, N., Kawasaki, K., Minoshima, S., Evans, G.A., Athanasiou, M., Schultz, R., Roe, B.A., Chen, F., Pan, H., Ramser, J., Lehrach, H., Reinhardt, R., McCombie, W.R., de la Bastide, M., Dedhia, N., Blocker, H., Hornischer, K., Nordsiek, G., Agarwala, R., Aravind, L., Bailey, J.A., Bateman, A., Batzoglou, S., Birney, E., Bork, P., Brown, D.G., Burge, C.B., Cerutti, L., Chen, H.C., Church, D., Clamp, M., Copley, R.R., Doerks, T., Eddy, S.R., Eichler, E.E., Furey, T.S., Galagan, J., Gilbert, J.G., Harmon, C., Hayashizaki, Y., Haussler, D., Hermjakob, H., Hokamp, K., Jang, W., Johnson, L.S., Jones, T.A., Kasif, S., Kasprzyk, A., Kennedy, S., Kent, W.J., Kitts, P., Koonin, E.V., Korf, I., Kulp, D., Lancet, D., Lowe, T.M., McLysaght, A., Mikkelsen, T., Moran, J.V., Mulder, N., Pollara, V.J., Ponting, C.P., Schuler, G., Schultz, J., Slater, G., Smit, A.F., Stupka, E., Szustakowki, J., Thierry-Mieg, D., Thierry-Mieg, J., Wagner, L., Wallis, J., Wheeler, R., Williams, A., Wolf, Y.I., Wolfe, K.H., Yang, S.P., Yeh, R.F., Collins, F., Guyer, M.S., Peterson, J., Felsenfeld, A., Wetterstrand, K.A., Patrinos, A., Morgan, M.J., de Jong, P., Catanese, J.J., Osoegawa, K., Shizuya, H., Choi, S., Chen, Y.J., Szustakowki, J. & International Human Genome Sequencing Consortium 2001, "Initial sequencing and analysis of the human genome", *Nature*, vol. 409, no. 6822, pp. 860-921.

- Laura, S.S., Gomez, D., Olga, A.C., Salmon, M., Gabriel, F.A., Ryan, M.H., Swiatlowska, P., Alexandra, A.C.N., Elizabeth, S.G., Adam, C.S., Isakson, B., Gwendalyn, J.R. & Gary, K.O. 2015, "KLF4- dependent phenotypic modulation of smooth muscle cells has a key role in atherosclerotic plaque pathogenesis", *Nature medicine*, .
- Lavine, K.J., Kovacs, A. & Ornitz, D.M. 2008, "Hedgehog signaling is critical for maintenance of the adult coronary vasculature in mice", *The Journal of clinical investigation*, vol. 118, no. 7, pp. 2404-2414.
- Lavine, K.J. & Ornitz, D.M. 2007, *Rebuilding the Coronary Vasculature: Hedgehog as a New Candidate for Pharmacologic Revascularization*, Elsevier Inc, United States.
- Lawson, N.D., Vogel, A.M. & Weinstein, B.M. 2002, "sonic hedgehog and vascular endothelial growth factor Act Upstream of the Notch Pathway during Arterial Endothelial Differentiation", *Developmental Cell*, vol. 3, no. 1, pp. 127-136.
- Lee, J.J., Ekker, S.C., Von Kessler, D.P., Porter, J.A., Sun, B.I. & Beachy, P.A. 1994, "Autoproteolysis in hedgehog protein biogenesis", *Science (New York, N.Y.)*, vol. 266, no. 5190, pp. 1528.
- Lee, M.H., Lu, K., Hazard, S., Yu, H., Shulenin, S., Hidaka, H., Kojima, H., Allikmets, R., Sakuma, N., Pegoraro, R., Srivastava, A.K., Salen, G., Dean, M. & Patel, S.B. 2001, "Identification of a gene, ABCG5, important in the regulation of dietary cholesterol absorption", *Nature genetics*, vol. 27, no. 1, pp. 79-83.
- Lee, S., Moskowitz, M.A. & Sims, J.R. 2007, "Sonic hedgehog inversely regulates the expression of angiopoietin-1 and angiopoietin-2 in fibroblasts", *International journal of molecular medicine*, vol. 19, no. 3, pp. 445.
- Lee, S.M., Nguyen, D., Hu, Z. & Abbott, G.W. 2015, "Kcne2 deletion promotes atherosclerosis and diet- dependent sudden death", *Journal of Molecular and Cellular Cardiology*, vol. 87, pp. 148-151.
- Lei, X., Basu, D., Li, Z., Zhang, M., Rudic, R.D., Jiang, X.C. & Jin, W. 2014, "Hepatic overexpression of the prodomain of furin lessens progression of atherosclerosis and reduces vascular remodeling in response to injury", *Atherosclerosis*, vol. 236, no. 1, pp. 121-130.
- Leitinger, N. 2003, "Oxidized phospholipids as modulators of inflammation in atherosclerosis", *Current opinion in lipidology*, vol. 14, no. 5, pp. 421-430.
- Lepor, N.E. & Kereiakes, D.J. 2015, "The PCSK9 Inhibitors: A Novel Therapeutic Target Enters Clinical Practice", *American Health & Drug Benefits*, vol. 8, no. 9, pp. 483-489.

- Li, A.C., Brown, K.K., Silvestre, M.J., Willson, T.M., Palinski, W. & Glass, C.K. 2000, "Peroxisome proliferator-activated receptor gamma ligands inhibit development of atherosclerosis in LDL receptor-deficient mice", *The Journal of clinical investigation*, vol. 106, no. 4, pp. 523-531.
- Li, F., Duman-Scheel, M., Yang, D., Du, W., Zhang, J., Zhao, C., Qin, L. & Xin, S. 2010, "Sonic hedgehog signaling induces vascular smooth muscle cell proliferation via induction of the G1 cyclin-retinoblastoma axis", *Arteriosclerosis, Thrombosis, and Vascular Biology*, vol. 30, no. 9, pp. 1787-1794.
- Liao, F., Andalibi, A., deBeer, F.C., Fogelman, A.M. & Lusis, A.J. 1993, "Genetic control of inflammatory gene induction and NF-kappa B-like transcription factor activation in response to an atherogenic diet in mice", *The Journal of clinical investigation*, vol. 91, no. 6, pp. 2572-2579.
- Libby, P., Ridker, P.M. & Hansson, G.K. 2011, "Progress and challenges in translating the biology of atherosclerosis", *Nature*, vol. 473, no. 7347, pp. 317-325.
- Libby, P., Ridker, P.M. & Maseri, A. 2002, "Inflammation and atherosclerosis", *Circulation*, vol. 105, no. 9, pp. 1135-1143.
- Libby, P. & Theroux, P. 2005, "Pathophysiology of coronary artery disease", *Circulation*, vol. 111, no. 25, pp. 3481-3488.
- Little, C. & Bagg, H. 1923, "The occurrence of two heritable types of abnormality among the descendants of X-rayed mice.", .
- Liu, S.Q., Tang, D., Tieche, C. & Alkema, P.K. 2003a, "Pattern formation of vascular smooth muscle cells subject to nonuniform fluid shear stress: mediation by gradient of cell density", *American journal of physiology.Heart and circulatory physiology*, vol. 285, no. 3, pp. H1072.
- Liu, S.Q., Tieche, C., Tang, D. & Alkema, P. 2003b, "Pattern formation of vascular smooth muscle cells subject to nonuniform fluid shear stress: role of PDGF-beta receptor and Src", *American journal of physiology.Heart and circulatory physiology*, vol. 285, no. 3, pp. H1081.
- Lu, H., Rateri, D.L. & Daugherty, A. 2007, "Immunostaining of mouse atherosclerotic lesions", *Methods in Molecular Medicine*, vol. 139, pp. 77.
- Lusis, A.J. 2000, "Atherosclerosis", *Nature*, vol. 407, no. 6801, pp. 233.
- Lusis, A.J., Mar, R. & Pajukanta, P. 2004, "Genetics of atherosclerosis", *Annual review of genomics and human genetics*, vol. 5, no. 1, pp. 189-218.
- Ma, Y., Wang, W., Zhang, J., Lu, Y., Wu, W., Yan, H. & Wang, Y. 2012, "Hyperlipidemia and atherosclerotic lesion development in Ldlr-deficient mice on a long-term high-fat diet", *PloS one*, vol. 7, no. 4, pp. e35835.

MacLeod, D.C., Strauss, B.H., de Jong, M., Escaned, J., Umans, V.A., van Suylen, R.J., Verkerk, A., de Feyter, P.J. & Serruys, P.W. 1994, "Proliferation and extracellular matrix synthesis of smooth muscle cells cultured from human coronary atherosclerotic and restenotic lesions", *Journal of the American College of Cardiology*, vol. 23, no. 1, pp. 59-65.

Majesky, M.W. 2007, "Developmental basis of vascular smooth muscle diversity", *Arteriosclerosis, Thrombosis, and Vascular Biology*, vol. 27, no. 6, pp. 1248.

Majesky, M.W., Dong, X.R., Hoggund, V., Mahoney, J., William M. & Daum, G. 2011, "The adventitia: a dynamic interface containing resident progenitor cells", *Arteriosclerosis, Thrombosis, and Vascular Biology*, vol. 31, no. 7, pp. 1530-1539.

Malkoff, J. 2005, "Non-invasive blood pressure for mice and rats", *Animal lab news, Kent Scientific corporation*, , pp. pp1-12.

Mansour, S.L., Thomas, K.R. & Capecchi, M.R. 1988, "Disruption of the proto-oncogene int-2 in mouse embryo-derived stem cells: a general strategy for targeting mutations to non-selectable genes", *Nature*, vol. 336, no. 6197, pp. 348-352.

Marcel Van, D.H. & Ingham, P.W. 1996, "smoothed encodes a receptor-like serpentine protein required for hedgehog signalling", *Nature*, vol. 382, no. 6591, pp. 547.

Marenberg, M.E., Risch, N., Berkman, L.F., Floderus, B. & de Faire, U. 1994, "Genetic Susceptibility to Death from Coronary Heart Disease in a Study of Twins", *The New England journal of medicine*, vol. 330, no. 15, pp. 1041-1046.

Marigo, V., Roberts, D.J., Lee, S.M., Tsukurov, O., Levi, T., Gastier, J.M., Epstein, D.J., Gilbert, D.J., Copeland, N.G. & Seidman, C.E. 1995, "Cloning, expression, and chromosomal location of SHH and IHH: two human homologues of the Drosophila segment polarity gene hedgehog", *Genomics*, vol. 28, no. 1, pp. 44-51.

Marigo, V. & Tabin, C.J. 1996, "Regulation of patched by sonic hedgehog in the developing neural tube", *Proceedings of the National Academy of Sciences of the United States of America*, vol. 93, no. 18, pp. 9346.

Marigo, V., Davey, R.A., Zuo, Y., Cunningham, J.M. & Tabin, C.J. 1996a, "Biochemical evidence that Patched is the Hedgehog receptor", *Nature*, vol. 384, no. 6605, pp. 176.

Marigo, V., Johnson, R.L., Vortkamp, A. & Tabin, C.J. 1996b, "Sonic hedgehog Differentially Regulates Expression of GLI and GLI3 during Limb Development", *Developmental biology*, vol. 180, no. 1, pp. 273-283.

Marmot, M.G., Smith, G.D., Stansfeld, S., Patel, C., North, F., Head, J., White, I., Brunner, E. & Feeney, A. 1991, "Health inequalities among British civil servants: the Whitehall II study", *Lancet (London, England)*, vol. 337, no. 8754, pp. 1387-1393.

Marsh, M.M., Walker, V.R., Curtiss, L.K. & Banka, C.L. 1999, "Protection against atherosclerosis by estrogen is independent of plasma cholesterol levels in LDL receptor-deficient mice", *Journal of lipid research*, vol. 40, no. 5, pp. 893-900.

Martin, G.R. 1981, "Isolation of a pluripotent cell line from early mouse embryos cultured in medium conditioned by teratocarcinoma stem cells", *Proceedings of the National Academy of Sciences of the United States of America*, vol. 78, no. 12, pp. 7634.

Massberg, S., Konrad, I., Nieswandt, B., Gawaz, M., Brand, K., Grüner, S., Page, S., Müller, E., Müller, I., Bergmeier, W., Richter, T. & Lorenz, M. 2002, "A critical role of platelet adhesion in the initiation of atherosclerotic lesion formation", *The Journal of experimental medicine*, vol. 196, no. 7, pp. 887-896.

Matsui, M., Takeda, Y., Uemura, S., Matsumoto, T., Seno, A., Onoue, K., Tsushima, H., Morimoto, K., Soeda, T., Okayama, S., Somekawa, S., Samejima, K., Kawata, H., Kawakami, R., Nakatani, K., Iwano, M. & Saito, Y. 2014, "Suppressed soluble Fms-like tyrosine kinase-1 production aggravates atherosclerosis in chronic kidney disease", *Kidney international*, vol. 85, no. 2, pp. 393-403.

McCarthy, M.I., Abecasis, G.R., Cardon, L.R., Goldstein, D.B., Little, J., Ioannidis, J.P. & Hirschhorn, J.N. 2008, "Genome-wide association studies for complex traits: consensus, uncertainty and challenges", *Nature reviews.Genetics*, vol. 9, no. 5, pp. 356-369.

McPherson, R., Pertsemlidis, A., Kavaslar, N., Stewart, A., Roberts, R., Cox, D.R., Hinds, D.A., Pennacchio, L.A., Tybjaerg-Hansen, A., Folsom, A.R., Boerwinkle, E., Hobbs, H.H. & Cohen, J.C. 2007, "A common allele on chromosome 9 associated with coronary heart disease", *Science (New York, N.Y.)*, vol. 316, no. 5830, pp. 1488-1491.

Meyers, E.N., Lewandoski, M. & Martin, G.R. 1998, "An Fgf8 mutant allelic series generated by Cre- and Flp-mediated recombination", *Nature genetics*, vol. 18, no. 2, pp. 136-141.

Mooney, C.J., Hakimjavadi, R., Fitzpatrick, E., Kennedy, E., Walls, D., Morrow, D., Redmond, E.M. & Cahill, P.A. 2015, "Hedgehog and Resident Vascular Stem Cell Fate", vol. 2015.

Moore, K. & Tabas, I. 2011, "Macrophages in the Pathogenesis of Atherosclerosis", *Cell*, vol. 145, no. 3, pp. 341-355.

Morrow, D., Cahill, P.A., Cullen, J.P., Liu, W., Guha, S., Sweeney, C., Birney, Y.A., Collins, N., Walls, D. & Redmond, E.M. 2009, "Sonic Hedgehog Induces Notch Target Gene Expression in Vascular Smooth Muscle Cells via VEGF-A", *Arteriosclerosis, Thrombosis, and Vascular Biology*, vol. 29, no. 7, pp. 1112-1118.

Morrow, D., Cahill, P.A., Sweeney, C., Birney, Y.A., Guha, S., Collins, N., Cummins, P.M., Murphy, R., Walls, D. & Redmond, E.M. 2007, "Biomechanical regulation of hedgehog signaling in vascular smooth muscle cells in vitro and in vivo", *AJP - Cell Physiology*, vol. 292, no. 1, pp. C488-496.

Mortensen, M.B., Kjolby, M., Gunnarsen, S., Larsen, J.V., Palmfeldt, J., Falk, E., Nykjaer, A. & Bentzon, J.F. 2014, "Targeting sortilin in immune cells reduces proinflammatory cytokines and atherosclerosis.(BRIEF REPORT)", *Journal of Clinical Investigation*, vol. 124, no. 12, pp. 5317.

Mouse Genome Sequencing Consortium, Waterston, R.H., Lindblad-Toh, K., Birney, E., Rogers, J., Abril, J.F., Agarwal, P., Agarwala, R., Ainscough, R., Alexandersson, M., An, P., Antonarakis, S.E., Attwood, J., Baertsch, R., Bailey, J., Barlow, K., Beck, S., Berry, E., Birren, B., Bloom, T., Bork, P., Botcherby, M., Bray, N., Brent, M.R., Brown, D.G., Brown, S.D., Bult, C., Burton, J., Butler, J., Campbell, R.D., Carninci, P., Cawley, S., Chiaromonte, F., Chinwalla, A.T., Church, D.M., Clamp, M., Clee, C., Collins, F.S., Cook, L.L., Copley, R.R., Coulson, A., Couronne, O., Cuff, J., Curwen, V., Cutts, T., Daly, M., David, R., Davies, J., Delehaunty, K.D., Deri, J., Dermitzakis, E.T., Dewey, C., Dickens, N.J., Diekhans, M., Dodge, S., Dubchak, I., Dunn, D.M., Eddy, S.R., Elnitski, L., Emes, R.D., Eswara, P., Eyras, E., Felsenfeld, A., Fewell, G.A., Flicek, P., Foley, K., Frankel, W.N., Fulton, L.A., Fulton, R.S., Furey, T.S., Gage, D., Gibbs, R.A., Glusman, G., Gnerre, S., Goldman, N., Goodstadt, L., Grafham, D., Graves, T.A., Green, E.D., Gregory, S., Guigo, R., Guyer, M., Hardison, R.C., Haussler, D., Hayashizaki, Y., Hillier, L.W., Hinrichs, A., Hlavina, W., Holzer, T., Hsu, F., Hua, A., Hubbard, T., Hunt, A., Jackson, I., Jaffe, D.B., Johnson, L.S., Jones, M., Jones, T.A., Joy, A., Kamal, M., Karlsson, E.K., Karolchik, D., Kasprzyk, A., Kawai, J., Keibler, E., Kells, C., Kent, W.J., Kirby, A., Kolbe, D.L., Korf, I., Kucherlapati, R.S., Kulbokas, E.J., Kulp, D., Landers, T., Leger, J.P., Leonard, S., Letunic, I., Levine, R., Li, J., Li, M., Lloyd, C., Lucas, S., Ma, B., Maglott, D.R., Mardis, E.R., Matthews, L., Mauceli, E., Mayer, J.H., McCarthy, M., McCombie, W.R., McLaren, S., McLay, K., McPherson, J.D., Meldrim, J., Meredith, B., Mesirov, J.P., Miller, W., Miner, T.L., Mongin, E., Montgomery, K.T., Morgan, M., Mott, R., Mullikin, J.C., Muzny, D.M., Nash, W.E., Nelson, J.O., Nhan, M.N., Nicol, R., Ning, Z., Nusbaum, C., O'Connor, M.J., Okazaki, Y., Oliver, K., Overton-Larty, E., Pachter, L., Parra, G., Pepin, K.H., Peterson, J., Pevzner, P., Plumb, R., Pohl, C.S., Poliakov, A., Ponce, T.C., Ponting, C.P., Potter, S., Quail, M., Reymond, A., Roe, B.A., Roskin, K.M., Rubin, E.M., Rust, A.G., Santos, R., Sapojnikov, V., Schultz, B., Schultz, J., Schwartz, M.S., Schwartz, S., Scott, C., Seaman, S., Searle, S., Sharpe, T., Sheridan, A., Shownkeen, R., Sims, S., Singer, J.B., Slater, G., Smit, A., Smith, D.R.,

Spencer, B., Stabenau, A., Stange-Thomann, N., Sugnet, C., Suyama, M., Tesler, G., Thompson, J., Torrents, D., Trevaskis, E., Tromp, J., Ucla, C., Ureta-Vidal, A., Vinson, J.P., Von Niederhausern, A.C., Wade, C.M., Wall, M., Weber, R.J., Weiss, R.B., Wendl, M.C., West, A.P., Wetterstrand, K., Wheeler, R., Whelan, S., Wierzbowski, J., Willey, D., Williams, S., Wilson, R.K., Winter, E., Worley, K.C., Wyman, D., Yang, S., Yang, S.P., Zdobnov, E.M., Zody, M.C. & Lander, E.S. 2002, "Initial sequencing and comparative analysis of the mouse genome", *Nature*, vol. 420, no. 6915, pp. 520-562.

Muller, H.J. 1927, "Artificial Transmutation of the Gene", *Science (New York, N.Y.)*, vol. 66, no. 1699, pp. 84-87.

Nagy, A., Moens, C., Ivanyi, E., Pawling, J., Gertsenstein, M., Hadjantonakis, A., Pirity, M. & Rossant, J. 1998, "Dissecting the role of N-myc in development using a single targeting vector to generate a series of alleles", *Current Biology*, vol. 8, no. 11, pp. 661-666.

Nakashima, Y., Plump, A.S., Raines, E.W., Breslow, J.L. & Ross, R. 1994, "ApoE-deficient mice develop lesions of all phases of atherosclerosis throughout the arterial tree", *Arteriosclerosis and Thrombosis : A Journal of Vascular Biology / American Heart Association*, vol. 14, no. 1, pp. 133.

Nelson, W.D., Zenovich, A.G., Ott, H.C., Stolen, C., Caron, G.J., Panoskaltis-Mortari, A., Barnes, S.A., 3rd, Xin, X. & Taylor, D.A. 2007, "Sex-dependent attenuation of plaque growth after treatment with bone marrow mononuclear cells", *Circulation research*, vol. 101, no. 12, pp. 1319-1327.

New, P., S., Goettsch, F., C., Aikawa, M., M., Marchini, M., J., Shibasaki, M., M., Yabusaki, M., K., Libby, M., P., Shanahan, M., C., Croce, M., K. & Aikawa, M., E. 2013, "Macrophage-Derived Matrix Vesicles: An Alternative Novel Mechanism for Microcalcification in Atherosclerotic Plaques", *Circulation research*, vol. 113, no. 1, pp. 72-77.

Nicholson, A.C., Han, J., Febbraio, M., Silverstein, R.L. & Hajjar, D.P. 2001, "Role of CD36, the Macrophage Class B Scavenger Receptor, in Atherosclerosis", *Annals of the New York Academy of Sciences*, vol. 947, no. 1, pp. 224-228.

Nielsen, H., Engelbrecht, J., Brunak, S. & von Heijne, G. 1997, "Identification of prokaryotic and eukaryotic signal peptides and prediction of their cleavage sites", *Protein engineering*, vol. 10, no. 1, pp. 1-6.

Nikpay, M., Goel, A., Won, H., Hall, L.M., Willenborg, C., Kanoni, S., Saleheen, D., Kyriakou, T., Nelson, C.P., Hopewell, J.C., Webb, T.R., Zeng, L., Dehghan, A., Alver, M., Armasu, S.M., Auro, K., Bjornes, A., Chasman, D.I., Chen, S., Ford, I., Franceschini, N., Gieger, C., Grace, C., Gustafsson, S., Huang, J., Hwang, S., Kim, Y.K., Kleber, M.E., Lau, K.W., Lu, X., Lu, Y., Lytikäinen, L., Mihailov, E., Morrison, A.C., Pervjakova, N., Qu, L., Rose, L.M., Salfati, E., Saxena, R., Scholz, M., Smith, A.V.,

Tikkanen, E., Uitterlinden, A., Yang, X., Zhang, W., Zhao, W., de Andrade, M., de Vries, P., S., van Zuydam, N., R., Anand, S.S., Bertram, L., Beutner, F., Dedoussis, G., Frossard, P., Gauguier, D., Goodall, A.H., Gottesman, O., Haber, M., Han, B., Huang, J., Jalilzadeh, S., Kessler, T., König, I., R., Lannfelt, L., Lieb, W., Lind, L., Lindgren, C.M., Lokki, M., Magnusson, P.K., Mallick, N.H., Mehra, N., Meitinger, T., Memon, F., Morris, A.P., Nieminen, M.S., Pedersen, N.L., Peters, A., Rallidis, L.S., Rasheed, A., Samuel, M., Shah, S.H., Sinisalo, J., Stirrups, K.E., Trompet, S., Wang, L., Zaman, K.S., Ardissino, D., Boerwinkle, E., Borecki, I.B., Bottinger, E.P., Buring, J.E., Chambers, J.C., Collins, R., Cupples, L.A., Danesh, J., Demuth, I., Elosua, R., Epstein, S.E., Esko, T., Feitosa, M.F., Franco, O.H., Franzosi, M.G., Granger, C.B., Gu, D., Gudnason, V., Hall, A.S., Hamsten, A., Harris, T.B., Hazen, S.L., Hengstenberg, C., Hofman, A., Ingelsson, E., Iribarren, C., Jukema, J.W., Karhunen, P.J., Kim, B., Kooner, J.S., Kullo, I.J., Lehtimäki, T., Loos, R.J.F., Melander, O., Metspalu, A., März, W., Palmer, C.N., Perola, M., Quertermous, T., Rader, D.J., Ridker, P.M., Ripatti, S., Roberts, R., Salomaa, V., Sanghera, D.K., Schwartz, S.M., Seedorf, U., Stewart, A.F., Stott, D.J., Thiery, J., Zalloua, P.A., O'Donnell, C., J., Reilly, M.P., Assimes, T.L., Thompson, J.R., Erdmann, J., Clarke, R., Watkins, H., Kathiresan, S., McPherson, R., Deloukas, P., Schunkert, H., Samani, N.J., Farrall, M. & =CARDIoGRAMplusC4D Consortium 2015, "A comprehensive 1,000 Genomes-based genome-wide association meta-analysis of coronary artery disease", *Nature genetics*, vol. 47, no. 10, pp. 1121-1130.

Nolan-Stevaux, O., Lau, J., Truitt, M.L., Chu, G.C., Hebrok, M., Fernandez-Zapico, M.E. & Hanahan, D. 2009, "GLI1 is regulated through Smoothed-independent mechanisms in neoplastic pancreatic ducts and mediates PDAC cell survival and transformation", *Genes & development*, vol. 23, no. 1, pp. 24-36.

Padmanabhan, S., Hastie, C., Prabhakaran, D. & Dominczak, A.F. 2010, "Genomic approaches to coronary artery disease", *The Indian journal of medical research*, vol. 132, pp. 567.

Paigen, B. 1995, "Genetics of responsiveness to high-fat and high-cholesterol diets in the mouse", *The American Journal of Clinical Nutrition*, vol. 62, no. 2, pp. 458S-462S.

Paigen, B., Holmes, P.A., Mitchell, D. & Albee, D. 1987a, "Comparison of atherosclerotic lesions and HDL-lipid levels in male, female, and testosterone-treated female mice from strains C57BL/6, BALB/c, and C3H", *Atherosclerosis*, vol. 64, no. 2-3, pp. 215-221.

Paigen, B., Morrow, A., Holmes, P.A., Mitchell, D. & Williams, R.A. 1987b, "Quantitative assessment of atherosclerotic lesions in mice", *Atherosclerosis*, vol. 68, no. 3, pp. 231-240.

Paigen, B.F., Morrow, A.F., Brandon, C.F., Mitchell, D.F. & Holmes, P. 1985, *Variation in susceptibility to atherosclerosis among inbred strains of mice*.

Pajukanta, P., Cargill, M., Viitanen, L., Nuotio, I., Kareinen, A., Perola, M., Terwilliger, J.D., Kempas, E., Daly, M., Lilja, H., Rioux, J.D., Brettin, T., Viikari, J.S.A., Rönnemaa, T., Laakso, M., Lander, E.S. & Peltonen, L. 2000, "Two Loci on Chromosomes 2 and X for Premature Coronary Heart Disease Identified in Early- and Late- Settlement Populations of Finland", *The American Journal of Human Genetics*, vol. 67, no. 6, pp. 1481-1493.

Parchure, A., Vyas, N., Ferguson, C., Parton, R.G. & Mayor, S. 2016, *Oligomerization and Endocytosis of Hedgehog is Necessary for its Efficient Exovesicular Secretion*.

Paré, G., Serre, D., Brisson, D., Anand, S.S., Montpetit, A., Tremblay, G., Engert, J.C., Hudson, T.J. & Gaudet, D. 2007, "Genetic Analysis of 103 Candidate Genes for Coronary Artery Disease and Associated Phenotypes in a Founder Population Reveals a New Association between Endothelin- 1 and High- Density Lipoprotein Cholesterol", *The American Journal of Human Genetics*, vol. 80, no. 4, pp. 673-682.

Park, H.L., Bai, C., Platt, K.A., Matise, M.P., Beeghly, A., Hui, C.C., Nakashima, M. & Joyner, A.L. 2000, "Mouse Gli1 mutants are viable but have defects in SHH signaling in combination with a Gli2 mutation", *Development (Cambridge, England)*, vol. 127, no. 8, pp. 1593.

Pasterkamp, W., G., Van, D.L., Haitjema, B., S., Foroughi Asl, J., Hassan, Siemelink, P.V., M., Bezemer, S., T., Van Setten, E., Jessica, Dichgans, C.A., M., Malik, L.M., R., Worrall, M., B., Schunkert, W., H., Samani, W., N., De Kleijn, W., Dominique, Markus, W., H., Hofer, W., I., Michoel, W., T., De Jager, W., Saskia, Björkegren, W., Johan, Den Ruijter, W., Hester & Asselbergs, W., F. 2016, "Human Validation of Genes Associated With a Murine Atherosclerotic Phenotype", *Arteriosclerosis, Thrombosis, and Vascular Biology*, vol. 36, no. 6, pp. 1240-1246.

Patel, M., K., Strong, R., A., Tohyama, J., J., Jin, J., X., Morales, J., C., Billheimer, J., J., Millar, J., J., Kruth, J., H. & Rader, J., D. 2015, "Macrophage Sortilin Promotes LDL Uptake, Foam Cell Formation, and Atherosclerosis", *Circulation research*, vol. 116, no. 5, pp. 789-796.

Peiser, L., Mukhopadhyay, S. & Gordon, S. 2002, "Scavenger receptors in innate immunity", *Current opinion in immunology*, vol. 14, no. 1, pp. 123-128.

Pepinsky, R.B., Zeng, C., Wen, D., Rayhorn, P., Baker, D.P., Williams, K.P., Bixler, S.A., Ambrose, C.M., Garber, E.A., Miatkowski, K., Taylor, F.R., Wang, E.A. & Galdes, A. 1998, "Identification of a palmitic acid- modified form of human Sonic hedgehog", *The Journal of biological chemistry*, vol. 273, no. 22, pp. 14037.

Peter J King, Leonardo Guasti & Ed Laufer 2008, "Hedgehog signalling in endocrine development and disease", *Journal of Endocrinology*, vol. 198, no. 3, pp. 439-450.

Petersen, T.N., Brunak, S., von Heijne, G. & Nielsen, H. 2011, "SignalP 4.0: discriminating signal peptides from transmembrane regions", *Nature methods*, vol. 8, no. 10, pp. 785-786.

Pettitt, S.J., Liang, Q., Rairdan, X.Y., Moran, J.L., Prosser, H.M., Beier, D.R., Lloyd, K.C., Bradley, A. & Skarnes, W.C. 2009, "Agouti C57BL/6N embryonic stem cells for mouse genetic resources", *Nature methods*, vol. 6, no. 7, pp. 493-495.

Plump, A.S., Smith, J.D., Hayek, T., Aalto-Setälä, K., Walsh, A., Verstuyft, J.G., Rubin, E.M. & Breslow, J.L. 1992, "Severe hypercholesterolemia and atherosclerosis in apolipoprotein E-deficient mice created by homologous recombination in ES cells", *Cell*, vol. 71, no. 2, pp. 343-353.

Pola, R., Asahara, T., Isner, J.M., Ling, L.E., Silver, M., Corbley, M.J., Kearney, M., Blake Pepinsky, R., Shapiro, R., Taylor, F.R. & Baker, D.P. 2001, "The morphogen Sonic hedgehog is an indirect angiogenic agent upregulating two families of angiogenic growth factors", *Nature medicine*, vol. 7, no. 6, pp. 706-711.

Pola, R., Losordo, D.W., Ling, L.E., Aprahamian, T.R., Barban, E., Bosch-Marce, M., Curry, C., Corbley, M., Kearney, M. & Isner, J.M. 2003, "Postnatal recapitulation of embryonic hedgehog pathway in response to skeletal muscle ischemia", *Circulation*, vol. 108, no. 4, pp. 479-485.

Ponnuswamy, P., Schrottle, A., Ostermeier, E., Gruner, S., Huang, P.L., Ertl, G., Hoffmann, U., Nieswandt, B. & Kuhlencordt, P.J. 2012, "eNOS protects from atherosclerosis despite relevant superoxide production by the enzyme in apoE mice", *PloS one*, vol. 7, no. 1, pp. e30193.

Porter, J.A., Young, K.E. & Beachy, P.A. 1996a, "Cholesterol modification of hedgehog signaling proteins in animal development", *Science (New York, N.Y.)*, vol. 274, no. 5285, pp. 255.

Porter, J.A., Young, K.E. & Beachy, P.A. 1996b, "Cholesterol modification of Hedgehog signalling proteins in animal development", *Science*, vol. 274, no. 5285, pp. 255.

Puimedon, M.S., Mergia, E., Al-Hasani, J., Aherrahrou, R., Freyer, J., Wit, C.d., Kosling, D., Schunkert, H., Erdmann, J. & Aherrahrou, Z. 2015, "Reduction of atherosclerosis in *gucy1a3* deficient mice.(Report)", vol. 132, no. 19.

Qi, F., Lin, S. & Fan, Q.C. 2004, "Development of retrovirus-mediated insertional mutagenesis in zebrafish and its application in saturation mutagenesis and gene screening", *Yi chuan xue bao = Acta genetica Sinica*, vol. 31, no. 7, pp. 750-757.

Queiroz, K.C.S., Bijlsma, M.F., Tio, R.A., Zeebregts, C.J., Dunaeva, M., Ferreira, C.V., Fuhler, G.M., Kuipers, E.J., Alves, M.M., Rezaee, F., Spek,

C.A. & Peppelenbosch, M.P. 2012, "Dichotomy in Hedgehog signaling between human healthy vessel and atherosclerotic plaques", *Molecular medicine (Cambridge, Mass.)*, vol. 18, pp. 1122.

Quinn, M.T., Parthasarathy, S., Fong, L.G. & Steinberg, D. 1987, "Oxidatively modified low density lipoproteins: a potential role in recruitment and retention of monocyte/macrophages during atherogenesis", *Proceedings of the National Academy of Sciences of the United States of America*, vol. 84, no. 9, pp. 2995.

Ramsbottom, S. & Pownall, M. 2016, "Regulation of Hedgehog Signalling Inside and Outside the Cell", *Journal of Developmental Biology*, vol. 4, no. 3, pp. 23.

Rapoport, T.A. 1992, "Transport of proteins across the endoplasmic reticulum membrane", *Science (New York, N.Y.)*, vol. 258, no. 5084, pp. 931-936.

Redmond, E.M., Guha, S., Walls, D. & Cahill, P.A. 2011, *Investigational Notch and Hedgehog inhibitors--therapies for cardiovascular disease*, England.

Redmond, E.M., Hamm, K., Cullen, J.P., Hatch, E., Cahill, P.A. & Morrow, D. 2013, "Inhibition of patched-1 prevents injury-induced neointimal hyperplasia", *Arteriosclerosis, Thrombosis, and Vascular Biology*, vol. 33, no. 8, pp. 1960-1964.

Renault, M.A., Chapouly, C., Yao, Q., Larrieu-Lahargue, F., Vandierdonck, S., Reynaud, A., Petit, M., Jaspard-Vinassa, B., Belloc, I., Traiffort, E., Ruat, M., Duplaa, C., Couffinhal, T., Desgranges, C. & Gadeau, A.P. 2013, "Desert hedgehog promotes ischemia-induced angiogenesis by ensuring peripheral nerve survival", *Circulation research*, vol. 112, no. 5, pp. 762-770.

Renault, M., Millay, M., Kamide, C., Scarpelli, A., Klyachko, E., Losordo, D.W., Roncalli, J., Tongers, J., Misener, S., Thorne, T., Jujo, K., Ito, A., Clarke, T. & Fung, C. 2009, "The Hedgehog transcription factor Gli3 modulates angiogenesis", *Circulation research*, vol. 105, no. 8, pp. 818-826.

Richardson, P.D., Davies, M.J. & Born, G.V. 1989, "Influence of plaque configuration and stress distribution on fissuring of coronary atherosclerotic plaques", *Lancet (London, England)*, vol. 2, no. 8669, pp. 941-944.

Riddle, R.D., Johnson, R.L., Laufer, E. & Tabin, C. 1993, "Sonic hedgehog mediates the polarizing activity of the ZPA", *Cell*, vol. 75, no. 7, pp. 1401-1416.

Ripatti, S., Sinisalo, J., Lokki, M., Nieminen, M.S., Melander, O., Salomaa, V., Peltonen, L., Kathiresan, S., Tikkanen, E., Orho-Melander, M.,

Havulinna, A.S., Silander, K., Sharma, A., Guiducci, C., Perola, M., Jula, A., Department of Clinical Sciences, M., Lund University, Sektionen för Barn/Urologi/Kvinnosjukvård/Endokrinologi, Emergency medicine/Medicine/Surgery, Internal Medicine, Lunds universitet, Institutionen för kliniska vetenskaper, M., Diabetes och endokrinologi, Hypertoni och hjärt-kärl sjukdom, Pediatrics/Urology/Gynecology/Endocrinology, Endocrinology, Hypertension and Cardiovascular Disease, Diabetes and Endocrinology, Faculty of Medicine, Medicin, Sektionen för Akut/Medicin/Kirurgi & Endokrinologi 2010, "A multilocus genetic risk score for coronary heart disease: case-control and prospective cohort analyses", *Lancet*, vol. 376, no. 9750, pp. 1393-1400.

Roelink, H., Porter, J.A., Chiang, C., Tanabe, Y., Chang, D.T., Beachy, P.A. & Jessell, T.M. 1995, "Floor plate and motor neuron induction by different concentrations of the amino-terminal cleavage product of sonic hedgehog autoproteolysis", *Cell*, vol. 81, no. 3, pp. 445-455.

Roselaar, S.E., Kakkanathu, P.X. & Daugherty, A. 1996, "Lymphocyte populations in atherosclerotic lesions of apoE ^{-/-} and LDL receptor ^{-/-} mice. Decreasing density with disease progression", *Arteriosclerosis, Thrombosis, and Vascular Biology*, vol. 16, no. 8, pp. 1013-1018.

Rosen, B., Schick, J. & Wurst, W. 2015, "Beyond knockouts: the International Knockout Mouse Consortium delivers modular and evolving tools for investigating mammalian genes", *Mammalian Genome*, vol. 26, no. 9, pp. 456-466.

Rosenfeld, M.E., Polinsky, P., Virmani, R., Kauser, K., Rubanyi, G. & Schwartz, S.M. 2000, "Advanced atherosclerotic lesions in the innominate artery of the ApoE knockout mouse", *Arteriosclerosis, Thrombosis, and Vascular Biology*, vol. 20, no. 12, pp. 2587-2592.

Ross, R. 1999, "Atherosclerosis--an inflammatory disease", *The New England journal of medicine*, vol. 340, no. 2, pp. 115.

Ross, R. 1993, "The pathogenesis of atherosclerosis: a perspective for the 1990s", *Nature*, vol. 362, no. 6423, pp. 801-809.

Roth, E.M. 2016, "Alirocumab for hyperlipidemia: ODYSSEY Phase III clinical trial results and US FDA approval indications", *Future cardiology*, vol. 12, no. 2, pp. 115-128.

Ruiz, I.A. 1999, "Gli proteins encode context-dependent positive and negative functions: implications for development and disease", *Development (Cambridge, England)*, vol. 126, no. 14, pp. 3205.

Russell, W.L., Hunsicker, P.R., Raymer, G.D., Steele, M.H., Stelzner, K.F. & Thompson, H.M. 1982, "Dose-- response curve for ethylnitrosourea-induced specific- locus mutations in mouse spermatogonia", *Proceedings of*

the National Academy of Sciences of the United States of America, vol. 79, no. 11, pp. 3589.

Russell, W.L., Kelly, E.M., Hunsicker, P.R., Bangham, J.W., Maddux, S.C. & Phipps, E.L. 1979, "Specific- locus test shows ethylnitrosourea to be the most potent mutagen in the mouse", *Proceedings of the National Academy of Sciences of the United States of America*, vol. 76, no. 11, pp. 5818.

Sachidanandam, R., Weissman, D., Schmidt, S.C., Kakol, J.M., Stein, L.D., Marth, G., Sherry, S., Mullikin, J.C., Mortimore, B.J., Willey, D.L., Hunt, S.E., Cole, C.G., Coggill, P.C., Rice, C.M., Ning, Z., Rogers, J., Bentley, D.R., Kwok, P.Y., Mardis, E.R., Yeh, R.T., Schultz, B., Cook, L., Davenport, R., Dante, M., Fulton, L., Hillier, L., Waterston, R.H., McPherson, J.D., Gilman, B., Schaffner, S., Van Etten, W.J., Reich, D., Higgins, J., Daly, M.J., Blumenstiel, B., Baldwin, J., Stange-Thomann, N., Zody, M.C., Linton, L., Lander, E.S., Altshuler, D. & International SNP Map Working Group 2001, "A map of human genome sequence variation containing 1.42 million single nucleotide polymorphisms", *Nature*, vol. 409, no. 6822, pp. 928-933.

Samani, N.J., Burton, P., Mangino, M., Ball, S.G., Balmforth, A.J., Barrett, J., Bishop, T., Hall, A. & BHF Family Heart Study, Research Group 2005, "A genomewide linkage study of 1,933 families affected by premature coronary artery disease: The British Heart Foundation (BHF) Family Heart Study", *PubMed*, .

Samani, N.J., Wichmann, H., Barrett, J.H., König, I.R., Stevens, S.E., Szymczak, S., Tregouet, D., Iles, M.M., Pahlke, F., Pollard, H., Lieb, W., Erdmann, J., Cambien, F., Fischer, M., Ouwehand, W., Blankenberg, S., Balmforth, A.J., Baessler, A., Ball, S.G., Strom, T.M., Braenne, I., Gieger, C., Hall, A.S., Deloukas, P., Tobin, M.D., Ziegler, A., Thompson, J.R., Schunkert, H., Hengstenberg, C., Mangino, M., Mayer, B., Dixon, R.J., Meitinger, T., Braund, P. & WTCCC and the Cardiogenics Consortium 2007, "Genomewide association analysis of coronary artery disease", *The New England journal of medicine*, vol. 357, no. 5, pp. 443.

Sayols-Baixeras, S., Lluís-Ganella, C., Lucas, G. & Elosua, R. 2014, "Pathogenesis of coronary artery disease: focus on genetic risk factors and identification of genetic variants", *The application of clinical genetics*, vol. 7, pp. 15.

Schildkraut, J.M., Myers, R.H., Cupples, L.A., Kiely, D.K. & Kannel, W.B. 1989, "Coronary risk associated with age and sex of parental heart disease in the Framingham Study", *The American Journal of Cardiology*, vol. 64, no. 10, pp. 555-559.

Schunkert, H., Gieger, C., Olivieri, O., Absher, D., Aherrahrou, Z., Allayee, H., Altshuler, D., Anand, S.S., Andersen, K., Anderson, J.L., Ardissino, D., Ball, S.G., König, I.R., Balmforth, A.J., Barnes, T.A., Becker, D.M., Becker, L.C., Berger, K., Bis, J.C., Boekholdt, S.M., Boerwinkle, E., Braund, P.S., Brown, M.J., Kathiresan, S., Burnett, M.S., Buyschaert, I., Carlquist, J.F.,

Chen, L., Cichon, S., Codd, V., Davies, R.W., Dedoussis, G., Dehghan, A., Demissie, S., Reilly, M.P., Devaney, J.M., Diemert, P., Do, R., Doering, A., Eifert, S., Mokhtari, N.E.E., Ellis, S.G., Elosua, R., Engert, J.C., Epstein, S.E., Assimes, T.L., de Faire, U., Fischer, M., Folsom, A.R., Freyer, J., Gigante, B., Girelli, D., Gretarsdottir, S., Gudnason, V., Gulcher, J.R., Halperin, E., Holm, H., Hammond, N., Hazen, S.L., Hofman, A., Horne, B.D., Illig, T., Iribarren, C., Jones, G.T., Jukema, J.W., Kaiser, M.A., Kaplan, L.M., Preuss, M., Kastelein, J.J.P., Khaw, K., Knowles, J.W., Kolovou, G., Kong, A., Laaksonen, R., Lambrechts, D., Leander, K., Lettre, G., Li, M., Stewart, A.F.R., Lieb, W., Loley, C., Lotery, A.J., Mannucci, P.M., Maouche, S., Martinelli, N., McKeown, P.P., Meisinger, C., Meitinger, T., Melander, O., Barbalic, M., Merlini, P.A., Mooser, V., Morgan, T., Mühleisen, T.W., Muhlestein, J.B., Münzel, T., Musunuru, K., Nahrstaedt, J., Nelson, C.P., Nöthen, M.M., Department of Clinical Sciences, M., CARDIoGRAM Consortium, Lund University, Emergency medicine/Medicine/Surgery, Internal Medicine, Lunds universitet, Institutionen för kliniska vetenskaper, M., Cardiogenics, Hypertoni och hjärtkärl sjukdom, Hypertension and Cardiovascular Disease, Faculty of Medicine, Medicin & Sektionen för Akut/Medicin/Kirurgi 2011, *Large-scale association analysis identifies 13 new susceptibility loci for coronary artery disease*, Nature Publishing Group, United States.

Shi, W., Wang, N.J., Shih, D.M., Sun, V.Z., Wang, X. & Lusis, A.J. 2000, "Determinants of atherosclerosis susceptibility in the C3H and C57BL/6 mouse model: evidence for involvement of endothelial cells but not blood cells or cholesterol metabolism", *Circulation research*, vol. 86, no. 10, pp. 1078-1084.

Skarnes, W.C., Moss, J.E., Hurtley, S.M. & Beddington, R.S. 1995, "Capturing genes encoding membrane and secreted proteins important for mouse development", *Proceedings of the National Academy of Sciences of the United States of America*, vol. 92, no. 14, pp. 6592.

Skarnes, W.C., Cox, T., Jackson, D., Severin, J., Biggs, P., Fu, J., Nefedov, M., de Jong, P.J., Stewart, A.F., Bradley, A., Rosen, B., West, A.P., Koutsourakis, M., Bushell, W., Iyer, V., Mujica, A.O., Thomas, M. & Harrow, J. 2011, "A conditional knockout resource for the genome-wide study of mouse gene function", *Nature*, vol. 474, no. 7351, pp. 337-342.

Skarnes, W.C., Tessier-Lavigne, M., Conklin, B.R., Stanford, W.L., Rossant, J., von Melchner, H., Wurst, W., Hicks, G., Nord, A.S., Cox, T., Young, S.G., Ruiz, P., Soriano, P. & International Gene Trap Consortium 2004, "A public gene trap resource for mouse functional genomics", *Nature genetics*, vol. 36, no. 6, pp. 543-544.

Small, D.M. 1988, "George Lyman Duff memorial lecture. Progression and regression of atherosclerotic lesions. Insights from lipid physical biochemistry", *Arteriosclerosis, Thrombosis, and Vascular Biology*, vol. 8, no. 2, pp. 103-129.

Smith, C.J., Nedwell, D.B., Dong, L.F. & Osborn, A.M. 2006, "Evaluation of quantitative polymerase chain reaction-based approaches for determining gene copy and gene transcript numbers in environmental samples", *Environmental microbiology*, vol. 8, no. 5, pp. 804-815.

Smith, D.D., Tan, X., Tawfik, O., Milne, G., Stechschulte, D.J. & Dileepan, K.N. 2010, "Increased aortic atherosclerotic plaque development in female apolipoprotein E-null mice is associated with elevated thromboxane A2 and decreased prostacyclin production", *Journal of physiology and pharmacology : an official journal of the Polish Physiological Society*, vol. 61, no. 3, pp. 309-316.

Smith, J.D., Trogan, E., Ginsberg, M., Grigaux, C., Tian, J. & Miyata, M. 1995, "Decreased atherosclerosis in mice deficient in both macrophage colony-stimulating factor (CSF-1) and apolipoprotein E", *Proceedings of the National Academy of Sciences of the United States of America*, vol. 92, no. 18, pp. 8264.

Smithies, O., Gregg, R.G., Boggs, S.S., Koralewski, M.A. & Kucherlapati, R.S. 1985, "Insertion of DNA sequences into the human chromosomal β -globin locus by homologous recombination", *Nature*, vol. 317, no. 6034, pp. 230.

Song, Y., Stampfer, M.J. & Liu, S. 2004, "Meta-analysis: Apolipoprotein E genotypes and risk for coronary heart disease.(Author Abstract)", *Annals of Internal Medicine*, vol. 141, no. 2, pp. 137.

Sonnhammer, E.L., von Heijne, G. & Krogh, A. 1998, "A hidden Markov model for predicting transmembrane helices in protein sequences", *Proceedings / ...International Conference on Intelligent Systems for Molecular Biology ; ISMB. International Conference on Intelligent Systems for Molecular Biology*, vol. 6, pp. 175-182.

Soutar, A.K. & Naoumova, R.P. 2007, "Mechanisms of disease: genetic causes of familial hypercholesterolemia", *Nature clinical practice. Cardiovascular medicine*, vol. 4, no. 4, pp. 214-225.

Strydom, H.C. 2000, "Natural history and histological classification of atherosclerotic lesions: an update", *Arteriosclerosis, Thrombosis, and Vascular Biology*, vol. 20, no. 5, pp. 1177-1178.

Strydom, H.C., Chandler, A.B., Glagov, S., Guyton, J.R., Insull, W., Jr, Rosenfeld, M.E., Schaffer, S.A., Schwartz, C.J., Wagner, W.D. & Wissler, R.W. 1994, "A definition of initial, fatty streak, and intermediate lesions of atherosclerosis. A report from the Committee on Vascular Lesions of the Council on Arteriosclerosis, American Heart Association", *Circulation*, vol. 89, no. 5, pp. 2462-2478.

Strydom, H.C., Wissler, R.W., Chandler, A.B., Dinsmore, R.E., Fuster, V., Glagov, S., Insull, J., Rosenfeld, M.E., Schwartz, C.J. & Wagner, W.D.

1995, "A Definition of Advanced Types of Atherosclerotic Lesions and a Histological Classification of Atherosclerosis: A Report From the Committee on Vascular Lesions of the Council on Arteriosclerosis, American Heart Association", *Arteriosclerosis Thrombosis and Vascular Biology*, vol. 15, no. 9, pp. 1512-1531.

Steven A. Vokes, Tatiana A. Yatskievych, Ronald L. Heimark, Jill McMahon, Andrew P. McMahon, Parker B. Antin & Paul A. Krieg 2004, "Hedgehog signaling is essential for endothelial tube formation during vasculogenesis", *Development*, vol. 131, no. 17, pp. 4371-4380.

Strachan T, Read A. Human molecular genetics. 3. London: Garland; 2003.

Stroes, E., Colquhoun, D., Sullivan, D., Civeira, F., Rosenson, R.S., Watts, G.F., Bruckert, E., Cho, L., Dent, R., Knusel, B., Xue, A., Scott, R., Wasserman, S.M., Rocco, M. & GAUSS-2 Investigators 2014, "Anti-PCSK9 antibody effectively lowers cholesterol in patients with statin intolerance: the GAUSS-2 randomized, placebo-controlled phase 3 clinical trial of evolocumab", *Journal of the American College of Cardiology*, vol. 63, no. 23, pp. 2541-2548.

Stylianou, I.M., Bauer, R.C., Reilly, M.P. & Rader, D.J. 2012, "Genetic Basis of Atherosclerosis: Insights From Mice and Humans", *Circulation research*, vol. 110, no. 2, pp. 337-355.

Surace, E.M., Balaggan, K.S., Tessitore, A., Mussolino, C., Cotugno, G., Bonetti, C., Vitale, A., Ali, R.R. & Auricchio, A. 2006, "Inhibition of ocular neovascularization by hedgehog blockade", *Molecular therapy : the journal of the American Society of Gene Therapy*, vol. 13, no. 3, pp. 573-579.

Surra, J.C., Guillen, N., Arbones-Mainar, J.M., Barranquero, C., Navarro, M.A., Arnal, C., Orman, I., Segovia, J.C. & Osada, J. 2010, "Sex as a profound modifier of atherosclerotic lesion development in apolipoprotein E-deficient mice with different genetic backgrounds", *Journal of Atherosclerosis and Thrombosis*, vol. 17, no. 7, pp. 712-721.

Takata, M., Sasaki, M.S., Sonoda, E., Morrison, C., Hashimoto, M., Utsumi, H., Yamaguchi-Iwai, Y., Shinohara, A. & Takeda, S. 1998, "Homologous recombination and non-homologous end-joining pathways of DNA double-strand break repair have overlapping roles in the maintenance of chromosomal integrity in vertebrate cells", *The EMBO journal*, vol. 17, no. 18, pp. 5497-5508.

Tangirala, R.K., Rubin, E.M. & Palinski, W. 1995, "Quantitation of atherosclerosis in murine models: correlation between lesions in the aortic origin and in the entire aorta, and differences in the extent of lesions between sexes in LDL receptor-deficient and apolipoprotein E-deficient mice", *Journal of lipid research*, vol. 36, no. 11, pp. 2320.

- Testa, G., Schaft, J., van der Hoeven, F., Glaser, S., Anastassiadis, K., Zhang, Y., Hermann, T., Stremmel, W. & Stewart, A.F. 2004, "A reliable lacZ expression reporter cassette for multipurpose, knockout-first alleles", *Genesis (New York, N.Y.: 2000)*, vol. 38, no. 3, pp. 151-158.
- Thomas, J.W., Lamantia, C. & Magnuson, T. 1998, "X-ray-induced mutations in mouse embryonic stem cells", *Proceedings of the National Academy of Sciences of the United States of America*, vol. 95, no. 3, pp. 1114.
- Thomas, K.R. & Capecchi, M.R. 1987, "Site-directed mutagenesis by gene targeting in mouse embryo-derived stem cells", *Cell*, vol. 51, no. 3, pp. 503-512.
- Traub, O. & Berk, B.C. 1998, "Laminar shear stress: mechanisms by which endothelial cells transduce an atheroprotective force", *Arteriosclerosis, Thrombosis, and Vascular Biology*, vol. 18, no. 5, pp. 677.
- Tuck, E., Estabel, J., Oellrich, A., Maguire, A.K., Adissu, H.A., Souter, L., Siragher, E., Lillistone, C., Green, A.L., Wardle-Jones, H., Carragher, D.M., Karp, N.A., Smedley, D., Adams, N.C., Bussell, J.N., Adams, D.J., Ramírez-Solis, R., Steel, K.P., Galli, A. & White, J.K. 2015, "A gene expression resource generated by genome-wide lacZ profiling in the mouse", *Disease models & mechanisms*, vol. 8, no. 11, pp. 1467.
- Tukachinsky, H., Kuzmickas, R., Jao, C., Liu, J. & Salic, A. 2012, "Dispatched and Scube Mediate the Efficient Secretion of the Cholesterol-Modified Hedgehog Ligand", *Cell Reports*, vol. 2, no. 2, pp. 308-320.
- Twisk, J., Gillian-Daniel, D.L., Tebon, A., Wang, L., Barrett, P.H.R. & Attie, A.D. 2000, "The role of the LDL receptor in apolipoprotein B secretion", *Journal of Clinical Investigation*, vol. 105, no. 4, pp. 521-532.
- Valenzuela, D.M., Murphy, A.J., Friendewey, D., Gale, N.W., Economides, A.N., Auerbach, W., Poueymirou, W.T., Adams, N.C., Rojas, J., Yasenchak, J., Chernomorsky, R., Boucher, M., Elsasser, A.L., Esau, L., Zheng, J., Griffiths, J.A., Wang, X., Su, H., Xue, Y., Dominguez, M.G., Noguera, I., Torres, R., Macdonald, L.E., Stewart, A.F., DeChiara, T.M. & Yancopoulos, G.D. 2003, "High-throughput engineering of the mouse genome coupled with high-resolution expression analysis", *Nature biotechnology*, vol. 21, no. 6, pp. 652-659.
- Vanderlaan, P.A., Reardon, C.A. & Getz, G.S. 2004, "Site specificity of atherosclerosis: site-selective responses to atherosclerotic modulators", *Arteriosclerosis, Thrombosis, and Vascular Biology*, vol. 24, no. 1, pp. 12.
- Vecerova, L., Strasky, Z., Rathouska, J., Slanarova, M., Brcakova, E., Micuda, S. & Nachtigal, P. 2012, "Activation of TGF-beta receptors and Smad proteins by atorvastatin is related to reduced atherogenesis in

ApoE/LDLR double knockout mice", *Journal of Atherosclerosis and Thrombosis*, vol. 19, no. 2, pp. 115-126.

Virmani, R., Burke, A.P., Farb, A. & Kolodgie, F.D. 2006, "Pathology of the Vulnerable Plaque", *Journal of the American College of Cardiology*, vol. 47, no. 8, pp. C13-C18.

Visel, A., Zhu, Y., May, D., Afzal, V., Gong, E., Attanasio, C., Blow, M.J., Cohen, J.C., Rubin, E.M. & Pennacchio, L.A. 2010, "Targeted deletion of the 9p21 non-coding coronary artery disease risk interval in mice", *Nature*, vol. 464, no. 7287, pp. 409-412.

Vokes, S.A., Ji, H., McCuine, S., Tenzen, T., Giles, S., Zhong, S., Longabaugh, W.J., Davidson, E.H., Wong, W.H. & McMahon, A.P. 2007, "Genomic characterization of Gli-activator targets in sonic hedgehog-mediated neural patterning", *Development (Cambridge, England)*, vol. 134, no. 10, pp. 1977-1989.

von der Thusen, J.H., van Vlijmen, B.J., Hoeben, R.C., Kockx, M.M., Havekes, L.M., van Berkel, T.J. & Biessen, E.A. 2002, "Induction of atherosclerotic plaque rupture in apolipoprotein E^{-/-} mice after adenovirus-mediated transfer of p53", *Circulation*, vol. 105, no. 17, pp. 2064-2070.

von Heijne, G. 1990, "The signal peptide", *The Journal of membrane biology*, vol. 115, no. 3, pp. 195-201.

Voyaziakis, E., Goldberg, I.J., Plump, A.S., Rubin, E.M., Breslow, J.L. & Huang, L.S. 1998, "ApoA- I deficiency causes both hypertriglyceridemia and increased atherosclerosis in human apoB transgenic mice", *Journal of lipid research*, vol. 39, no. 2, pp. 313.

Wang, G., Zhang, Z., Xu, Z., Yin, H., Bai, L., Ma, Z., Decoster, M.A., Qian, G. & Wu, G. 2010, "Activation of the sonic hedgehog signaling controls human pulmonary arterial smooth muscle cell proliferation in response to hypoxia", *Biochimica et biophysica acta*, vol. 1803, no. 12, pp. 1359-1367.

Wang, L., W., Tang, R., Y., Wang, R., Y., Tascau, R., L., Balcerak, R., J., Tong, R., W., Levine, R., R., Welch, R., C., Tall, R., A. & Wang, R., N. 2016, "LNK/ SH2B3 Loss of Function Promotes Atherosclerosis and Thrombosis", *Circulation research*, .

Wentzel, J.J., Chatzizisis, Y.S., Gijssen, F.J.H., Giannoglou, G.D., Feldman, C.L. & Stone, P.H. 2012, "Endothelial shear stress in the evolution of coronary atherosclerotic plaque and vascular remodelling: current understanding and remaining questions", *Cardiovascular research*, vol. 96, no. 2, pp. 234.

West, D.B., De Jong, P.J., Pasumarthi, R.K., Baridon, B., Djan, E., Trainor, A., Griffey, S.M., Engelhard, E.K., Rapp, J., Li, B. & Lloyd, K.C.K. 2015, "A

lacZ reporter gene expression atlas for 313 adult KOMP mutant mouse lines", *Genome research*, vol. 25, no. 4, pp. 598-607.

Westerterp, M., Berbée, J.,F.P., Pires, N.M.M., van Mierlo, G.,J.D., Kleemann, R., Romijn, J.A., Havekes, L.M. & Rensen, P.C.N. 2007, "Apolipoprotein C- I is crucially involved in lipopolysaccharide- induced atherosclerosis development in apolipoprotein E- knockout mice", *Circulation*, vol. 116, no. 19, pp. 2173.

White, J., Gerdin, A., Karp, N., Ryder, E., Buljan, M., Bussell, J., Salisbury, J., Clare, S., Ingham, N., Podrini, C., Houghton, R., Estabel, J., Bottomley, J., Melvin, D., Sunter, D., Adams, N., Tannahill, D., Logan, D.W., Macarthur, D.G., Flint, J., Mahajan, V.B., Tsang, S.H., Smyth, I., Watt, F.M., Skarnes, W.C., Dougan, G., Adams, D.J., Ramirez-Solis, R., Bradley, A. & Steel, K.P. 2013, "Genome- wide Generation and Systematic Phenotyping of Knockout Mice Reveals New Roles for Many Genes", *Cell*, vol. 154, no. 2, pp. 452-464.

Whitman, S.C. 2004, "A practical approach to using mice in atherosclerosis research", *The Clinical biochemist.Reviews / Australian Association of Clinical Biochemists*, vol. 25, no. 1, pp. 81-93.

Wicking, C., Smyth, I. & Bale, A. 1999, "The hedgehog signalling pathway in tumorigenesis and development", *Oncogene*, vol. 18, no. 55, pp. 7844.

Wilson, K., Fry, G.L., Chappell, D.A., Sigmund, C.D. & Medh, J.D. 2001, "Macrophage- specific expression of human lipoprotein lipase accelerates atherosclerosis in transgenic apolipoprotein e knockout mice but not in C57BL/ 6 mice", *Arteriosclerosis, Thrombosis, and Vascular Biology*, vol. 21, no. 11, pp. 1809.

Wilson, P.W., D'Agostino, R.B., Levy, D., Belanger, A.M., Silbershatz, H. & Kannel, W.B. 1998, "Prediction of coronary heart disease using risk factor categories", *Circulation*, vol. 97, no. 18, pp. 1837-1847.

Witek, R.P., Agboola, K.M., Chen, W., Diehl, A.M., Yang, L., Liu, R., Jung, Y., Omenetti, A., Syn, W., Choi, S.S., Cheong, Y. & Fearing, C.M. 2009, "Liver cell-derived microparticles activate hedgehog signaling and alter gene expression in hepatic endothelial cells", *Gastroenterology*, vol. 136, no. 1, pp. 320-330.e2.

Wu, J.E., Basso, F., Shamburek, R.D., Amar, M.J.A., Vaisman, B., Szakacs, G., Joyce, C., Tansey, T., Freeman, L., Paigen, B.J., Thomas, F., Brewer, H.B. & Santamarina-Fojo, S. 2004, "Hepatic ABCG5 and ABCG8 overexpression increases hepatobiliary sterol transport but does not alter aortic atherosclerosis in transgenic mice", *The Journal of biological chemistry*, vol. 279, no. 22, pp. 22913.

Yamagishi, H., Maeda, J., Hu, T., McAnally, J., Conway, S.J., Kume, T., Meyers, E.N., Yamagishi, C. & Srivastava, D. 2003, "Tbx1 is regulated by

tissue- specific forkhead proteins through a common Sonic hedgehog-responsive enhancer", *Genes & development*, vol. 17, no. 2, pp. 269.

Yao, Q., Renault, M.A., Chapouly, C., Vandierdonck, S., Belloc, I., Jaspard-Vinassa, B., Daniel-Lamaziere, J.M., Laffargue, M., Merched, A., Desgranges, C. & Gadeau, A.P. 2014, "Sonic hedgehog mediates a novel pathway of PDGF-BB-dependent vessel maturation", *Blood*, vol. 123, no. 15, pp. 2429-2437.

Yoon, J.W., Kita, Y., Frank, D.J., Majewski, R.R., Konicek, B.A., Nobrega, M.A., Jacob, H., Walterhouse, D. & Iannaccone, P. 2002, "Gene expression profiling leads to identification of GLI1- binding elements in target genes and a role for multiple downstream pathways in GLI1-induced cell transformation", *The Journal of biological chemistry*, vol. 277, no. 7, pp. 5548.

Yusuf, S., Hawken, S., Ounpuu, S., Dans, T., Avezum, A., Lanas, F., McQueen, M., Budaj, A., Pais, P., Varigos, J., Lisheng, L. & INTERHEART Study Investigators 2004, "Effect of potentially modifiable risk factors associated with myocardial infarction in 52 countries (the INTERHEART study): case-control study", *Lancet (London, England)*, vol. 364, no. 9438, pp. 937-952.

Zadelaar, A.S., von der Thusen, J.H., Boesten, L.S., Hoeben, R.C., Kockx, M.M., Versnel, M.A., van Berkel, T.J., Havekes, L.M., Biessen, E.A. & van Vlijmen, B.J. 2005, "Increased vulnerability of pre-existing atherosclerosis in ApoE-deficient mice following adenovirus-mediated Fas ligand gene transfer", *Atherosclerosis*, vol. 183, no. 2, pp. 244-250.

Zaman, A.G., Helft, G., Worthley, S.G. & Badimon, J.J. 2000, "The role of plaque rupture and thrombosis in coronary artery disease", *Atherosclerosis*, vol. 149, no. 2, pp. 251-266.

Zdravkovic, S., Wienke, A., Pedersen, N.L., Marenberg, M.E., Yashin, A.I. & De Faire, U. 2002, "Heritability of death from coronary heart disease: a 36-year follow-up of 20 966 Swedish twins", *Journal of internal medicine*, vol. 252, no. 3, pp. 247-254.

Zhang, S.H., Reddick, R.L., Piedrahita, J.A. & Maeda, N. 1992, "Spontaneous hypercholesterolemia and arterial lesions in mice lacking apolipoprotein E", *Science (New York, N.Y.)*, vol. 258, no. 5081, pp. 468-471.

Zhou, X. & Hansson, G.K. 1999, "Detection of B cells and proinflammatory cytokines in atherosclerotic plaques of hypercholesterolaemic apolipoprotein E knockout mice", *Scandinavian Journal of Immunology*, vol. 50, no. 1, pp. 25-30.

